High Energy Phenomenology using the Impact Parameter Representation and the Quark Model

Nathan W. Dean

Churchill College

Cambridge

Submitted for the Degree of Doctor of Philosophy

in the University of Cambridge

June 1968

Preface

The research described in this thesis has been undertaken during a period of three years as a research student in Cambridge University. It is the author's original work except where explicitly stated, and no part of it has been submitted for any other degree or diploma. Much of the content of Chapters II-IV has appeared already in Il Nuovo Cimento, 52A, 1129 (1967). The consideration of the antisymmetric sum rule in Chapter VII also has been published, in Nuclear Physics, B4, 534 (1968), and the analysis of double exchange reactions has been submitted for publication in the same journal.

It is with pleasure that I express my appreciation to my supervisor, Dr. R. J. Eden, for his excellent guidance and continued encouragement. I also wish to thank Professor L. Van Hove, who served as my adviser during the period from September 1, 1967 through April 1, 1968, which I spent at the Centre Europeene pour la Recherche Nucleaire, Geneva, Switzerland. Stimulating conversations with Dr. Eden, with Professor Van Hove, and with my friends and colleagues at CERN and at the Cavendish Laboratory played a great part in the formulation of my ideas.

I am grateful to the United States Churchill Foundation for a Churchill Scholarship, which opened the possibility of studying

at Cambridge and supported me financially during my first year of research; and to the U.S. National Science Foundation for a Graduate Fellowship during the last two years. The hospitality extended to me in the High Energy Physics group and at CERN is also gratefully acknowledged. My thanks go too to Miss Carol McCall for her careful typing of the manuscript.

Nathan W. Dean

Contents

CHAPTER I

Introduction

> To say that technopolitan man is pragmatic means that he is a kind of modern ascetic. He disciplines himself to give up certain things. He approaches problems by isolating them from irrelevant considerations, by bringing to bear the knowledge of different specialists, and by getting ready to grapple with a new series of problems when these have been provisionally solved. Life for him is a set of problems, not an unfathomable mystery. He brackets off the things that cannot be dealt with and deals with those that can. He wastes little time thinking about "ultimate" or "religious" questions. And he can live with highly provisional solutions.
>
> Harvey Cox [1]

These lines, although written to describe generally the style of life in a secular society, state remarkably well the basic philosophy of phenomenological high energy physics. It is, at

heart, a philosophy of parametrization. While waiting for the lightning stroke of genius that will explain the universe, we busy ourselves by describing it. We seek to wed the accumulated data to a few basic ideas by means of simple parametric representations. In so doing we ask not so much why as how. It is this pragmatic attitude that will characterize the following thesis.

The work we shall present consists of two parts, each essentially self-contained and discrete. The first part consists of a study of the application of techniques similar to the Sommerfeld-Watson transformation to an impact parameter representation of the scattering amplitude. We investigate the implications of pole terms in the complex impact parameter plane and their relation to the complex angular momentum plane of Regge theory. Such terms are shown to be present in a potential theoretic model and to be related to the behaviour of Regge amplitudes at large momentum transfer. The energy dependence of large angle scattering seems compatible with the amplitude resulting from an impact parameter pole; we therefore present the results obtained by fitting experimental data on high energy proton-proton scattering near 90° in the centre-of-mass system on this basis. The fits obtained are reasonably good.

The second part of the thesis is concerned with multiple scattering in the quark model. The success of the relations derived from the additivity assumption can be explained in terms of a simple physical picture of independent quarks. If this view-

point is taken, however, rescattering effects, which can be calculated by means of the well-known Glauber formalism, may not be negligible. We present evidence, both by direct calculation and by fitting experimental data, that the quark model with multiple scattering is capable of describing the high energy interactions of hadrons. We begin by studying two situations in which the single scattering effects do not appear; then we assume a simple form of Regge behaviour and parametrize the meson-nucleon total cross sections. Finally we extend the model to include spin effects and obtain a reasonably good fit to the data on pion-proton interactions, including particularly the charge exchange polarization. Our analysis shows that multiple scattering effects are sizeable and vanish extremely slowly with increasing energy.

Apart from a pragmatic interest in approximating the observed experimental situation, the two parts are related only in the fact that both begin from an impact parameter representation of the scattering amplitude. They differ primarily in approach; the first investigates a mathematically motivated parametrization form, while the second studies a rather intuitive physical model.

Although our notation is standard, we have attempted throughout to define all symbols as they are introduced. Vectors are signified by bars, e.g. $\bar{z}$, and we consistently employ natural units in which $\hbar = c = 1$. Although k generally indicates a momentum, we point out that in part I it refers to the centre of mass frame,

whereas in part II it denotes the laboratory momentum.

Reference

1. Harvey Cox, The Secular City (London: SCM, 1965) p.63.

PART I

REGGE-LIKE POLES IN THE IMPACT PARAMETER PLANE

CHAPTER II

Poles in the Impact Parameter Plane

The partial wave expansion, which serves admirably as a general theoretical framework for the description of scattering processes in the low energy region, becomes less satisfactory at higher energies. Above about 6 GeV/c, the angular behaviour of hadronic differential cross sections becomes essentially diffractive. Both elastic and inelastic processes show a strong forward peak, decreasing rapidly as the momentum transfer increases, and quite small differential cross sections in the large angle region. In some cases there is also a peak in the backward direction. The description of such processes by a partial wave expansion clearly requires that a large number of partial wave amplitudes must be known accurately in order to obtain simultaneously the necessary addition of terms to form the forward peak and the cancellations which must occur at larger angles. As a result, reliable partial wave analyses become very difficult to do.

An appealing alternative framework has its origins in the classical description of the scattering of light, and is variously known as the eikonal approximation, the optical model, or the impact parameter representation. This method of description, which, although

approximate, corresponds to an intuitive physical picture of the scattering process, was first suggested in this context by Moliere[1] some twenty years ago. Although the theory was developed further by numerous authors[2] it has played a relatively minor role in strong interaction physics until very recently. The partial wave expansion, although poorly suited to high energy phenomenology, has dominated theoretical development because it can be formulated rigorously for general relativistic scattering amplitudes. The impact parameter representation, although excellent phenomenologically, remained for many years an approximate and inherently non-relativistic theory. Both of these unsatisfactory facets of its nature can be exhibited by giving the usual potential theoretic derivation of the eikonal approximation.

The familiar quantum mechanical description of the interaction between an incident particle of momentum k and a potential $V(\bar{r})$ is contained in the Schrödinger equation, written in natural units ($\hbar = c = m = 1$) as

$$[\nabla^2 + k^2 - 2V(\bar{r})]\, \psi(\bar{r}) = 0 \quad . \tag{2.1}$$

We look for a solution of this equation of the form

$$\psi(\bar{r}) = \phi(\bar{b},z)\, e^{ikz} \tag{2.2}$$

where the z direction has been defined to be that of the incident momentum and $\bar{b}$ is a vector in the plane perpendicular to it. We expect $\phi(\bar{b},z)$ to be a slowly varying function in the high-energy

situation, so we neglect $\nabla^2\phi(\bar{b},z)$ and obtain from (2.1)

$$\frac{\partial\phi}{\partial z}(\bar{b},z) = \frac{1}{ik} V\phi(\bar{b},z) \quad . \tag{2.3}$$

Since the solution (2.2) should asymptotically represent the incident plane wave as $z \to -\infty$ the boundary condition on (2.3) is $\phi(\bar{b},-\infty) = 1$, which implies that

$$\phi(\bar{b},z) = \exp\left[\frac{1}{ik}\int_{-\infty}^{z} dz'\, V(\bar{r}')\right] \quad . \tag{2.4}$$

For a central potential the approximate wave function is therefore

$$\psi(\bar{r}) = \exp\left[ikz + \frac{1}{ik}\int_{-\infty}^{z} d\zeta\; V\left(\sqrt{\zeta^2+b^2}\right)\right] \tag{2.5}$$

and the corresponding elastic scattering amplitude is

$$f(k,\theta) = -\frac{1}{4\pi}\int d^3\bar{r}\; e^{-i\bar{k}'.\bar{r}}\, V(\bar{r})\, \psi(\bar{r})$$

$$= -\frac{1}{4\pi}\int d^3\bar{r}\; e^{i(\bar{k}-\bar{k}').(\bar{b}+\hat{k}z)}\, V(\bar{r}) \times$$

$$\times \exp\left(\frac{1}{ik}\int_{-\infty}^{z} d\zeta\; V\left(\sqrt{\zeta^2+b^2}\right)\right) , \tag{2.6}$$

where $\bar{k}'$ is the final momentum and θ denotes the scattering angle. Now for small scattering angles we have

$$e^{i(\bar{k}-\bar{k}').\hat{k}z} \approx 1 \tag{2.7}$$

and with this approximation (2.6) becomes

$$f(k,\theta) = -\frac{1}{4\pi}\int d^2\bar{b}\,dz\; e^{i(\bar{k}-\bar{k}').\bar{b}}\; V(r)\; e^{\frac{1}{ik}\int_{-\infty}^{z} d\zeta\; V(\sqrt{\zeta^2+b^2})}$$

$$= -\frac{ik}{2\pi}\int d^2\bar{b}\; e^{i(\bar{k}-\bar{k}').\bar{b}} \int_{-\infty}^{\infty} dz\; \frac{d}{dz}\left[e^{\frac{1}{ik}\int_{-\infty}^{z} d\zeta\; V(\sqrt{\zeta^2+b^2})}\right]$$

$$= -\frac{ik}{2\pi}\int b\,db\,d\phi\; e^{i|\bar{k}-\bar{k}'|b\cos\phi}\left[e^{\frac{1}{ik}\int_{-\infty}^{\infty} d\zeta\; V(\sqrt{\zeta^2+b^2})} - 1\right]$$

yielding finally

$$f(k,\theta) = -ik\int_0^{\infty} b\,db\; J_o\,(b\sqrt{-s})\;[e^{2i\chi(b)} - 1] \tag{2.8}$$

where $J_o(z)$ is the zero-order Bessel function,

$$J_o(z) = \frac{1}{2\pi}\int_0^{2\pi} d\phi\; e^{iz\cos\phi}\ ,$$

and we have used the notations

$$\sqrt{-s} = |\bar{k}-\bar{k}'| = 2k\sin\frac{\theta}{2} \tag{2.9}$$

$$\chi(b) = -\frac{1}{2k}\int_{-\infty}^{\infty} d\zeta\; V(\sqrt{\zeta^2+b^2})\ . \tag{2.10}$$

Equation (2.8) defines the impact parameter expansion of the scattering amplitude in this basic case.

The non-relativistic nature of this derivation, implicit in the use of the Schrödinger equation, is not a serious problem; it is readily shown that the same procedure can be followed starting from a relativistic wave equation. The result (2.8) remains nonetheless conceptually tied to potential theory, and furthermore it is only obtained by means of an approximate solution, using WKB methods, of the original equation. Phenomenologically, this does not matter so much; the representation is an excellent one for use in constructing models to explain the experimental situation. Among many examples are the "coherent droplet" model of Byers and Yang[3], the analysis by Serber[4] of large angle scattering, and a vast amount of work in the absorption model[5]. For rigorous theoretical analysis, however, the use of the impact parameter expansion is hindered by its approximate foundation.

The partial wave expansion, on the other hand, can be obtained naturally as an exact expansion of the scattering amplitude in terms of Legendre polynomials, and thus depends only on the most basic properties of functional representation in an orthonormal basis. Since the expression (2.8) is essentially a type of Hankel transform, it should be possible to obtain it similarly in a more rigorous manner. The first step toward such a formulation was taken by Cottingham and Peierls[6], and extensive further developments came independently but almost simultaneously from Adachi and Kotani[7] and

from Predazzi and Lüming[8]. Their technique starts from the familiar partial wave expansion

$$f(k,\theta) = \frac{1}{2ik} \sum_{\ell=0}^{\infty} (2\ell+1)\, f_\ell(k)\, P_\ell(\cos\theta) \tag{2.11}$$

and makes use of the relation

$$\int_0^\infty dx\, J_0(x \sin\tfrac{\theta}{2})\, J_{2\ell+1}(x) = P_\ell(\cos\theta) \tag{2.12}$$

to obtain by interchanging summation and integration

$$f(k,\theta) = -ik \int_0^\infty bdb\, J_0(2bk \sin\tfrac{\theta}{2})\, h(b,k) \tag{2.13}$$

with

$$h(b,k) = \frac{1}{bk} \sum_{\ell=0}^{\infty} (2\ell+1)\, f_\ell(k)\, J_{2\ell+1}(2bk) \quad . \tag{2.14}$$

More will be said in Chapter IV regarding this elegant method for defining rigorously and exactly an impact parameter representation of the scattering amplitude. For the moment, we emphasize only that it does exist. This formulation of the amplitude can therefore be treated on the same formal basis as the partial wave analysis. The particular point we wish to make in this chapter is that the

mathematical framework which leads to the very important concept of "Reggeization" of the partial wave series can be applied equally well to the impact parameter representation.

One of the most fruitful implications of the partial wave expansion for strong interaction physics has been the Regge pole analysis. Both fundamental and phenomenological insights have resulted from the idea of extending the summation index ℓ away from the real integers into the complex angular momentum plane. The basic mathematical nature of the impact parameter b is not essentially different from that of ℓ; both serve as parameters permitting a representation of the scattering amplitude in terms of the special functions of mathematical physics. It follows naturally that we should consider the extension of the impact parameter to complex values in a way exactly analogous to Regge theory. That this extension can indeed be performed we shall now show; and in the following chapters, some of the consequences of this idea will be investigated in more detail.

In order to make clear the procedure to be followed we shall give here a brief statement of the essential ingredients of Regge theory. Every term in the partial wave series (2.11) can be written as a contour integral, since

$$(2\ell+1)f_\ell(k)P_\ell(\cos\theta) = \int_{C_\ell} d\lambda \frac{(2\lambda+1)f(k,\lambda)P_\lambda(-\cos\theta)}{\sin \pi\lambda} \qquad (2.15)$$

where C_ℓ encloses only the point $\lambda = \ell$ in the complex λ plane, and $f(k,\ell)$ is a continuation of $f_\ell(k)$ to complex ℓ. To make the Sommerfeld-Watson transformation, we join the contours C_ℓ to form a single contour C, as shown in Figure 2-1, obtaining

$$f(k,\theta) = \frac{1}{2ik}\int_C d\lambda \frac{(2\lambda+1)}{\sin \pi\lambda} f(k,\lambda) P_\lambda(-\cos\theta) \quad . \tag{2.16}$$

We now assume that $f(k,\lambda)$ vanishes as $|\lambda| \to \infty$ for Re $\lambda > -\frac{1}{2}$; Carlson's theorem guarantees the uniqueness of such a continuation. It follows that the contour can be deformed into that shown in Figure 2-2, consisting of the line Re $\lambda = -\frac{1}{2} + \epsilon$ plus the contributions due to any singularities of $f(k,\lambda)$. If these singularities are only poles, as indicated in Figure 2-2, the resulting expression for the scattering amplitude is

$$f(k,\theta) = \frac{1}{2ik}\sum_i R_i(k) P_{\alpha_i(k)}(-\cos\theta) + \frac{i}{2k}\int_{-\frac{1}{2}-i\infty}^{-\frac{1}{2}+i\infty} d\lambda \frac{2\lambda+1}{\sin\pi\lambda} f(k,\lambda) P_\lambda(-\cos\theta) \quad , \tag{2.17}$$

where $\alpha_i(k)$ is the position of the i^{th} pole of $f(k,\lambda)$ and $R_i(k)$ is related to the residue $r_i(k)$ of this pole by

$$R_i(k) = \frac{2\alpha_i(k) + 1}{\sin \pi\alpha_i(k)} r_i(k) \quad . \tag{2.18}$$

Now we enquire into the behaviour of $f(k,\theta)$ in the limit of large negative values of cos θ, which in relativistic theory corresponds

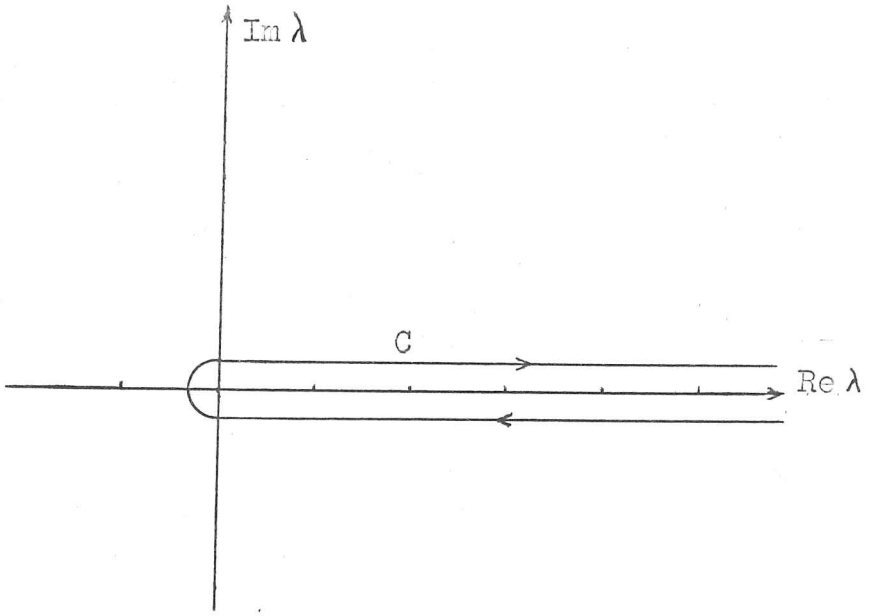

Figure 2-1. The contour C.

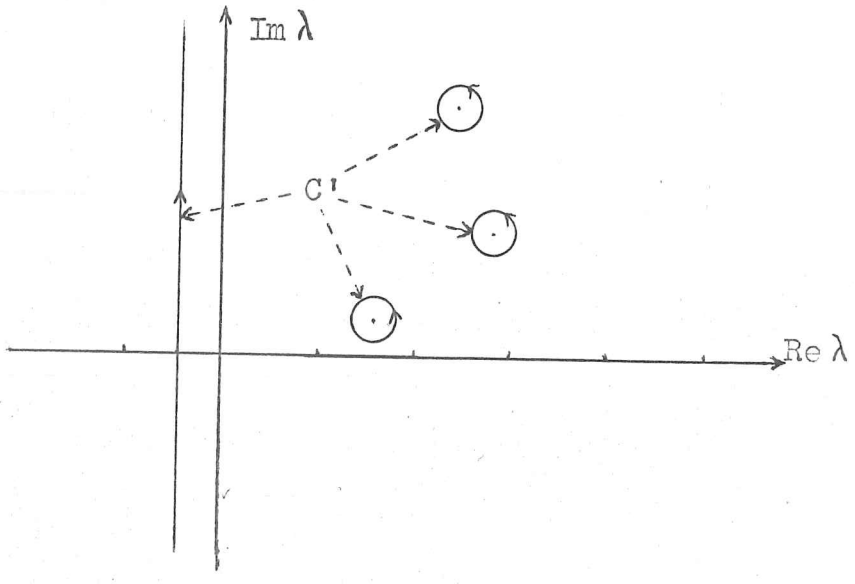

Figure 2-2. The contour C'.

to high energy scattering in the crossed channel. The asymptotic behaviour of the Legendre function is given by $P_\alpha(z) \sim z^\alpha$, and as a result the background integral along Re $\lambda = -\frac{1}{2}$ is of order $(-\cos\theta)^{-\frac{1}{2}}$ and is therefore negligible. The dominant contribution to the scattering amplitude comes from the pole $\alpha_o(k)$ which has the largest real part, i.e.

$$f(k,\theta) \approx \frac{1}{2ik} R_o(k) (-\cos\theta)^{\alpha_o(k)} . \qquad (2.19)$$

These are the bare bones of Regge theory, avoiding all inessential complications. Our purpose in reviewing them is to see the basic manipulations of the parameter involved. Briefly stated, these consist of three steps: the transformation of the parametrization into a closed contour integral, the appropriate deformation of the contour, and the study of the asymptotic behaviour of the resulting expression in the high energy region of the crossed channel.

The first of these three steps can be performed more easily for the impact parameter representation than for the partial wave series. The artifice of the Sommerfeld-Watson transformation is unnecessary, since the parameter is defined over a continuous range of values rather than at a discrete set of points. Therefore there is no ambiguity in the definition of a continuation into the complex parameter space. We write a more convenient general form of the impact parameter representation

$$F(t,s) = \int_0^\infty d\beta \; J_o(\sqrt{-\beta s}) \; H(\beta,t) \tag{2.20}$$

in terms of the usual Mandelstam variables s and $t = 4(k^2 + 1)$, with $\beta = b^2$. Our choice of variables corresponds to consideration of the t channel rather than the usual s channel; the reason for this approach will shortly be evident. Using the formula[9]

$$\int_0^\infty d\zeta \; J_\mu(b\zeta)(\zeta^2+z^2)^{-\nu}\zeta^{\mu+1} = \frac{1}{\Gamma(\nu)} \left(\frac{b}{2}\right)^{\nu-1} z^{1+\mu-\nu} \; K_{\nu-\mu-1}(bz) \tag{2.21}$$

with $\mu = 0$, $\nu = 1$, we obtain, on substituting $x = \zeta^2$, $-y = z^2$, $b = 1$,

$$\int_0^\infty dx \; \frac{J_o(\sqrt{x})}{x - y} = 2 \, K_o(\sqrt{-y}) \; . \tag{2.22}$$

This relation is valid throughout the complex y-plane with the proviso Re $\sqrt{y} \geq 0$, and can be considered a definition of the modified Bessel function. It implies that $K_o(\sqrt{-y})$ is analytic in the complex y-plane cut along the positive real axis and has a discontinuity there given by

$$\frac{1}{2i} \{K_o(\sqrt{-|y|+i\epsilon}) - K_o(\sqrt{-|y|-i\epsilon})\} = \frac{\pi}{2} J_o(\sqrt{|z|}) \; . \tag{2.23}$$

Therefore since $s < 0$ we can write (2.20) in the form

$$F(s,t) = \int_C d\beta\, K_o(\sqrt{\beta}s)\, H(\beta,t) \tag{2.24}$$

where C is a contour surrounding the positive real β axis.

The contour can be deformed by recognizing the asymptotic behaviour of the modified Bessel function,

$$K_o(\sqrt{-y}) \approx \sqrt{\frac{\pi}{2}}\, \frac{\exp(-\sqrt{-y})}{(-y)^{\frac{1}{4}}} \tag{2.25}$$

which permits us to expand the contour to infinity provided $H(\beta,t)$ is suitably bounded. Equation (2.24) then becomes

$$F(s,t) = \int_{C'} d\beta\, K_o(\sqrt{\beta}s)\, H(\beta,t) \tag{2.26}$$

where C′ is a contour surrounding the singularities of $H(\beta,t)$. We note here that, in contrast to Regge theory, no "background integral" results from the properties of the representation; the amplitude is determined fully by the singularity structure of $H(\beta,t)$. In particular, if $H(\beta,s)$ has t-dependent single poles at $\beta = \beta_i(t)$,

$$H(\beta,t) = \tfrac{1}{2} \sum_i \frac{R_i(t)}{\beta - \beta_i(t)} + H'(\beta,t)\ , \tag{2.27}$$

then

$$F(t,s) = F_p(t,s) + \frac{1}{i\pi} \int_{C'} d\beta\, K_o(\sqrt{\beta}s)\, H'(\beta,t) \tag{2.28}$$

with the contribution of the pole terms given by

$$F_p(t,s) = \sum_i F_i(t,s)$$

$$F_i(t,s) = R_i(t)\, K_o(\sqrt{\beta_i(t)}s) \quad . \tag{2.29}$$

We now take the third step listed above by assuming that if (2.28) is continued in t and s to the region corresponding to high energy scattering in the crossed (s) channel it still provides a valid representation of the amplitude. As s becomes large and positive the pole terms behave as indicated by (2.25),

$$F_i(t,s) \approx \sqrt{\frac{\pi}{2}}\, R_i(t)\, \frac{\exp(-\sqrt{\beta_i(t)}s)}{(\beta_i(t)s)^{\frac{1}{4}}} \quad . \tag{2.30}$$

Neglecting for the moment the presence of $H'(\beta,t)$, we find that the dominant contribution to $F(t,s)$ comes from that pole having the smallest value of Re $\sqrt{\beta_i(t)}$. The resulting form (2.30) must be contrasted with the asymptotic Regge form $s^{\alpha(t)}$. In terms of the diffraction peak, the impact parameter pole clearly leads to a more rapid shrinkage, whereas experimentally it appears that a less rapid shrinkage, or none, is needed. Although a non-shrinking diffraction peak might be reproduced by using several pole terms, as has been done for Regge theory, it seems more likely that the relevance of this result may be in large angle scattering, where a

strong energy dependence very similar to (2.30) has indeed been observed. The behaviour $\frac{d\sigma}{d\Omega} \sim s^{\frac{1}{2}} e^{-a\sqrt{s}}$ is in fact quite compatible with the experimental situation in the region $-2t \approx s \gg 4$. In Chapters IV and V we shall investigate this possibility in more detail.

Let us close this chapter by pointing out the general nature of the procedure we have followed. It is not essential that the Bessel functions were used; in (2.20), $J_o(\sqrt{-\beta s})$ could be replaced by any appropriate function of β, s, and t. A similar result would then follow in terms of a second function defined analogously to equation (2.22). We see therefore that Reggeization is but one form of a more basic technique applicable to any parametric representation of the scattering amplitude, and in particular to the impact parameter representation. For this case the important properties of the transformed amplitude $H(\beta,t)$ can be studied both in relation to potential theoretic approximations and as determined from the exact formulation in terms of partial waves. In the next chapter, we shall apply the ideas we have developed here to a number of potentials. Then in Chapter IV we shall discuss some of the more formal considerations and compare Regge poles with those in the impact parameter plane. Finally, in Chapter V, we shall present the results obtained by fitting the suggested forms to the available data on proton-proton elastic scattering near 90° in the centre-of-mass system.

References

1. G. Moliere, Zeits. Naturforsch. 2A, 133 (1947).

2. The most comprehensive reference on all aspects of the eikonal approach is the article by R. J. Glauber, in Lectures in Theoretical Physics, edited by W. E. Brittin and L. G. Dunham (New York: Interscience, 1958), p.315.

3. N. Byers and C. N. Yang, Phys. Rev. 142, 976 (1966).

4. R. Serber, Phys. Rev. Letters 10, 357 (1963).

5. See, for example, L. Durand III and Y. T. Chiu, Phys. Rev. 137, B1530 (1965).

6. W. N. Cottingham and R. N. Peierls, Phys. Rev. 137, B147 (1965).

7. T. Adachi and T. Kotani, Prog. Theor. Phys., Extra Number, 1965; Tokyo Metropolitan Technical College preprint, 1967; and further references listed there.

8. E. Predazzi, Annals of Phys. 36, 228, 250 (1966); M. Lüming and E. Predazzi, Nuovo Cimento 42, 878 (1966).

9. A. Erdelyi, The Bateman Manuscript Project (New York: McGraw-Hill, 1953), p.95.

CHAPTER III

Examples in Potential Theory

We shall now attempt to put into practice the formalism developed in the preceding chapter by studying the analytic structure in the β-plane resulting from a number of simple potentials. The basic connection with potential theory has been forged in terms of the eikonal approximation

$$f(k,\theta) = -ik \int_0^\infty bdb\, J_o(b\sqrt{-s})\, [e^{2i\chi(b)} - 1] \tag{3.1}$$

with $\chi(b)$ determined from the potential by

$$\chi(b) = -\frac{1}{2k} \int_{-\infty}^{\infty} dz\, V\left(\sqrt{z^2+b^2}\right) . \tag{3.2}$$

Unfortunately this approximation, although convenient in derivation, cannot be carried out for meaningful potentials; the exponential in the kernel tends to produce essential singularities in the b-plane, and the integration cannot be performed.

A similar failing, the production of essential singularities in the k-plane, has been pointed out by Blankenbecler and Goldberger[1].

As a remedy they propose an alternative representation, derivable from unitarity, which can be written

$$f_{BG}(k,\theta) = -ik\int_0^\infty bdb\, J_o(b\sqrt{-s})\,\frac{2i\chi(b)}{1-i\chi(b)} \quad . \tag{3.3}$$

The kernel $h_{BG}(b,k) = 2i\chi(b)/(1-i\chi(b))$ is in agreement with the exponential kernel of the eikonal approximation up to order k^{-3} and is much more satisfactory in both the k-plane and the b-plane. Consequently the representation (3.3) is far superior to the eikonal approximation if the technique of continuation into the complex b^2-plane is to be used. We shall therefore rewrite the Blankenbecler-Goldberger representation in an invariant form analogous to (2.20),

$$F(t,s) = \frac{\sqrt{t}}{2}\int_0^\infty d\beta\, J_o(\sqrt{-\beta s})\,\frac{n(\beta)}{1+\frac{n(\beta)}{\sqrt{4-t}}} \quad , \tag{3.4}$$

and employ it for potential analysis. In (3.4) the explicit k-dependence of $\chi(b)$ has been removed by defining

$$n(\beta) = -\int_{-\infty}^{\infty} dz\, V\left(\sqrt{z^2+\beta}\right) \quad , \tag{3.5}$$

and the factor $\sqrt{t}$ necessary to convert the non-relativistic expression (3.3) into a proper relativistically invariant amplitude has been added. The relationship of this amplitude to the direct

channel differential cross section is

$$\frac{d\sigma}{d\Omega} = \frac{1}{t} |F(t,s)|^2$$

and the corresponding expression of the optical theorem yields a total cross section

$$\sigma = \frac{4\pi}{k\sqrt{t}} \operatorname{Im} F(t,0) \quad .$$

The s-channel quantities are defined in a similar manner. Although our emphasis will remain primarily on the crossed channel amplitude and the analogy to Regge theory, we shall be able in some cases to study the direct channel as well.

It is apparent in (3.4) that a pole term appears in the amplitude when $n(\beta) = -\sqrt{4-t}$. We shall investigate in this chapter the expressions which result when the Blankenbecler-Goldberger representation is analysed in this way for the power law potentials and the Gaussian potential. These potentials divide naturally into two classes according to the analytic structure of $n(\beta)$; for odd integer power laws and the Gaussian potential the kernel function is meromorphic in the β-plane, whereas more general power laws produce a branch point at the origin. This branch point results from a pinch of the contour in (3.5) caused by the singular nature of the potential as $r \to 0$; it is avoided only by potentials $V(r)$ such that $rV(r)$ is free of branch points at the origin of the r^2-plane. For example, if we write

$$rV(r) = \int_0^\infty d\rho^2 \, \frac{v(\rho^2)}{\rho^2 + r^2}$$

it follows readily that

$$n(\beta) = \pi \int_0^\infty d\rho \, \frac{v(\rho^2)}{\sqrt{\rho^2+\beta}} \log\left[\frac{\sqrt{\beta+\rho^2} + \rho}{\sqrt{\beta+\rho^2} - \rho}\right]$$

implying that $n(\beta)$ has a cut along the negative real axis. In the presence of such cuts the analysis we wish to attempt becomes very difficult, particularly in the crossed channel, and it will not be possible to show that the pole terms dominate.

We begin with the power law potentials, which we write in the form

$$V(r) = \frac{V_\alpha(t)}{r^\alpha} \tag{3.6}$$

to emphasize that the strength of the potential may be energy-dependent. From (3.5) it follows that

$$n(\beta) = -n_\alpha \, \beta^{\frac{1-\alpha}{2}} \tag{3.7a}$$

with

$$n_\alpha = 2\sqrt{\pi} \, \frac{\Gamma(\frac{\alpha-1}{2})}{\Gamma(\frac{\alpha}{2})} \, V_\alpha(t) \tag{3.7b}$$

provided $\alpha > 1$. If $\alpha \leq 1$, the integral in (3.5) diverges; for the limiting case $\alpha = 1$, corresponding to the Coulomb potential, the divergence appears in the term $\Gamma(\frac{\alpha-1}{2})$.

The scattering amplitude for the potential (3.6) is therefore given in the Blankenbecler-Goldberger representation by

$$F(t,s) = -\frac{\sqrt{t}}{2}\int_0^\infty d\beta\, J_o(\sqrt{-\beta}s)\, \frac{n_\alpha}{\beta^{\frac{\alpha-1}{2}} - \frac{n_\alpha}{\sqrt{4-t}}} . \tag{3.8}$$

It is clear in (3.8) that the kernel possesses a branch point at $\beta = 0$ unless α is an odd integer. We shall examine first the archetypal case $\alpha = 3$, for which there is a single pole in the β-plane located at

$$\beta_o(s) = \frac{n_\alpha}{\sqrt{4-t}} . \tag{3.9}$$

Consequently the scattering amplitude is

$$F(s,t) = -\frac{\sqrt{t}}{2}\int_0^\infty d\beta\, J_o(\sqrt{-\beta}s)\, \frac{n_3}{\beta - \frac{n_3}{\sqrt{4-t}}}$$

$$= -n_3\sqrt{t}\, K_o\left(\frac{\sqrt{n_3}s}{(4-t)^{\frac{1}{4}}}\right) \tag{3.10}$$

The expression (3.10), being exact, can be studied in either channel. In the crossed channel it has the decreasing behaviour

provided $\alpha > 1$. If $\alpha \leq 1$, the integral in (3.5) diverges; for the limiting case $\alpha = 1$, corresponding to the Coulomb potential, the divergence appears in the term $\Gamma(\frac{\alpha-1}{2})$.

The scattering amplitude for the potential (3.6) is therefore given in the Blankenbecler-Goldberger representation by

$$F(t,s) = -\frac{\sqrt{t}}{2}\int_0^\infty d\beta\, J_o(\sqrt{-\beta}s)\, \frac{n_\alpha}{\beta^{\frac{\alpha-1}{2}} - \frac{n_\alpha}{\sqrt{4-t}}} . \tag{3.8}$$

It is clear in (3.8) that the kernel possesses a branch point at $\beta = 0$ unless α is an odd integer. We shall examine first the archetypal case $\alpha = 3$, for which there is a single pole in the β-plane located at

$$\beta_o(s) = \frac{n_\alpha}{\sqrt{4-t}} . \tag{3.9}$$

Consequently the scattering amplitude is

$$F(s,t) = -\frac{\sqrt{t}}{2}\int_0^\infty d\beta\, J_o(\sqrt{-\beta}s)\, \frac{n_3}{\beta - \frac{n_3}{\sqrt{4-t}}}$$

$$= -n_3\sqrt{t}\, K_o\left(\frac{\sqrt{n_3 s}}{(4-t)^{\frac{1}{4}}}\right) \tag{3.10}$$

The expression (3.10), being exact, can be studied in either channel. In the crossed channel it has the decreasing behaviour

for large positive s which was emphasized in Chapter II. It must be noted, however, that if n_3 is energy-independent the pole trajectory $\beta_0(t) = n_3/\sqrt{4-t}$ decreases with increasing -t. The s-channel amplitude therefore increases with momentum transfer, whereas physically we expect it to decrease. A different facet of the same problem arises in the direct channel, where the decrease of $\beta_0(t)$ corresponds to an increase with energy of the amplitude. Specifically, the behaviour of the modified Bessel function

$$K_0(z) \to -\ln \frac{\gamma z}{2} \qquad \text{as} \quad z \to 0 \tag{3.11}$$

implies that

$$F(t,s) \propto |t|^{\frac{1}{2}} \ln |t| \qquad \text{as} \quad |t| \to \infty \tag{3.12}$$

in disagreement with the observed behaviour in either channel.

The resolution of this problem requires that the potential be energy-dependent in such a way that $\beta_0(t)$ is non-decreasing; that is, the strength $V_3(t)$ must increase at least as rapidly as k. Such behaviour is obtained if, for example, the Klein-Gordon equation is used to describe the scattering[2]; n_3 is then proportional to the energy, and $\beta_0(t)$ is asymptotically constant. This conclusion is also in qualitative agreement with the results obtained by Tiktopoulos[3], who fitted high energy large angle scattering by means of a WKB analysis of power law potentials with strength proportional to k^2. Unfortunately his analysis involved

$\alpha = 2$, so we can make no direct comparison with his numerical results, nor with those obtained subsequently by Kouris[4] using $\alpha = 4$.

The most unsatisfactory aspect of this potential arises if we consider the implications of (3.10) for forward scattering. In the s channel, the precise form of the amplitude as $t \to 0$ is determined by the corresponding behaviour of $V_3(t)$; whatever this behaviour is, it turns out that the amplitude vanishes. The opposite situation occurs in the direct channel, where the impact parameter pole leads automatically to a logarithmically divergent amplitude as $s \to 0$. This divergence is inherent in the form of the pole term, and reinforces our earlier belief that the relevance of this method of analysis lies in the consideration of large angle scattering.

The results we have obtained for $\alpha = 3$ can be extended straightforwardly to the other odd powers $\alpha = 2m + 1$, for which the amplitude is given by

$$F_m(s,t) = \frac{\sqrt{t(4-t)}}{m} \sum_{j=1}^{m} \beta_j(t)\, K_o\left(\sqrt{\beta_j(t)}s\right) , \qquad (3.13)$$

where the $\beta_j(t)$ denote the m solutions of

$$\beta^m = \frac{n_{2m+1}}{\sqrt{4-t}} . \qquad (3.14)$$

There is no change in the conclusions reached for non-forward

$\alpha = 2$, so we can make no direct comparison with his numerical results, nor with those obtained subsequently by Kouris[4] using $\alpha = 4$.

The most unsatisfactory aspect of this potential arises if we consider the implications of (3.10) for forward scattering. In the s channel, the precise form of the amplitude as $t \to 0$ is determined by the corresponding behaviour of $V_3(t)$; whatever this behaviour is, it turns out that the amplitude vanishes. The opposite situation occurs in the direct channel, where the impact parameter pole leads automatically to a logarithmically divergent amplitude as $s \to 0$. This divergence is inherent in the form of the pole term, and reinforces our earlier belief that the relevance of this method of analysis lies in the consideration of large angle scattering.

The results we have obtained for $\alpha = 3$ can be extended straightforwardly to the other odd powers $\alpha = 2m + 1$, for which the amplitude is given by

$$F_m(s,t) = \frac{\sqrt{t(4-t)}}{m} \sum_{j=1}^{m} \beta_j(t)\, K_o\left(\sqrt{\beta_j(t)}s\right) , \qquad (3.13)$$

where the $\beta_j(t)$ denote the m solutions of

$$\beta^m = \frac{n_{2m+1}}{\sqrt{4-t}} . \qquad (3.14)$$

There is no change in the conclusions reached for non-forward

scattering in either channel; agreement with the observed physical behaviour still requires that $V_{2m+1}(t)$ increase with energy. While the s-channel amplitude again vanishes as $t \to 0$, the forward direct channel amplitude is well-behaved for $m > 1$. The logarithmic singularities which occur in the pole terms as $s \to 0$ cancel each other in the summation, leading to

$$F_m(t,0) = \frac{\pi}{m} \sqrt{t(t-4)}\ \beta_o(t) \quad . \tag{3.15}$$

where β_o is the pole with the smallest phase. This result can be obtained directly, of course, by integration of (3.8) with $s = 0$. The total cross section in the t channel corresponding to this potential therefore has the same energy dependence as $\beta_o(t)$; it follows that a decrease with energy of the large momentum transfer scattering requires an increasing total cross section.

We turn now to the more general case in which α is no longer restricted to the odd integers. The pole terms are still present in (3.8) and are located at the solutions of

$$\beta^{\frac{\alpha-1}{2}} = \frac{n_\alpha}{\sqrt{4-t}} \quad . \tag{3.16}$$

There are a finite or infinite number of these solutions, depending on whether α is rational or irrational, but only those with phase between 0 and 2π contribute to the integral. The branch point in the kernel at $\beta = 0$ leads to an integral of the discontinuity over the corresponding cut, and the resulting expression for the scattering

amplitude is

$$F(t,s) = \frac{2\sqrt{t(4-t)}}{\alpha - 1} \sum_{\{j\}} \beta_j(t)\, K_o(\sqrt{\beta_j(t)}s) + F_c(t,s) \qquad (3.17)$$

with

$$F_c(t,s) = \frac{\sqrt{t}\, n_\alpha}{\pi} \cos\frac{\pi\alpha}{2} \int_0^{-\infty} d\beta \; \frac{K_o(\sqrt{\beta}s)(-\beta)^{\frac{\alpha-1}{2}}}{(-\beta)^{\alpha-1} - 2\frac{n_\alpha}{\sqrt{4-t}} \sin\frac{\pi\alpha}{2} (-\beta)^{\frac{\alpha-1}{2}} + \frac{n_\alpha^2}{4-t}} \cdot \qquad (3.18)$$

The summation over the pole terms makes a contribution which is similar to that we have already studied for $\alpha = 2m + 1$, so our concern here is the analysis of the cut term (3.18).

In the direct channel we can evaluate $F_c(t,s)$ approximately by neglecting appropriate terms in the denominator. For this purpose it is convenient to change variables in (3.18) and write

$$F_c(t,s) = \frac{\sqrt{t}\, n_\alpha (-s)^{\frac{\alpha-3}{2}}}{\pi} \cos\frac{\pi\alpha}{2} \int_0^{\infty} dx \; \frac{K_o(\sqrt{x})\, x^{\frac{\alpha-1}{2}}}{x^{\alpha-1} - 2\lambda x^{\frac{\alpha-1}{2}} \sin\frac{\pi\alpha}{2} + \lambda^2} \qquad (3.19)$$

where

$$\lambda^2 \equiv \frac{n_\alpha^2}{4 - t} (-s)^{\alpha-1} \; . \qquad (3.20)$$

The integrand is bounded, since the pole terms have been removed, and the decrease of $K_o(\sqrt{x})$ depresses the contributions of large x.

Consequently when λ^2 is very large (3.19) becomes

$$F_c(t,s) \approx \frac{\sqrt{t}\, n_\alpha(-s)^{\frac{\alpha-3}{2}}}{\pi\lambda^2} \cos\frac{\pi\alpha}{2} \int_0^\infty dx\, K_o(\sqrt{x})\, x^{\frac{\alpha-1}{2}}$$

$$= \frac{2^\alpha \sqrt{t}\,(t-4)}{\pi n_\alpha} \cos\frac{\pi\alpha}{2} \left[\Gamma\left(\frac{\alpha+1}{2}\right)\right]^2 \frac{1}{(-s)^{\frac{\alpha+1}{2}}} \quad . \tag{3.21}$$

We see from (3.20) that this limit corresponds either to large momentum transfers or to high energies in the case that the potential increases with t. The opposite limit, $\lambda^2 \to 0$, can sometimes be taken also; the amplitude $F_c(t,s)$ then becomes

$$F_c(t,s) \underset{\lambda^2\to 0}{=} \frac{\sqrt{t}\, n_\alpha(-s)^{\frac{\alpha-3}{2}}}{\pi} \cos\frac{\pi\alpha}{2} \int_0^\infty dx\, K_o(\sqrt{x})\, x^{\frac{1-\alpha}{2}} \tag{3.22}$$

which converges provided $\alpha < 3$ to yield

$$F_c(t,s) = \frac{2^{2-\alpha}\sqrt{t}\, n_\alpha}{\pi} \cos\frac{\pi\alpha}{2} \left[\Gamma\left(\frac{3-\alpha}{2}\right)\right]^2 (-s)^{\frac{\alpha-3}{2}} \quad . \tag{3.23}$$

This result is relevant for the near-forward scattering. It is instructive to note that (3.23) can be considered for $\alpha = 1$, corresponding to the Coulomb potential; the divergence we have noticed in n_α is cancelled by the factor $\cos\frac{\pi\alpha}{2}$, and we obtain

$$F_c^{\text{Coulomb}}(t,s) = \frac{2\,V_1(s)\,\sqrt{t}}{s}\,, \tag{3.24}$$

reproducing the t-channel Coulomb scattering amplitude except for its divergent phase. (This divergence was shifted into the pole term because we took the limit $s \to 0$ before letting $\alpha \to 1$.)

In order to attempt a similar analysis of (3.18) in the s channel we must make use of the analytic properties of $K_o(z)$. The appropriate continuation as s moves from negative real values to the upper side of the real axis is

$$K_o(e^{-\frac{i\pi}{2}} z) = \frac{i\pi}{2}\, H_o^{(1)}(z) \tag{3.25}$$

where $H_o^{(1)}(z) \equiv J_o(z) + i\,Y_o(z)$ is the Hankel function of the first kind. Then we have in place of (3.19)

$$F_c(t,s) = \sqrt{-t}\; n_\alpha\, s^{\frac{\alpha-3}{2}} \cos\frac{\pi\alpha}{2} \int_0^\infty dx\, \frac{H_o^{(1)}(\sqrt{x})\, x^{\frac{\alpha-1}{2}}}{x^{\alpha-1} - 2\eta x^{\frac{\alpha-1}{2}} \sin\frac{\pi\alpha}{2} + \eta^2} \tag{3.26}$$

where

$$\eta^2 = \frac{n_\alpha^2}{4 - t}\; s^{\alpha-1}\,.$$

In this case the high energy limit is $\eta^2 \to \infty$. Unfortunately the Hankel function does not decrease sufficiently rapidly to enable

us to follow the procedure used in the direct channel; but from the form of (3.26) we see that in any case $F_c(t,s)$ will probably depend on a power of s. Therefore in either channel the pole terms decrease more rapidly with $|s|$ than the contribution of the cut.

Consequently we cannot show generally for these potentials that the dominant behaviour of the crossed channel scattering amplitude is supplied by poles in the impact parameter plane. It remains a valid assertion that such terms are present, however, and it is interesting that at least in some cases, namely $\alpha = 2m+1$, they are entirely responsible for the resulting amplitude. In order to present a second case in which this result is obtained we now consider a Gaussian potential

$$V(r) = V_o\, e^{-\mu^2 r^2} \tag{3.27}$$

which clearly satisfies the aforementioned requirement of analyticity in the r^2-plane.

For this potential it follows immediately from (3.5) that

$$n(\beta) = -\sqrt{\pi}\, V_o\, e^{-\mu^2\beta} \equiv -n_o\, e^{-\mu^2\beta} \tag{3.28}$$

so we have

$$F(t,s) = -\frac{\sqrt{t}}{2}\int_0^\infty d\beta\, J_o(\sqrt{-\beta s})\, \frac{n_o}{e^{\mu^2\beta} - \frac{n_o}{\sqrt{4-t}}}\ . \tag{3.29}$$

The kernel of (3.29) is analytic in β except for an infinite set of poles located at

$$\beta_m(t) = \frac{1}{\mu^2}\left[\ln\left(\frac{n_o}{\sqrt{4-t}}\right) + 2\pi mi\right] \tag{3.30}$$

with residues $R_m(s) = \sqrt{4-t}\,/\,\mu^2 V_o$ independent of m. The amplitude is correspondingly given by the infinite sum of these pole terms,

$$F(t,s) = \frac{\sqrt{t(4-t)}}{2\mu^2}\sum_{m=-\infty}^{\infty} K_o\left(\sqrt{\frac{s}{\mu^2}\left[\ln\left(\frac{n_o}{\sqrt{4-t}}\right) + 2\pi mi\right]}\right) . \tag{3.31}$$

In the limit of large $|s|$, pertinent for either high energy in the crossed channel or large momentum transfer in the direct channel, we have seen that the term with the smallest value of Re $\sqrt{\beta_m(t)}$ is dominant. It is easily shown that this occurs for m = 0, so we obtain

$$F(t,s) \approx \frac{\sqrt{t(4-t)}}{2\mu^2} K_o\left(\sqrt{\frac{s}{2\mu^2}\ln\left(\frac{n_o^2}{4-t}\right)}\right)$$

$$\approx \frac{\sqrt{t(4-t)}}{2\mu^2}\sqrt{\frac{\pi}{2}}\left\{\frac{s}{2\mu^2}\ln\left(\frac{n_o^2}{4-t}\right)\right\}^{-\frac{1}{4}}\exp\left[-\sqrt{\frac{s}{2\mu^2}\ln\left(\frac{n_o^2}{4-t}\right)}\right] . \tag{3.32}$$

As $|t|$ increases, the trajectories $\beta_m(t)$ also increase in magnitude provided $|t-4| > |n_o|^2$; the energy dependence of the potential is therefore restricted similarly. The strength of the potential can again be related to the direct channel total cross section, however,

since for $s = 0$ the integral in (3.29) can be evaluated exactly with the result

$$F(t,0) = \frac{\sqrt{t(4-t)}}{2\mu^2} \ln\left(1 + \frac{n_o}{\sqrt{4-t}}\right) . \qquad (3.33)$$

In contrast to the power laws, then, the Gaussian potential implies the same behaviour with t for the total cross section and the large momentum transfer scattering; an energy independent potential produces reasonable physical behaviour for the large angle region but leads to a decreasing total cross section.

It is evident that the procedure we have followed in these examples can be carried out for any potential provided the analytic structure of $n(\beta)$ can be established. In general we shall expect to find pole terms present, but it is difficult to guarantee their dominance. If there is a cut on the negative real β axis, as in the case of the general power laws, the evaluation of the amplitude may be very difficult and its asymptotic s-dependence may be obscured.

The potentials for which complex impact parameter methods are pertinent, therefore, are those for which branch points in the resulting $n(\beta)$ either are absent or are less important asymptotically than the pole terms. It is possible to invent forms of $n(\beta)$ with the appropriate analytic structure; there arises then the inverse problem of determining the potential from $n(\beta)$. Omnes[5] has shown that this inversion can be performed, since (3.5) is essentially a

recondite form of Abel's integral equation, with the result

$$V(r) = -\frac{1}{\pi r^2}\int_{r^2}^{\infty} d\beta \; \frac{\sqrt{\beta}\,\frac{\partial}{\partial\beta}\left[\sqrt{\beta}\; n\;(\beta)\right]}{\sqrt{\beta - r^2}} \quad . \tag{3.34}$$

Using (3.34) a potential can be produced which leads to any desired simple analytic properties for $n(\beta)$.

Consequently we shall conclude here our potential theoretic considerations. The cases we have studied are interesting in themselves as examples of the application of the Blankenbecler-Goldberger representation. A broader significance, however, can perhaps be discerned in the procedural analogy with Regge theory drawn in Chapter II. Just as Regge's analysis of potential scattering provided heuristic motivation for the intensive study and use of complex angular momentum ideas, so the present chapter suggests the further investigation, both formally and phenomenologically, of the possibility and implications of poles in the impact parameter plane.

References

1. R. Blankenbecler and M. L. Goldberger, Phys. Rev. 126, 766 (1962).

2. M. M. Islam, "Impact Parameter Description of High Energy Scattering", lectures delivered at the 1967 Summer Institute for Theoretical Physics, University of Colorado, Boulder, Colorado.

3. G. Tiktopoulos, Phys. Rev. 138, B1550 (1965).

4. C. Kouris, Nuovo Cimento 44, 598 (1966).

5. R. Omnes, Phys. Rev. 137, B653 (1965).

CHAPTER IV

Connections with Regge Poles

In our introduction of the concept of a complex impact parameter plane we have stressed the similarity of the mathematical techniques involved to those employed in Regge theory. The examples presented in the preceding chapter of the application of these techniques to potential theory serve as justification for the possibility of poles in the impact parameter amplitude; in the Blankenbecler-Goldberger representation such terms do exist, and in some cases they produce the dominant part of the high energy scattering amplitude. The phenomenological relevance of this possibility lies in the fact that the strong energy dependence of large angle differential cross sections seems compatible with the amplitude resulting from an impact parameter pole. Before turning to a direct comparison with the experimental data, however, we wish to look more closely at the relationship between these terms and Regge poles, both from a very naive viewpoint and through the rigorous formulation of the impact parameter amplitude.

It is evident in the designation "impact parameter" that the quantity b has a physical significance as well as a mathematical usefulness. This significance is visible in the derivation of the

eikonal model, where b corresponds to the classical impact parameter; consequently it is physically related to the angular momentum and thereby the partial wave index ℓ. The parallel is made clear in the simplest quantum-mechanical approach to an impact parameter representation; if the partial wave series

$$f(k,\theta) = \frac{1}{2ik} \sum_{\ell} (2\ell + 1)\, f_\ell(k)\, P_\ell(\cos\theta) \tag{4.1}$$

contains important contributions from a large number of terms, it is appropriate to replace the summation by an integration. Making for large ℓ the substitution

$$P_\ell(\cos\theta) \approx J_o((2\ell + 1)\sin\frac{\theta}{2}) \ , \tag{4.2}$$

we find in this approach

$$f(k,\theta) \approx \frac{1}{2ik} \int_0^\infty d\ell\, J_o((2\ell + 1)\sin\frac{\theta}{2})\, [(2\ell + 1) f_\ell(k)] \ .$$

In other words, we expect by analogy with the eikonal model

$$bk \approx \ell + \tfrac{1}{2} \ . \tag{4.3}$$

This relation can in fact be shown to hold both in the eikonal approximation and in the rigorous formulation mentioned in Chapter II. The quantity bk is the classical angular momentum, and thus the equivalence of impact parameter and partial wave techniques is emphasized.

If the naive metaphor expressed by (4.3) is intuitively extended to the complex angular momentum plane, we see that a Regge pole should be somehow analogous to a pole in the complex impact parameter plane. In the notation we have been using, the pole positions would be related in this view by

$$\beta(t) \approx \frac{4}{t-4} \left(\alpha(t) + \tfrac{1}{2}\right)^2 . \tag{4.4}$$

Although the reasoning which leads to (4.4) is rather crude, it brings to light an interesting result. We have noted already that if the scattering amplitude produced by an impact parameter pole is to behave reasonably well physically, $\beta(t)$ must be an increasing function of t; consequently (4.4) implies that $(\alpha(t) + \frac{1}{2})$ must likewise increase in magnitude with t. If our analogy holds, therefore, we expect that the Regge trajectory must move to fairly large negative values as the momentum transfer increases.

A firmer foundation for these conjectures can be constructed by considering in the s channel the Mandelstam form of the Regge pole amplitude

$$F_r(t,s) = r(t)\, Q_{-1-\alpha(t)} \left(-1 - \frac{2s}{t-4}\right) , \tag{4.5}$$

which is relevant when $\alpha(t) < -\frac{1}{2}$. The similarity between this amplitude and that resulting from an impact parameter pole can be established by using the relation between Bessel functions and

Legendre functions of large order, analogous to (4.2)[1],

$$Q_\nu(\cosh\xi) \approx e^{-(\nu+\frac{1}{2})(\xi-\tanh\xi)} \sqrt{\operatorname{sech}\xi}\, K_0((\nu+\tfrac{1}{2})\tanh\xi) \quad , \tag{4.6}$$

which is valid for large $|\nu|$ with Re $\nu > 0$. If $\alpha(t)$ becomes sufficiently negative, then (4.5) resembles an impact parameter pole term of the form implied by (4.6), namely

$$F_r(t,s) \propto K_0\left(2(-\alpha(t)-\tfrac{1}{2})\left[\frac{\sqrt{s+t-4}}{2s+t-4}\right]\sqrt{s}\right) . \tag{4.7}$$

While (4.7) thus reproduces the functional character that we have studied in preceding chapters, it does not isolate the s-dependence in quite the same way. In fact it is not difficult to see that the appearance of the hyperbolic tangent in (4.7) corresponds to the appearance of $\frac{1}{2}\tan\theta$ rather than $\sin\frac{\theta}{2}$ in the derivation of the eikonal approximation. This is indeed a trivial change, since in the small-angle approximation which was pertinent there $\sin\frac{\theta}{2} \approx \frac{1}{2}\tan\theta \approx \frac{\theta}{2}$.

Perhaps, then, the source of the compatibility between the large angle scattering and the crossed channel impact parameter pole amplitude is that both resemble the behaviour of a Regge pole term such as (4.5) at large negative values of t. The necessity for the increasing magnitude of $\alpha(t)$ is in fact evident in (4.5), since $Q_\nu(z)$ is known to be a decreasing function of ν; if $F_r(t,s)$ is to shrink in the crossed channel as the momentum transfer increases, $\nu = -1 - \alpha(t)$ must increase. This situation can be

seen from the asymptotic expansion of $Q_\nu(\cosh\xi)$ pertinent in the case of Re $\nu \to \infty$ [2],

$$Q_\nu(\cosh\xi) \approx \sqrt{\frac{\pi}{2}\,\mathrm{csch}\,\xi}\;\frac{\Gamma(\nu+1)}{\Gamma(\nu+\frac{3}{2})}\;e^{-(\nu+\frac{1}{2})\xi}\,, \tag{4.8}$$

which implies that

$$F_r(t,s) \approx \sqrt{\frac{\pi}{2}}\;r(t)\left[\frac{4s}{t-4}\left(1+\frac{s}{t-4}\right)\right]^{-\frac{1}{4}}\frac{\Gamma(-\alpha(t))}{\Gamma(\frac{1}{2}-\alpha(t))}\;e^{(\frac{1}{2}+\alpha(t))\cosh^{-1}(\frac{2s}{4-t}-1)}\,. \tag{4.9}$$

We note in particular in equation (4.9) that the amplitude can be written naturally in terms of the two variables t and $x \equiv \frac{s}{4-t}$. If both s and $|t|$ are much greater than 4, it is possible to express x approximately in terms of the s-channel scattering angle θ_s as

$$x = \frac{2}{1-\cos\theta_s}\,. \tag{4.10}$$

Consequently the form (4.9) suggests the study of large angle scattering as a function of scattering angle and momentum transfer instead of energy. The x-dependence of the exponential factor in (4.9) is then on the quantity $\cosh^{-1}(2x-1) = \cosh^{-1}(\frac{3+\cos\theta_s}{1-\cos\theta_s})$, and a logarithmic plot of

$$x^{3/2}(1+x)^{\frac{1}{2}}\,|F_r(t,s)|^2 = \frac{\sqrt{3-\cos\theta}}{(1-\cos\theta)^2}\,\frac{d\sigma}{d\Omega} \qquad (4.11)$$

against this variable at fixed t should be linear. The importance of the quantity $(3+\cos\theta_s)/(1-\cos\theta_s)$ has recently been stressed by Freund[3] in an approach similar to the above but rather more approximate; he concludes from a consideration of straight-line Regge trajectories that the expected behaviour does exist and that the pion pole is the one responsible. In the next chapter we shall present results of fitting the experimental data which indicate that such behaviour is indeed present and is described reasonably well by either a Regge pole with negative trajectory or an impact parameter pole.

For the moment, however, we prefer to continue our further investigation of poles in the impact parameter plane. We have shown that this concept is analogous procedurally to that of Regge poles, and we have established the similarity of the two types of amplitude in the region of large momentum transfer. There remains, however, the question of a more direct connection between the two theories. Does a Regge pole amplitude directly imply the existence of an impact parameter pole, and vice versa? There are several ways to approach this question, but to consider it correctly requires that we present in rather more detail the rigorous definition of the impact parameter amplitude.

We shall employ for this purpose a formulation due to Islam[4]

which makes clear certain pertinent points regarding the Adachi-Kotani representation. An amplitude is defined by

$$\begin{aligned} A(k,y) &= T(k,y) \quad , \qquad 0 \leqslant y < 1 \\ &= \bar{T}(k,y) \quad , \qquad 1 < y \end{aligned} \tag{4.12}$$

where $y \equiv \sin\frac{\theta}{2}$ and $T(k,\sin\frac{\theta}{2}) \equiv f(\mathbf{k},\theta)$. The function $\bar{T}(k,y)$ is arbitrary except for certain convergence conditions, namely (i) $\int_1^\infty y^{\frac{1}{2}}\,\bar{T}(s,y)dy$ is absolutely convergent and (ii) $\bar{T}(k,y)$ is of bounded variation for $1 < y < \infty$. These conditions are sufficient to ensure that $A(k,y)$ has a Fourier-Bessel representation for $0 < y < \infty$, which we write as

$$A(k,y) = \frac{1}{2ik}\int_0^\infty b\,db\; J_o(2kby)\; a(k,b) \tag{4.13a}$$

$$a(k,b) = 2ik\int_0^\infty y\,dy\; J_o(2kby)\; A(k,y) \quad . \tag{4.13b}$$

We now split $a(k,b)$ into two parts, writing

$$a(k,b) = a_1(k,b) + a_2(k,b) \tag{4.14a}$$

$$a_1(k,b) = 2ik\int_0^1 y\;dy\; J_o(2kby)\; T(k,y) \tag{4.14b}$$

$$a_2(k,b) = 2ik\int_1^\infty y\;dy\; J_o(2kby)\; \bar{T}(k,y) \quad . \tag{4.14c}$$

which makes clear certain pertinent points regarding the Adachi-Kotani representation. An amplitude is defined by

$$\begin{aligned} A(k,y) &= T(k,y) \quad , \qquad 0 \leq y < 1 \\ &= \bar{T}(k,y) \quad , \qquad 1 < y \end{aligned} \tag{4.12}$$

where $y \equiv \sin\frac{\theta}{2}$ and $T(k,\sin\frac{\theta}{2}) \equiv f(\mathbf{k},\theta)$. The function $\bar{T}(k,y)$ is arbitrary except for certain convergence conditions, namely (i) $\int_1^\infty y^{\frac{1}{2}} \bar{T}(s,y)dy$ is absolutely convergent and (ii) $\bar{T}(k,y)$ is of bounded variation for $1 < y < \infty$. These conditions are sufficient to ensure that $A(k,y)$ has a Fourier-Bessel representation for $0 < y < \infty$, which we write as

$$A(k,y) = \frac{1}{2ik}\int_0^\infty bdb\, J_o(2kby)\, a(k,b) \tag{4.13a}$$

$$a(k,b) = 2ik\int_0^\infty ydy\, J_o(2kby)\, A(k,y) \quad . \tag{4.13b}$$

We now split $a(k,b)$ into two parts, writing

$$a(k,b) = a_1(k,b) + a_2(k,b) \tag{4.14a}$$

$$a_1(k,b) = 2ik\int_0^1 y\, dy\, J_o(2kby)\, T(k,y) \tag{4.14b}$$

$$a_2(k,b) = 2ik\int_1^\infty y\, dy\, J_o(2kby)\, \bar{T}(k,y) \quad . \tag{4.14c}$$

The function $a_1(k,b)$ therefore contains the dynamical description of the direct channel amplitude $T(k,y)$, while $a_2(k,y)$ depends only on the extension $\bar{T}(k,y)$ used outside the physical region.

If we assume a partial wave expansion for $T(k,y)$,

$$T(k,\sin\frac{\theta}{2}) = \frac{1}{ik}\sum_{\ell=0}^{\infty}(2\ell+1)\,f_\ell(k)\,P_\ell(\cos\theta)\quad , \tag{4.15}$$

then the relation

$$\int_0^1 y\,dy\,J_0(2kby)\,P_\ell(1-2y^2) = \frac{1}{2kb}\,J_{2\ell+1}(2kb) \tag{4.16}$$

leads directly to

$$a_1(k,b) = \frac{1}{kb}\sum_{\ell=0}^{\infty}(2\ell+1)\,f_\ell(k)\,J_{2\ell+1}(2kb)\quad . \tag{4.17}$$

Consequently $a_1(k,b)$ is the same representation we have already mentioned as $h(b,k)$ in Chapter II.

Adachi and Kotani have pointed out that this function is an entire function of b of exponential type 1. Therefore the poles in the $\beta = b^2$ plane which we wish to study cannot be present in $a_1(k,b)$; the only possible singularity in the finite β plane is a branch point at the origin induced by the mapping from b to β. In particular a Regge pole cannot cause a pole in $a_1(k,b)$. This

result can be confirmed explicitly by applying the Sommerfeld-Watson transformation to the series (4.17) with $f_\ell(k)$ given by a single Regge pole term,

$$f_\ell^R(k) = \frac{r(k)}{\ell - \alpha(k)} \quad . \tag{4.18}$$

Using the asymptotic behaviour of the Bessel functions

$$J_\nu(z) \sim \frac{1}{\sqrt{2\pi\nu}} \left(\frac{ez}{2\nu}\right)^\nu \qquad \text{as} \quad |\nu| \to \infty \tag{4.19}$$

we obtain by a straightforward calculation

$$H^R(k,\beta) = a_1^R(k,\sqrt{\beta}) = \sqrt{\beta}\, \frac{(2\alpha+1)r(k)}{\cos[\pi(\alpha+\frac{1}{2})]}\, J_{2\alpha+1}(-2k\sqrt{\beta}) + B(k,\beta) \tag{4.20a}$$

where

$$B(k,\beta) = \int_{-\frac{1}{2}-i\infty}^{-\frac{1}{2}+i\infty} d\lambda\, \frac{(2\lambda+1)\, r(k)\, J_{2\lambda+1}(-2k\sqrt{\beta})}{\pi\cos[\pi(\lambda+\frac{1}{2})]\,(\lambda - \alpha(k))} \tag{4.20b}$$

is a "background integral" term which can be shown to be convergent. It is evident that $H^R(k,\beta)$ as given by (4.20) is indeed free of poles in the β plane; in fact it is, as expected, an entire function of b.

We would not expect, however, to find a term supplying the crossed channel asymptotic behaviour by means of $a_1(k,b)$, since it contains dynamical information about the direct channel only. The scattering amplitude which it produces,

$$\int_0^\infty bdb\, J_o(2kby)\, a_1(k,b) = T(k,y) \quad , \qquad 0 \leq y < 1$$
$$= 0 \quad , \qquad 1 < y \quad , \tag{4.21}$$

clearly does not extend beyond the boundaries of the direct channel physical region. Instead we must consider the analytic properties of the function $a(k,b) = a_1(k,b) + a_2(k,b)$ obtained when $\bar{T}(k,y)$ is taken to be the analytic continuation of $T(k,y)$ away from this physical region, in accord with the principle of S-matrix theory. The usual method of expressing this continuation, based on the Lehmann ellipse, is to write $T(k, \sin\frac{\theta}{2})$ as a dispersion integral in the $\cos\theta$ plane,

$$T(k,y) = \frac{1}{\pi}\int_{z_o}^{\infty} dz\, \frac{\rho_+(k,z)}{z-1+2y^2} + \frac{1}{\pi}\int_{-z_o}^{-\infty} dz\, \frac{\rho_-(k,z)}{z-1+2y^2} \tag{4.22}$$

where $\cos\theta = 1 - 2y^2$ and $z_o > 1$; this function is then understood to describe both $T(k,y)$ and the appropriate $\bar{T}(k,y)$.

The expression (4.22) can now be inserted in (4.13b) to define the correct impact parameter amplitude. The first term yields

$$a_+(k,b) = \frac{2ik}{\pi}\int_0^\infty y\, dy\, J_o(2kby) \int_{z_o}^{\infty} dz\, \frac{\rho_+(k,z)}{z-1+2y^2}$$
$$= \frac{ik}{\pi}\int_{z_o}^{\infty} dz\, \rho_+(k,z)\, K_o\left(2kb\sqrt{\frac{z-1}{2}}\right) \tag{4.23}$$

because of (2.21). This definition of the impact parameter representation was first given by Henzi[5]. A similar result is obtained for the second term except that the integration over negative values of z causes the argument of the Bessel function to be on its cut. Although we could resort to the analytic continuation of $K_o(\sqrt{z})$ mentioned in Chapter III, it is more reasonable to take note of the well-known fact that this term corresponds to the u channel, describing "backward" scattering. It is therefore naturally described in terms of the angle $\pi-\theta$ rather than θ, that is, by $\cos\frac{\theta}{2} = [1 - y^2]^{\frac{1}{2}}$ instead of y. Consequently we write

$$a_-(k,b) \equiv \frac{2ik}{\pi}\int_0^\infty y\,dy\,J_o(2kby)\int_{-z_o}^{-\infty} dz\,\frac{\rho_-(k,z)}{z+1-2y^2}$$

$$= \frac{ik}{\pi}\int_{-z_o}^{-\infty} dz\,\rho_-(k,z)\,K_o\left(2kb\sqrt{\frac{-z-1}{2}}\right) \qquad (4.24)$$

in terms of which the second term of (4.22) has an impact parameter representation in $\cos\frac{\theta}{2}$. Thus the amplitude can be expressed in the form

$$T(k,y) = \int_0^\infty b\,db[J_o(2kby)a_+(k,b) + J_o(2kb\sqrt{1-y^2})a_-(k,b)] \quad . \qquad (4.25)$$

It is appropriate to note here that equation (4.25) can be separated in a manner analogous to the definition of the signature in the partial wave series,

$$T(k,y) = T^{(+)}(k,y) + T^{(-)}(k,y)$$

$$T^{(\pm)}(k,y) = \int_0^\infty b\, db\, a^{(\pm)}(k,b)[J_o(2kby) \pm J_o(2kb\sqrt{1-y^2})] \qquad (4.26a)$$

with

$$a^{(\pm)}(k,b) = \tfrac{1}{2}[a_+(k,b) \pm a_-(k,b)] \; ; \qquad (4.26b)$$

however, there is no simple relation between $J_o(2kb \sin\frac{\theta}{2})$ and $J_o(2kb \cos\frac{\theta}{2})$, so not much is gained. In particular we point out that the phase of an impact parameter pole term cannot be determined as naturally as in Regge theory.

We see, then, that the impact parameter amplitude appropriate to our arguments is $a^{(\pm)}(k,b)$, or equivalently $a_\pm(k,b)$ as defined by (4.23) or (4.24); in other words, the pertinent form is

$$a(k,b) = \frac{ik}{\pi}\int_{z_o}^\infty dz\, \rho(k,z)\, K_o(2kb\sqrt{\tfrac{z-1}{2}}) \qquad (4.27)$$

with $\rho(k,z)$ chosen appropriately as $\rho_+(k,z)$ or $\rho_-(k,-z)$. The difference between this definition and that of Adachi and Kotani can be written simply by defining two functions

$$\lambda_1(x,\xi) = \int_0^1 y\,dy\ \frac{J_o(xy)}{y^2+\xi^2} \tag{4.28a}$$

$$\lambda_2(x,\xi) = \int_1^\infty y\,dy\ \frac{J_o(xy)}{y^2+\xi^2} \tag{4.28b}$$

which satisfy $\lambda_1(x,\xi) + \lambda_2(x,\xi) = K_o(x\xi)$. Then

$$h(b,k) = a_1(k,b) = \frac{ik}{\pi}\int_{z_o}^\infty dz\ \rho(k,z)\ \lambda_1(2kb,\sqrt{\frac{z-1}{2}}) \ . \tag{4.29a}$$

The dynamics of the crossed channel region, and therefore any possible impact parameter poles, are contained in the remainder of the amplitude, i.e.

$$a_2(k,b) = \frac{ik}{\pi}\int_{z_o}^\infty dz\ \rho(k,z)\ \lambda_2(2kb,\sqrt{\frac{z-1}{2}}) \ . \tag{4.29b}$$

The question of a direct connection between a Regge pole and an impact parameter pole can now be considered correctly. We define a Regge amplitude

$$T_R(k,y) = \frac{r(k)}{\sin\pi\alpha(k)}\ P_{\alpha(k)}(2y^2-1) \tag{4.30a}$$

which can be written in dispersed form

$$T_R(k,y) = -\frac{r(k)}{\pi}\int_1^\infty dz\ \frac{P_{\alpha(k)}(z)}{z-1+2y^2} \tag{4.30b}$$

because of the analytic properties of the Legendre function. (In reality the dispersion relation (4.30b) is valid only for $-1 < \alpha(k) < 0$; larger values of $\alpha(k)$ require subtractions. The essential conclusions we seek are adequately shown by (4.30), however, and are unchanged if $\alpha(k)$ is larger.) It follows that the impact parameter amplitude corresponding to a Regge pole is

$$a_R(k,b) = -\frac{ik}{\pi}\, r(k)\int_1^\infty dz\ P_{\alpha(k)}(z)\ K_o\left(2bk\sqrt{\frac{z-1}{2}}\right) . \tag{4.31}$$

The integral can readily be shown to converge for Re $b > 0$; consequently the only singularity in the β plane is a branch point at $\beta = 0$.

Therefore a Regge pole leads to a cut in the impact parameter amplitude but not to poles. In fact, it can be seen from the general form (4.27) that singularities away from the origin of the β plane cannot be produced by any $\rho(k,z)$ which converges sufficiently rapidly to permit the existence of the dispersion relation (4.32). It appears, then, that probably the impact parameter amplitude contains only a cut on the negative real axis of the β plane, and no poles are present.

The concept of impact parameter poles may nonetheless be relevant in that the contribution of the integral over the cut in the β-plane may be well approximated by a pole term; for example, the discontinuity across the cut could be strongly peaked about a certain value of β. Indeed, the Blankenbecler-Goldberger representation, which we have used in Chapter III, is such an approximation. It reproduces the unknown analytic structure in the β-plane by means of an N/D solution of a dispersion relation in the k-plane for $a(k,b)$, using the well-known approximate unitarity of the impact parameter representation.

We conclude therefore that it is reasonable to hope that the asymptotic behaviour of the scattering amplitude in the large angle region may be parametrized quite well by the form

$$F_p(s,t) \approx R(t)\, K_o(\sqrt{\beta(t)}s)$$

which is suggested by a pole in the impact parameter plane. We have seen that this form is suggested by potential theory. Its compatibility with Regge poles and with rigorous formulations of the impact parameter amplitude have been studied. The remaining question, which will be investigated in the next chapter, is its phenomenological importance: how well does it agree with nature?

References

1. G. N. Watson, A Treatise on the Theory of Bessel Functions (Cambridge: University Press, 1922), p.158.

2. Handbook of Mathematical Functions, edited by M. Abramowitz and I. Stegun (New York: Dover, 1965), p.336.

3. P. G. O. Freund, "Large Angle Scattering and the Pion's Regge Trajectory", University of Chicago preprint EFINS 68-02 (1968).

4. M. M. Islam, Lectures delivered at the 1967 Summer Institute for Theoretical Physics, University of Colorado, Boulder, Colorado.

5. R. Henzi, Nuovo Cimento 46, 370 (1966).

CHAPTER V

Comparison with Experiment

The ultimate test of a theory is, of course, its comparison with the experimental data, to which we now turn. The prediction of the theoretical considerations of the previous chapters is essentially that the behaviour of the scattering amplitude at large momentum transfer $\sqrt{-t}$ and high energy $\sqrt{s}$ should be given, to a good approximation, by

$$F_P(s,t) \sim R(t)\, K_0\, (\sqrt{\beta(t)s}) \tag{5.1}$$

if a pole in the crossed channel impact parameter amplitude is the dominant mechanism. If the pole is in the direct channel instead, the only modification necessary is the interchange of s and t. In addition to examining both these cases, we shall also consider the possibility, mentioned in Chapter IV, that the above behaviour is reproducing the effect of a Regge trajectory moving to large negative values. In that case the amplitude is given approximately by

$$F_R(s,t) \sim R'(t)\, Q_{-1-\alpha(t)}\, (-1 - \frac{2s}{t-4m^2}) \quad . \tag{5.2}$$

Since both of the forms (5.1) and (5.2) involve arbitrary functions of momentum transfer, the direct comparison of either with experiment

requires data at fixed large values of -t for varying values of s. Unfortunately, such data are not available. Although there do exist measurements for some different t values at fixed s, the majority of the data have variations in both s and t in the points measured. We must therefore follow the less desirable procedure of comparing with experiment by fitting simple forms of (5.1) and (5.2) to the data available.

We shall begin this section by giving a review of the experimental situation in large angle proton-proton scattering. Voluminous data on this reaction in the angular region 30°-90° in the centre-of-mass system have recently become available, and we have used them to obtain minimized chi-square fits with simple parametrizations of the residue and trajectory functions. The data themselves, however, have produced a considerable amount of controversy and phenomenological speculation, and we feel it is appropriate here to describe the current situation in some detail.

The first experiment to measure large angle elastic proton-proton scattering was performed by Cocconi et al.[1] in 1965. It was found by Orear[2] that these data, covering a large range of s and t values, could be fitted quite well by a simple exponential distribution in the transverse momentum $p_{\perp} = p \sin\theta$: specifically, he found

$$s \frac{d\sigma}{d\Omega} = A\, e^{-p_{\perp}/b} \qquad (5.3)$$

with $A = (595 \pm 135)\ \mathrm{GeV}^2 \frac{\mathrm{mb}}{\mathrm{sr}}$, $b = (158 \pm 3)$ MeV/c. This strikingly simple distribution led to much speculation about the possible

universality of the form (5.3), and attempts were made to derive it from more general principles. In particular a statistical model[3] met with some temporary success, until it was shown by Ericson[4] that in such a model one must find statistical fluctuations in the differential cross section. A more precise measurement of the angular distribution was made by Allaby et al.[5] in 1966; there was no sign of the predicted fluctuations. These data nonetheless could be fitted to Orear's formula provided that a different slope ($b = (225 \pm 4)$ MeV/c) was used. Further measurements were made by Akerlof et al.[6], who measured the differential cross section at 90° in the centre of mass system for momenta between 5 and 13 GeV/c; and again by Allaby et al.[7] The former experiment showed very clearly a break at which the slope in a fit using the form (5.3) changed, while the latter observed a corresponding break in the angular distribution.

As the amount of data available increased, so did the complexity of the fitting efforts which various groups made. The Akerlof group fitted the proton-proton scattering data over the entire angular range using an "onion" model of the nucleon, which pictured scattering at larger angles as the result of interactions with the core region of the nucleon. On the basis of three different interaction regions they used correspondingly three exponential terms

$$\frac{d\sigma}{d\Omega} = \sum_{i=1}^{3} A_i \, e^{-a_i (\beta p_\perp)^2} \qquad (5.4)$$

where β is the centre of mass frame velocity of the proton. It should be noted that in their parametrization the variable employed is $(\beta p_\perp)^2$ rather than $p_\perp$, which Orear used. This variable is particularly simple when expressed in terms of the usual invariants s, t, and u, namely

$$(\beta p_\perp)^2 = \frac{tu}{s} \quad . \tag{5.5}$$

An extension of this work was made by Krisch[8], who attempted to remove the effects of the symmetry under interchange of t and u which follows from the indistinguishability of the two protons. Krisch's approach involved multiplying the observed differential cross-section by a factor which was unity in the forward direction but decreased monotonically to $\frac{1}{2}$ at 90° and to zero at 180°. Using this "effective cross section for distinguishable protons," he was able to fit the general behaviour of the data reasonably well over an impressive range of twelve orders of magnitude.

A different approach was taken by the Allaby group, who, after experimenting with various parametrizations, concluded that the most effective one is

$$\frac{d\sigma}{dt} = B \exp\left(- s \sin\theta/g\right) \quad . \tag{5.6}$$

In terms of this expression the data are found to lie quite closely on two curves; for $s \sin\theta < 16$ GeV^2, the parameters in (5.6) are $B = (134.6 \pm 11.7)$ mb/GeV^2, $g = (1.24 \pm 0.01)$ GeV^2, while for

$s \sin\theta > 20$ GeV^2, they are $B = (56.4 \pm 3.4)$ μb/GeV^2, $g = (2.77 \pm 0.02)$ GeV^2.

Both these parametrization techniques are purely phenomenological; not only do they have no firm theoretical basis, but in fact either (5.4) or (5.6) contradicts the Cerulus-Martin bound[9]

$$|F(s,\cos\theta)| > e^{-C(z)\sqrt{s}\ln s} \quad . \tag{5.7}$$

Our result (5.1) is compatible with this bound, however, and has some theoretical justification if the previous chapters are accepted. It therefore seems reasonable to hope that it will be possible to describe the large angle scattering differential cross sections by means of an impact parameter pole formalism. The investigation of that possibility is the primary concern of this chapter.

The work we shall describe was performed at CERN in the latter part of 1967, but was completed before the latest data of the Allaby group[10] were made available. These detailed measurements, in the region near the "break" in their parametrization, show that neither of the parametrizations (5.4) or (5.6) is capable of describing accurately the full angular behaviour of the scattering amplitude. It is perhaps even questionable whether the breaks seen in the earlier fits are in fact truly drastic changes in the differential cross section or merely an effect induced by the fitting of a regular variation to an unfortunately chosen variable. To show the situation clearly we reproduce as Figure 5-1 a collection of all available data, given in reference 10. It will be of interest in the future to see whether our

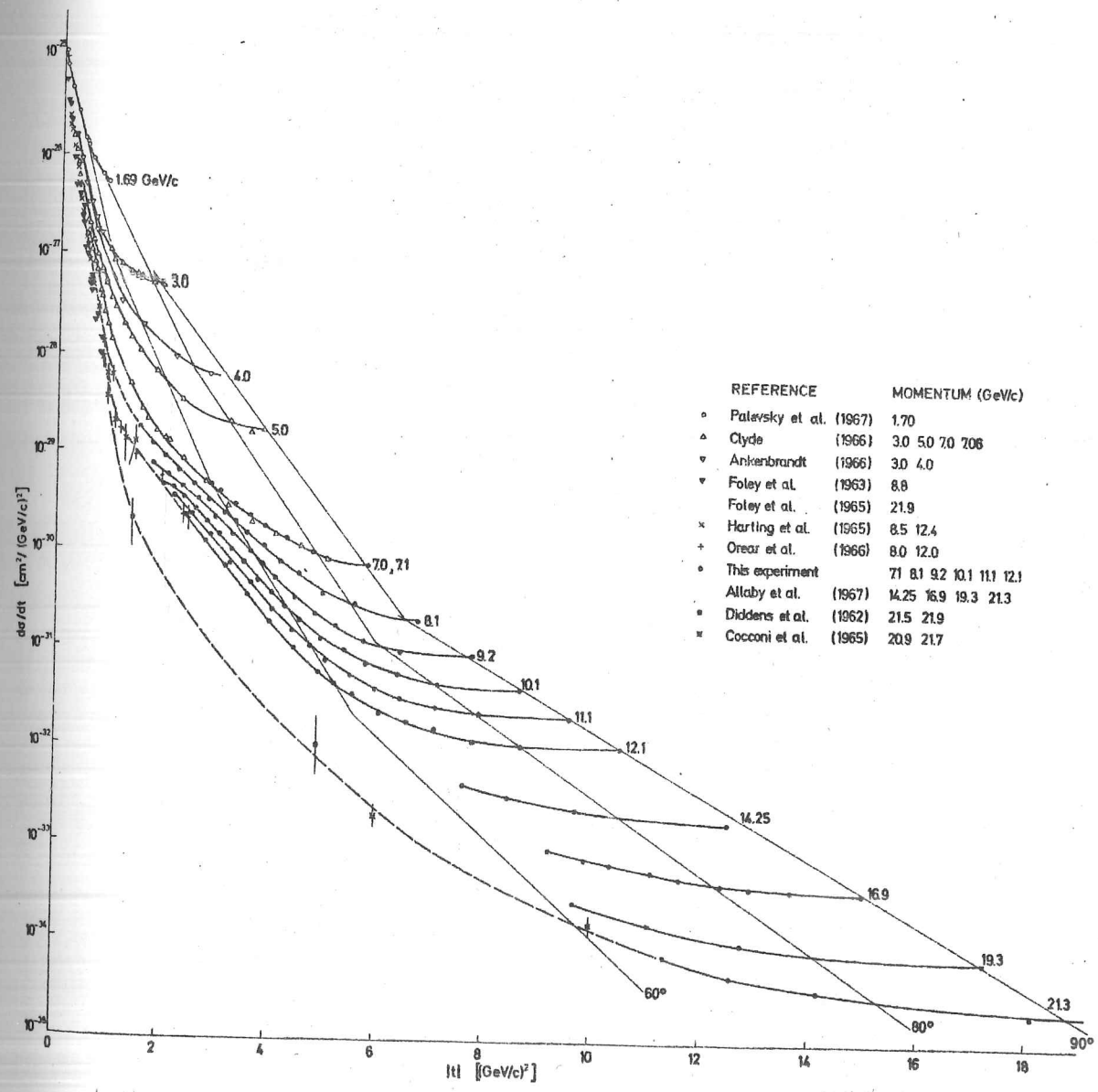

Figure 5-1 Proton-proton differential cross sections, taken from reference 10.

form (5.1) can fit the new data reported there.

The current state of affairs regarding the experimental data can be summarized, then, by saying that some very interesting structure is clearly present, but present phenomenological fits cannot adequately describe more than the gross features of the large angle differential cross sections.

Our procedure for comparing the experimental data with the forms (5.1) and (5.2) involved using the MINROS function minimization program to find the best fit of the data, in the sense of the smallest value of chi-squared, resulting from a simple parametrization with the appropriate functions. The MINROS program is a standard one, and we shall not give any detailed description of it. The fitting was carried out using the CERN CDC 6400 and CDC 6600 computers. For (5.1) the residue and trajectory functions were parametrized by writing

$$|R(t)| = \exp [R_0 + R_1 t + R_2 t^2] \tag{5.8}$$

and

$$\sqrt{\beta(t)} = \beta_0 + \beta_1 t + \beta_2 t^2 \ . \tag{5.9}$$

In order to take account of the existence of the u-channel, we symmetrize the amplitude by using

$$F^T(s,t) = F_p(s,t) + F_p(s,u) \tag{5.10a}$$

$$|F_p(s,t)| = \exp(R_0+R_1 t+R_2 t^2) K_0((\beta_0+\beta_1 t+\beta_2 t^2)\sqrt{s}), \tag{5.10b}$$

At 90° in the centre of mass system the modification made by (5.10) is trivial, since $t = u$. In order to extend the fitting away from 90°, however, it is necessary to know the phase of $F_p(s,t)$ as defined in (5.1). As we have pointed out earlier, the phase cannot be determined as naturally as in Regge theory. We therefore take a simple ansatz

$$F_p(s,t) = e^{i\phi(t)} |F_p(s,t)| \tag{5.11}$$

and assume that near 90° it is sufficient to use a linear t-dependence,

$$\phi(t) = \phi_0 + \phi_1 t \ . \tag{5.12}$$

We have neglected the possibility of s dependence in the phase in writing (5.11). Adding to (5.12) any term independent of t, such as one linear in s, produces no change in $|F^T(s,t)|^2$, and is therefore irrelevant to the calculation of the differential cross sections.

In order to consider also the possibility of the pole being in the direct channel impact parameter amplitude we have followed the same fitting procedure using the amplitude

$$F^d(s,t) = F_p(t,s) + F_p(u,s) \tag{5.13a}$$

$$|F_p(t,s)| = \exp(R_0^d + R_1^d t + R_2^d t^2)\ K_0((\beta_0^d + \beta_1^d t + \beta_2^d t^2)\sqrt{-t}) \tag{5.13b}$$

instead of (5.10). The phase of the pole term was, however, still

assumed to be linear in t as given by (5.12). The Regge theoretic form (5.2) was also parametrized in a similar way, putting in $F_R(s,t)$

$$|R'(t)| = \exp\left[R'_0 + R'_1 t + R'_2 t^2\right] \tag{5.14}$$

$$\alpha(t) = \alpha_0 + \alpha_1 t + \alpha_2 t^2 \tag{5.15}$$

and symmetrizing in t and u by defining

$$F^R(s,t) = F_R(s,t) + F_R(s,u) \tag{5.16a}$$

$$|F_R(s,t)| = \exp[R'_0+R'_1 t+R'_2 t^2]\, Q_{-1-\alpha_0-\alpha_1 t-\alpha_2 t^2}\left(-1 - \frac{2s}{t-4m^2}\right). \tag{5.16b}$$

The phase of $F_R(s,t)$, however, is known to come from the signature factor $(1 + \tau\, e^{-i\pi\alpha(t)})$, where τ is the signature of the Regge pole involved. For the fits we shall present we have assumed that the magnitude of the residue is the exponential as in (5.14), and the phase is then just

$$\phi_R(t) = -\frac{\pi}{2}\left(\alpha(t) - \frac{\tau - 1}{2}\right). \tag{5.17}$$

Since a constant in the phase is immaterial, the fit does not depend upon the signature of the pole exchanged.

It did not prove possible to fit all the data with a single parametrization in any of the forms above. This result is not surprising, since we expect that the "break" mentioned earlier may reflect the change occurring when a near trajectory becomes the

dominant one. We have therefore divided the data into two sets in roughly the same manner as in reference 7. A list of the data points used in the fitting program along with pertinent kinematical quantities is given in Tables 5-A and 5-B. These points do not include the entirety of the data; they are primarily representative of the 90° scattering in the c.m.s. system plus a number of points at angles near 90°. Points far from 90° in the centre of mass system were excluded on the basis that fitting them provided a test rather of the phase parametrization (5.12) than of the original formula (5.1) or (5.2). A further factor limiting the number of data points fitted was the excessive amount of computer time used in recalculating the Bessel functions for the parametrizations (5.10) and (5.13), and the Legendre functions for (5.16), on each loop of the minimization procedure.

We begin with the more asymptotic region for which $s \sin\theta > 18.5$ GeV^2. The fits obtained to the 37 data points listed in Table 5-A using the parametrizations (5.10), (5.13), and (5.16) are summarized in Table 5-C. We give the value of χ^2 in each case for all thirty-seven points and also for the twenty-eight points at 90° in the centre of mass system in order to show the efficiency with which the assumptions (5.11) and (5.12) and the result (5.17) were able to parametrize the phase of the amplitude. The fits are generally good, and we shall elaborate briefly upon each of them. The graphical presentation of the results is made rather clumsy by the fact that we are dealing with two independent variables s and t. In the detailed results, to be found at the end of this chapter,

we have elected therefore to give in tabular form the full fits to the data, and to plot explicitly in the graphs only the fits to the points at 90°. As an indication of the effect of our symmetrization technique we show in these tables the ratio of the u channel amplitude to the t channel amplitude. The values of this parameter, listed as FU/FT, are uniformly less than one and decreasing for angles away from 90°. Finally we point out that the units we use for the parameters R_1, R_1^d, R_1', β_1, β_1^d, α_1, and ϕ, are GeV^{-2}; of R_2, R_2^d, R_2', β_2, β_2^d, and α_2, GeV^{-4}.

Fit	Parametrization	Number of parameters	χ^2	$\chi^2(90^{\circ})$
D	(5.10)	7	31.08	25.71
E	(5.10)	3	62.58	50.87
F	(5.13)	7	36.67	28.21
G	(5.16)	6	35.87	30.21
H	(5.16)	4	41.59	38.38

Table 5-C Summary of results for the fitting of the three parametrizations being studied to the data in Table 5-A.

Beginning, then, with the parametrization (5.10), we find a good fit to the data, shown in Figure 5-2 and Table 5-D, with $\chi^2 = 31.08$, corresponding to the parameters

$$R_0 = (4.08 \pm 0.50) \qquad R_1 = (0.011 \pm 0.141)$$

$$R_2 = (2.89 \pm 5.49) \times 10^{-3}$$

$$\beta_0 = -(0.272 \pm 0.111) \qquad \beta_1 = (0.0703 \pm 0.0195) \qquad (5.18)$$

(Fit D)

$$\beta_2 = -(9.21 \pm 7.00) \times 10^{-4}$$

$$\phi_1 = -(0.133 \pm 0.054) \ .$$

It is apparent that this parametrization is in good agreement with experiment. We show in Figure 5-4 the variation with t of the best fit residue and trajectory functions

$$R(t) = \exp(4.08 + 0.011\ t + 0.00289\ t^2) \qquad (5.19a)$$

$$\sqrt{\beta(t)} = -0.272 - 0.0703\ t - 0.000921\ t^2 \ . \qquad (5.19b)$$

The large standard deviations of some of these parameters as given in (5.18) are interpreted to mean that the functional form being used is so compatible with the shape of the data that a good fit can be obtained for a large range of values of R(t) and $\beta(t)$. We have therefore reduced the number of free parameters to three by setting $R_1 = R_2 = \beta_2 = \phi_1 = 0$, corresponding to the assumption of a constant residue

and a linear t-dependence for the square root of the trajectory $\sqrt{\beta(t)}$. Despite the rather austere limitations thereby imposed on $F_p(s,t)$, a reasonably good fit is still obtained. The value of χ^2 is approximately doubled, to 62.58, of which more than 25 is due to only two points. The results for this fit are given in Table 5-E, the comparison with the 90° points being shown in Figure 5-3. The best fit values of the free parameters are

$$\begin{aligned} R_0 &= (5.36 \pm 0.27) \\ \beta_0 &= (0.280 \pm 0.082) \\ \beta_1 &= -(0.0288 \pm 0.0024) \ . \end{aligned} \qquad \begin{matrix} (5.20) \\ (\text{Fit E}) \end{matrix}$$

We have also indicated on Figure 5-4 the value $\exp(R_0)$ and the straight-line trajectory resulting from (5.20).

Following a similar procedure using the parametrization (5.13), we find an almost equally good fit with $\chi^2 = 36.67$. The parameters have the following values:

$$\begin{aligned} R_0 &= (3.04 \pm 0.02) \qquad & R_1 &= (0.142 \pm 0.002) \\ & & R_2 &= -(0.00206 \pm 0.00002) \\ \beta_0 &= -(0.311 \pm 0.068) \qquad & \beta_1 &= (0.0698 \pm 0.0007) \\ & & \beta_2 &= -(7.83 \pm 0.09) \times 10^{-4} \\ & & \phi_1 &= -(0.0233 \pm 0.0001) \ . \end{aligned} \qquad \begin{matrix} (5.21) \\ (\text{Fit F}) \end{matrix}$$

and a linear t-dependence for the square root of the trajectory $\sqrt{\beta(t)}$. Despite the rather austere limitations thereby imposed on $F_p(s,t)$, a reasonably good fit is still obtained. The value of χ^2 is approximately doubled, to 62.58, of which more than 25 is due to only two points. The results for this fit are given in Table 5-E, the comparison with the 90^o points being shown in Figure 5-3. The best fit values of the free parameters are

$$\begin{aligned} R_0 &= (5.36 \pm 0.27) \\ \beta_0 &= (0.280 \pm 0.082) \\ \beta_1 &= -(0.0288 \pm 0.0024) \ . \end{aligned} \qquad \begin{matrix} (5.20) \\ (\text{Fit E}) \end{matrix}$$

We have also indicated on Figure 5-4 the value $\exp(R_0)$ and the straight-line trajectory resulting from (5.20).

Following a similar procedure using the parametrization (5.13), we find an almost equally good fit with $\chi^2 = 36.67$. The parameters have the following values:

$$\begin{aligned} R_0 &= (3.04 \pm 0.02) \qquad & R_1 &= (0.142 \pm 0.002) \\ & & R_2 &= -(0.00206 \pm 0.00002) \\ \beta_0 &= -(0.311 \pm 0.068) \qquad & \beta_1 &= (0.0698 \pm 0.0007) \\ & & \beta_2 &= -(7.83 \pm 0.09) \times 10^{-4} \\ & & \phi_1 &= -(0.0233 \pm 0.0001) \ . \end{aligned} \qquad \begin{matrix} (5.21) \\ (\text{Fit F}) \end{matrix}$$

In Table 5-F we list the results for this fit, and in Figure 5-5 is shown the comparison of the calculated values with experiment for the 90° points. The best fit residue and trajectory functions

$$R^{d}(s) = \exp(3.04 + 0.142\ s - 0.00206\ s^{2}) \tag{5.22a}$$

$$\sqrt{\beta^{d}(s)} = -0.311 + 0.0698\ s - 0.000783\ s^{2} \tag{5.22b}$$

are pictured in Figure 5-6. The standard deviations of the parameters listed in (5.21) are all quite small, implying that the fit depends rather strongly on the actual parametrization used for the residue and trajectory.

The final parametrization fitted to these data is that given by (5.16), employing a Regge-pole term. With this form also we find quite good agreement with experiment, obtaining for the thirty-seven data points a least value of χ^{2} of 35.87 using the parameters

$$R'_{0} = (5.50 \pm 1.62) \qquad R'_{1} = (0.410 \pm 0.288)$$

$$R'_{2} = (0.0120 \pm 0.0116)$$

$$\alpha_{0} = -1 + (0.089 \pm 0.670) \qquad \alpha_{1} = -(0.076 \pm 0.120) \tag{5.23}$$

$$\alpha_{2} = -(0.00591 \pm 0.00461) \qquad \text{(Fit G)}$$

Again the compatibility of the functional form (5.2) used with the shape of the data is indicated by the large standard deviations attached to the parameter values in (5.23). We therefore attempt a more stringent fit, reducing the number of free parameters to four, by eliminating the quadratic terms in $R'(t)$ and $\alpha(t)$. With

$R_2' = \alpha_2 = 0$ a good fit is still obtained, the parameters

$$R_0' = (4.699 \pm 0.001) \qquad R_1' = (0.1598 \pm 0.0001)$$
$$\alpha_0 = -1 + (0.5490 \pm 0.0001) \qquad \alpha_1 = (0.05115 \pm 0.0001) \qquad \text{(Fit H)} \tag{5.24}$$

yielding a χ^2 value of 41.59. The standard deviations have receded to the fourth significant figure for this fit.

As before, we show the full results for these two fits in Tables 5-G and 5-H respectively, and the comparison with the 90° data points in Figures 5-7 and 5-8. The residues and trajectories for both are plotted together in Figure 5-9. We note that the trajectory values are in agreement with our earlier conjecture that $\alpha(t)$ should move away from zero. The intercept of either the linear or the quadratic trajectory at $t = 0$ is negative, corresponding to a low-lying pole, but it is presumptuous to imagine that these values can be extrapolated so far beyond the range of t in which they were fitted.

We turn next to the lower-energy data in the range 11 GeV^2 < s sin θ < 17 GeV^2. Table 5-I summarizes in the previous way the results obtained for the three parametrizations. The fits to the twenty-two data points at 90° are about equally as good as those to all twenty-nine, so the phase parametrization again seems satisfactory.

Fit	Parametrization	Number of parameters	χ^2	$\chi^2(90^\circ)$
J	(5.10)	7	20.90	18.53
K	(5.10)	3	41.41	38.96
L	(5.13)	7	34.68	33.27
M	(5.16)	6	21.19	17.89
N	(5.16)	3	40.96	38.95

Table 5-I Values of χ^2 for the twenty-nine data points and the twenty-two at 90° in the centre of mass system obtained by fitting the data in Table 5-B.

Beginning with the parametrization (5.10), we find that the assumption of a pole in the crossed channel impact parameter amplitude is capable of producing good agreement with experiment using the parameters

$$R_0 = (6.83 \pm 1.21) \qquad R_1 = (0.266 \pm 0.028)$$
$$R_2 = -(0.0146 \pm 0.0716)$$
$$\beta_0 = -(0.614 \pm 0.121) \qquad \beta_1 = -(0.245 \pm 0.125) \qquad (5.25)$$
$$\beta_2 = -(0.0187 \pm 0.0303) \qquad \text{(Fit J)}$$
$$\phi_1 = (0.225 \pm 0.270) \ .$$

The resulting value of χ^2 is 20.90, indicating quite a good fit. Once again we note that the standard deviations are fairly large and that as a result some of the parameters are consistent with zero. This fact indicates that the considerable curvature present in $\sqrt{\beta(t)}$ is not of much importance to the fit. As before we therefore reduce the number of parameters; in this case it appears compatible with (5.25) to use a linear residue and a constant trajectory. Setting $R_2 = \beta_1 = \beta_2 = \phi_1 = 0$, we obtain a fit which still has a reasonably low χ^2 of 41.41 corresponding to the parameters

$$R_0 = (8.02 \pm 1.16) \qquad R_1 = (0.537 \pm 0.183)$$
$$\beta_0 = (0.209 \pm 0.063) \ . \qquad \text{(5.26)}$$
$$\text{(Fit K)}$$

Even with this more stringent parametrization the freedom in $R(t)$ and $\beta(t)$ is fairly large. We give the full results of these two cases in Tables 5-J and 5-K and Figures 5-10 - 5-12.

For the parametrization (5.13) corresponding to a direct channel impact parameter pole, the best fit is considerably poorer than that of the previous case. The parameters

$$R_0^d = (3.85 \pm 0.08) \qquad R_1^d = (0.790 \pm 0.015)$$
$$R_2^d = -(0.0337 \pm 0.0008)$$
$$\beta_0^d = (0.0593 \pm 0.0017) \qquad \beta_1^d = (0.280 \pm 0.007) \qquad \text{(5.27)}$$
$$\text{(Fit L)}$$
$$\beta_2^d = -(0.0110 \pm 0.0002)$$
$$\phi_1 = -(0.0723 \pm 0.0025)$$

produce a χ^2 value of 34.68, which, although not extraordinarily large, is nonetheless 65% larger than the comparable value resulting from a crossed channel impact parameter pole. The details of this fit are given in Table 5-L and Figures 5-13 and 5-14.

Finally we consider the Regge pole parametrization (5.16) for these data. The fit obtained here is fully as good as that using (5.10), obtaining a value of 21.19 for χ^2 corresponding to the parameters

$$R_0' = (4.67 \pm 1.41) \qquad R_1' = (0.231 \pm 0.119)$$

$$R_2' = -(0.0866 \pm 0.0197)$$

$$\alpha_0 = -1 + (0.817 \pm 0.224) \qquad \alpha_1 = -(0.0327 \pm 0.0325) \qquad \text{(Fit M)} \tag{5.28}$$

$$\alpha_2 = -(0.00116 \pm 0.00225) \ .$$

Once again the specific form of the residue and trajectory is not very well determined because of large standard deviations attached to the parameters. We have shown in previous cases that a more spartan parametrization usually succeeds in obtaining a good fit when this situation arises. For the results (5.28), however, we notice from Figure 5-17 that the trajectory

$$\alpha(t) = -0.183 - 0.0327\, t - 0.00116\, t^2 \tag{5.29}$$

has not fulfilled our expectation that it would be reasonably far from zero in the region of interest. We therefore attempt to ameliorate this problem by fixing the parameters α_0, α_1, and α_2 at

values one standard deviation from those in (5.28), in the appropriate direction to remove the value of $\alpha(t)$ from zero. This improved curve,

$$\alpha_f(t) = -0.407 - 0.0002\,t - 0.00341\,t^2 \qquad (5.30)$$

is also shown in Figure 5-17. We then find a fit to the data having χ^2 approximately doubled, to 40.96, with the residue parameters given by

$$R_0' = (6.62 \pm 0.15) \qquad R_1' = (0.589 \pm 0.062)$$
$$R_2' = (0.00819 \pm 0.00625)\ . \qquad (5.31)$$
(Fit N)

The full results for both cases are given in Tables 5-M and 5-N; the comparisons with the data at 90° in the centre of mass system and the residue and trajectory parametrizations are shown in Figures 5-15 - 5-18.

We conclude from the results of the fitting procedures we have presented here that in general the formalism described in the preceding chapters based on the quasi-Reggeisation of an impact parameter representation is capable of describing the experimental data on proton-proton scattering near 90° in the centre of mass system. Comparing the results obtained by the use of a pole in the crossed channel impact parameter amplitude with those of a pole in the direct channel amplitude indicates that the crossed channel pole is in rather better agreement with experiment, although a reasonable

fit can be obtained on either basis. The connection noted in the preceding chapter between the amplitude resulting from an impact parameter pole and the Mandelstam form of a Regge amplitude is also substantiated by the excellent fit to the data which are obtained by parametrizing the latter.

We bring to an end the first part of this thesis by remarking that the problems of high energy physics must be considered as pragmatic ones. Unlike quantum electrodynamics, the theory of strong interactions cannot, as yet, attempt to calculate experimental quantities from first principles; instead it must rely on finding the proper conjunction of basic ideas and simple parametrizations. From the most pragmatic viewpoint, the choice of parametrizations is decided by convenient representation of the experimental situation. Thus the partial wave expansion is particularly appropriate in, for example, the study of resonant structure, where it is intimately connected with the angular momentum of the resonance. On the other hand, diffractive scattering is much more aptly described by an impact parameter expansion.

A second, and less obvious, importance of parametrization techniques is their suggestive nature. By way of Regge theory, the partial wave expansion provides a rationalization of the behaviour $R(t)s^{\alpha(t)}$, which is itself an excellent parametrization of high energy scattering in the s-channel. We view our considerations of the complex impact parameter plane in a similar light;

they suggest a form for the scattering amplitude which, in its dependence on s and t, seems to be reasonably compatible with the large angle scattering. We hope therefore that the concept of poles in the impact parameter plane may be phenomenologically useful in high energy physics.

P_{lab}, GeV/c	s, GeV^2	-t, GeV^2	θ, degrees	s sin θ, GeV^2	$\frac{d\sigma}{d\Omega}$, $\frac{\text{nanobarns}}{\text{steradian}}$	reference
9,00	18,74	7,61	90,00	18,74	80,900 ± 3,721	6
9,20	19,11	7,79	90,00	19,11	78,000 ± 3,354	6
9,40	19,48	7,98	90,00	19,48	67,600 ± 3,583	6
9,60	19,86	8,17	90,00	19,86	58,900 ± 2,886	6
9,80	20,23	8,35	90,00	20,23	53,600 ± 2,519	6
10,00	20,60	8,54	90,00	20,60	46,800 ± 2,293	6
10,20	20,98	8,73	90,00	20,98	44,100 ± 2,117	6
10,40	21,35	8,92	90,00	21,35	38,600 ± 1,814	6
10,60	21,72	9,10	90,00	21,72	35,600 ± 1,709	6
10,80	22,10	9,29	90,00	22,10	30,300 ± 1,485	6
11,00	22,47	7,51	78,00	21,98	29,600 ± ,700	7
11,00	22,47	9,48	90,00	22,47	28,400 ± 1,562	7
11,00	22,47	8,81	86,00	22,42	26,900 ± ,900	7
11,20	22,84	9,66	90,00	22,84	25,500 ± 1,377	6
11,40	23,22	9,85	90,00	23,22	20,200 ± 1,091	6
11,60	23,59	10,04	90,00	23,59	19,000 ± ,988	6
11,80	23,97	10,22	90,00	23,97	15,300 ± ,826	6
12,00	24,34	10,41	90,00	24,34	14,300 ± ,772	6
12,20	24,71	10,60	90,00	24,71	11,800 ± ,625	6
12,40	25,09	10,78	90,00	25,09	11,600 ± ,626	6
12,60	25,46	10,97	90,00	25,46	9,530 ± ,600	6
12,80	25,84	11,16	90,00	25,84	8,670 ± ,494	6
13,00	26,21	11,35	90,00	26,21	7,390 ± ,436	6
13,20	26,59	11,53	90,00	26,59	7,220 ± ,513	6
13,40	26,96	11,72	90,00	26,96	5,250 ± ,299	6
14,30	28,64	9,74	77,00	27,91	4,360 ± ,140	7
14,30	28,64	12,56	90,00	28,64	3,310 ± ,090	7
16,90	33,51	11,62	77,00	32,65	1,030 ± ,030	7
16,90	33,51	12,39	80,00	33,00	,920 ± ,040	7
16,90	33,51	12,91	82,00	33,19	,860 ± ,030	7
16,90	33,51	13,69	85,00	33,39	,810 ± ,040	7
16,90	33,51	15,00	90,00	33,51	,750 ± ,050	7
19,30	38,01	17,25	90,00	38,01	,188 ± ,017	7
21,30	41,76	18,12	87,00	41,70	,061 ± ,009	7
18,00	35,57	14,91	86,00	35,49	,365 ± ,082	1
21,90	42,88	19,68	90,00	42,88	,052 ± ,014	1
30,90	59,76	28,12	90,00	59,76	,001 ± ,001	1

Table 5A Data points used in our fitting procedures in the region s sin θ > 18.5 GeV^2.

P_{lab}, GeV/c	s, GeV^2	$-t$, GeV^2	θ, degrees	s sinθ, GeV^2	$\frac{d\sigma}{d\Omega}$, $\frac{\text{nanobarns}}{\text{steradian}}$	reference
4,98	11,27	3,59	85,80	11,24	9248,2 ± 616,5	11
5,00	11,30	3,65	86,40	11,28	9168,4 ± 568,4	12
4,98	11,27	3,64	86,54	11,25	9063,3 ± 431,6	11
5,00	11,30	3,89	90,00	11,30	8510,0 ± 246,8	6
5,10	11,49	3,98	90,00	11,49	7900,0 ± 237,0	6
5,20	11,67	4,08	90,00	11,67	7090,0 ± 219,8	6
5,30	11,86	4,17	90,00	11,86	6490,0 ± 233,6	6
5,40	12,04	4,26	90,00	12,04	5530,0 ± 171,4	6
5,50	12,23	4,35	90,00	12,23	4900,0 ± 166,6	6
5,60	12,41	4,45	90,00	12,41	4470,0 ± 138,6	6
5,70	12,60	4,54	90,00	12,60	3720,0 ± 122,8	6
5,80	12,78	4,63	90,00	12,78	3370,0 ± 111,2	6
5,90	12,97	4,72	90,00	12,97	2740,0 ± 95,9	6
6,00	13,15	4,82	90,00	13,15	2440,0 ± 75,6	6
6,08	13,30	4,44	84,71	13,24	2413,1 ± 155,7	11
6,07	13,28	4,66	87,40	13,27	2330,9 ± 155,4	11
6,10	13,34	4,91	90,00	13,34	2190,0 ± 81,0	6
6,20	13,52	5,00	90,00	13,52	1830,0 ± 67,7	6
6,40	13,89	5,19	90,00	13,89	1500,0 ± 55,5	6
6,60	14,27	5,37	90,00	14,27	1070,0 ± 50,3	6
6,80	14,64	5,56	90,00	14,64	796,0 ± 36,6	6
7,06	15,12	5,04	82,45	14,99	721,1 ± 38,8	12
7,00	15,01	5,75	90,00	15,01	645,0 ± 26,4	6
7,08	15,16	5,67	88,53	15,15	583,5 ± 64,8	11
7,20	15,38	5,93	90,00	15,38	515,0 ± 20,6	6
7,40	15,75	6,12	90,00	15,75	386,0 ± 18,5	6
7,60	16,13	6,30	90,00	16,13	305,0 ± 16,5	6
7,80	16,50	6,49	90,00	16,50	253,0 ± 11,4	6
8,00	16,87	6,68	90,00	16,87	217,0 ± 9,8	6

Table 5B Data points used in our fitting procedures in the region 11 GeV^2 < s sin θ < 17 GeV^2.

S	T	EXPTL VAL	ERR	FIT	CHISQUARE	FU/FT
18.735	7.608	80.900	3.721	86.658	2.394	1.000
19.109	7.795	78.000	3.354	77.034	.083	1.000
19.482	7.981	67.600	3.583	68.426	.053	1.000
19.855	8.168	58.900	2.886	60.738	.405	1.000
20.229	8.355	53.600	2.519	53.881	.012	1.000
20.602	8.542	46.800	2.293	47.774	.180	1.000
20.976	8.728	44.100	2.117	42.339	.692	1.000
21.350	8.915	38.600	1.814	37.507	.363	1.000
21.723	9.102	35.600	1.709	33.216	1.947	1.000
22.097	9.289	30.300	1.485	29.406	.362	1.000
22.471	7.506	29.600	.700	29.574	.001	.325
22.471	9.476	28.400	1.562	26.027	2.307	1.000
22.471	8.815	26.900	.900	26.398	.312	.689
22.845	9.663	25.500	1.377	23.032	3.213	1.000
23.219	9.850	20.200	1.091	20.378	.027	1.000
23.593	10.037	19.000	.988	18.027	.970	1.000
23.967	10.224	15.300	.826	15.946	.611	1.000
24.341	10.411	14.300	.772	14.104	.064	1.000
24.715	10.598	11.800	.625	12.475	1.163	1.000
25.089	10.785	11.600	.626	11.033	.819	1.000
25.463	10.972	9.530	.600	9.759	.145	1.000
25.837	11.159	8.670	.494	8.632	.006	1.000
26.211	11.346	7.390	.436	7.636	.317	1.000
26.586	11.533	7.220	.513	6.755	.822	1.000
26.960	11.720	5.250	.299	5.977	5.900	1.000
28.644	9.737	4.360	.140	4.527	1.421	.259
28.644	12.563	3.310	.090	3.453	2.521	1.000
33.513	11.623	1.030	.030	1.025	.030	.247
33.513	12.393	.920	.040	.887	.670	.341
33.513	12.910	.860	.030	.826	1.307	.423
33.513	13.690	.810	.040	.766	1.199	.584
33.513	14.997	.750	.050	.732	.134	1.000
38.010	17.245	.188	.017	.187	.002	1.000
41.758	18.119	.061	.009	.066	.251	.741
35.574	14.909	.365	.082	.400	.179	.650
42.882	19.682	.052	.014	.048	.078	1.000
59.755	28.118	.001	.001	.001	.120	1.000

Table 5D Detailed results for fit D.

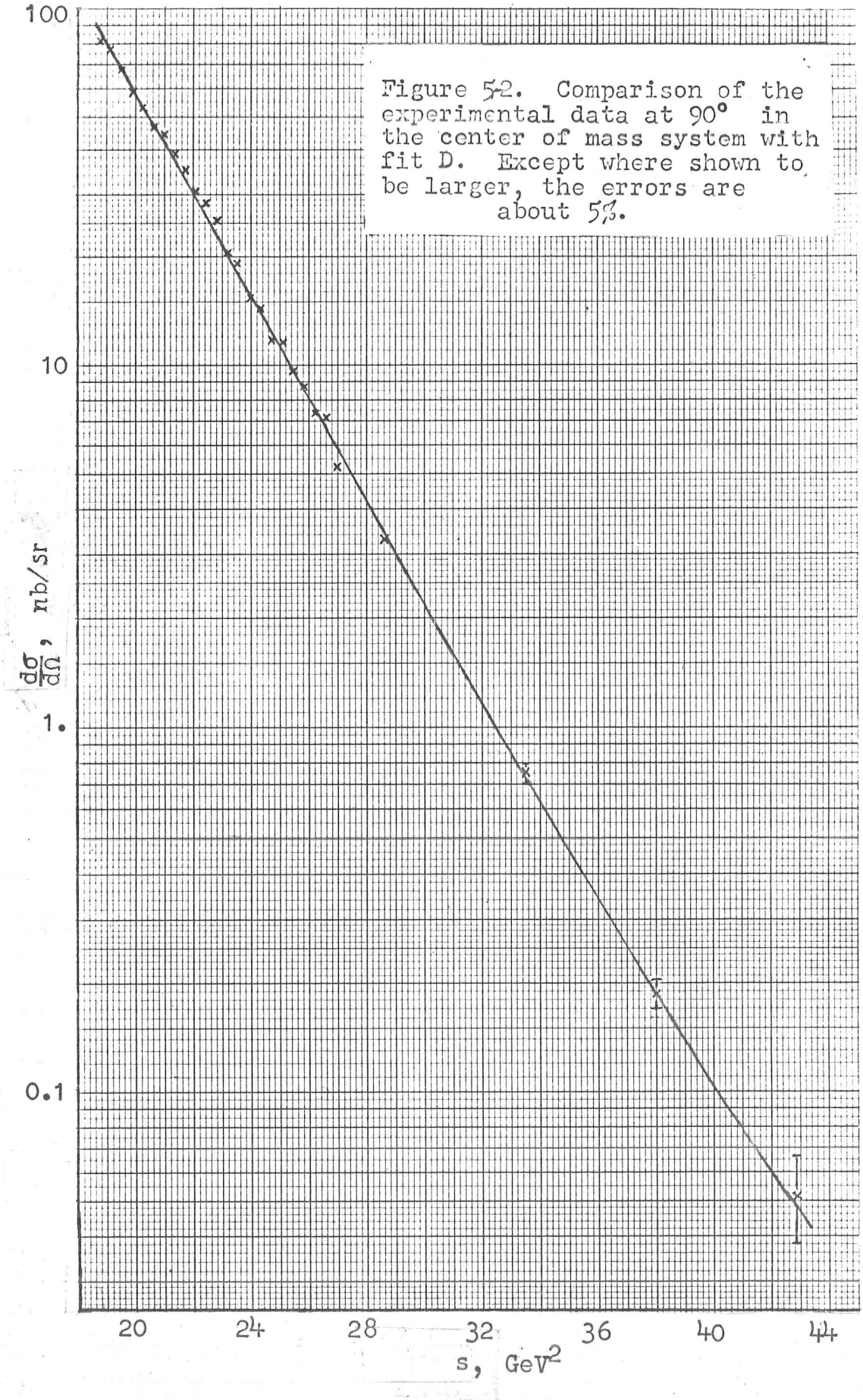

Figure 5-2. Comparison of the experimental data at 90° in the center of mass system with fit D. Except where shown to be larger, the errors are about 5%.

S	T	EXPTL VAL	ERR	FIT	CHISQUARE	FU/FT
18.735	7.608	80.900	3.721	85.271	1.379	1.000
19.109	7.795	78.000	3.354	75.807	.427	1.000
19.482	7.981	67.600	3.583	67.394	.003	1.000
19.855	8.168	58.900	2.886	59.914	.123	1.000
20.229	8.355	53.600	2.519	53.262	.018	1.000
20.602	8.542	46.800	2.293	47.346	.057	1.000
20.976	8.728	44.100	2.117	42.085	.906	1.000
21.350	8.915	38.600	1.814	37.405	.434	1.000
21.723	9.102	35.600	1.709	33.243	1.902	1.000
22.097	9.289	30.300	1.485	29.541	.261	1.000
22.471	7.506	29.600	.700	28.118	4.482	.531
22.471	9.476	28.400	1.562	26.249	1.897	1.000
22.471	8.815	26.900	.900	26.455	.245	.809
22.845	9.663	25.500	1.377	23.320	2.506	1.000
23.219	9.850	20.200	1.091	20.716	.224	1.000
23.593	10.037	19.000	.988	18.400	.369	1.000
23.967	10.224	15.300	.826	16.340	1.584	1.000
24.341	10.411	14.300	.772	14.509	.073	1.000
24.715	10.598	11.800	.625	12.880	2.984	1.000
25.089	10.785	11.600	.626	11.433	.071	1.000
25.463	10.972	9.530	.600	10.146	1.053	1.000
25.837	11.159	8.670	.494	9.003	.453	1.000
26.211	11.346	7.390	.436	7.986	1.871	1.000
26.586	11.533	7.220	.513	7.084	.071	1.000
26.960	11.720	5.250	.299	6.281	11.879	1.000
28.644	9.737	4.360	.140	4.367	.002	.371
28.644	12.563	3.310	.090	3.648	14.090	1.000
33.513	11.623	1.030	.030	.993	1.519	.285
33.513	12.393	.920	.040	.884	.809	.380
33.513	12.910	.860	.030	.830	1.005	.460
33.513	13.690	.810	.040	.773	.835	.615
33.513	14.997	.750	.050	.738	.054	1.000
35.574	14.909	.365	.082	.384	.055	.654
38.010	17.245	.188	.017	.162	2.279	1.000
41.758	18.119	.061	.009	.046	2.760	.667
42.882	19.682	.052	.014	.030	2.302	1.000
59.755	28.118	.001	.001	.000	1.593	1.000

Table 5E Detailed results for fit E.

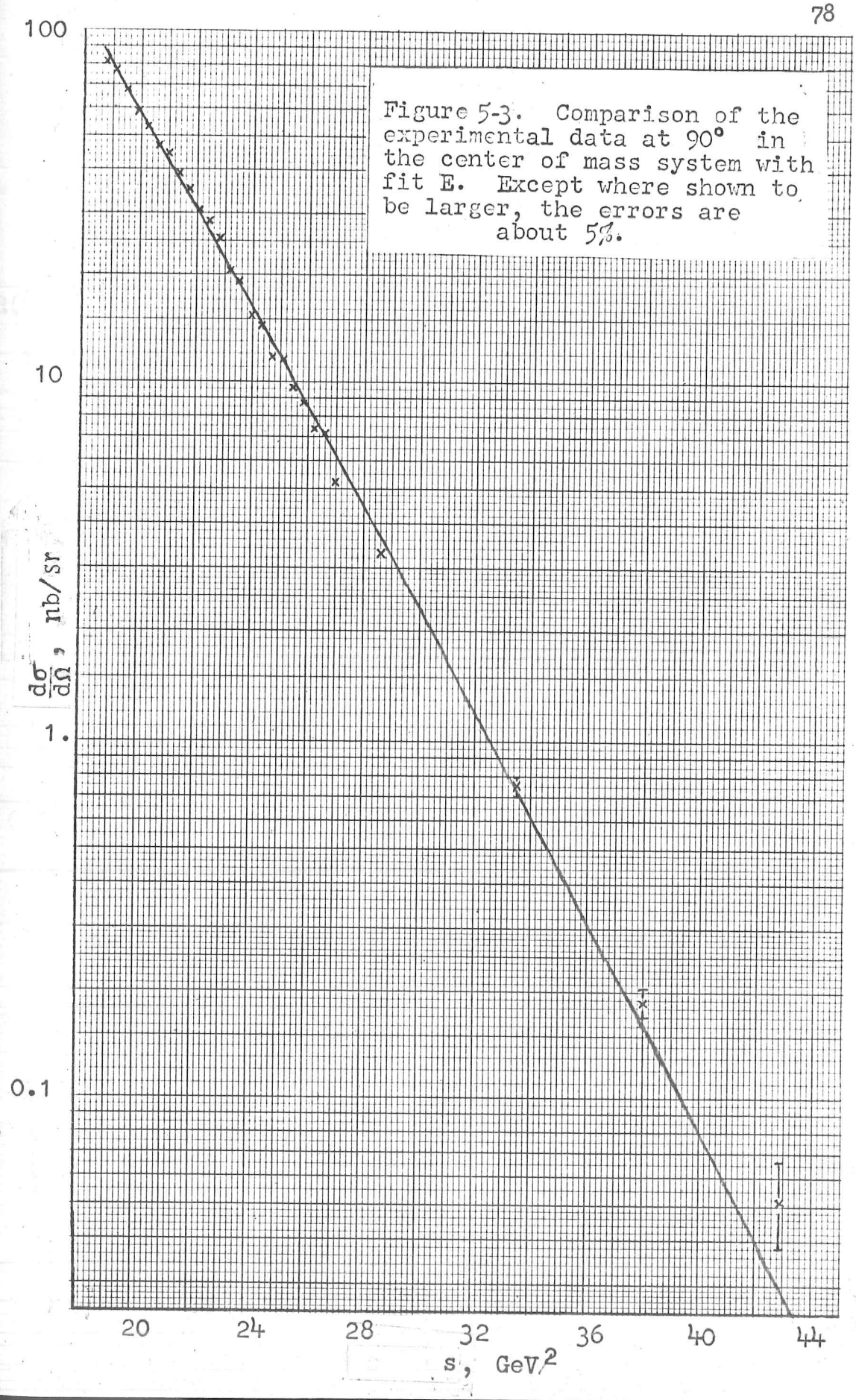

Figure 5-3. Comparison of the experimental data at 90° in the center of mass system with fit E. Except where shown to be larger, the errors are about 5%.

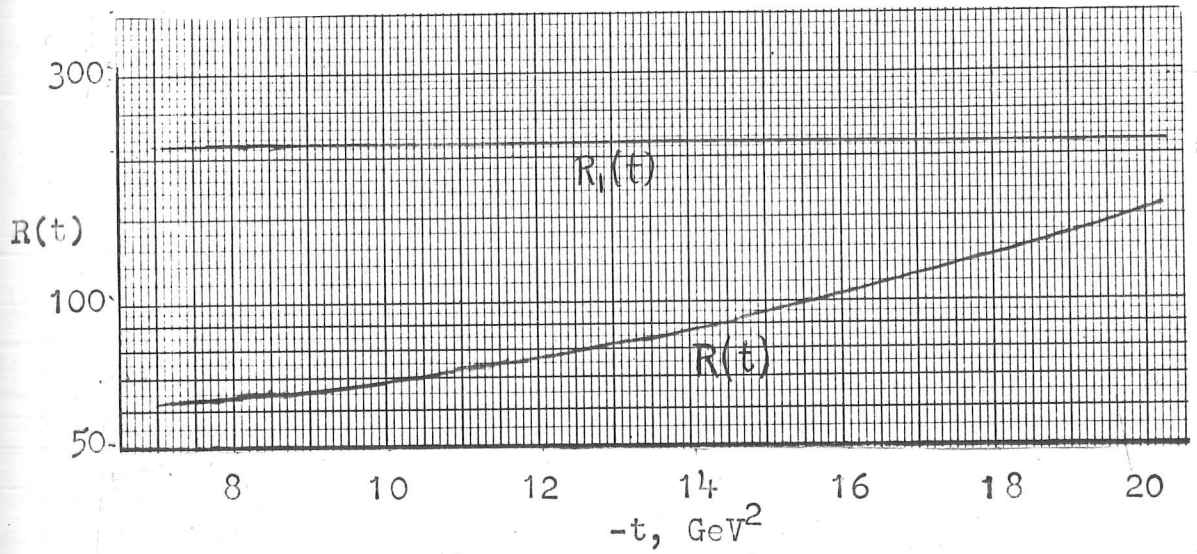

(a) $R(t) = \exp(4.08 + 0.0107t + 0.00289t^2)$
and $R_1(t) = \exp(5.36)$.

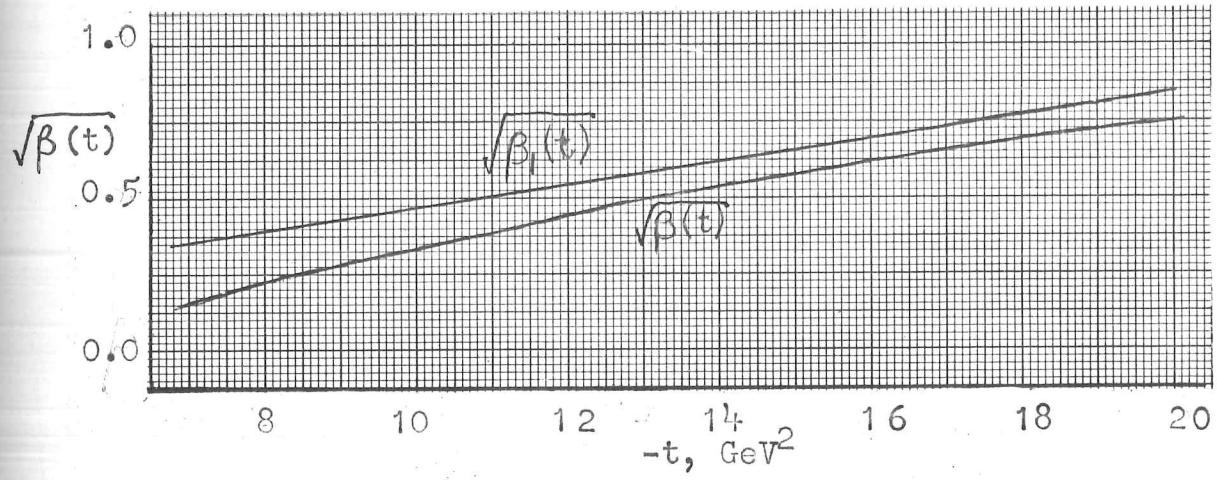

(b) $\sqrt{\beta(t)} = -0.272 - 0.0703t - 0.000921t^2$
and $\sqrt{\beta_1(t)} = 0.280 - 0.0288t$.

Figure 5-4 Residue (a) and trajectory (b) functions for fits D and E.

S	T	EXPTL VAL	ERR	FIT	CHISQUARE	FU/FT
18.735	7.608	80.900	3.721	84.259	.815	1.000
19.109	7.795	78.000	3.354	75.202	.696	1.000
19.482	7.981	67.600	3.583	67.062	.023	1.000
19.855	8.168	58.900	2.886	59.756	.088	1.000
20.229	8.355	53.600	2.519	53.206	.025	1.000
20.602	8.542	46.800	2.293	47.339	.055	1.000
20.976	8.728	44.100	2.117	42.091	.900	1.000
21.350	8.915	38.600	1.814	37.401	.437	1.000
21.723	9.102	35.600	1.709	33.214	1.950	1.000
22.097	9.289	30.300	1.485	29.479	.306	1.000
22.471	7.506	29.600	.700	30.137	.589	.520
22.471	9.476	28.400	1.562	26.150	2.075	1.000
22.471	8.815	26.900	.900	26.570	.134	.804
22.845	9.663	25.500	1.377	23.186	2.824	1.000
23.219	9.850	20.200	1.091	20.549	.102	1.000
23.593	10.037	19.000	.988	18.204	.650	1.000
23.967	10.224	15.300	.826	16.120	.986	1.000
24.341	10.411	14.300	.772	14.270	.001	1.000
24.715	10.598	11.800	.625	12.629	1.757	1.000
25.089	10.785	11.600	.626	11.173	.464	1.000
25.463	10.972	9.530	.600	9.883	.346	1.000
25.837	11.159	8.670	.494	8.740	.020	1.000
26.211	11.346	7.390	.436	7.728	.600	1.000
26.586	11.533	7.220	.513	6.832	.574	1.000
26.960	11.720	5.250	.299	6.039	6.953	1.000
28.644	9.737	4.360	.140	4.552	1.884	.388
28.644	12.563	3.310	.090	3.465	2.974	1.000
33.513	11.623	1.030	.030	1.017	.192	.327
33.513	12.393	.920	.040	.880	.992	.423
33.513	12.910	.860	.030	.815	2.260	.503
33.513	13.690	.810	.040	.749	2.358	.651
33.513	14.997	.750	.050	.708	.693	1.000
38.010	17.245	.188	.017	.175	.625	1.000
41.758	18.119	.061	.009	.061	.002	.734
35.574	14.909	.365	.082	.384	.051	.695
42.882	19.682	.052	.014	.043	.332	1.000
59.755	28.118	.001	.001	.002	.942	1.000

Table 5F Detailed results for fit F.

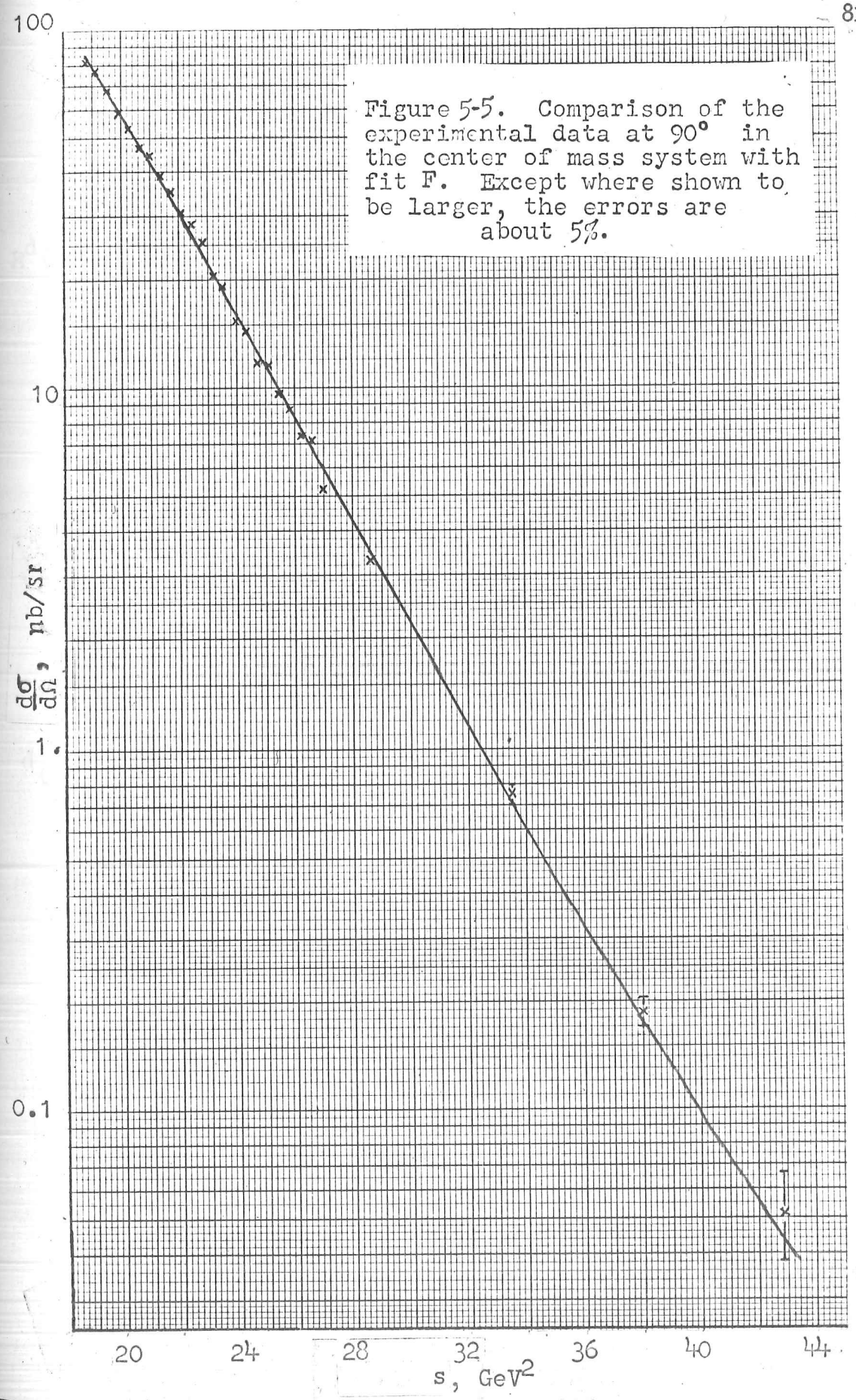

Figure 5-5. Comparison of the experimental data at 90° in the center of mass system with fit F. Except where shown to be larger, the errors are about 5%.

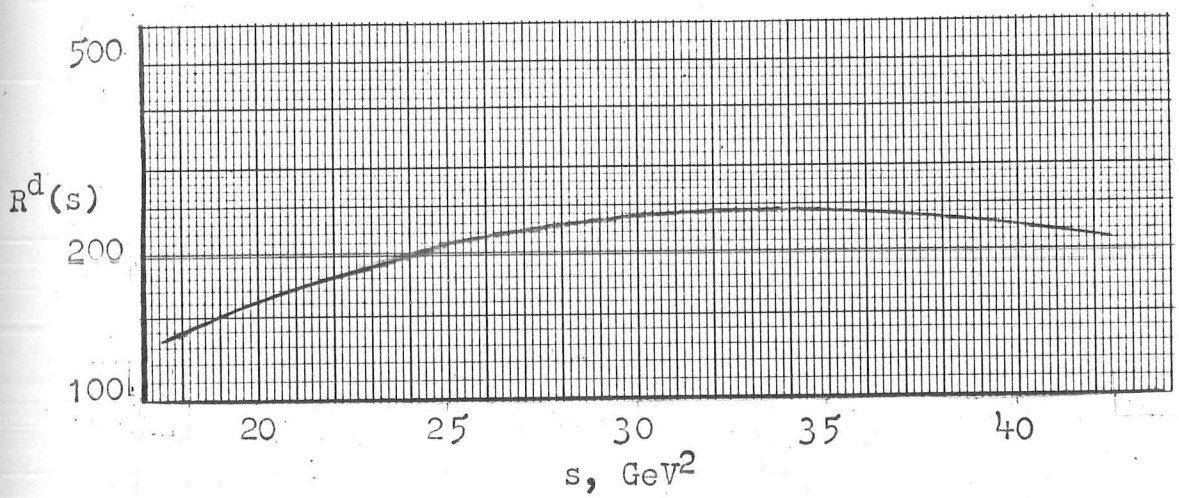

(a) $R^d(s) = \exp(3.04 + 0.142s - 0.00206s^2)$.

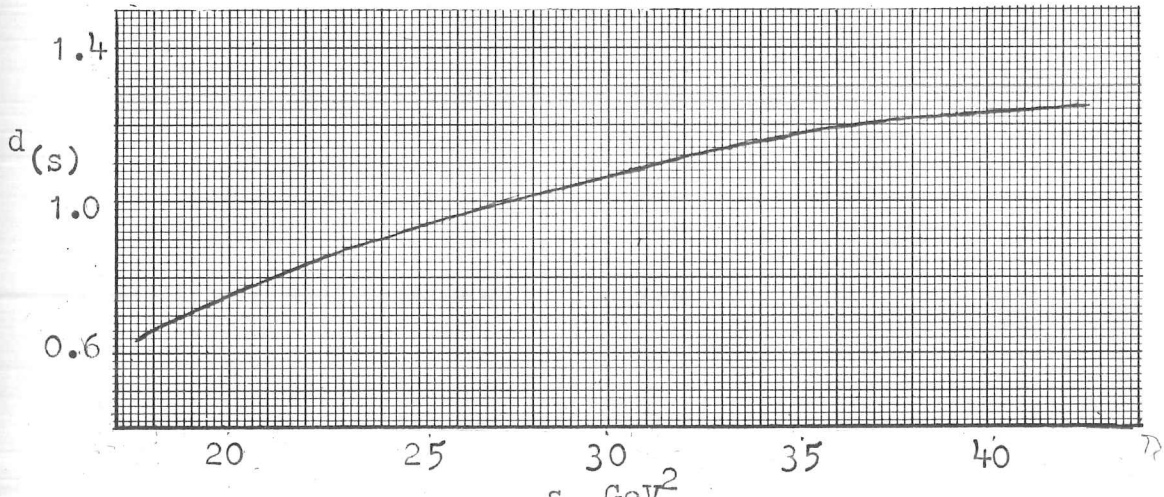

(b) $\sqrt{\beta^d(s)} = -0.311 + 0.0698s - 0.000783s^2$.

Figure 5-6 **Residue (a) and trajectory (b) functions for fit F.**

S	T	EXPTL VAL	ERR	FIT	CHISQUARE	FU/FT
18.735	7.608	80.900	3.721	88.977	4.711	1.000
19.109	7.795	78.000	3.354	78.551	.027	1.000
19.482	7.981	67.600	3.583	69.362	.242	1.000
19.855	8.168	58.900	2.886	61.259	.668	1.000
20.229	8.355	53.600	2.519	54.113	.041	1.000
20.602	8.542	46.800	2.293	47.808	.193	1.000
20.976	8.728	44.100	2.117	42.243	.769	1.000
21.350	8.915	38.600	1.814	37.332	.489	1.000
21.723	9.102	35.600	1.709	32.996	2.323	1.000
22.097	9.289	30.300	1.485	29.167	.582	1.000
22.471	7.506	29.600	.700	29.264	.231	.496
22.471	9.476	28.400	1.562	25.786	2.801	1.000
22.471	8.815	26.900	.900	26.173	.652	.786
22.845	9.663	25.500	1.377	22.799	3.847	1.000
23.219	9.850	20.200	1.091	20.161	.001	1.000
23.593	10.037	19.000	.988	17.831	1.401	1.000
23.967	10.224	15.300	.826	15.772	.326	1.000
24.341	10.411	14.300	.772	13.952	.203	1.000
24.715	10.598	11.800	.625	12.345	.759	1.000
25.089	10.785	11.600	.626	10.924	1.165	1.000
25.463	10.972	9.530	.600	9.668	.053	1.000
25.837	11.159	8.670	.494	8.559	.051	1.000
26.211	11.346	7.390	.436	7.577	.185	1.000
26.586	11.533	7.220	.513	6.710	.989	1.000
26.960	11.720	5.250	.299	5.943	5.368	1.000
28.644	9.737	4.360	.140	4.596	2.838	.356
28.644	12.563	3.310	.090	3.452	2.493	1.000
33.513	11.623	1.030	.030	1.028	.003	.313
33.513	12.393	.920	.040	.897	.345	.402
33.513	12.910	.860	.030	.836	.633	.479
33.513	13.690	.810	.040	.777	.678	.628
33.513	14.997	.750	.050	.743	.022	1.000
38.010	17.245	.188	.017	.190	.013	1.000
41.758	18.119	.061	.009	.063	.059	.749
35.574	14.909	.365	.082	.404	.228	.682
42.882	19.682	.052	.014	.046	.129	1.000
59.755	28.118	.001	.001	.001	.356	1.000

Table 5G Detailed results for fit G.

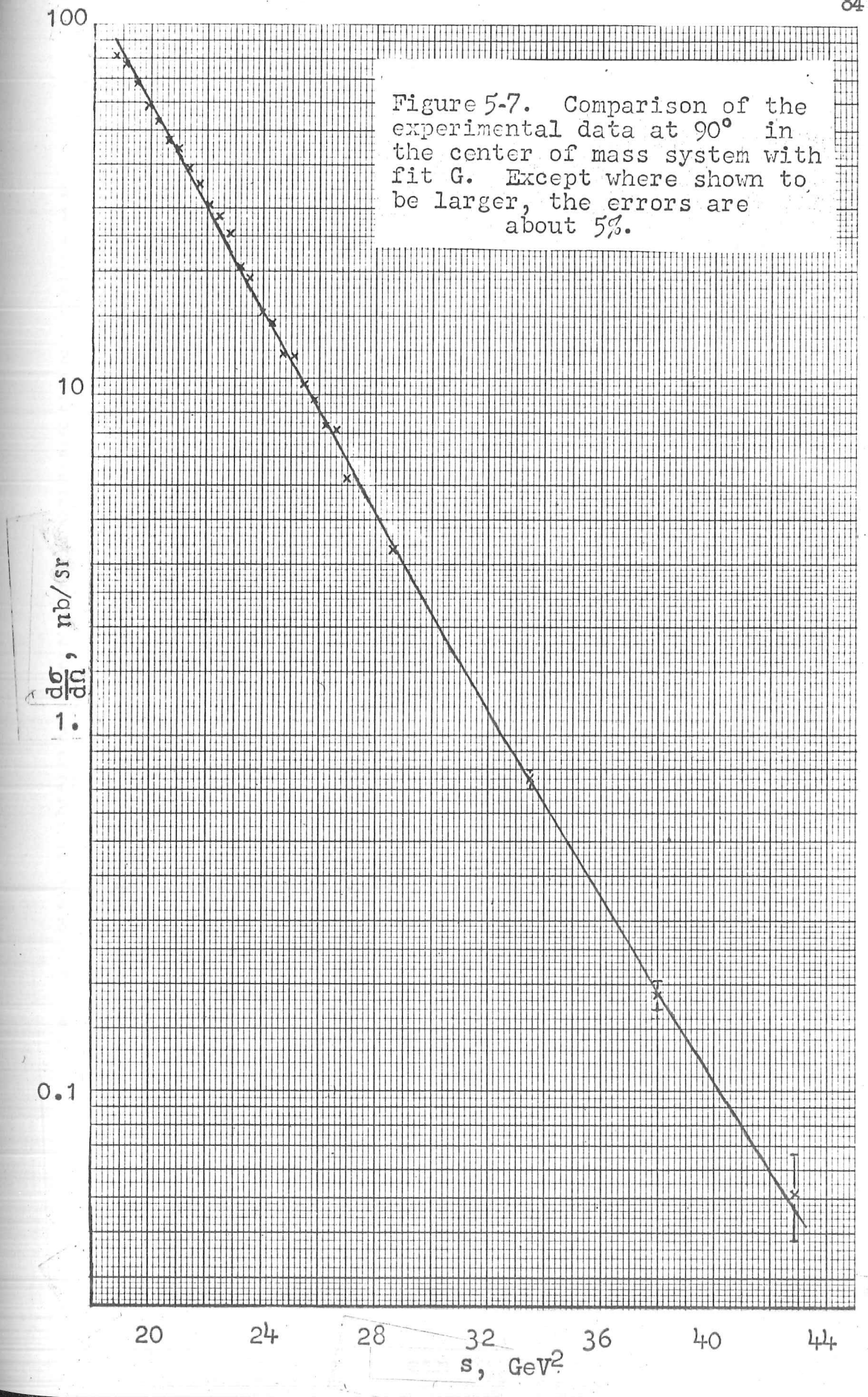

Figure 5-7. Comparison of the experimental data at 90° in the center of mass system with fit G. Except where shown to be larger, the errors are about 5%.

S	T	EXPTL VAL	ERR	FIT	CHISQUARE	FU/FT
18.735	7.608	80.900	3.721	92.217	9.248	1.000
19.109	7.795	78.000	3.354	80.908	.752	1.000
19.482	7.981	67.600	3.583	71.035	.919	1.000
19.855	8.168	58.900	2.886	62.407	1.476	1.000
20.229	8.355	53.600	2.519	54.861	.251	1.000
20.602	8.542	46.800	2.293	48.257	.404	1.000
20.976	8.728	44.100	2.117	42.473	.591	1.000
21.350	8.915	38.600	1.814	37.403	.435	1.000
21.723	9.102	35.600	1.709	32.956	2.394	1.000
22.097	9.289	30.300	1.485	29.053	.705	1.000
22.471	7.506	29.600	.700	28.924	.933	.537
22.471	9.476	28.400	1.562	25.626	3.154	1.000
22.471	8.815	26.900	.900	25.976	1.053	.811
22.845	9.663	25.500	1.377	22.614	4.392	1.000
23.219	9.850	20.200	1.091	19.966	.046	1.000
23.593	10.037	19.000	.988	17.636	1.906	1.000
23.967	10.224	15.300	.826	15.585	.119	1.000
24.341	10.411	14.300	.772	13.778	.456	1.000
24.715	10.598	11.800	.625	12.186	.382	1.000
25.089	10.785	11.600	.626	10.783	1.701	1.000
25.463	10.972	9.530	.600	9.545	.001	1.000
25.837	11.159	8.670	.494	8.452	.194	1.000
26.211	11.346	7.390	.436	7.488	.050	1.000
26.586	11.533	7.220	.513	6.635	1.301	1.000
26.960	11.720	5.250	.299	5.882	4.465	1.000
28.644	9.737	4.360	.140	4.366	.002	.397
28.644	12.563	3.310	.090	3.435	1.933	1.000
33.513	11.623	1.030	.030	1.049	.411	.326
33.513	12.393	.920	.040	.916	.009	.420
33.513	12.910	.860	.030	.853	.055	.499
33.513	13.690	.810	.040	.789	.271	.647
33.513	14.997	.750	.050	.751	.000	1.000
35.574	14.909	.365	.082	.414	.359	.687
38.010	17.245	.188	.017	.191	.032	1.000
41.758	18.119	.0610	.0090	.0641	.119	.712
42.882	19.682	.0521	.0140	.0452	.233	1.000
59.755	28.118	.0011	.0010	.0003	.842	1.000

Table 5H Detailed results for fit H.

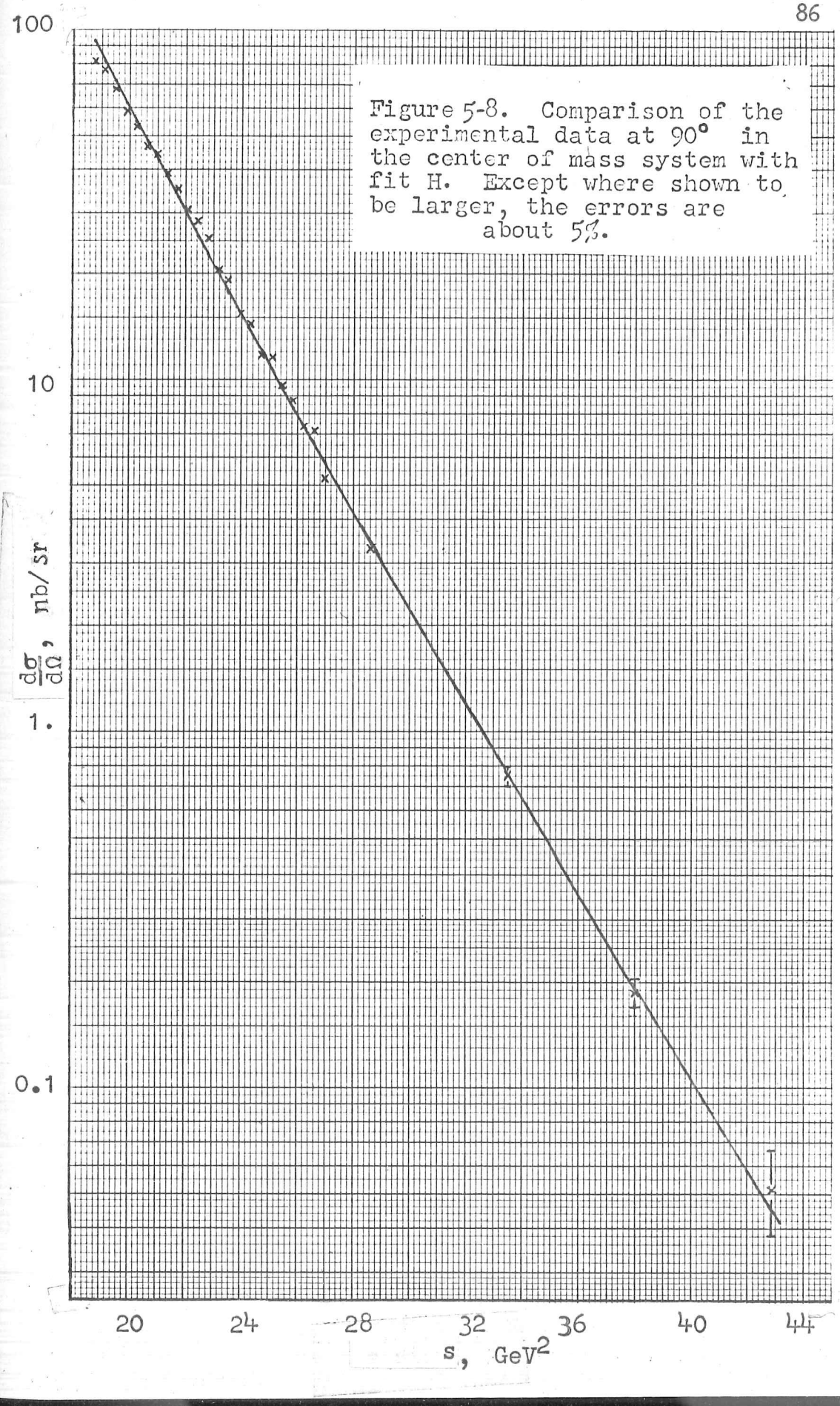

Figure 5-8. Comparison of the experimental data at 90° in the center of mass system with fit H. Except where shown to be larger, the errors are about 5%.

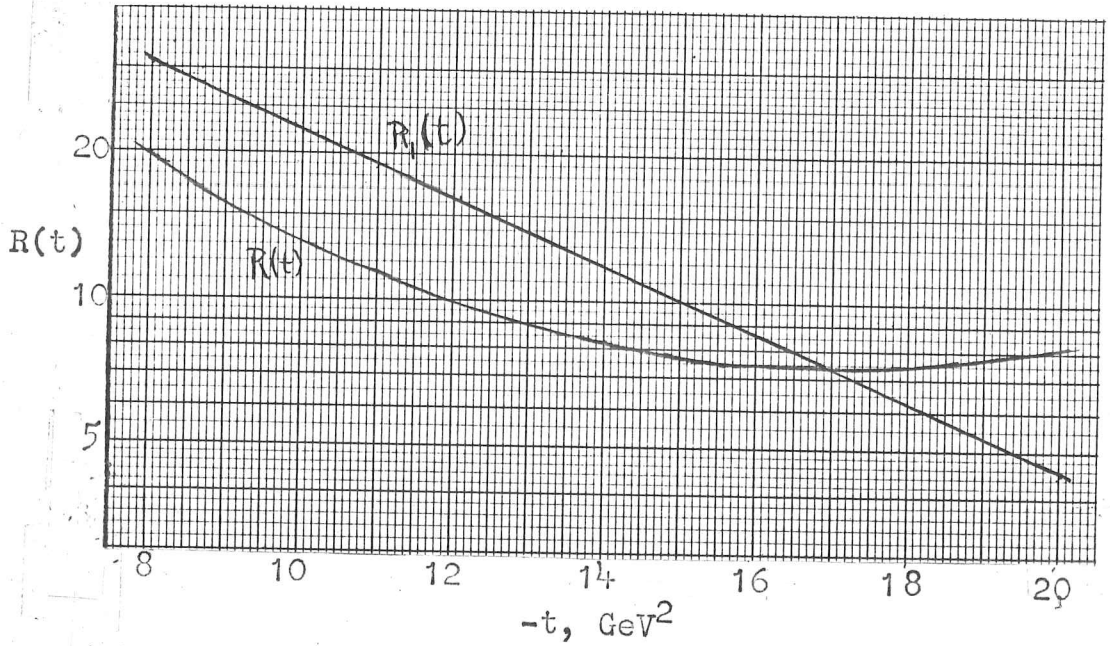

(a) $R(t) = \exp(5.50 + 0.410t + 0.0120t^2)$ and
$R_1(t) = \exp(4.70 + 0.160t)$.

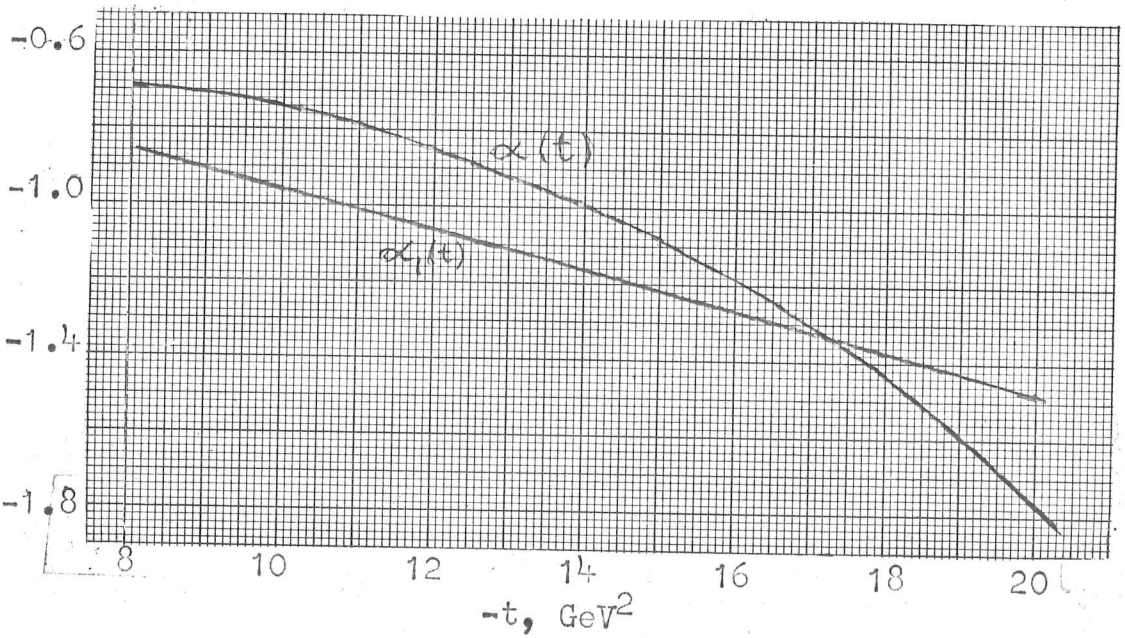

(b) $\alpha(t) = -0.911 - 0.0762t - 0.00591t^2$ and
$\alpha_1(t) = -0.451 + 0.0512t$.

Figure 5-9 Residue (a) and trajectory (b) functions for fits G and H.

S	T	EXPTL VAL	ERR	FIT	CHISQUARE	FO/FT
11.267	3.590	9243.2	616.5	8626.9	1.016	.453
11.304	3.648	9160.4	568.4	8682.4	.731	.517
11.267	3.640	9063.3	431.6	8857.2	.220	.527
11.304	3.892	8910.0	240.8	9022.4	4.311	1.000
11.483	3.965	7900.0	237.0	8063.6	.476	1.000
11.673	4.077	7080.8	219.8	7149.0	.072	1.000
11.857	4.169	6490.0	233.6	6303.4	.635	1.000
12.042	4.262	5530.0	171.4	5536.6	.001	1.000
12.227	4.354	4960.0	166.6	4650.1	.090	1.000
12.412	4.446	4470.0	138.6	4241.1	2.730	1.000
12.597	4.539	3720.0	122.8	3704.1	.017	1.000
12.782	4.632	3379.8	111.2	3232.8	1.523	1.000
12.967	4.724	2740.0	95.9	2820.6	.706	1.000
13.153	4.817	2440.0	75.6	2460.9	.076	1.000
13.301	4.440	2413.1	155.7	2363.6	.101	.476
13.283	4.666	2330.9	155.4	2275.1	.129	.695
13.338	4.910	2190.0	81.0	2147.6	.274	1.000
13.524	5.002	1630.0	67.7	1875.1	.443	1.000
13.895	5.188	1500.0	55.5	1432.4	1.482	1.000
14.266	5.374	1070.0	50.3	1098.4	.320	1.000
14.630	5.559	796.0	36.6	846.3	1.690	1.000
15.121	5.039	721.1	38.6	734.3	.117	.391
15.909	5.745	645.0	26.4	655.7	.164	1.000
15.150	5.670	583.5	64.8	597.4	.046	.634
15.381	5.931	515.0	20.6	511.2	.034	1.000
15.754	6.117	386.0	18.5	401.2	.675	1.000
16.126	6.303	305.8	16.5	317.2	.550	1.000
16.498	6.490	253.0	11.4	252.7	.001	1.000
16.671	6.676	217.0	9.8	203.0	2.058	1.000

Table 5J Detailed results for fit J.

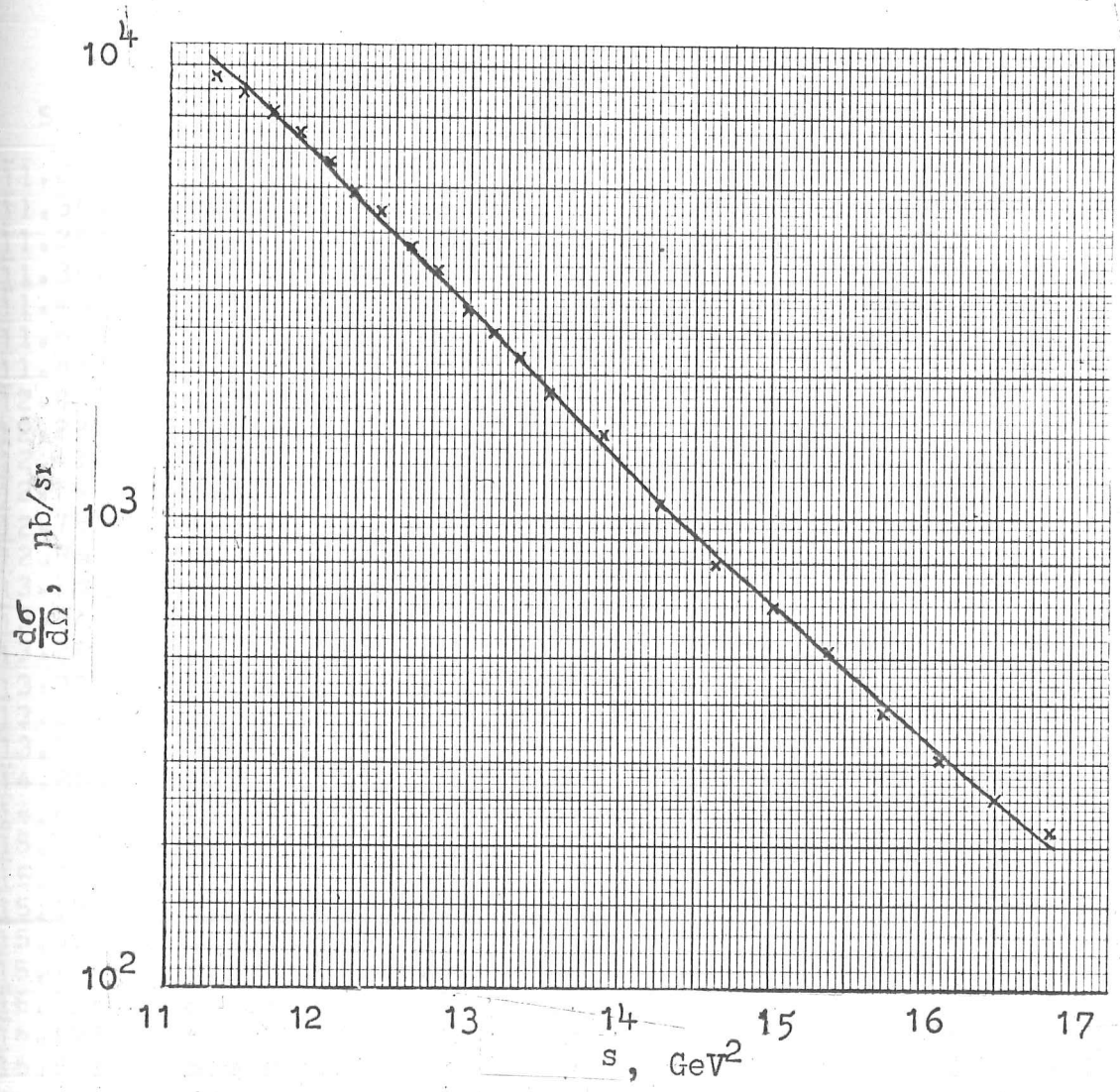

Fig. 5-10. Comparison of the experimental data at 90^o in the center of mass system with fit J. The errors of the data points are approximately 5%.

S	T	EXPTL VAL	ERR	FIT	CHISQUARE	FU/FT
11.267	3.590	9248.2	616.5	9615.8	.355	.737
11.304	3.648	9168.4	568.4	9306.6	.059	.769
11.267	3.640	9063.3	431.6	9544.8	1.245	.778
11.304	3.892	8510.0	246.8	9148.5	6.694	1.000
11.488	3.985	7900.0	237.0	8006.9	.204	1.000
11.673	4.077	7090.0	219.8	7010.3	.131	1.000
11.857	4.169	6490.0	233.6	6140.0	2.244	1.000
12.042	4.262	5530.0	171.4	5379.6	.770	1.000
12.227	4.354	4900.0	166.6	4715.0	1.234	1.000
12.412	4.446	4470.0	138.6	4133.8	5.886	1.000
12.597	4.539	3720.0	122.8	3625.5	.593	1.000
12.782	4.632	3370.0	111.2	3180.7	2.898	1.000
12.967	4.724	2740.0	95.9	2791.3	.287	1.000
13.153	4.817	2440.0	75.6	2450.4	.019	1.000
13.301	4.440	2413.1	155.7	2340.3	.219	.616
13.283	4.660	2330.9	155.4	2269.0	.158	.788
13.338	4.910	2190.0	81.0	2151.7	.223	1.000
13.524	5.002	1830.0	67.7	1890.0	.786	1.000
13.895	5.188	1500.0	55.5	1459.5	.532	1.000
14.266	5.374	1070.0	50.3	1128.3	1.344	1.000
14.638	5.559	796.0	36.6	873.2	4.442	1.000
15.121	5.039	721.1	38.8	737.4	.178	.441
15.009	5.745	645.0	26.4	676.4	1.412	1.000
15.158	5.670	583.5	64.8	614.9	.234	.852
15.381	5.931	515.0	20.6	524.5	.214	1.000
15.754	6.117	386.0	18.5	407.1	1.298	1.000
16.126	6.303	305.0	16.5	316.3	.468	1.000
16.498	6.490	253.0	11.4	245.9	.388	1.000
16.871	6.676	217.0	9.8	191.4	6.891	1.000

Table 5K Detailed results for fit K.

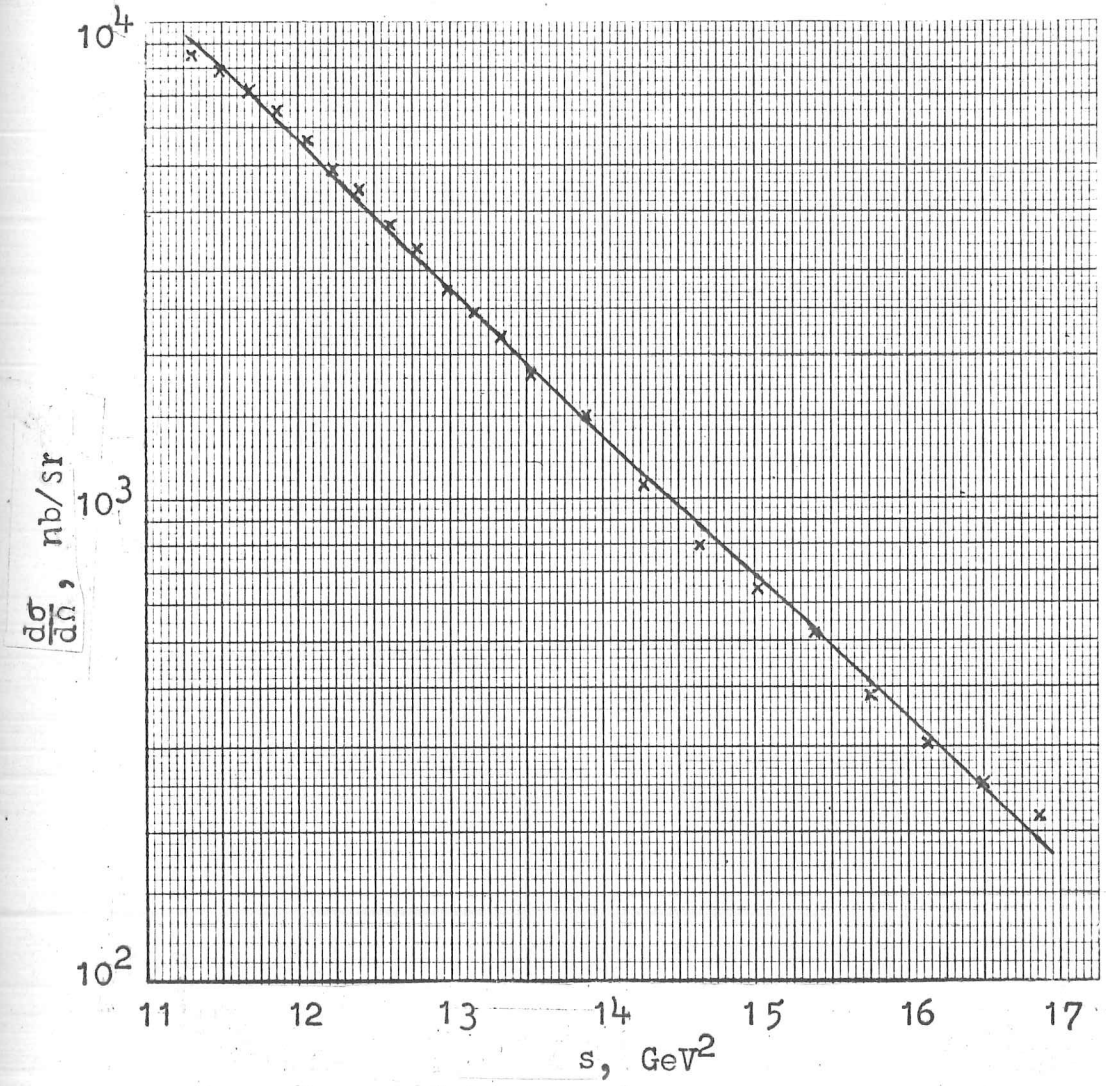

Fig. 5-11. Comparison of the experimental data at 90° in the center of mass system with fit K. The errors of the data points are approximately 5 %.

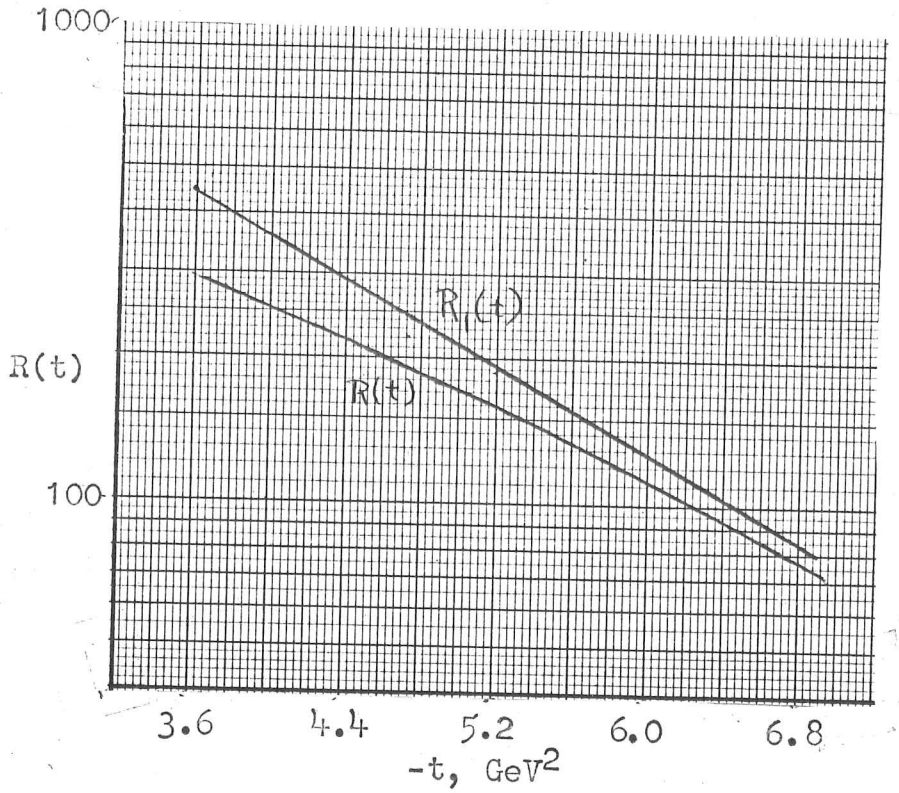

(a) $R(t) = \exp(6.83 + 0.266t - 0.0146t^2)$ and $R_1(t) = \exp(8.02 + 0.537t)$.

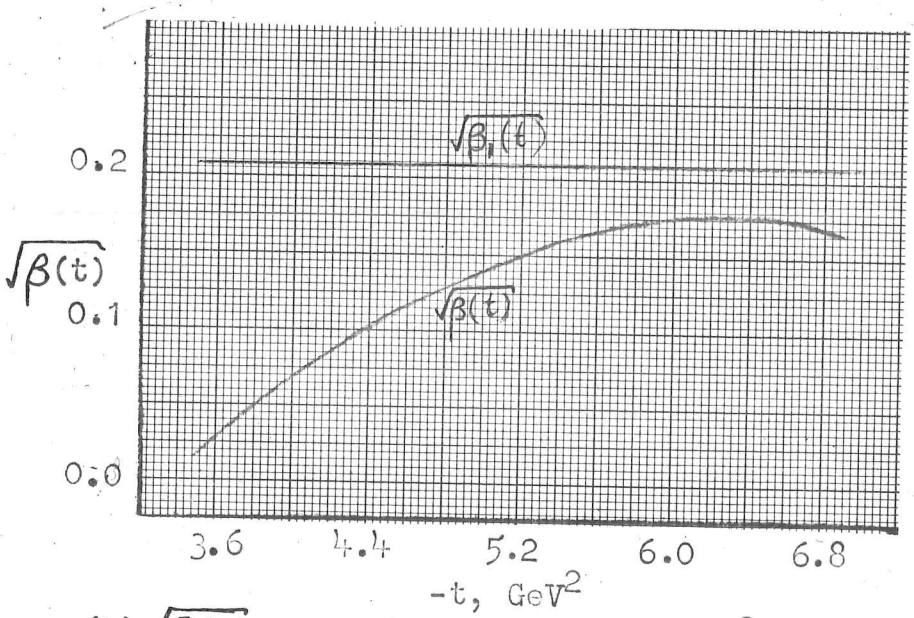

(b) $\sqrt{\beta(t)} = -0.614 + 0.245t - 0.0187t^2$ and $\sqrt{\beta_1(t)} = 0.209$.

Figure 5-12 Residue (a) and trajectory (b) functions for fits J and K.

S	T	EXPTL VAL	ERR	FIT	CHISQUARE	FU/FT
11.267	3.590	9248.2	616.5	9518.7	.192	.742
11.304	3.648	9168.4	568.4	9214.9	.007	.774
11.267	3.640	9063.3	431.6	9434.3	.739	.782
11.304	3.892	8510.0	246.8	9028.3	4.411	1.000
11.488	3.985	7900.0	237.0	7958.0	.060	1.000
11.673	4.077	7090.0	219.8	7009.5	.134	1.000
11.857	4.169	6490.0	233.6	6170.1	1.875	1.000
12.042	4.262	5530.0	171.4	5428.0	.354	1.000
12.227	4.354	4900.0	166.6	4772.6	.585	1.000
12.412	4.446	4470.0	138.6	4194.4	3.955	1.000
12.597	4.539	3720.0	122.8	3684.8	.082	1.000
12.782	4.632	3370.0	111.2	3236.0	1.451	1.000
12.967	4.724	2740.0	95.9	2841.1	1.112	1.000
13.153	4.817	2440.0	75.6	2493.9	.507	1.000
13.301	4.440	2413.1	155.7	2370.3	.076	.657
13.283	4.660	2330.9	155.4	2306.0	.026	.813
13.338	4.910	2190.0	81.0	2188.7	.000	1.000
13.524	5.002	1830.0	67.7	1920.8	1.798	1.000
13.895	5.188	1500.0	55.5	1479.3	.140	1.000
14.266	5.374	1070.0	50.3	1139.7	1.919	1.000
14.638	5.559	796.0	36.6	878.8	5.117	1.000
15.121	5.039	721.1	38.8	706.5	.140	.533
15.009	5.745	645.0	26.4	678.6	1.616	1.000
15.158	5.670	583.5	64.8	615.0	.236	.884
15.381	5.931	515.0	20.6	525.0	.235	1.000
15.754	6.117	386.0	18.5	407.1	1.296	1.000
16.126	6.303	305.0	16.5	316.6	.493	1.000
16.498	6.490	253.0	11.4	247.0	.281	1.000
16.871	6.676	217.0	9.8	193.4	5.847	1.000

Table 5L Detailed results for fit L.

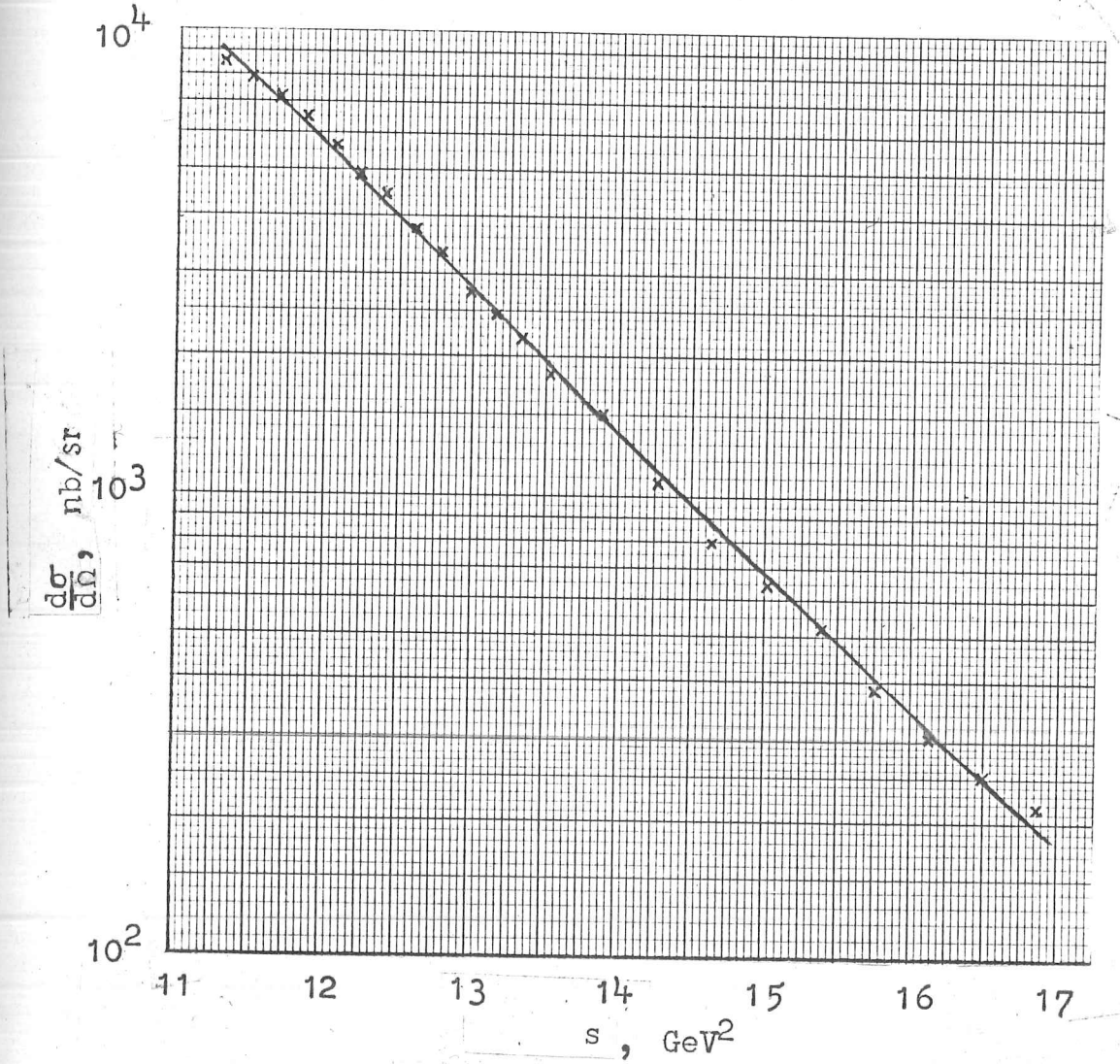

Fig. 5-13. Comparison of the experimental data at 90^o in the center of mass system with fit L. The errors of the data points are approximately 5 %.

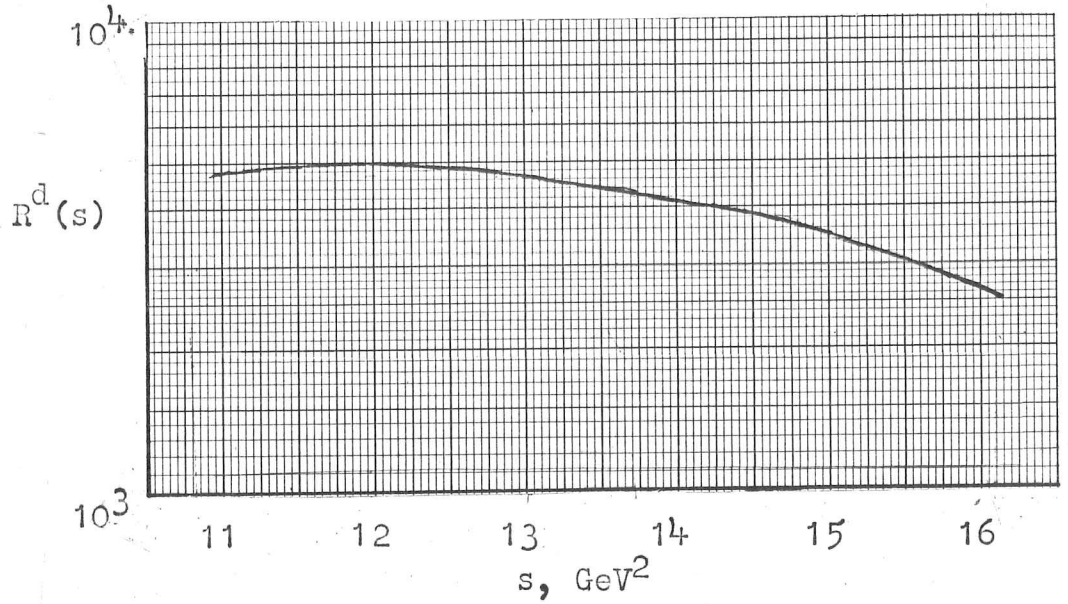

(a) $R^d(s) = \exp(3.85 - 0.790s - 0.0337s^2)$.

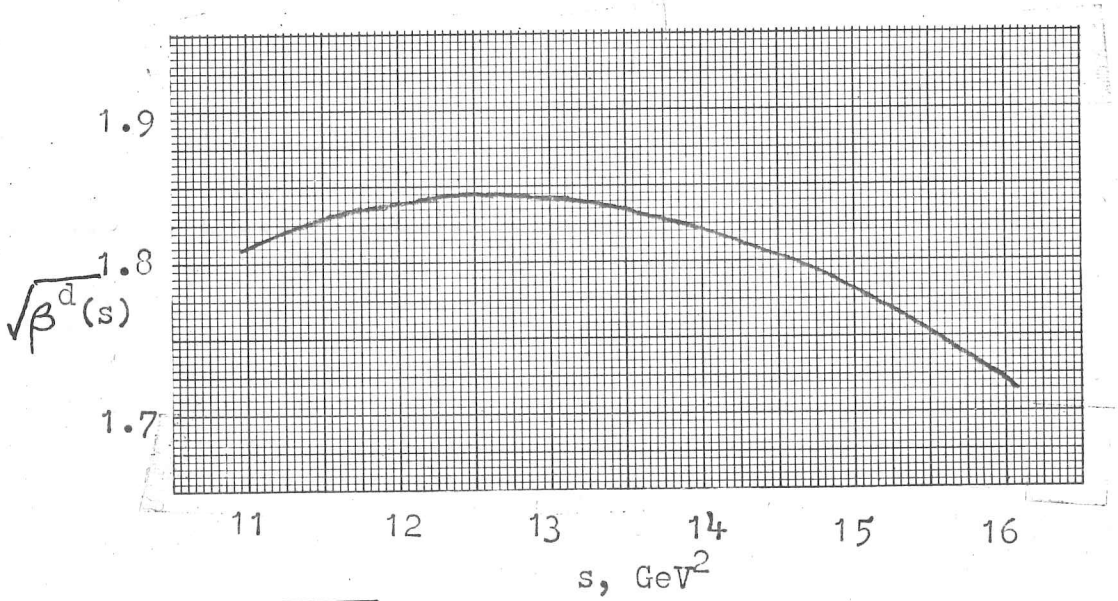

(b) $\sqrt{\beta^d(s)} = 0.0593 + 0.280s - 0.0110s^2$.

Figure 5-14 Residue (a) and trajectory (b) functions for fit L.

S	T	EXPTL VAL	ERR	FIT	CHISQUARE	FU/FT
11.267	3.590	9248.2	616.5	9466.2	.125	.729
11.304	3.648	9168.4	568.4	9199.5	.003	.761
11.267	3.640	9063.3	431.6	9419.2	.680	.771
11.304	3.892	8510.0	246.8	9092.0	5.562	1.000
11.488	3.985	7900.0	237.0	8027.0	.287	1.000
11.673	4.077	7090.0	219.8	7076.9	.004	1.000
11.857	4.169	6490.0	233.6	6230.9	1.230	1.000
12.042	4.262	5530.0	171.4	5479.0	.088	1.000
12.227	4.354	4900.0	166.6	4812.1	.278	1.000
12.412	4.446	4470.0	138.6	4221.5	3.215	1.000
12.597	4.539	3720.0	122.8	3699.6	.028	1.000
12.782	4.632	3370.0	111.2	3239.1	1.386	1.000
12.967	4.724	2740.0	95.9	2833.4	.949	1.000
13.153	4.817	2440.0	75.6	2476.7	.236	1.000
13.301	4.440	2413.1	155.7	2387.6	.027	.563
13.283	4.660	2330.9	155.4	2293.0	.059	.753
13.338	4.910	2190.0	81.0	2163.6	.106	1.000
13.524	5.002	1830.0	67.7	1889.2	.764	1.000
13.895	5.188	1500.0	55.5	1439.1	1.203	1.000
14.266	5.374	1070.0	50.3	1096.5	.278	1.000
14.638	5.559	796.0	36.6	837.1	1.262	1.000
15.121	5.039	721.1	38.8	781.2	2.409	.406
15.009	5.745	645.0	26.4	642.0	.013	1.000
15.158	5.670	583.5	64.8	584.9	.000	.830
15.381	5.931	515.0	20.6	496.0	.847	1.000
15.754	6.117	386.0	18.5	387.8	.010	1.000
16.126	6.303	305.0	16.5	308.6	.049	1.000
16.498	6.490	253.0	11.4	252.1	.006	1.000
16.871	6.676	217.0	9.8	214.1	.087	1.000

Table 5M Detailed results for fit M.

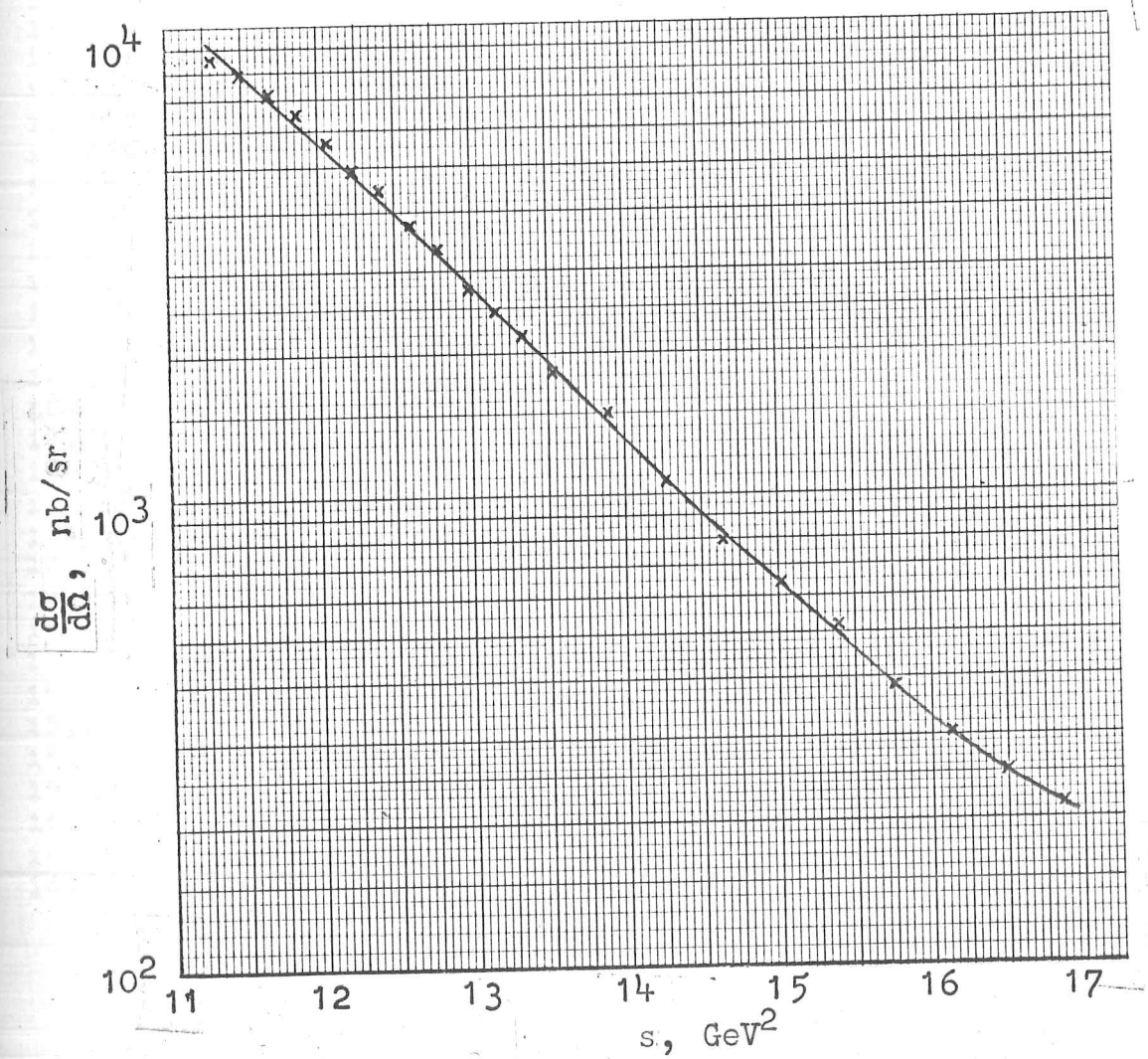

Fig. 5-15. Comparison of the experimental data at 90^o in the center of mass system with fit M. The errors of the data points are approximately 5%.

S	T	EXPTL VAL	ERR	FIT	CHISQUARE	FU/FT
11.267	3.590	9248.2	616.5	9560.4	.256	.760
11.304	3.648	9168.4	568.4	9262.5	.027	.789
11.267	3.640	9063.3	431.6	9499.8	1.023	.797
11.304	3.892	8510.0	246.8	9126.9	6.249	1.000
11.488	3.985	7900.0	237.0	7994.1	.158	1.000
11.673	4.077	7090.0	219.8	7003.9	.153	1.000
11.857	4.169	6490.0	233.6	6138.3	2.266	1.000
12.042	4.262	5530.0	171.4	5381.1	.754	1.000
12.227	4.354	4900.0	166.6	4718.7	1.185	1.000
12.412	4.446	4470.0	138.6	4138.9	5.709	1.000
12.597	4.539	3720.0	122.8	3631.3	.522	1.000
12.782	4.632	3370.0	111.2	3186.8	2.714	1.000
12.967	4.724	2740.0	95.9	2797.4	.358	1.000
13.153	4.817	2440.0	75.6	2456.1	.046	1.000
13.301	4.440	2413.1	155.7	2332.9	.265	.638
13.283	4.660	2330.9	155.4	2271.5	.146	.802
13.338	4.910	2190.0	81.0	2157.1	.165	1.000
13.524	5.002	1830.0	67.7	1894.8	.917	1.000
13.895	5.188	1500.0	55.5	1463.1	.442	1.000
14.266	5.374	1070.0	50.3	1130.8	1.460	1.000
14.638	5.559	796.0	36.6	874.6	4.612	1.000
15.121	5.039	721.1	38.8	729.6	.048	.463
15.009	5.745	645.0	26.4	677.1	1.471	1.000
15.158	5.670	583.5	64.8	615.0	.235	.860
15.381	5.931	515.0	20.6	524.6	.215	1.000
15.754	6.117	386.0	18.5	406.7	1.250	1.000
16.126	6.303	305.0	16.5	315.6	.413	1.000
16.498	6.490	253.0	11.4	245.0	.488	1.000
16.871	6.676	217.0	9.8	190.4	7.410	1.000

Table 5N Detailed results for fit N.

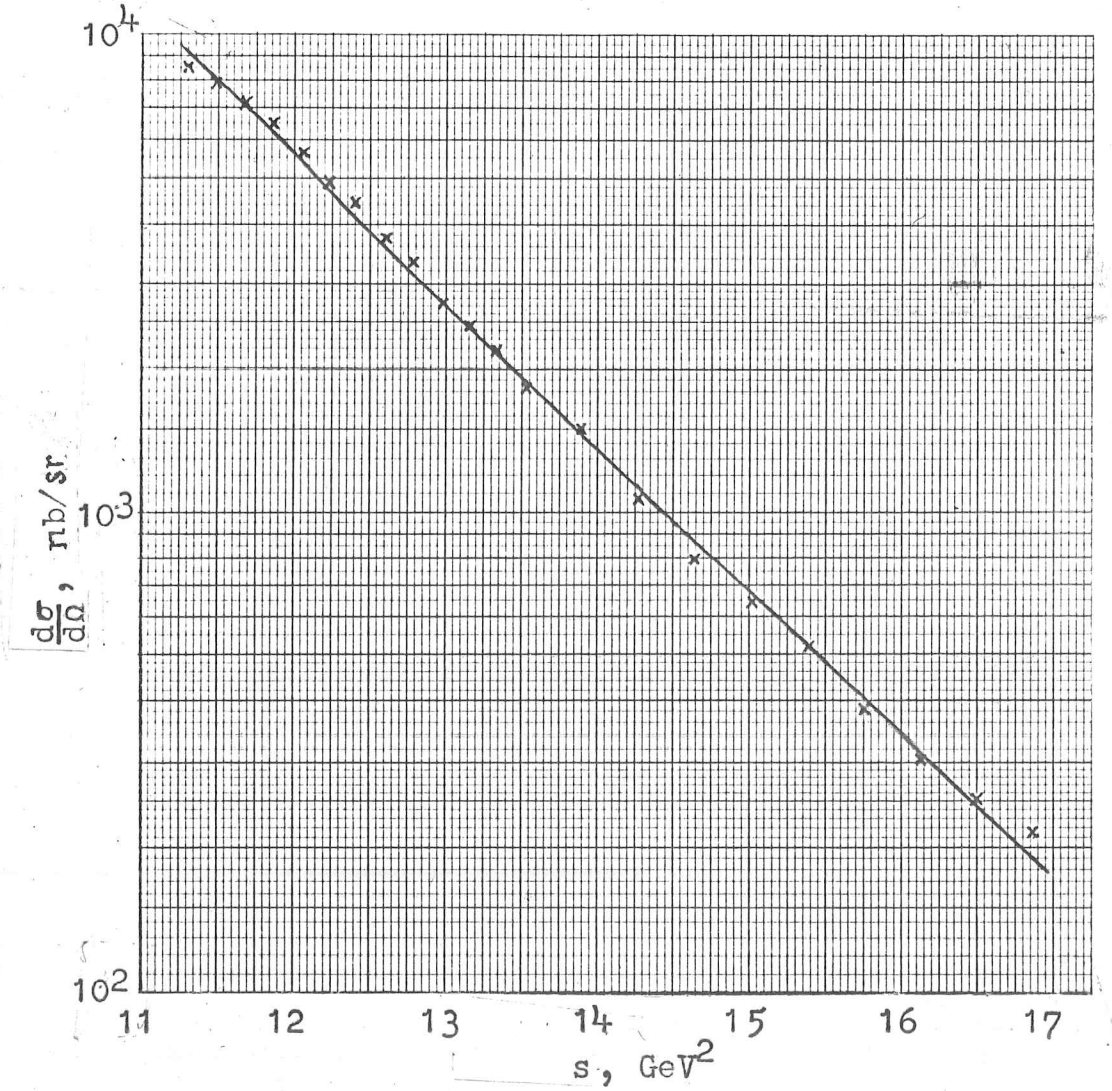

Fig. 5-16. Comparison of the experimental data at 90^o in the center of mass system with fit N. The errors of the data points are approximately 5%.

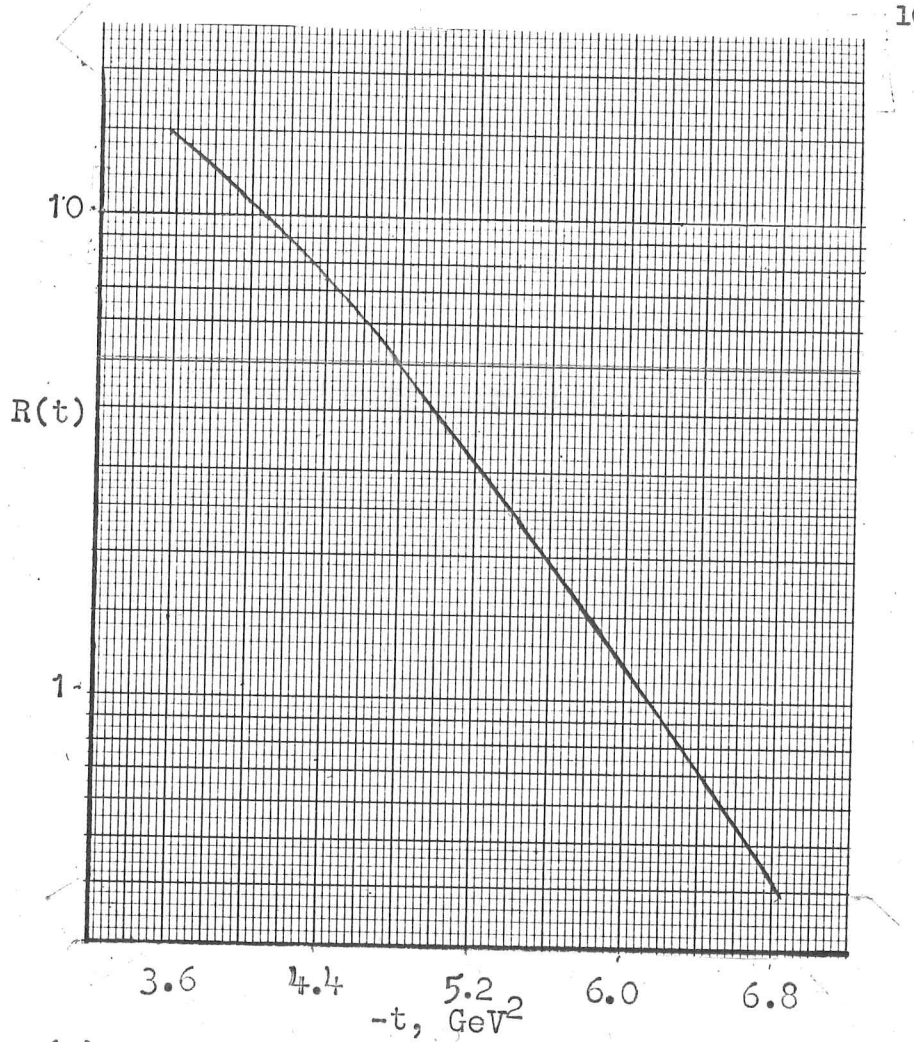

(a) $R(t) = \exp(4.67 + 0.231t - 0.0866t^2)$.

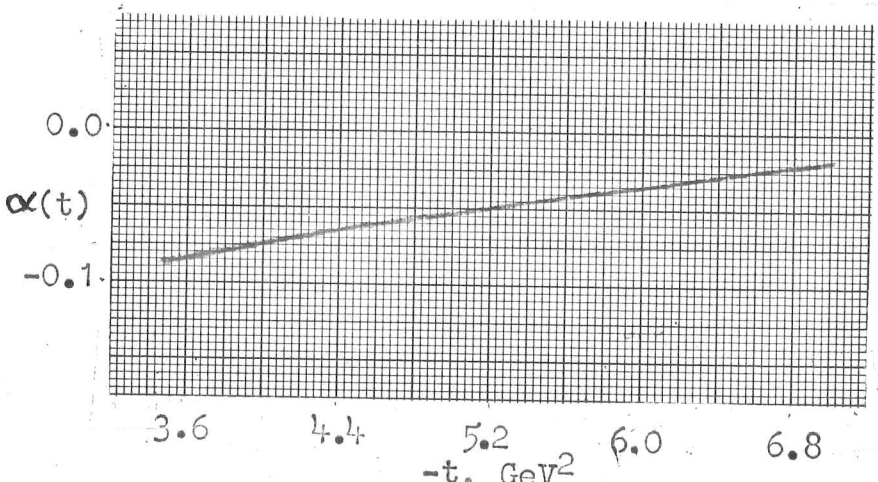

(b) $\alpha(t) = -0.183 - 0.0327t - 0.00116t^2$.

Figure 5-17 Residue (a) and trajectory (b) functions for fit M.

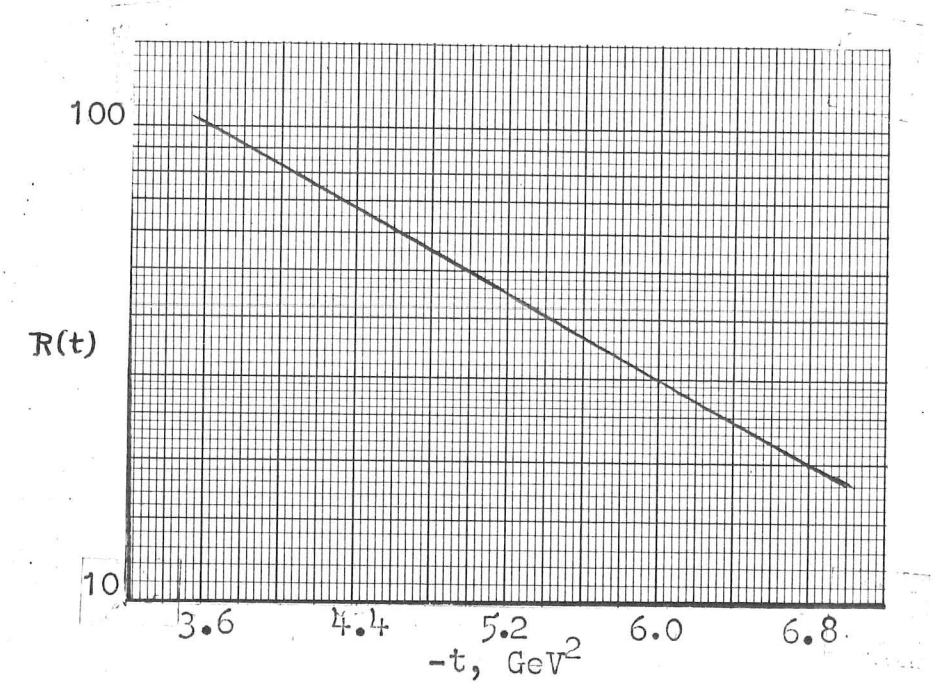

(a) $R_f(t) = \exp(6.62 + 0.589t + 0.00819t^2)$.

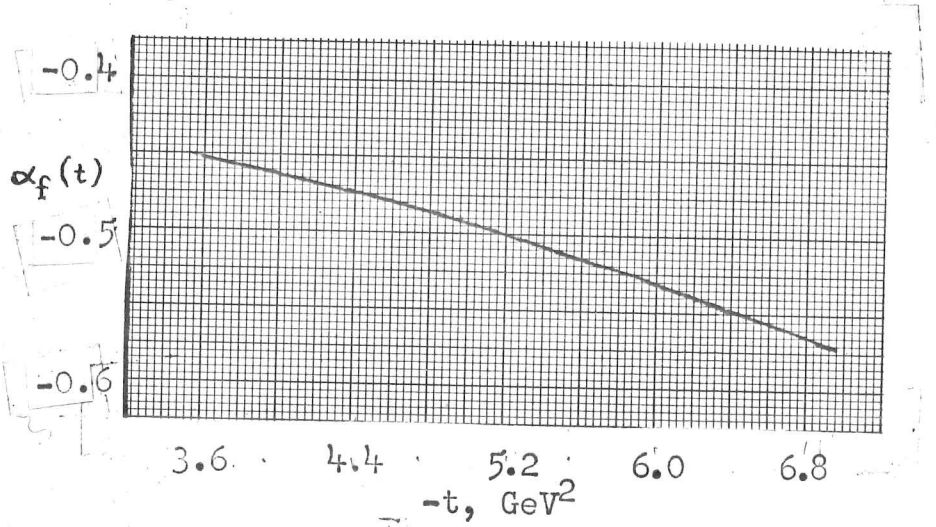

(b) $\alpha_f(t) = -0.407 - 0.0002t - 0.00341t^2$

Figure 5-18 Residue (a) and trajectory (b) functions for fit N.

References

1. G. Cocconi et al., Phys. Rev. 138, B165 (1965).

2. J. Orear, Phys. Letters 13, 190 (1964).

3. G. Fast and R. Hagedorn, Nuovo Cimento 27, 208 (1963); R. Hagedorn, Nuovo Cimento 35, 216 (1965).

4. T. Ericson, Ann. of Phys. 23, 390 (1963) and CERN report TH406 (1964).

5. J. V. Allaby et al., Phys. Letters 23, 389 (1966).

6. C. W. Akerlof et al., Phys. Rev. 159, 1138 (1967).

7. J. V. Allaby et al., Phys. Letters 25B, 156 (1967).

8. A. D. Krisch, Phys. Rev. Letters 19, 1149 (1967).

9. F. Cerulus and A. Martin, Phys. Letters 8, 80 (1964); T. Kinoshita, Phys. Rev. Letters 12, 256 (1964).

10. J. V. Allaby et al., report presented at the "Topical Conference on High Energy Collisions of Hadrons", CERN, January 15-18, 1968.

11. C. M. Ankenbrandt, Report UCRL-17257 (1966).

12. A. R. Clyde, Report UCRL-16275 (1966).

PART II

MULTIPLE SCATTERING IN THE QUARK MODEL

CHAPTER VI

Introduction and Apologia for the Quark Model

"Beyond thy telescope or spectroscope observer keen, beyond
all mathematics,
Beyond the doctor's surgery, anatomy, beyond the chemist
with his chemistry,
The entities of entities, eidolons."

Whitman[1]

One of the most frustrating facts in fundamental particle physics is that nature apparently does not permit the existence of the free quark. When Gell-Mann[2] and Zweig[3], prompted by the outstanding success of the eightfold way, suggested these elementary objects as a physical source of the observed symmetries, the way seemed open to an understanding of the hadrons as a newer and deeper form of nuclear physics. The principal proviso on this conjecture was the necessity of observing the free quark, the "hydrogen nucleus" of the system, which would be distinguished by its fractional electric charge. Such particles were not known to exist at that time, nor have they been discovered since. The

emphasis of research activity therefore turned quite quickly, and with justification, to a more recondite mathematical viewpoint which regarded quarks as a group theoretic abstraction rather than a physical entity. In other words, physical quarks became mathematical quirks. Although the fruit borne by the intensive study of group theory has hardly been sufficient to fulfill its original promise, this basic attitude is still commonly held.

The first indication of a return to a more literal physical picture of the quark model came in papers published independently by Levin and Frankfurt[4] and by Lipkin and Scheck[5]. The principal observations of these papers can be encapsulated in the statement that if mesons consist of two quarks while baryons consist of three, then the ratio of mesonic to baryonic cross sections at asymptotic energies should logically be 2/3. This startlingly simple conjecture, which is certainly not incompatible with the experimental situation, has prompted the development in some detail of what is now most usually called simply "the quark model". Its pragmatic philosophy has been aptly described by Lipkin[6] as a " 'broom and rug' model in which one uses a broom to sweep all aspects of the problem which one does not understand under a rug." One then hopes to be able to calculate physically meaningful quantities from only the ideas which remain visible above the rug. Among these are a vague picture of quarks with some undefined physical presence and various postulates for explaining their behaviour. Two principal areas of enquiry have developed, dealing respectively with low-energy and high-energy quark

phenomena.

The former area of these two concerns itself with questions of how quarks are bound to form hadrons and how static gross properties of the hadrons can be related in terms of quark structure. The question of "free quarks" is essentially swept under the rug, but it can be rationalized by the observation that the existence of particles having no free states (for example, particles obeying parastatistics laws) is certainly conceivable. Some success has been achieved in the derivation of mass splitting rules, electromagnetic decay widths, etc., although, as Lipkin points out, most of these are obtainable from other assumptions and therefore are not definitive evidence for the quark model. Dalitz's[7] classification of pion-nucleon resonances on the basis of a quark shell model of hadron structure cannot be duplicated by any other hypothesis, however, and is impressively successful. In particular the resonant behaviour observed in the most recent phase shift analysis by Lovelace[8] and his collaborators is quite well described.

The second area of investigation, and the one with which the second half of this thesis will be concerned, is the quark model of high energy scattering. Its fundamental tenet is the assumption commonly called the additivity principle, stating that the scattering amplitude resulting from the collision of an n-component composite particle with an arbitrary target is the sum of amplitudes corresponding to each of the n constituent particles. By way of introduction we shall give some examples of the results which can be obtained from

additivity. The literature which has developed in this field is voluminous, however, and a comprehensive review of it will not be attempted.

Following the recipe provided by additivity, we can write down immediately the amplitudes for elastic scattering of nucleons, antinucleons, and mesons by nucleons. With capital letters denoting particles and small letters denoting quarks, these are

$$F_{PP} = 10\,F_{pp} + 8\,F_{pn} \tag{6.1a}$$

$$F_{PN} = 8\,F_{pp} + 10\,F_{pn} \tag{6.1b}$$

$$F_{\bar{P}P} = 10\,F_{\bar{p}p} + 8\,F_{\bar{p}n} \tag{6.1c}$$

$$F_{\bar{P}N} = 8\,F_{\bar{p}p} + 10\,F_{\bar{p}n} \tag{6.1d}$$

$$F_{\pi^+P} = 4\,F_{pp} + 2\,F_{pn} + 2\,F_{\bar{p}p} + 4\,F_{\bar{p}n} \tag{6.2a}$$

$$F_{\pi^-P} = 2\,F_{pp} + 4\,F_{pn} + 4\,F_{\bar{p}p} + 2\,F_{\bar{p}n} \tag{6.2b}$$

$$F_{K^+P} = 4\,F_{pp} + 2\,F_{pn} + 6\,F_{\bar{\lambda}p} \tag{6.2c}$$

$$F_{K^+N} = 2\,F_{pp} + 4\,F_{pn} + 6\,F_{\bar{\lambda}p} \tag{6.2d}$$

$$F_{K^-P} = 6F_{\lambda p} + 4F_{\bar{p}p} + 2F_{\bar{p}n} \tag{6.2e}$$

$$F_{K^-N} = 6F_{\lambda p} + 2F_{\bar{p}p} + 4F_{\bar{p}n} \,. \tag{6.2f}$$

In writing these equations we have assumed isosymmetry for the quark-quark amplitudes, which in turn leads to isosymmetry for the particle amplitudes. Among these ten expressions it is possible to find four independent linear relations by eliminating the six quark terms. We write these in the form

$$F_{PP} - F_{PN} = F_{K^+P} - F_{K^+N} \tag{6.3a}$$

$$F_{\bar{P}P} - F_{\bar{P}N} = F_{K^-P} - F_{K^-N} \tag{6.3b}$$

$$F_{PP} + F_{\bar{P}N} = 2F_{\pi^+P} + F_{\pi^-P} \tag{6.3c}$$

$$F_{\bar{P}P} + F_{PN} = 2F_{\pi^-P} + F_{\pi^+P} \,. \tag{6.3d}$$

Equation (6.3a) relates the differences of roughly equal quantitites, so that both sides are near zero, and therefore agreement with experiment is quite satisfactory (Figure 6-1). The same is roughly true of (6.3b), although it should be noted that the two sides of the equation seem experimentally to be of opposite signs. Equations (6.3c) and (6.3d) clearly correspond in the asymptotic (Pomeranchuk) limit to the 2/3 ratio mentioned above. A formidable problem arises,

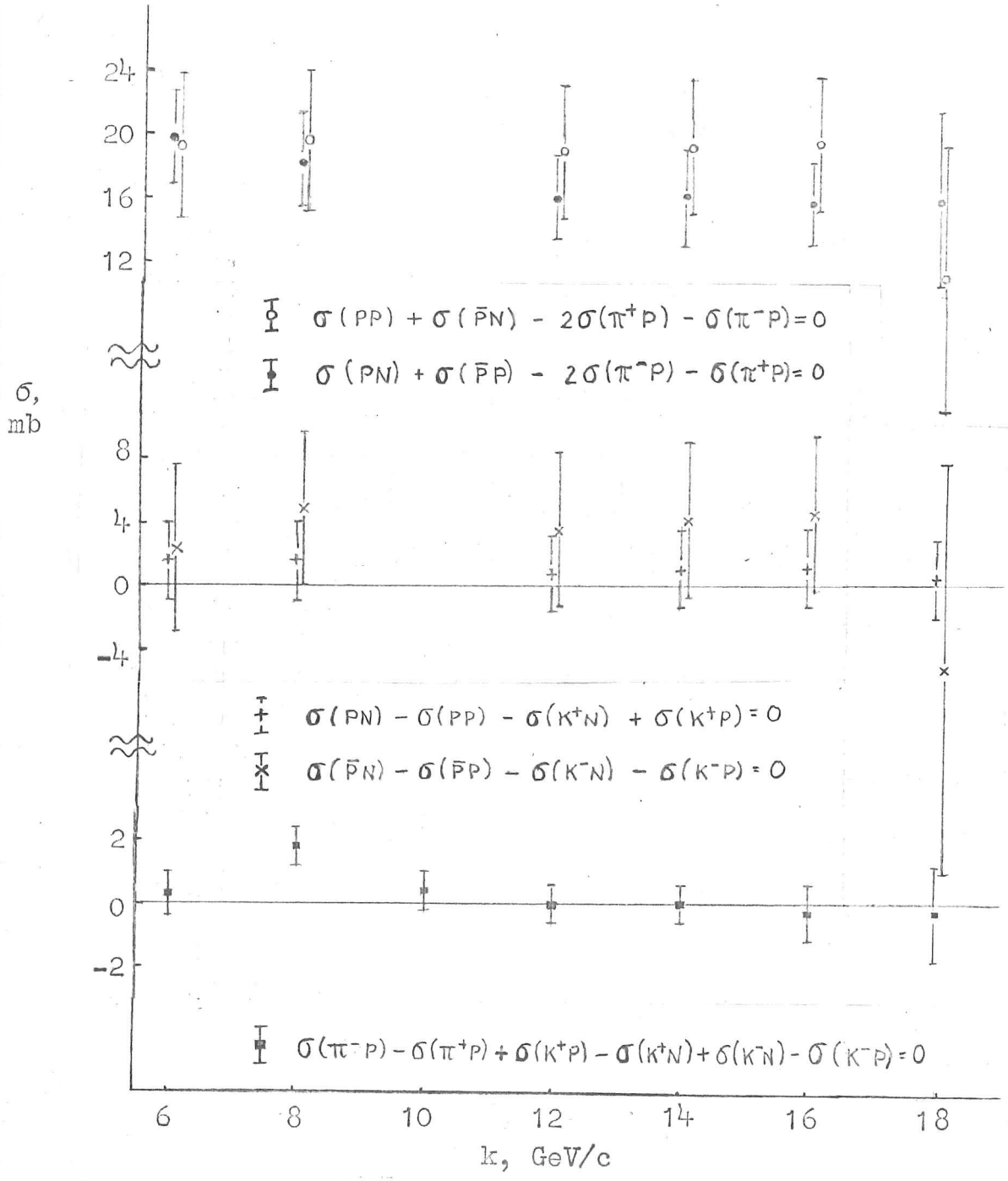

Figure 6-1 Comparison with experiment of relations predicted by the additive quark model, using the data of reference 25.

however, in attempting to compare these results with experiment at finite energies. If the same energy is used for the meson-nucleon amplitudes as for the baryon-nucleon ones, the data contradict both of these equations quite badly, as can be seen in Figure 6-1. But should the amplitudes be taken at the same energy, or should some allowance be made for the difference between meson and baryon? This question is clearly important for these equations; it is even more vital if the quantities being compared involve inelastic amplitudes, which vanish rapidly with energy.

Kokkedee and Van Hove[9] have suggested that the quarks should share equally in the kinetic energy of the hadron. The comparison should then be made at equal quark energies, which means that the meson laboratory momentum should be 2/3 of that of the baryon. This procedure does improve the situation noted above, but it has the side effect that it destroys the 2/3 ratio of total cross sections. This failing, which has been generally overlooked, results from the fact that the quark amplitudes must be taken proportional to the quark energy. If we write asymptotically

$$F_{NN} \approx F_{\bar{N}N} \approx i\,\sigma_N\,\frac{k}{4\pi}$$

$$F_{\pi N} \approx i\,\sigma_\pi\,\frac{k}{4\pi}$$

$$F_{qq} \approx F_{\bar{q}q} \approx i\,\sigma_q\,\frac{k_q}{4\pi}$$

where k is the laboratory frame momentum and k_q the corresponding quark momentum, and use the prescription $k_q = \frac{k}{3}$ $(\frac{k}{2})$ for baryons (mesons), then it follows from the relations (6.1) and (6.2) that

$$\sigma_N = \sigma_\pi = 6\,\sigma_q \,. \tag{6.4}$$

This technique therefore leads to asymptotic equality of mesonic and baryonic cross sections. Other conjectures have been put forward to explain the failure of (6.3c) and (6.3d), involving, for example, the use of three-quark interactions in (6.1) and (6.2)[10], or of only the non-annihilative parts of the nucleon-antinucleon amplitudes[11]. None of these explanations is entirely satisfactory, however, and it does not seem possible at present to resolve the problem unambiguously. We shall not pursue it any farther; the remaining chapters of this thesis will deal almost exclusively with meson-nucleon reactions, and none of the calculations we attempt will require us to compare unlike types of amplitudes.

In fact the six equations (6.2) are degenerate, and consequently there exists a relation which involves only the meson-nucleon interactions. It is the antisymmetric sum rule of Barger and Rubin[12],

$$F_{\pi^+P} - F_{\pi^-P} + F_{K^+N} - F_{K^+P} + F_{K^-P} - F_{K^-N} = 0 \,,$$

sometimes called the weak Johnson-Treiman relation. Figure 6-1 shows that it is in excellent agreement with the experimental data. This result is simultaneously the most fundamental and the most satisfactory of those obtained in the quark model, since in reality

it requires additivity and quark structure for only the mesons. As such, it will be of particular interest to us in the next chapter, where multiple scattering corrections to it will be derived.

For the moment, however, we shall use it in another sense, namely, the consideration of charge exchange reactions. Because of isosymmetry the relation (6.5) is equivalent to

$$\sqrt{2}\, F_{\pi^- P \to \pi^0 N} = F_{K^+ N \to K^0 P} - F_{K^- P \to \bar{K}^0 N} \tag{6.6}$$

which follows also from using the quark isosymmetry relations

$$f_{\bar{p}p \to \bar{n}n} = f_{\bar{p}n} - f_{\bar{p}p} \tag{6.7a}$$

$$f_{pn \to np} = f_{pp} - f_{pn} \,. \tag{6.7b}$$

If we consider similarly the quark structure of the isosinglet η^0 meson, we find trivially that

$$\sqrt{6}\, F_{\pi^- P \to \eta^0 N} = F_{K^+ N \to K^0 P} + F_{K^- P \to \bar{K}^0 N} \,. \tag{6.8}$$

This relation has also been obtained from Regge theory with SU(3) symmetric vertices[13]. A convenient test of (6.6) and (6.8) is made possible by noting that to a good approximation $F_{K^+N \to K^0P}$ is real while $F_{K^-P \to \bar{K}^0N}$ is imaginary; this fact is predicted by Regge theory and confirmed by experiment[14]. Assuming thus that

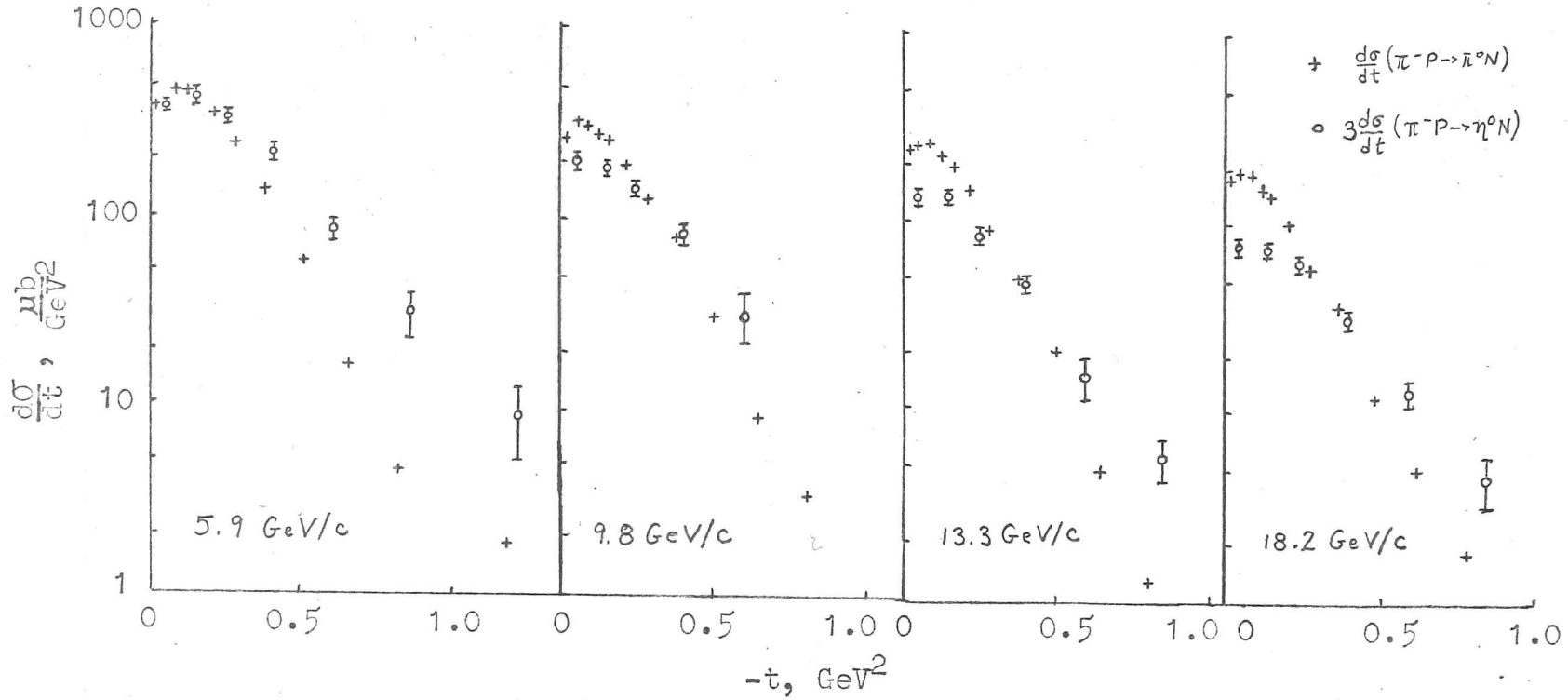

Figure 6-2 Comparison with experiment of equation (6.9). The data are taken from references 15 and 16.

these two amplitudes are out of phase, we conclude that

$$\frac{d\sigma}{dt}(\pi^- P \to \pi^0 N) = 3\frac{d\sigma}{dt}(\pi^- P \to \eta^0 N) \quad . \tag{6.9}$$

Although the agreement seems to be deteriorating at higher energies, this equation is moderately well satisfied by the experimental data, as we show in Figure 6-2.

The results we have given here are simple examples indicating the philosophy of the additive quark model. Much greater detail can be considered, and a host of authors have done so. We mention particularly the extension of these ideas to helicity amplitudes initiated by Itzykson and Jacob[17] and subsequently pursued by Friar and Trefil[18] and by Białas and collaborators[19]; and the application to production processes due to Satz[20]. The journals are rife with reports of relations obtained from additivity, which meet with more or less experimental corroboration.

Surely, however, it is most important here not to lose sight of the basic physical premise on which this work is founded. What does the additivity assumption mean? In the language of nuclear physics the answer is clear: it is essentially the impulse approximation. It neglects entirely the correlations between the quarks. Once we accept the actual presence of bound quarks, we can do much better than this crude approximation. The apparatus for considering scattering by a composite system was formulated in 1955 by Glauber[21], and is well known in nuclear theory. Our purpose in the remainder of this thesis is to investigate some of the applications of the

Glauber formalism to the quark model.

In the next chapter we shall give a derivation of this formalism; for the moment we merely catalogue its general features to indicate the principal characteristics of the expected results. The Glauber model permits us to derive the scattering amplitude for the composite particle, including the "multiple scattering" corrections resulting from correlation effects, in terms of the amplitudes for the corresponding free particles. The leading contribution is essentially the sum of these single-scattering amplitudes, reproducing thereby the crux of the additivity assumption. The correction terms involve integrations over products of single scattering amplitudes, and are therefore non-additive. In the relevant case of diffractive scattering, it turns out that the contribution of each order of multiple scattering is successively smaller in the forward direction, but less strongly peaked, than that of the preceding order. At sufficiently large momentum transfers, then, there will be interference between, for example, single and double scattering, resulting in the appearance of structure in the differential cross section. This characteristic behaviour is very well known in processes involving scattering off light nuclei such as deuterium or helium.

The first use of these techniques in the quark model was by Deloff[22], who fitted a simple model to the meson-nucleon diffraction peaks. The non-additivity of the multiple scattering terms was pointed out and explored by Franco[23], while Harrington and Pagnamenta[24]

have attempted to use them to explain structure in the hadron-nucleon differential cross sections. In general, however, the application of the Glauber formalism to the quark model has only just begun.

In the following three chapters, then, we propose to consider the high energy scattering of hadrons from the viewpoint of the quark model with multiple scattering. In Chapter VII we introduce the Glauber model by means of its usual derivation and make two simple, and relatively successful, applications which require no knowledge of the variations with energy of the amplitudes involved. Chapter VIII studies in a simplified model the effects of Regge behaviour on the multiple scattering terms and presents the results obtained by fitting such forms to the experimental data on total cross sections. The fact that multiple scattering terms mimic Regge cuts leads us in Chapter IX to consider a more comprehensive application of these ideas, in a formalism replete with all spin complications, to pion-nucleon interactions. We are able to fit a large amount of scattering data, including the charge exchange polarization, reasonably well with a multiple scattering quark model.

References

1. From "Eidolons", in Leaves of Grass, by Walt Whitman.

2. M. Gell-Mann, Phys. Letters 8, 214 (1964).

3. G. Zweig, CERN preprint 8419/Th 412 (1964).

4. E. M. Levin and L. L. Frankfurt, JETP Letters 2, 65 (1965).

5. H. J. Lipkin and F. Scheck, Phys. Rev. Letters 16, 71 (1966).

6. H. J. Lipkin, "Quarks, Symmetries and Groups", presented at the Fifth Coral Gables Conference on Symmetries at High Energies, January 1968.

7. R. H. Dalitz, "Excited Nucleons and the Baryonic Supermultiplets", presented at the Topical Conference on πN Scattering at Irvine, California, December 1967.

8. A. Donnachie, R. Kirsopp, and C. Lovelace, Phys. Letters 26B, 161 (1968); C. Lovelace, "Nucleon Resonances and Low Energy Scattering", presented at the Heidelberg Conference on Elementary Particles, September 1967.

9. J. J. J. Kokkedee and L. Van Hove, Nuovo Cimento 42A, 711 (1966).

10. R. J. Oakes, Nuovo Cimento 49A, 316 (1967).

11. J. J. J. Kokkedee and L. Van Hove, Nucl. Phys. B1, 169 (1967).

12. V. Barger and M. H. Rubin, Phys. Rev. 140, B1365 (1965).

13. R. J. N. Phillips and W. Rarita, Phys. Rev. 140, B200 (1965); Phys. Rev. Letters 15, 807 (1965).

14. See, among others, E. Leader, Rev. Mod. Phys. 38, 476 (1966), and reference 9.

15. A. V. Stirling et al., Phys. Rev. Letters 14, 763 (1965).

16. O. Guisan et al., Phys. Letters 18, 200 (1965).

17. C. Itzykson and M. Jacob, Nuovo Cimento 48A, 909 (1967).

18. J. L. Friar and J. Trefil, Nuovo Cimento 49A, 642 (1967).

19. A. Białas, review talk at the Topical Conference on High Energy Collisions on Hadrons, CERN, January 1968.

20. H. Satz, Phys. Letters 25B, 220 (1967) and Phys. Rev. Letters 19, 1453 (1967).

21. R. J. Glauber, Phys. Rev. 100, 242 (1955).

22. A. Deloff, Nucl. Phys. B2, 597 (1967).

23. V. Franco, Phys. Rev. Letters 18, 1159 (1967).

24. D. Harrington and A. Pagnamenta, Phys. Rev. Letters 18, 1147 (1967) and Rutgers University preprint.

25. W. Galbraith et al., Phys. Rev. 138, B913 (1965).

CHAPTER VII

The Quark Model in the Glauber Formalism

A simple derivation of the Glauber multiple scattering formalism can be based upon the eikonal model we have described in the beginning of Chapter II. Its most well-known application in high energy physics is probably in the analysis of hadron-deuteron interactions to obtain the hadron-neutron scattering cross-sections, and we shall present briefly the argument for this simplest case. We therefore consider the process pictured in Figure 7-1, in which an incident proton with momentum $\bar{k}$ scatters elastically from a deuteron composed of two nucleons.

INITIAL STATE FINAL STATE

Figure 7-1. Elastic proton-deuteron scattering.

For the moment we shall neglect spin and isospin effects. The eikonal approximation must be generalized somewhat, since the scattering centre no longer possesses the axial symmetry obtained in the simpler case of a single scatterer. Franco and Glauber[1] have shown that the appropriate expression for the scattering amplitude is

$$f(\bar{k},\bar{k}') = \frac{ik}{2\pi} \int d^2\bar{b}\, \exp[i(\bar{k}-\bar{k}').\bar{b}]\, \{e^{2i\chi(\bar{b})} - 1\} \qquad (7.1)$$

where $\bar{b}$ is an impact parameter vector perpendicular to the direction of the incident particle's momentum, and $\chi(\bar{b})$ is the phase shift associated with that impact parameter. The relationship of $\chi(\bar{b})$ to the interaction potential $V(\bar{r})$ between the particles is the same as that already encountered in the simple eikonal model, namely

$$\chi(\bar{b}) = -\frac{1}{2k} \int_{-\infty}^{\infty} d\bar{z}\, V(\bar{b} + \bar{z}) \qquad (7.2)$$

where $\bar{z}$ is a vector parallel to the incident momentum $\bar{k}$. If we assume that the potential $V_0(\bar{r})$ describing the interaction between the proton and the deuteron is simply the sum of the effective two-body nucleon potentials $V_N(\bar{r}-\bar{r}')$, we have

$$V_0(\bar{r}) = \int d\bar{r}' \int d\bar{r}''\, |\psi_0(\bar{r}',\bar{r}'')|^2 \{V_N(\bar{r}-\bar{r}') + V_N(\bar{r}-\bar{r}'')\} \qquad (7.3)$$

where the integration over the modulus-square of the deuteron wave function $\psi_0(\bar{r}', \bar{r}'')$ is performed to take account of the nucleon density distribution in the obvious way. The form assumed by (7.3) clearly suggests, although it does not directly imply, that we should write

$$e^{i\chi(\bar{b})} = \langle f|\ e^{i\chi_{total}(\bar{b}\ ,\ \bar{r})}\ |i\rangle \qquad (7.4)$$

where $\langle f|$ and $|i\rangle$ denote the initial and final deuteron bound-state wave functions, which we shall hereafter take to be the same since we

wish to consider elastic scattering. The function $\chi_{total}(\bar{b},\bar{r})$ is defined by

$$\chi_{total}(\bar{b},\bar{r}) = \chi_N(\bar{b} - \bar{r}/2) + \chi_N(\bar{b} + \bar{r}/2) \tag{7.5}$$

with

$$\chi_N(\bar{b}) = -\frac{1}{2k}\int_{-\infty}^{\infty} d\bar{z}\, V_N(\bar{b} + \bar{z}) \quad . \tag{7.6}$$

Now it is easily seen that if we define

$$\Gamma_D(\bar{b},\bar{s}) = e^{2i\chi_{tot}(\bar{b},\bar{s})} - 1 \tag{7.7a}$$

and

$$\Gamma_N(\bar{b}) = e^{2i\chi_N(\bar{b})} - 1 \tag{7.7b}$$

then we obtain the algebraic relation

$$\Gamma_D(\bar{b},\bar{r}) = \Gamma_N(\bar{b}+\bar{r}/2) + \Gamma_N(\bar{b}-\bar{r}/2) - \Gamma_N(\bar{b}+\bar{r}/2)\,\Gamma_N(\bar{b}-\bar{r}/2) \quad . \tag{7.8}$$

Then if we write the deuteron scattering amplitude as

$$f_D(\bar{k},\bar{q}) = \frac{ik}{2\pi}\int d^2\bar{b}\; e^{i\bar{q}\cdot\bar{b}}\,\langle D|\Gamma_D(\bar{b},\bar{r})|D\rangle \tag{7.9}$$

where $\bar{q} = \bar{k} - \bar{k}'$ is the momentum transfer and $|D\rangle$ is the deuteron state, we have

$$f_D(\bar{k},\bar{q}) = \frac{ik}{2\pi}\int d^2\bar{b}\; e^{i\bar{q}\cdot\bar{b}}\,\langle D|[\Gamma_N(\bar{b}+\bar{r}/2) + \Gamma_N(\bar{b}-\bar{r}/2) - \Gamma_N(\bar{b}+\bar{r}/2)\Gamma_N(\bar{b}-\bar{r}/2)]|D\rangle \tag{7.10}$$

For the first two terms in (7.10) we have by simply changing variables

$$\int d^2\bar{b}\; e^{i\bar{q}\cdot\bar{b}}\langle D|\Gamma_N(\bar{b}\pm\bar{r}/2)|D\rangle = \langle D|e^{\mp i\bar{q}\cdot\bar{r}/2}|D\rangle \int d^2\bar{b}'e^{i\bar{q}\cdot\bar{b}'}\Gamma_N(\bar{b}') \; . \qquad (7.11)$$

The latter term of (7.11) is clearly to be identified with the single scattering amplitude for the nucleon-nucleon system,

$$f_N(\bar{k},\bar{q}) \;=\; \frac{ik}{2\pi}\int d^2\bar{b}'e^{i\bar{q}\cdot\bar{b}'}\Gamma_N(\bar{b}') \quad ; \qquad (7.12)$$

the former term is just the deuteron elastic form factor,

$$S_D(\mp\,\bar{q}/2) \;=\; \langle D|e^{\mp i\bar{q}\cdot\bar{r}/2}|D\rangle \; . \qquad (7.13)$$

The last term of (7.10) can also be expressed in terms of the single scattering amplitude and the deuteron form factor by making use of the Fourier-integral representation of the two-dimensional Dirac delta function

$$\delta(\bar{q}) \;=\; \int d^2\bar{b}\; \frac{e^{i\bar{q}\cdot\bar{b}}}{2\pi} \qquad (7.14)$$

yielding the result

$$\frac{ik}{2\pi}\int d^2\bar{b}\; e^{i\bar{q}\cdot\bar{b}}\;\langle D|\Gamma_N(\bar{b}+\bar{r}/2)\;\Gamma_N(\bar{b}-\bar{r}/2)\;|D\rangle \;=$$

$$-\frac{i}{2\pi k}\int d^2\bar{q}'S_D(\bar{q}')\;f_N(\bar{k},\;\bar{q}/2+\bar{q}')\;f_N(\bar{k},\;\bar{q}/2-\bar{q}') \; . \qquad (7.15)$$

We therefore finally obtain

$$f_D(\bar{k},\bar{q}) = f_N(\bar{k},\bar{q})\left\{S_D(\frac{\bar{q}}{2}) + S_D(-\frac{\bar{q}}{2})\right\} + \frac{i}{2\pi k}\int d^2\bar{q}' S_D(\bar{q}')\, f_N(\bar{k}, \frac{\bar{q}}{2} + \bar{q}')$$

$$f_N(\bar{k}, \frac{\bar{q}}{2} - \bar{q}') \quad . \tag{7.16}$$

This equation, which forms the basis for the calculations which we shall present, is familiar in lower energy nuclear physics where it has been used frequently with considerable success[2]. It should be pointed out here that although the validity of the original derivation of (7.1) is limited to near-forward scattering, equation (7.16) has been able to describe successfully scattering in very light nuclei at momentum transfers much larger than might have been expected.

In order to evaluate simply the essential results of the Glauber model embodied in equation (7.16), we shall now make two simplifying assumptions. First, we assume that the scattering amplitudes $f_N(\bar{k},\bar{q})$ are effectively exponential in the square of the momentum transfer,

$$f_N(\bar{k},\bar{q}) = f_N\, e^{-\gamma q^2} \quad .$$

This form is generally correct in most simple scattering processes at sufficiently high energies and small momentum transfer. Secondly, we shall assume that the form factor $S_D(\bar{q})$ is effectively unity in the region of interest. This assumption is strictly tenable only in the extreme forward direction. In fact in the case of nucleon-deuteron scattering it is known that the variation of the deuteron form factor is responsible for a substantial part of the angular variations of the differential cross-section, even in the diffraction region. Our

considerations will not apply to the deuteron, however; we shall instead decompose either nucleons or mesons into their constituent quarks. The present understanding of the form factors of hadrons on the basis of the quark model is far from complete, and the experimental work on meson form factors is often meagre. It is true, however, that the form factors of the hadrons seem to decrease less rapidly than that of the deuteron, corresponding to the expectation that the quarks forming the hadrons are tightly bound. Furthermore, it often seems in nuclear scattering that the results are rather insensitive to the form factor. This result is not surprising when we consider that if we make the exponential approximation in the double scattering term, the main contribution to the scattering amplitude must come from momentum transfers for which both $|\frac{\bar{q}}{2} + \bar{q}'|$ and $|\frac{\bar{q}}{2} - \bar{q}'|$ are small, i.e. in which $|\bar{q}'|$ is small. This insensitivity is particularly significant in our applications to the quark model because the single scattering amplitudes, which would involve free quarks, are not known. As an example we consider the possibility that the form factor is also exponential in q^2. A trivial calculation shows that the difference between the definitions

$$f_N(\bar{k},\bar{q}) = f\, e^{-\gamma q^2} \quad , \quad S_D(\tfrac{\bar{q}}{2}) = 1$$

and

$$f_N(\bar{k},\bar{q}) = f\, e^{-(\gamma-\beta/4)q^2} \quad , \quad S_D(\tfrac{q}{2}) = e^{-\beta q^2/4}$$

comes only from the double scattering terms, and that these terms are in the ratio

$$\frac{\gamma}{\gamma + \beta/4} \; e^{\beta q^2/8} \; .$$

Since we expect that $\beta << \gamma$ if the quarks are tightly bound, we see that for reasonably small momentum transfers the difference should be quite small. In all the applications we shall consider only small momentum transfers are involved, so it is reasonable to hope that the effect of this assumption will not be severe[3].

Making these two assumptions, then, we find from (7.16)

$$f_D(\bar{k},\bar{q}) \; = \; 2 \, f_N \, e^{-\gamma q^2} \; + \; \frac{i f_N^2}{2k\gamma} \; e^{-\frac{\gamma}{2} q^2} \; . \qquad (7.17)$$

This relation serves as prototype for all the multiple scattering processes we shall consider. It is easily extended to more general circumstances; for example, spin and isospin can be included quite naturally, as we shall presently show. If the scattering in question is that of a k-particle composite system by an ℓ-particle one, the algebraic result analogous to (7.8) is similarly obtained, and contains $\frac{(k\ell)!}{n!(k\ell-n)!}$ terms describing n-tuple scattering[4]. The possibility of two different types of scattering process being involved in the multiple scattering (which is the case in the deuteron, of course) is also easily considered. The double-scattering integral can be performed even if the slopes of the two diffraction peaks are different, since

$$\int d^2\bar{p} \; e^{-\gamma_1(\frac{\bar{q}}{2} + \bar{p})^2 - \gamma_2(\frac{\bar{q}}{2} - \bar{p})^2} \; = \; \frac{2\pi}{\gamma_1+\gamma_2} \; e^{-\frac{\gamma_1 \gamma_2}{\gamma_1+\gamma_2} q^2} \; . \qquad (7.18)$$

This result can in fact be extended to n-tuple scattering, since it is quickly proved by induction that the relevant form is

$$\int d^2\bar{p}_1 \cdots d^2\bar{p}_n \delta(\bar{q} - \sum_{i=1}^{n} \bar{p}_i) e^{-\sum_{i=1}^{n} \gamma_i p_i^2} = \frac{(2\pi)^{n-1}}{(\prod_{i=1}^{n} \gamma_i)(\sum_{i=1}^{n} \gamma_i^{-1})} e^{-\frac{1}{\sum_{i=1}^{n} \gamma_i^{-1}} q^2} \tag{7.19}$$

For the moment, however, we shall postpone any major extensions of the model and examine two simple applications of the formalism already developed. In the first of these applications we shall show that the relation which seems in the simple additive quark model to be outstandingly in agreement with the experimental data is not substantially altered by the inclusion of multiple scattering effects; then we shall present an investigation of processes which involve double charge or hypercharge exchange and therefore require double scattering terms in the quark model.

Of the various predictions obtained in the independent quark model, the most nearly ubiquitous is the antisymmetric sum rule among meson-nucleon elastic scattering amplitudes

$$F_{\pi^+P} + F_{K^+N} + F_{K^-P} - F_{\pi^-P} - F_{K^-N} - F_{K^-P} = 0 \tag{7.20}$$

which was first found by Barger and Rubin[5]. The ease with which this result is obtained follows from the fact that it depends on only the two most basic assumptions of the model, namely, quark structure for the mesons and the additivity of the quark-nucleon amplitudes. Since

the multiple scattering effects are clearly non-additive, we wish to investigate whether they can significantly alter the excellent agreement of (7.20) with the meson-nucleon total cross section data. We shall find that within reasonable approximations it is possible to derive the correction terms, and that the amount by which they remove the right-hand side of (7.20) from zero is quite small as a result of cancellations among the various terms.

We begin by assuming that the meson-nucleon scattering amplitude can be written as in (7.9),

$$F_{MN}(\bar{k},\bar{q}) = \frac{ik}{2\pi}\int d^2\bar{b}\, e^{i\bar{q}\cdot\bar{b}}\, \Gamma_{MN}(\bar{k},\bar{b}) \quad . \tag{7.21}$$

F_{MN} and Γ_{MN} are now taken to be matrices in the isospace of the meson-nucleon system. We neglect complications due to spin, since we shall only consider forward scattering. Resolving the meson into its component quark and antiquark, we write analogously to (7.8)

$$\Gamma_{MN}(\bar{k},\bar{b}) = \langle M|\Gamma_{qN}(\bar{b}+\tfrac{\bar{r}}{2})+\Gamma_{\bar{q}N}(\bar{b}-\tfrac{\bar{r}}{2})-\tfrac{1}{2}\{\Gamma_{qN}(\bar{b}+\tfrac{\bar{r}}{2}),\Gamma_{\bar{q}N}(\bar{b}-\tfrac{\bar{r}}{2})\}_+|M\rangle \tag{7.22}$$

where the anticommutator $\{A,B\}_+ \equiv AB + BA$ has been taken to symmetrize the double scattering term. The nucleon could also be considered in terms of its quark structure, of course, but we shall not find it necessary to do so.

The most general form of the function Γ_{qN} describing the interaction between a nucleon and an isodoublet quark is conveniently written in terms of two scalar functions A and B as

$$\Gamma_{qN}(\bar{k},\bar{b}) = A(\bar{k},\bar{b}) + 4\, B(\bar{k},\bar{b})\, \bar{T}_q \cdot \bar{T}_N \tag{7.23}$$

where $\bar{T}_q$ and $\bar{T}_N$ are the isospin operators for the quark and the nucleon respectively. For the isosinglet λ quark there is only one function, which we define as

$$\Gamma_{\lambda N}(\bar{k},\bar{b}) = C(\bar{k},\bar{b}) \ . \tag{7.24}$$

We define similarly functions $\bar{A}(\bar{k},\bar{b})$, $\bar{B}(\bar{k},\bar{b})$, and $\bar{C}(\bar{k},\bar{b})$ describing nucleon-antiquark interactions. Using these definitions in (7.22) we easily find the following results:

$$\Gamma_{\pi^+P}(\bar{k},\bar{b}) = \langle \pi^+ | A + B + \bar{A} + \bar{B} - A\bar{A} - A\bar{B} - B\bar{A} - B\bar{B} | \pi^+ \rangle \tag{7.25a}$$

$$\Gamma_{\pi^-P}(\bar{k},\bar{b}) = \langle \pi^- | A - B + \bar{A} - \bar{B} - A\bar{A} + A\bar{B} + B\bar{A} - B\bar{B} | \pi^- \rangle \tag{7.25b}$$

$$\Gamma_{K^+P}(\bar{k},\bar{b}) = \langle K^+ | A + B + \bar{C} - A\bar{C} - B\bar{C} | K^+ \rangle \tag{7.25c}$$

$$\Gamma_{K^+N}(\bar{k},\bar{b}) = \langle K^+ | A - B + \bar{C} - A\bar{C} + B\bar{C} | K^+ \rangle \tag{7.25d}$$

$$\Gamma_{K^-N}(\bar{k},\bar{b}) = \langle K^- | C + \bar{A} + \bar{B} - C\bar{A} - C\bar{B} | K^- \rangle \tag{7.25e}$$

$$\Gamma_{K^-P}(\bar{k},\bar{b}) = \langle K^- | C + \bar{A} - \bar{B} - C\bar{A} + C\bar{B} | K^- \rangle \tag{7.25f}$$

where the argument of A, B, C is $(\bar{b} + \frac{\bar{r}}{2})$, and of $\bar{A}$, $\bar{B}$, $\bar{C}$ is $(\bar{b} - \frac{\bar{r}}{2})$.

We now proceed as described above and define "effective quark-nucleon scattering amplitudes" by

$$f_A(\bar{k},\bar{q}) = \frac{ik}{2\pi}\int d^2\bar{b}\; e^{i\bar{q}\cdot\bar{b}}\; A(\bar{k},\bar{b}) \tag{7.26}$$

and similarly for B, C, $\bar{A}$, $\bar{B}$, and $\bar{C}$, and assume that these amplitudes are effectively exponential,

$$f_A(\bar{k},\bar{q}) = A\, e^{-\gamma q^2} \tag{7.27a}$$

$$f_{\bar{A}}(\bar{k},\bar{q}) = \bar{A}\, e^{-\bar{\gamma} q^2}\ , \tag{7.27b}$$

etc. Then on taking the meson form factors to be essentially unity we find the following expressions for the forward scattering amplitudes including multiple scattering effects:

$$F_{\pi^+P}(\bar{k},0) = A + \bar{A} + B + \bar{B} - \frac{(A+B)(\bar{A}+\bar{B})}{2ik(\gamma+\bar{\gamma})} \tag{7.28a}$$

$$F_{\pi^-P}(\bar{k},0) = A + \bar{A} - B - \bar{B} - \frac{(A-B)(\bar{A}-\bar{B})}{2ik(\gamma+\bar{\gamma})} \tag{7.28b}$$

$$F_{K^+P}(\bar{k},0) = A + B + \bar{C} - \frac{(A+B)\bar{C}}{2ik(\gamma+\bar{\gamma})} \tag{7.28c}$$

$$F_{K^+N}(\bar{k},0) = A - B + \bar{C} - \frac{(A-B)\bar{C}}{2ik(\gamma+\bar{\gamma})} \tag{7.28d}$$

$$F_{K^-N}(\bar{k},0) = C + \bar{A} + \bar{B} - \frac{C(\bar{A}+\bar{B})}{2ik(\gamma+\bar{\gamma})} \tag{7.28e}$$

$$F_{K^-P}(\bar{k},0) = C + \bar{A} - \bar{B} - \frac{C(\bar{A} - \bar{B})}{2ik(y + \bar{y})} \quad . \tag{7.28f}$$

If we now define

$$G_{MN}(k) \equiv 1 + \frac{i}{2k(y + \bar{y})} F_{MN}(\bar{k},0) \tag{7.29}$$

then equations (7.28) imply that

$$G_{\pi^+P}(k)\, G_{K^+N}(k)\, G_{K^-P}(k) = G_{\pi^-P}(k)\, G_{K^+P}(k)\, G_{K^-N}(k) \quad . \tag{7.30}$$

After some algebra we can write this equation, suppressing the arguments of the amplitudes, in the following form:

$$F_{\pi^+P} + F_{K^+N} + F_{K^-P} - F_{\pi^-P} - F_{K^+P} - F_{K^-N} = i(S + T) \tag{7.31}$$

$$S = \frac{1}{2k(y + \bar{y})} \left\{ F_{\pi^-P} F_{K^+P} + F_{\pi^-P} F_{K^-N} + F_{K^-N} F_{K^+P} - F_{\pi^+P} F_{K^+N} - F_{\pi^+P} F_{K^-P} - F_{K^-P} F_{K^+N} \right\} \tag{7.32a}$$

$$T = i \left(\frac{1}{2k(y + \bar{y})} \right)^2 \left\{ F_{\pi^-P} F_{K^+P} F_{K^-N} - F_{\pi^+P} F_{K^+N} F_{K^-P} \right\} \quad . \tag{7.32b}$$

The equality (7.30) predicted by the quark model with multiple scattering therefore relates the sum of amplitudes appearing in the antisymmetric sum rule to the correction terms S and T. In order to obtain a simple estimate of the magnitudes of these corrections we

now assume that all amplitudes are purely imaginary and use the optical theorem

$$\sigma_{MN}(k) = \frac{4\pi}{k} \operatorname{Im} F_{MN}(k,0) \tag{7.33}$$

to express (7.30), (7.31), and (7.32) in terms of the meson-nucleon total cross sections σ_{MN}. We obtain from (7.30)

$$\left(1 - \frac{\sigma_{\pi^+P}}{8\pi(y+\bar{y})}\right)\left(1 - \frac{\sigma_{K^+N}}{8\pi(y+\bar{y})}\right)\left(1 - \frac{\sigma_{K^-P}}{8\pi(y+\bar{y})}\right) = \left(1 - \frac{\sigma_{\pi^-P}}{8\pi(y+\bar{y})}\right)\left(1 - \frac{\sigma_{K^+P}}{8\pi(y+\bar{y})}\right)\left(1 - \frac{\sigma_{K^-N}}{8\pi(y+\bar{y})}\right) \tag{7.34}$$

and from (7.31) and (7.32)

$$\sigma_{\pi^+P} + \sigma_{K^+N} + \sigma_{K^-P} - \sigma_{\pi^-P} - \sigma_{K^+P} - \sigma_{K^-N} = \sigma^{(S)} + \sigma^{(T)} \tag{7.35}$$

$$\sigma^{(S)} = -\frac{1}{8\pi(y+\bar{y})}\left\{\sigma_{\pi^-P}\sigma_{K^+P} + \sigma_{\pi^-P}\sigma_{K^-N} + \sigma_{K^+P}\sigma_{K^-N} - \sigma_{\pi^+P}\sigma_{K^+N} - \sigma_{\pi^+P}\sigma_{K^-P} - \sigma_{K^+N}\sigma_{K^-P}\right\} \tag{7.36a}$$

$$\sigma^{(T)} = \left(\frac{1}{8\pi(y+\bar{y})}\right)^2\left\{\sigma_{\pi^-P}\sigma_{K^+P}\sigma_{K^-N} - \sigma_{\pi^+P}\sigma_{K^-P}\sigma_{K^+N}\right\}. \tag{7.36b}$$

We naturally expect the values of y and $\bar{y}$ to be about the same as those of the slopes of the meson-nucleon diffraction peaks, so we choose

k_{LAB}, GeV/c	6.0	8.0	10.0	12.0	14.0	16.0	18.0
L.H.S. of (7.34)	.410 ± .006	.419 ± .005	.429 ± .005	.438 ± .006	.443 ± .006	.446 ± .007	.448 ± .009
R.H.S. of (7.34)	.411 ± .006	.429 ± .006	.431 ± .006	.438 ± .006	.442 ± .006	.445 ± .007	.445 ± .010
L.H.S. of (7.35), mb	0.3 ± 0.7	1.8 ± 0.6	0.4 ± 0.6	0.0 ± 0.6	0.0 ± 0.6	-0.3 ± 0.9	-0.3 ± 1.5
$\sigma^{(S)}$, mb	0.4	1.0	0.3	0.09	0.07	-0.02	-0.06
$\sigma^{(T)}$, mb	0.08	0.1	0.04	0.02	0.01	0.003	0.004

Table 7-1

k_{LAB}, GeV/c	6.0	8.0	10.0	12.0	14.0	16.0	18.0
L.H.S. of (7.34)	.410 ± .006	.419 ± .005	.429 ± .005	.438 ± .006	.443 ± .006	.446 ± .007	.448 ± .009
R.H.S. of (7.34)	.411 ± .006	.429 ± .006	.431 ± .006	.438 ± .006	.442 ± .006	.445 ± .007	.445 ± .010
L.H.S. of (7.35), mb	0.3 ± 0.7	1.8 ± 0.6	0.4 ± 0.6	0.0 ± 0.6	0.0 ± 0.6	-0.3 ± 0.9	-0.3 ± 1.5
$\sigma^{(S)}$, mb	0.4	1.0	0.3	0.09	0.07	-0.02	-0.06
$\sigma^{(T)}$, mb	0.08	0.1	0.04	0.02	0.01	0.003	0.004

Table 7-1

$(y + \bar{y}) = 3.5$ mb as a reasonable value. Then we obtain the values shown in Table 7-1 for the comparison of the two sides of (7.34), the values of the antisymmetric sum on the left-hand side of (7.35), and the correction terms $\sigma^{(S)}$ and $\sigma^{(T)}$, calculated from the total cross section data of Galbraith et al.[6]. We see that (7.34) is in excellent agreement with the experimental results. It is correspondingly noteworthy also that the values obtained for the left-hand side of (7.35), although smaller generally than the observed errors, tend to agree well with the values of $\sigma^{(S)}$ and $\sigma^{(T)}$. The values of $\sigma^{(S)}$ are quite small, and those of $\sigma^{(T)}$ are completely negligible; this smallness is due to cancellations among the terms in (7.36a) and in (7.36b). A typical term in the equation for $\sigma^{(S)}$ is of the order of 5 mb, however, and is certainly not a negligible correction term; similarly the two terms in $\sigma^{(T)}$ are about 1 mb each. The good agreement of (7.20) with experiment, therefore, is the result of the near-cancellation, rather than of the actual negligibility, of the multiple-scattering effects. We note further that, although the assumption that only two slopes, y and $\bar{y}$, are involved is necessary for the exact derivation of (7.34), the general features of the calculation are independent of any precise knowledge of the slopes of the diffraction peaks or the quark structure of the nucleon.

As a second simple application we now consider the inelastic processes requiring double scattering in the quark model. The very small cross-sections observed for inelastic two-body processes which require double charge exchange, such as $\pi^- p \to K^+ \Sigma^-$, or double

strangeness exchange, such as $K^-P \to K^0\Xi^0$, are explained quite naturally by the additive quark model. The intuitively expected suppression of reactions requiring I = 2 or S = 2 meson states in the t channel corresponds simply to the fact that such states cannot be formed in quark-quark or quark-antiquark interactions. That these cross-sections are not identically zero is a measure of the failure of the additivity assumption, since they can proceed only by means of double inelastic scattering terms which are inherently non-additive. These terms can be calculated under the assumptions we have used above, however, and it seems a natural test of the idea of multiple scattering in the quark model to do so.

We shall consider in detail the process $K^-P \to \pi^+\Sigma^-$. Other reactions of this type, in particular $K^-P \to K^+\Xi^-$, $K^-P \to K^0\Xi^0$, $\pi^-P \to K^+\Sigma^-$, and the antibaryon reactions $\bar{P}P \to \bar{\Sigma}^+\Sigma^-$, $\bar{P}P \to \bar{\Xi}^0\Xi^0$, and $\bar{P}P \to \bar{\Xi}^+\Xi^-$, can then be studied by a simple generalization of the results we obtain for the first reaction. Again neglecting spin complications, we begin as before by writing the scattering amplitude in the form

$$F_{K^-P \to \pi^+\Sigma^-}(\bar{k},\bar{q}) = \frac{ik}{2\pi}\int d^2\bar{b}\, e^{i\bar{q}\cdot\bar{b}}\, \Gamma_{K^-P \to \pi^+\Sigma^-}(\bar{k},\bar{b})$$

but now we decompose both meson and nucleon into their respective quark structures. The collision matrix for the meson-nucleon system is then represented by a sum of terms corresponding to single, double, ... sextuple scattering of the meson quark and antiquark by the three quarks of the nucleon. A straightforward application of the

Glauber formalism yields the following form for the double scattering amplitude, which is the leading term for the double charge exchange amplitude:

$$F_{K^-P \to \pi^+\Sigma^-}(\bar{k},\bar{q}) = \frac{i}{2\pi k}\int d^2p\, S_{K^-\pi^+}(\bar{p})\, f_{\bar{p}p \to \bar{n}n}(\bar{k}, \tfrac{\bar{q}}{2} + \bar{p}) \tag{7.37}$$

$$\times f_{p\lambda \to \lambda p}(\bar{k}, \tfrac{\bar{q}}{2} - \bar{p})\, T_{P\Sigma^-}(\tfrac{\bar{q}}{2} + \bar{p}, \tfrac{\bar{q}}{2} - \bar{p})$$

with the form factors

$$S_{K^-\pi^+}(\bar{p}) = \int d^3\bar{s}\, \phi_{K^-}(\bar{s})\, e^{i\bar{p}\cdot\bar{s}}\, \phi^*_{\pi^+}(\bar{s})$$

$$T_{P\Sigma^-}(\bar{p},\bar{q}) = \int d^3\bar{r}_1 \int d^3\bar{r}_2 \int d^3\bar{r}_3\, \delta(\bar{r}_1+\bar{r}_2+\bar{r}_3)\, \psi^*_{\Sigma^-}(\bar{r}_1,\bar{r}_2,\bar{r}_3)$$

$$\times e^{i(\bar{q}\cdot\bar{r}_1 + \bar{p}\cdot\bar{r}_2)}\, \psi_P(\bar{r}_1,\bar{r}_2,\bar{r}_3)$$

where $\phi_M(s)$ is the bound state spatial wave function of the meson M with quark and antiquark located at $\frac{\bar{s}}{2}$ and $-\frac{\bar{s}}{2}$ respectively, and $\psi_B(\bar{r}_1,\bar{r}_2,\bar{r}_3)$ is the symmetric bound state spatial wave function of the baryon B. The functions $f_{\bar{p}p \to \bar{n}n}(\bar{k},\bar{q})$ and $f_{p\lambda \to \lambda p}(\bar{k},\bar{q})$ are effective inelastic quark scattering amplitudes for the quark processes indicated.

To evaluate this expression we now make again the assumptions made previously, that the form factors can be set equal to unity and that the quark scattering amplitudes are exponentials in q^2. The

former assumption now implies, in addition to "tight binding", that we neglect the differences in the hadron wave functions which must result from the mass splitting. We write the four inelastic quark scattering amplitudes in the following exponential form:

$$f_{\bar{p}p \to \bar{n}n}(\bar{k},\bar{q}) = \frac{k}{\sqrt{\pi}} A^{\frac{1}{2}} e^{-\frac{a}{2} q^2} \tag{7.38a}$$

$$f_{p\lambda \to \lambda p}(\bar{k},\bar{q}) = \frac{k}{\sqrt{\pi}} B^{\frac{1}{2}} e^{-\frac{b}{2} q^2} \tag{7.38b}$$

$$f_{\bar{p}p \to \bar{\lambda}\lambda}(\bar{k},\bar{q}) = \frac{k}{\sqrt{\pi}} C^{\frac{1}{2}} e^{-\frac{c}{2} q^2} \tag{7.38c}$$

$$f_{pn \to np}(\bar{k},\bar{q}) = \frac{k}{\sqrt{\pi}} D^{\frac{1}{2}} e^{-\frac{d}{2} q^2} \tag{7.38d}$$

The inelastic quark reactions described by (7.38a) - (7.38d) are individually responsible for other scattering processes; for example, if we keep only the leading single scattering terms we can write

$$f_{\bar{p}p \to \bar{n}n}(\bar{k},\bar{q}) = F_{K^-P \to \bar{K}^0N}(\bar{k},\bar{q}) \tag{7.39a}$$

$$f_{p\lambda \to \lambda p}(\bar{k},\bar{q}) = F_{K^-P \to \pi^-\Sigma^+}(\bar{k},\bar{q}) \tag{7.39b}$$

$$f_{\bar{p}p \to \bar{\lambda}\lambda}(\bar{k},\bar{q}) = F_{\pi^+P \to K^+\Sigma^+}(\bar{k},\bar{q}) \tag{7.39c}$$

$$f_{pn \to np}(\bar{k},\bar{q}) = F_{K^+N \to K^oP}(\bar{k},\bar{q}) \quad . \tag{7.39d}$$

The coefficients A, B, C, D and a, b, c, d are thus determined from the differential cross sections of the single exchange processes. Specifically, from equations (7.39) we have

$$\frac{d\sigma}{dt}(K^-P \to \bar{K}^oN) = A\, e^{-aq^2} \tag{7.40a}$$

$$\frac{d\sigma}{dt}(K^-P \to \pi^-\Sigma^+) = B\, e^{-bq^2} \tag{7.40b}$$

$$\frac{d\sigma}{dt}(\pi^+P \to K^+\Sigma^+) = C\, e^{-cq^2} \tag{7.40c}$$

$$\frac{d\sigma}{dt}(K^+N \to K^oP) = D\, e^{-dq^2} \tag{7.40d}$$

It should be noted, of course, that differential cross sections of charge and hypercharge exchange processes are not exactly exponentials; in addition to the non-diffractive large angle region, there are in some cases dips in the forward direction. In general, however, the approximate forms above are sufficiently accurate for our purposes.

Inserting (7.38a) and (7.38b) into (7.37), then, we find

$$F_{K^-P \to \pi^+\Sigma^-}(\bar{k},\bar{q}) = -\frac{ik}{\pi(a+b)} A^{\frac{1}{2}} B^{\frac{1}{2}} e^{-\frac{1}{2/a+2/b} q^2} \tag{7.41}$$

which yields immediately

$$\frac{d\sigma}{dt}(K^-P \to \pi^+\Sigma^-) = \frac{1}{\pi}\frac{AB}{(a+b)^2} e^{-\frac{1}{1/a+1/b} q^2} . \qquad (7.42)$$

The differential cross section for the double charge exchange is thus completely determined, with no free parameters, by the diffraction peaks of the single exchange processes involved. Equations analogous to (7.42) can be written down immediately for the other double exchange processes listed above by substituting appropriately the parameters of the other quark reactions. For the other meson-induced reactions we obtain

$$\frac{d\sigma}{dt}(K^-P \to K^+\Xi^-) = \frac{d\sigma}{dt}(K^-P \to K^0\Xi^0) = \frac{1}{\pi}\frac{BC}{(b+c)^2} e^{-\frac{1}{1/b+1/c} q^2} \qquad (7.43)$$

$$\frac{d\sigma}{dt}(\pi^-P \to K^+\Sigma^-) = \frac{1}{\pi}\frac{CD}{(c+d)^2} e^{-\frac{1}{1/c+1/d} q^2} \qquad (7.44)$$

for the differential cross sections of the double exchange processes. The procedure for the antiproton reactions is identical except that we shall determine the necessary coefficients by using single-exchange antiproton processes, thereby avoiding the necessity of choosing the appropriate energy for comparison of meson-baryon and antibaryon-baryon amplitudes. We therefore use in place of (7.39a) and (7.39c)

$$f_{\bar{p}p \to \bar{n}n}(\bar{k},\bar{q}) = F_{\bar{P}P \to \bar{N}N}(\bar{k},\bar{q}) = \frac{k}{\sqrt{\pi}} A'^{\frac{1}{2}} e^{-\frac{a'}{2} q^2} \qquad (7.39e)$$

and

$$f_{\bar{p}p \to \bar{\lambda}\lambda}(\bar{k},\bar{q}) = F_{\bar{P}P \to \bar{\Sigma}^-\Sigma^+}(\bar{k},\bar{q}) = \frac{k}{\sqrt{\pi}}\, C'^{\frac{1}{2}}\, e^{-\frac{c'}{2}q^2} \qquad (7.39f)$$

in terms of which

$$\frac{d\sigma}{dt}(\bar{P}P \to \bar{N}N) = A'\, e^{-a'q^2} \qquad (7.40e)$$

and

$$\frac{d\sigma}{dt}(\bar{P}P \to \bar{\Sigma}^-\Sigma^+) = C'\, e^{-c'q^2}\,. \qquad (7.40f)$$

We find then that

$$\frac{d\sigma}{dt}(\bar{P}P \to \bar{\Sigma}^+\Sigma^-) = \frac{1}{\pi}\,\frac{A'C'}{(a'+c')^2}\, e^{-\frac{1}{1/a'+1/c'}q^2} \qquad (7.45)$$

and

$$\frac{d\sigma}{dt}(\bar{P}P \to \bar{\Xi}^+\Xi^-) = \frac{d\sigma}{dt}(\bar{P}P \to \bar{\Xi}^o\Xi^o) = \frac{1}{\pi}\,\frac{C'^2}{4c'^2}\, e^{-\frac{c'}{2}q^2}\,. \qquad (7.46)$$

There are several salient features which equations (7.42) - (7.46) have in common. In particular we notice that since the ratio of the forward differential cross section to the square of the slope of the diffraction peak is small for inelastic processes, the double charge or hypercharge exchange cross sections are predicted to be quite small. If a sufficient number of events is collected to permit a study of the angular variations, the diffraction peak resulting from the double scattering process is expected to be considerably flatter than that from single scattering, the ratio of slopes being approximately $\frac{1}{2}$.

It is possible, furthermore, to estimate the variation with energy of the double exchange processes if the behaviour of the single exchange processes is known. Morrison[7] has classified inelastic two-body processes by writing for the total reaction cross-section $\sigma \approx K\, s^{-n}$, with $n = 1.6$ and $n = 2.0$ for those reactions corresponding respectively to non-strange and strange meson exchange. By integrating the differential cross sections we have obtained we find immediately $\sigma \approx K\, s^{-3.6}$ for the reactions producing Σ's, which correspond to $S = 1$, $I = 2$ exchange, and $\sigma \approx K\, s^{-4.0}$ for those producing Ξ's, equivalent to $S = 2$ meson exchange. Further s dependence may arise as a result of variation of the slope of the diffraction peak; assumption of Regge behaviour, for example, leads to a factor $(\ln s)^{-1}$ in this way.

We notice also the equality of the amplitudes for the production of Ξ^0 and Ξ^- in (7.43) and (7.46), which results from the assumption of isosymmetry in the quark processes $\bar{p}p \to \bar{\lambda}\lambda$ and $\bar{n}n \to \bar{\lambda}\lambda$. This result corresponds to the dominance of $I = 1$ in the direct channel. Alternatively it can be expressed in terms of the crossed channel, implying the equality of the amplitudes for exchange of mesons with $S = 2$, $I = 1$ and $S = 2$, $I = 0$.

We shall now present a very rough comparison of the experimental data with the predictions made above. The data on the double exchange processes generally consist of only a few events, and the errors on the single exchange cross sections are often quite large; consequently we shall not attempt to estimate the errors on the values we calculate.

We wish also to point out that in most cases we are limited by the availability of data to rather low energies, where it is not clear that our model should be valid. The approximation that the diffraction peaks are exponential is less reliable at low energies. In the mesonic reactions, furthermore, the dominant mechanism seems to be baryon exchange, which cannot be considered in our formalism[8]. The peak from baryon exchange is in the backward direction, however, so we may hope to separate the two effects.

Beginning with equation (7.42), we estimate from data[9] at 2.24 GeV/c laboratory momentum

$$\frac{d\sigma}{dt}(K^-P \to \bar{K}^0N) \approx 850\, e^{-1.5q^2}\ \mu b/GeV^2 \qquad (7.47a)$$

$$\frac{d\sigma}{dt}(K^-P \to \pi^-\Sigma^+) \approx 300\, e^{-1.5q^2}\ \mu b/GeV^2 \ . \qquad (7.47b)$$

Although the energy is quite low, the data for these reactions seem to agree quite well with the exponential approximation. Using these constants in (7.42), we obtain

$$\frac{d\sigma}{dt}(K^-P \to \pi^+\Sigma^-) \approx 23\, e^{-0.75q^2}\ \mu b/GeV^2 \ . \qquad (7.47c)$$

In this case it is possible to separate clearly the forward double charge exchange reactions from the backward peak corresponding to baryon exchange. The prediction (7.47c) agrees with the experimental data quite well, as is shown in Figure 7-2. The differential cross section has a value of $\sim 19\ \mu b/GeV^2$ in the near-forward direction and

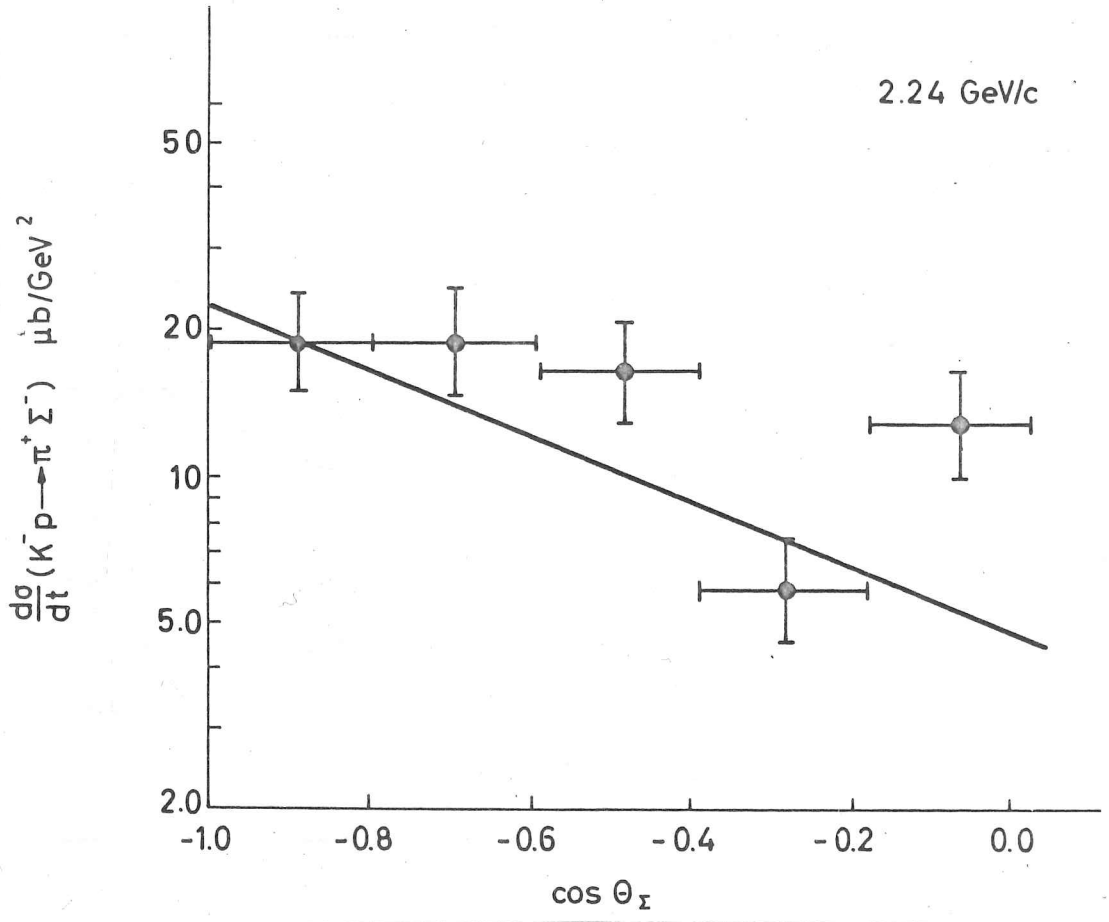

Figure 7-2 Comparison of prediction and experiment for $\frac{d\sigma}{dt}(K^- P \rightarrow \pi^+ \Sigma^-)$. The data are taken from reference 9 with one event set equal to $(1.17 \pm 0.17)\ \mu b/GeV^2$; the straight line is our predicted value.

decreases slowly with increasing momentum transfer. At a somewhat higher energy, the data[10,11] indicate that at 3.5 GeV/c

$$\frac{d\sigma}{dt}(K^-P \to \bar{K}^oN) \approx 800\, e^{-3.3q^2}\ \mu b/GeV^2 \qquad (7.48a)$$

$$\frac{d\sigma}{dt}(K^-P \to \pi^-\Sigma^+) \approx 280\, e^{-1.7q^2}\ \mu b/GeV^2 \qquad (7.48b)$$

yielding

$$\frac{d\sigma}{dt}(K^-P \to \pi^+\Sigma^-) \approx 7.0\, e^{-1.7q^2}\ \mu b/GeV^2 \ . \qquad (7.48c)$$

The very sparse data on the double charge exchange at this energy show no events in the forward hemisphere, where the above estimate predicts about four.

Turning next to equation (7.43), we use data[12] at 2.3 GeV/c laboratory momentum to estimate that

$$\frac{d\sigma}{dt}(\pi^+P \to K^+\Sigma^+) \approx 800\, e^{-7.0q^2}\ \mu b/GeV^2 \ . \qquad (7.49a)$$

Combining this figure with (7.47b) we find

$$\frac{d\sigma}{dt}(K^-P \to K^+\Xi^-) \approx 2.7\, e^{-1.2q^2}\ \mu b/GeV^2 \ , \qquad (7.49b)$$

whereas the data show a forward differential cross section of about 6 $\mu b/GeV^2$ and a large backward peak. Going to a higher energy[13], we estimate that at 3.23 GeV/c

$$\frac{d\sigma}{dt}(\pi^+P \to K^+\Sigma^+) \approx 1100\, e^{-9.6q^2}\ \mu b/GeV^2 \ , \qquad (7.50a)$$

and using (7.48b) we obtain

$$\frac{d\sigma}{dt}(K^-P \to K^+\Xi^-) \approx 2.6\, e^{-2.6q^2}\ \mu b/GeV^2 \qquad (7.50b)$$

at laboratory momenta around 3.4 GeV/c. Again the experimental data are very scant, showing five events in the forward hemisphere; from (7.50b) we would expect one or two.

Comparison of (7.44) with experiment requires data for $\frac{d\sigma}{dt}(K^+N \to K^oP)$, which are only available[14] at the low energy of 2.3 GeV/c and are not very well on an exponential; a rough estimate of

$$\frac{d\sigma}{dt}(K^+N \to K^oP) \approx 2300\, e^{-2.9q^2}\ \mu b/GeV^2 \qquad (7.51a)$$

can be combined with (7.49a) to yield

$$\frac{d\sigma}{dt}(\pi^-P \to K^+\Sigma^-) \approx 15\, e^{-2.0q^2}\ \mu b/GeV^2 \ . \qquad (7.51b)$$

The data on this process are dominated by a strong backward peak, but in the near-forward direction the differential cross section is $(6.0 \pm 4.0)\ \mu b/GeV^2$, compatible with (7.51b) although somewhat low.

We consider next the antiproton processes, which provide a better test of the model because there is no possibility of baryon exchange as a competing mechanism for the reactions. Beginning with (7.45), we estimate from data[15,16] in the momentum range 3.0 - 3.6 GeV/c that

$$\frac{d\sigma}{dt}(\bar{P}P \to \bar{N}N) \approx 8000\, e^{-5.1q^2}\ \mu b/GeV^2 \qquad (7.52a)$$

and

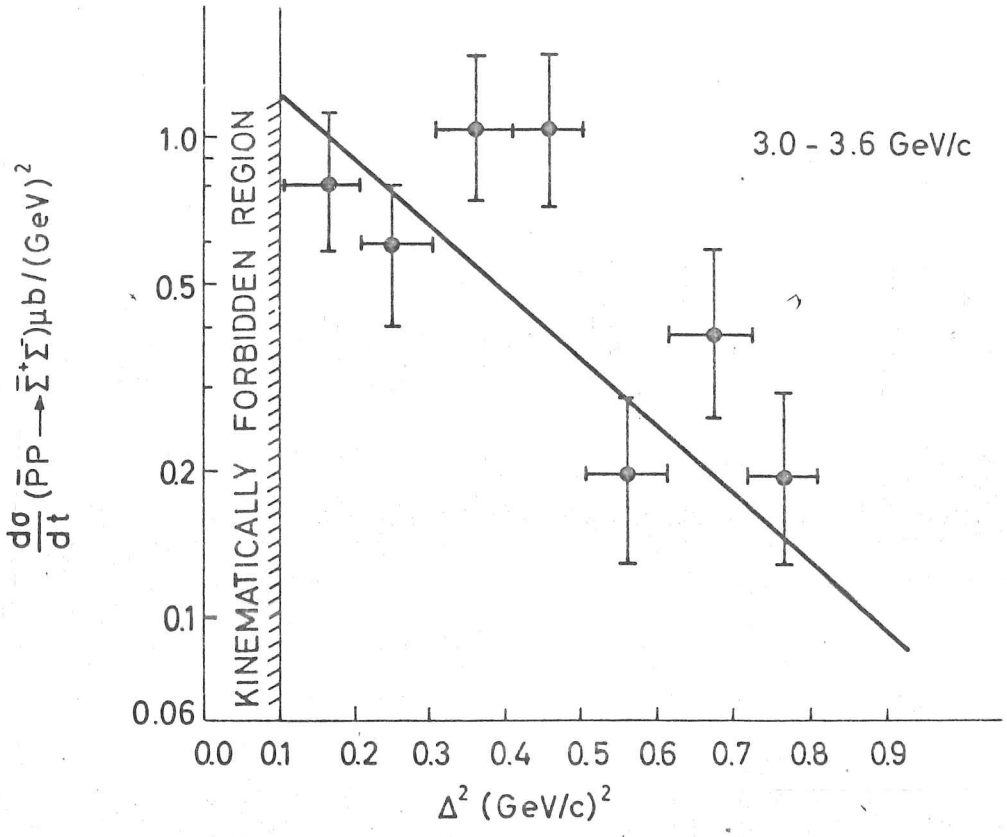

Figure 7-3 Comparison of prediction and experiment for $\frac{d\sigma}{dt}(\bar{P}P \rightarrow \bar{\Sigma}^+\Sigma^-)$. The data are taken from reference 15 with one event set equal to $(1.17 \pm 0.17)\ \mu b/GeV^2$; the straight line is our predicted value.

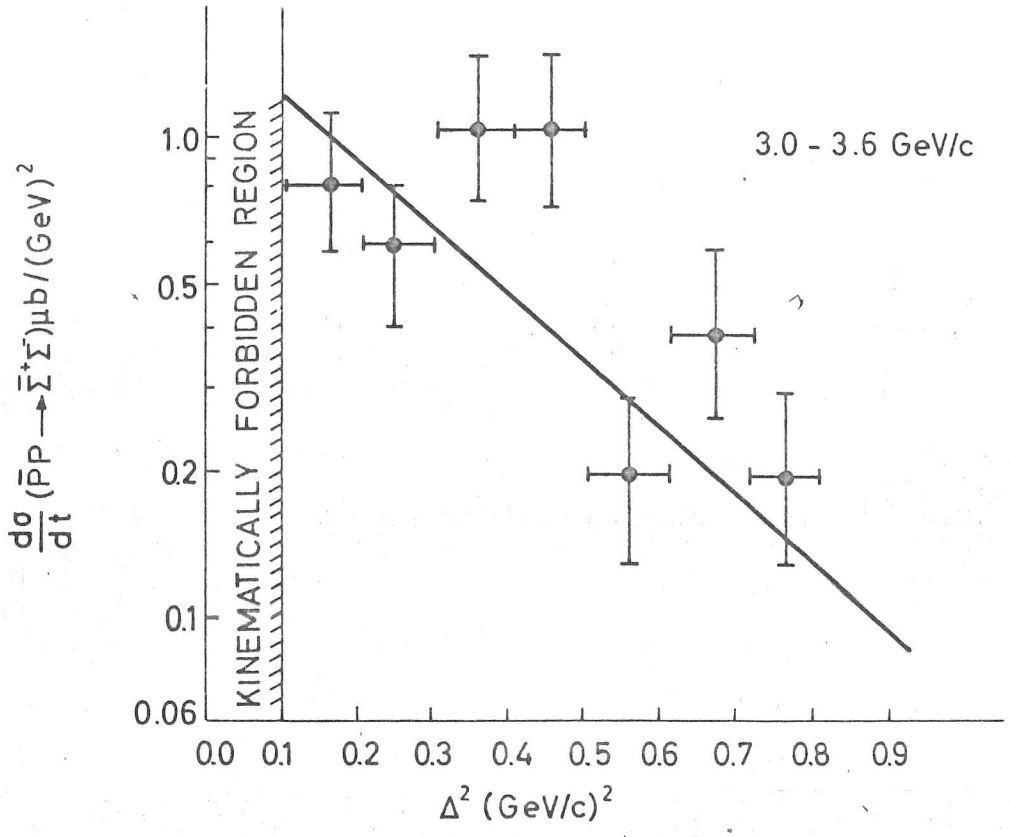

Figure 7-3 Comparison of prediction and experiment for $\frac{d\sigma}{dt}(\bar{P}P \rightarrow \bar{\Sigma}^+\Sigma^-)$. The data are taken from reference 15 with one event set equal to $(1.17 \pm 0.17)\ \mu b/GeV^2$; the straight line is our predicted value.

$$\frac{d\sigma}{dt}(\bar{P}P \to \bar{\Sigma}^-\Sigma^+) \approx 340\, e^{-8.3q^2}\ \mu b/GeV^2 \qquad (7.52b)$$

from which we predict that

$$\frac{d\sigma}{dt}(\bar{P}P \to \bar{\Sigma}^+\Sigma^-) \approx 12.4\, e^{-3.2q^2}\ \mu b/GeV^2 \ . \qquad (7.52c)$$

This result also compares excellently with the experimental data. In Figure 7-3 we have plotted the measured cross sections with (7.52c) shifted so that $q^2 = 0$ corresponds to the minimal momentum transfer, which is non-zero because of the P-Σ mass difference. At a higher energy we estimate from data[17,18] at 7.0 GeV/c laboratory momentum that

$$\frac{d\sigma}{dt}(\bar{P}P \to \bar{\Sigma}^-\Sigma^+) \approx 160\, e^{-9.0q^2}\ \mu b/GeV^2 \qquad (7.53a)$$

$$\frac{d\sigma}{dt}(\bar{P}P \to \bar{N}N) \approx 1650\, e^{-4.4q^2}\ \mu b/GeV^2 \qquad (7.53b)$$

from which we obtain

$$\frac{d\sigma}{dt}(\bar{P}P \to \bar{\Sigma}^+\Sigma^-) \approx 1.2\, e^{-2.9q^2}\ \mu b/GeV^2 \ . \qquad (7.53c)$$

Two events of this type were seen, corresponding to a total reaction cross section of $\sigma_R = (3 \pm 2)\ \mu b$; by integrating (7.53c) we would estimate $\sigma_R = 0.41\ \mu b$.

Finally, for equation (7.46) we use (7.52b) to estimate that for laboratory momenta (3.0 - 3.6) GeV/c

$$\frac{d\sigma}{dt}(\bar{P}P \to \bar{\Xi}^+\Xi^-) \approx 0.35\, e^{-4.1q^2}\ \mu b/GeV^2 \qquad (7.54)$$

yielding a total reaction cross section of less than 0.1 μb. At 3.0 GeV/c, two events of this type were seen in the experiment of reference 15, corresponding to a cross section of (2 ± 1) μb; no events were seen at 3.6 GeV/c. Further data[19] at 3.7 GeV/c give a very similar estimate for $\frac{d\sigma}{dt}(\bar{P}P \to \bar{\Sigma}^-\Sigma^+)$ and assign a reaction cross section for the double hypercharge exchange of 2 μb on the basis of three events. The prediction of equation (7.54) therefore seems to be an order of magnitude smaller than the experimental result. We note that such a discrepancy can be explained by the existence of a heavy boson resonance of mass 2.5 - 3.0 GeV. The good agreement of equation (7.45) with experimental data at the same energy indicates that this resonance must couple much more weakly to $\bar{\Sigma}^+\Sigma^-$ than to $\bar{\Xi}^+\Xi^-$.

At 7 GeV/c, we predict from (7.53a) a miniscule differential cross section for this process

$$\frac{d\sigma}{dt}(\bar{P}P \to \bar{\Xi}^+\Xi^-) \approx 0.06\, e^{-4.5q^2}\ \mu b/GeV^2 \ . \qquad (7.55)$$

In agreement with this result is the fact that the reaction was not seen in the data of reference 17.

We conclude therefore on the basis of these two simple applications that the calculation of scattering amplitudes by means of the quark model with multiple scattering seems to lead to results that are

generally quite good. The elastic meson-nucleon scattering amplitudes are connected by a non-linear equation which can be related to the antisymmetric sum rule and is in excellent agreement with the experimental results. Application of the multiple scattering formalism to the description of double charge of hypercharge exchange leads to results that are in most cases, within the large errors, in good qualitative agreement with the experimental data.

References

1. V. Franco and R. J. Glauber, Phys. Rev. 142, 1195 (1966).

2. Excellent reviews of the applications of the Glauber model in nuclear physics are given by C. Wilkin, BNL preprint 11722, and R. J. Glauber, in High Energy Physics and Nuclear Structure (North-Holland, 1967).

3. We are very grateful to Professor R. J. Glauber for a stimulating discussion on the effects of the form factor in the multiple scattering formalism.

4. This result has also been noticed by A. Pagnamenta, private correspondence.

5. V. Barger and M. H. Rubin, Phys. Rev. 140, B1365 (1965).

6. W. Galbraith et al., Phys. Rev. 138, B913 (1965).

7. D. R. O. Morrison, Phys. Letters 22, 528 (1966).

8. The baryon exchange mechanism in the quark model has been considered by P. J. S. Watson, Phys. Letters 25B, 287 (1967).

9. G. W. London et al., Phys. Rev. 143, 1034 (1966).

10. The ($K^- P \to \bar{K}^0 N$) parameters have been estimated using reference 9 and the data of P. Astbury et al., Phys. Letters 23, 396 (1966).

11. Birmingham-Glasgow-London (I.C.)-Oxford-Rutherford Collaboration, Phys. Rev. 152, 1148 (1966).

12. O. I. Dahl et al., Phys. Rev. 163, 1430 (1967).

13. R. R. Kofler et al., Phys. Rev. 163, 1479 (1967).

14. I. Butterworth et al., Phys. Rev. Letters 15, 734 (1965).

15. B. Musgrave et al., Nuovo Cimento 35, 735 (1965).

16. O. Czyzewski et al., Phys. Letters 20, 554 (1966).

17. C. Y. Chien et al., Phys. Rev. 152, 1171 (1966).

18. P. Astbury et al., Phys. Letters 23, 160 (1966).

19. C. Baltay et al., Phys. Rev. 140, B1027 (1965).

CHAPTER VIII

Multiple Scattering and Regge Theory

We have shown in the preceding chapter that if the six meson-nucleon elastic amplitudes which are commonly measured are expressed in terms of six quark-nucleon amplitudes, a relation between them exists even with the inclusion of multiple scattering effects. It is therefore impossible to invert the equations and solve explicitly for the quark-nucleon amplitudes. Consequently no direct calculation of the magnitude of the multiple scattering terms can be obtained. If the behaviour with energy of the single scattering amplitude is known, however, we may estimate the importance of the various terms by parametrizing the total amplitude and fitting it to the data at several energies. The logical assumption for the energy dependence of the single scattering amplitude is that corresponding to a Regge pole. To begin this chapter, then, we must investigate the effects on the multiple scattering terms which result from the Regge behaviour of the single scattering. The results obtained by fitting a simple spin-independent Regge model to the experimental total cross sections will then be presented.

CHAPTER VIII

Multiple Scattering and Regge Theory

We have shown in the preceding chapter that if the six meson-nucleon elastic amplitudes which are commonly measured are expressed in terms of six quark-nucleon amplitudes, a relation between them exists even with the inclusion of multiple scattering effects. It is therefore impossible to invert the equations and solve explicitly for the quark-nucleon amplitudes. Consequently no direct calculation of the magnitude of the multiple scattering terms can be obtained. If the behaviour with energy of the single scattering amplitude is known, however, we may estimate the importance of the various terms by parametrizing the total amplitude and fitting it to the data at several energies. The logical assumption for the energy dependence of the single scattering amplitude is that corresponding to a Regge pole. To begin this chapter, then, we must investigate the effects on the multiple scattering terms which result from the Regge behaviour of the single scattering. The results obtained by fitting a simple spin-independent Regge model to the experimental total cross sections will then be presented.

Since an integration over momentum transfer is involved in the multiple scattering terms, it is necessary to employ a simplified version of the Regge pole amplitude. The traditional form, used by Phillips and Rarita[1] among many others, is

$$F(s,t) = (2\alpha(t)+1)\,\beta(t)\,\frac{(1+\tau e^{-i\pi\alpha(t)})}{\sin\pi\alpha(t)}\,s^{\alpha(t)} \qquad (8.1)$$

where $\beta(t)$ is the residue function, $\alpha(t)$ the pole's trajectory, τ the signature, and s and t have their usual meanings. The extraneous factors in (8.1) clearly prohibit the exact integration over t of this amplitude in any but pathological cases. We therefore adopt a much simpler form which contains nonetheless all of the essential features of (8.1) by writing

$$F_R^+(s,t) = -c_+\left(\frac{s}{is_0}\right)^{\alpha_+(t)} \qquad \text{for } \tau = +1 \qquad (8.2a)$$

$$F_R^-(s,t) = i\,c_-\left(\frac{s}{is_0}\right)^{\alpha_-(t)} \qquad \text{for } \tau = -1\ . \qquad (8.2b)$$

It is simply a result of analyticity plus crossing symmetry that the dependence on (s/i) in equations (8.2) correctly reproduces the phase of the Regge amplitude given, in (8.1), by the signature factor $(1+\tau e^{-i\pi\alpha(t)})$.[2] The constants $c_\pm$ and s_0 are chosen so that they reproduce the t-dependence of the residue function; that is, we assume that it is possible to write approximately, for $\tau = +1$,

$$2(2\alpha(t)+1)\,\beta(t)\,\frac{\cos\left(\frac{\pi\alpha(t)}{2}\right)}{\sin\left(\pi\alpha(t)\right)} = -\,c_{+}\,(s_0)^{-\alpha_{+}(t)} \tag{8.3a}$$

and for $\tau = -1$, similarly,

$$2(2\alpha(t)+1)\,\beta(t)\,\frac{\sin\left(\frac{\pi\alpha(t)}{2}\right)}{\sin\left(\pi\alpha(t)\right)} = -\,c_{-}\,(s_0)^{-\alpha_{-}(t)}\,. \tag{8.3b}$$

The exponential t-dependence in the residue function often invoked in order to fit the experimental diffraction peaks is thus pictured as representing an incorrect normalization of the energy. A trivial calculation shows that the value of s_0 necessary for compatibility with typical high-energy data is between 0.001 GeV^2 and 0.1 GeV^2, depending on the slope of the Regge trajectory.

As a simple example in which the essential results following from the definitions (8.2) can easily be seen we consider the same scattering process pictured in the introduction of the Glauber model in the preceding chapter. The kinematic quantities defined there are related to the invariant variables by

$$s = M^2 + m^2 + 2M\sqrt{k^2 + m^2} \tag{8.4}$$

$$t = 2M(M - \sqrt{q^2 + M^2}) \;; \tag{8.5}$$

the final momentum k' of the incident particle is determined by

$$\sqrt{k'^2 + m^2} = \sqrt{k^2 + m^2} + \sqrt{q^2 + M^2} - M\,. \tag{8.6}$$

The relation between t and q^2 in (8.5) is easily inverted to give

$$q^2 = -t\left(1 - \frac{t}{4M^2}\right) . \tag{8.7}$$

In these equations we have denoted the mass of the incident particle by m, and that of the target by M. The principal features of the Glauber formalism are insensitive to the frame in which it is derived, and therefore to the choice of which of these is to represent the composite particle. A pertinent question is whether the mass of the composite particle itself or that of the component particle involved should be used; since we do not know the quark mass, we shall naturally use the mass of the physical particle. In fact we shall soon see that, at least at asymptotic energies, where $s \approx 2Mk$, this choice is quite free.

To be definite we assume that the Regge pole involved is the Pomeranchuk, with positive signature and $\alpha(0) = 1$. The required exponential dependence on q^2 is obtained by writing

$$\alpha(t) = 1 - \beta q^2 = 1 + \beta t\left(1 - \frac{t}{4M^2}\right) . \tag{8.8}$$

The scattering amplitude can now be written down by making in (7.17) the substitution

$$f_N\, e^{-\gamma q^2} = -C\left(\frac{s}{is_o}\right)^{1-\beta q^2} , \tag{8.9}$$

that is,

$$f_N = -C\left(\frac{s}{is_o}\right) \quad , \quad \gamma = \beta \ln\left(\frac{s}{is_o}\right) \quad ,$$

yielding

$$f_R(s,q^2) = -2C\left(\frac{s}{is_o}\right)^{1-\beta q^2} + \frac{iC^2}{2k\beta \ln\left(\frac{s}{is_o}\right)} \left(\frac{s}{is_o}\right)^{2-\frac{\beta}{2}q^2} . \quad (8.10)$$

We notice at once that the double scattering term has the s-dependence which typifies a Regge cut. It is in fact a well known general result that the iteration of a Regge pole term, whether as a multiple scattering integral or in some other guise, leads to the apperance of terms having this behaviour. This point was made as long ago as 1962 by Amati, Stanghellini, and Fubini[3] in considering the multiperipheral model of high energy scattering. It was subsequently shown in a treatment of Feynman diagram singularity structure by Mandelstam[4], however, that the cut they found was cancelled by other terms, and that only non-planar diagrams could lead to Regge cuts. Such diagrams appear only if the structure of both particles involved in the scattering process is considered. This result is therefore difficult to reconcile with the Glauber formalism, which produces a cut regardless of the structure of the non-composite particle. The contrast, even in language, between the physical assumptions of Glauber theory and the ponderous mathematical apparatus of diagrammatic techniques is a formidable one, and the resolution of the problems involved is far from apparent[5]. The viewpoint we shall adopt is a phenomenological

one; we regard the Glauber formalism as a tool supplying an eminently reasonable parametrization of the scattering amplitude. As such, it can be used independently of whether the actual form of the cut term is ultimately vindicated or not.

It is sufficient for our examination of the essential features of the amplitude (8.10) to study its asymptotic form, using the high energy approximation $s \approx 2Mk$. Then (8.10) becomes

$$f_R(s,q^2) \approx -2C\left(\frac{s}{is_o}\right)^{1-\beta q^2} + \frac{C^2 M}{\beta s_o \ln\left(\frac{s}{is_o}\right)} \left(\frac{s}{is_o}\right)^{1-\frac{\beta}{2}q^2} . \qquad (8.11)$$

We examine first the total cross section, which is obtained by using the optical theorem. Assuming for the moment that $s >> s_o$, so that $\ln\left(\frac{s}{is_o}\right)$ is essentially real, we have

$$\sigma_T(s) = \frac{4\pi}{k} \operatorname{Im} f_R(s,o)$$

$$\approx 8\pi \left\{ 2\left(\frac{MC}{s_o}\right) - \frac{1}{\beta \ln\left(\frac{s}{s_o}\right)} \left(\frac{MC}{s_o}\right)^2 \right\} . \qquad (8.12)$$

The multiple scattering contribution is immediately seen to be subtractive, implying that the total cross section increases to a constant value. The opposite situation is observed in experimental hadronic total cross sections. If several trajectories are involved, however, the increasing behaviour may be hidden. More simply, a positive double scattering contribution can result

from a pole with negative signature because of the extra i in the definition (8.2b); or from the inclusion of double isoflip terms because of the Clebsch-Gordan coefficients. In any case, however, the multiple scattering contribution vanishes with increasing energy at least logarithmically because of the shrinkage of the diffraction peak. We also note in (8.12) that the mass M and the constant C appear only in the combination $(\frac{MC}{s_o})$, so that this result does not depend directly on the choice of M, as mentioned above. Except for the term $\beta \ln(\frac{s}{s_o})$, which represents the slope of the single-scattering diffraction peak, the result is also insensitive to s_o.

We look next at the differential cross-section. For the large energy, small momentum transfer limit being considered, we obtain

$$\frac{d\sigma}{dt} \approx \frac{\pi}{k^2} |f_R|^2$$

$$\approx 16\pi \left(\frac{MC}{s_o}\right)^2 \left[\left(\frac{s}{s_o}\right)^{-2\beta q^2} - \frac{\cos(\frac{\pi\beta q^2}{4})}{\ln(s/s_o)} \left(\frac{MC}{s_o}\right) \left(\frac{s}{s_o}\right)^{-\frac{3}{2}\beta q^2} + \right.$$

$$\left. + \frac{1}{4(\beta \ln \frac{s}{s_o})^2} \left(\frac{MC}{s_o}\right)^2 \left(\frac{s}{s_o}\right)^{-\beta q^2} \right] . \qquad (8.13)$$

Once again M and C appear only as $(\frac{MC}{s_o})$, and β and s_o appear always as related to the single-scattering diffraction peak slope. Of

particular interest in (8.13) is the energy dependence of the three terms. We have seen already in the total cross section that for $q^2 = 0$ the single scattering is dominant at $s \to \infty$. For non-zero values of q^2, however, the opposite result is obtained. The ratio of the double scattering term to the single is proportional to $(\frac{s}{s_o})^{\beta q^2}/(\ln \frac{s}{s_o})^2$, and therefore for sufficiently high energies the former dominates. The behaviour implied by (8.13) is pictured in Figure 8-1; at very small q^2 we see mainly the single scattering term. For larger q^2 the interference between single and double scattering becomes more important and may cause dips in the differential cross section. Finally, at sufficiently large values of q^2, the double scattering term becomes dominant. A convenient measure of how rapidly the limiting behaviour is approached is obtained by finding the value of q^2 for which the contributions of single and double scattering are equally important. Setting

$$(\frac{s}{s_o})^{-2\beta q_o^2} = \frac{1}{4(\beta \ln \frac{s}{s_o})^2} \; (\frac{MC}{s_o})^2 \; (\frac{s}{s_o})^{-\beta q_o^2} \qquad (8.14)$$

we find

$$q_o^2 = 2[\ln(\ln \frac{s}{s_o}) - \ln (\frac{MC}{2\beta s_o}) \,] \,/\, (\beta \ln \frac{s}{s_o}) \;, \qquad (8.15)$$

which has only the slightest decreasing behaviour with increasing s. The structure of the differential cross section therefore changes

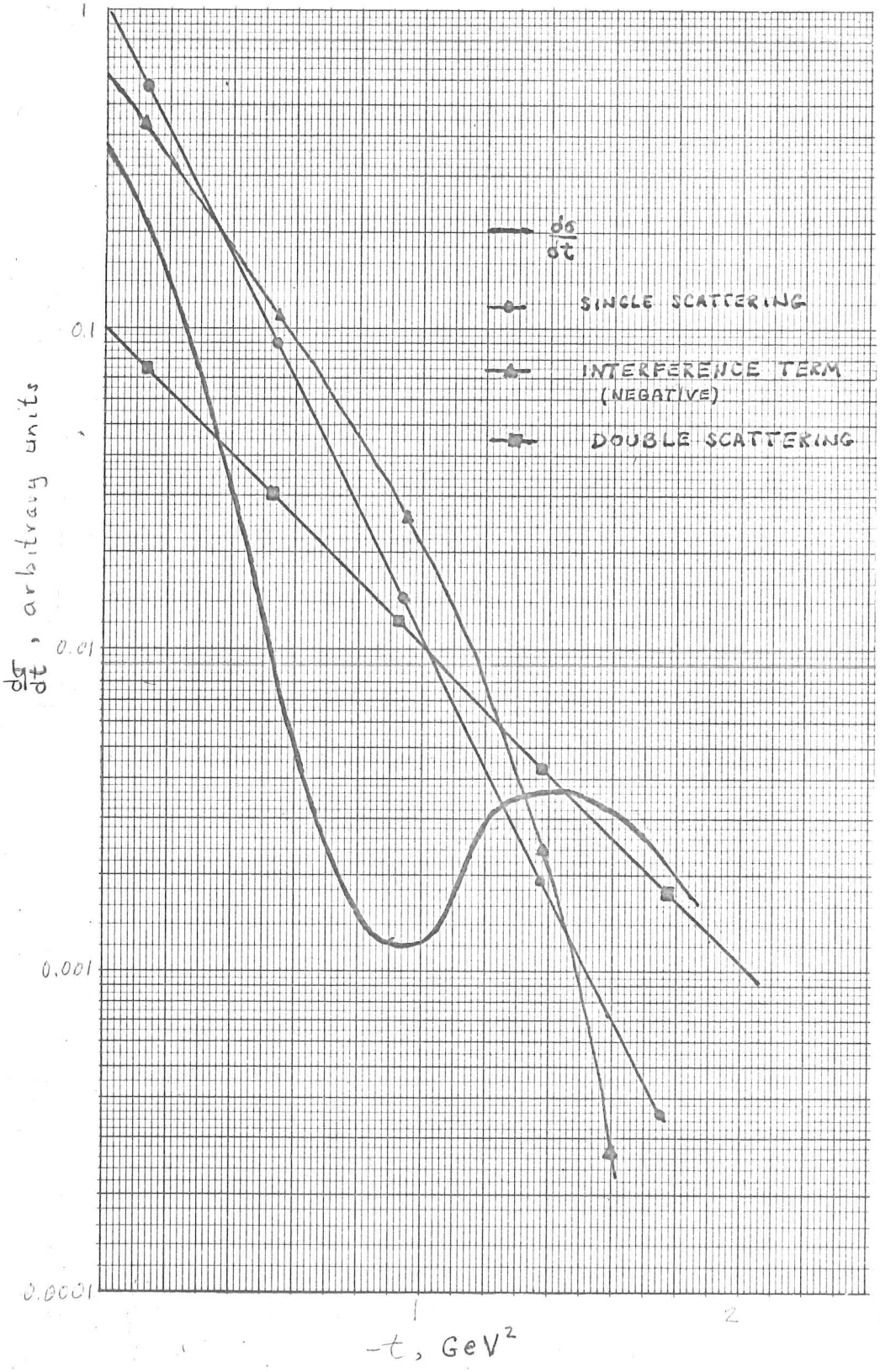

Figure 8-1 Contributions of single and double scattering and of the interference between them to the differential cross section in the one-pole model.

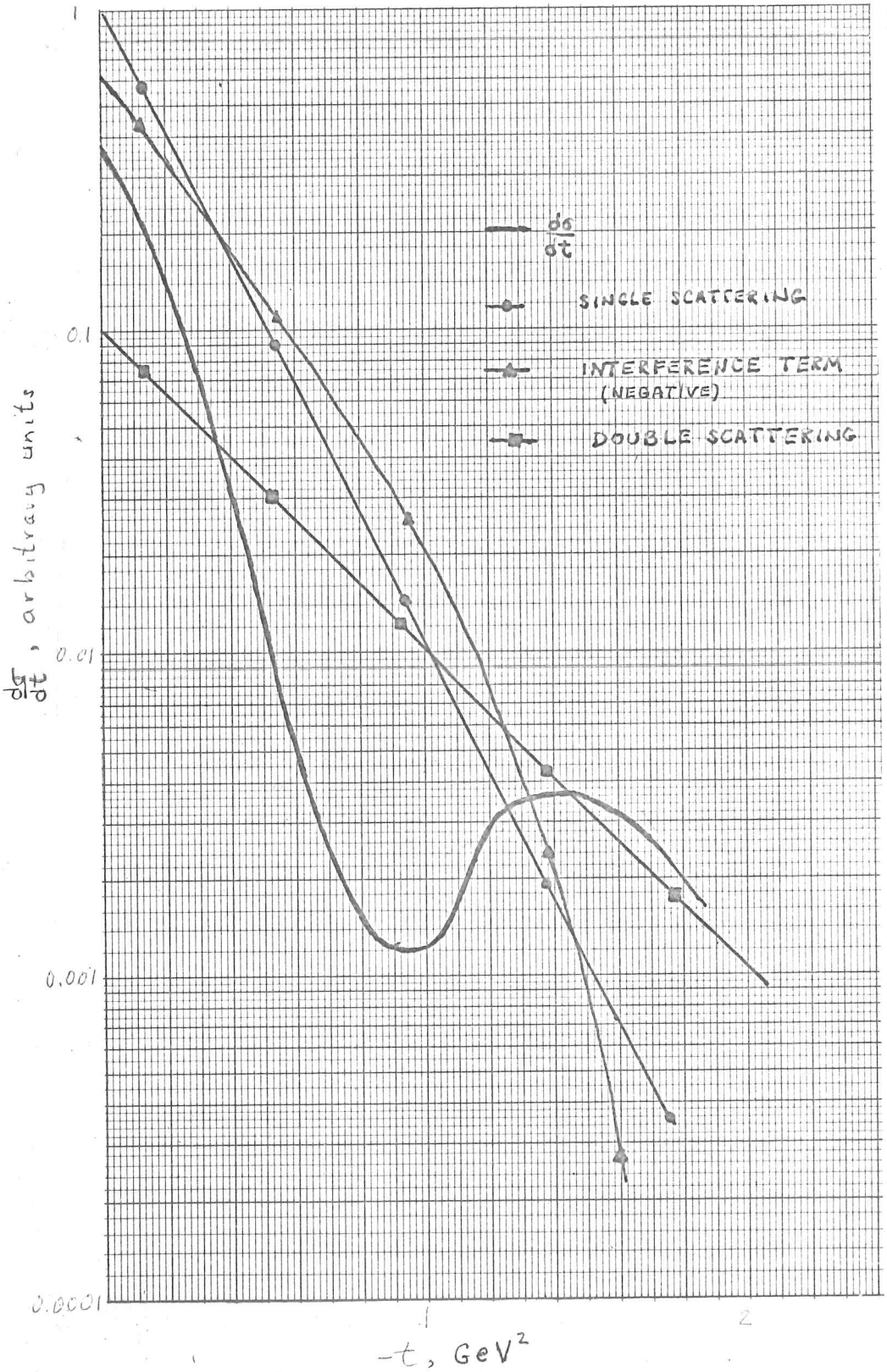

Figure 8-1 Contributions of single and double scattering and of the interference between them to the differential cross section in the one-pole model.

very slowly with increasing energy, but ultimately arrives at a limit in which the contribution of the simple scattering term is visible only within an arbitrarily small range of momentum transfer. From this limit it is possible to estimate whether the multiple scattering contributions to the total cross section are important, since their smallness implies that even at small momentum transfers only double scattering is seen. It follows that the extrapolated forward scattering is much smaller than the optical theorem value if the multiple scattering is negligible in σ_T. This is not the case in the presently available data, so we conclude that the multiple scattering effects are of some importance.

In order to estimate more accurately the magnitudes of these effects, we have applied this Regge formalism to the parametrization of the meson-nucleon scattering amplitudes. An immediate problem in such an application is choosing which interaction to Reggeize. The most basic level of elementarity indicates that the quark-quark amplitudes should be chosen, but it is also conceivable that quark-nucleon or quark-meson amplitudes might be more appropriate. Because the consideration of the antisymmetric sum rule in the preceding chapter required the decomposition of only the meson we shall begin by considering the quark-nucleon amplitudes to have the forms (8.2). Most of the formalism already developed can then be taken over directly. For comparison we shall also consider the quark-quark interaction to be Reggeized as the second stage of this calculation. We shall present the results of fitting the meson-nucleon

total cross section data of Galbraith et al.[6] with these parametrizations. The third possibility, decomposing only the nucleon and Reggeizing the quark-meson interaction, is not compatible with the treatment of the preceding chapter and will be temporarily neglected. It is, however, the simplest procedure to follow if spin complications are to be considered, and it will be used in the next chapter for this purpose.

We start therefore with the expressions for the scattering amplitudes analogous to (7.28). The six quark-nucleon amplitudes f_A, f_B, f_C, $f_{\bar{A}}$, $f_{\bar{B}}$, and $f_{\bar{C}}$ are to be set equal to the appropriate Regge-pole terms. For the non-strange quarks this procedure is exactly equivalent to the treatment of nucleon-nucleon scattering by means of Regge poles, which involves basically four poles with different sets of quantum numbers. These four poles we denote as usual by P, ρ, ω, and R, and their amplitudes are given respectively by

$$F_P(s,q^2) = - P \left(\frac{s}{is_o}\right)^{\alpha_P(q^2)} \tag{8.16a}$$

$$F_\rho(s,q^2) = + i\,\rho \left(\frac{s}{is_o}\right)^{\alpha_\rho(q^2)} \tag{8.16b}$$

$$F_\omega(s,q^2) = - i\,\omega \left(\frac{s}{is_o}\right)^{\alpha_\omega(q^2)} \tag{8.16c}$$

$$F_R(s,q^2) = + R \left(\frac{s}{is_o}\right)^{\alpha_R(q^2)} . \tag{8.16d}$$

The trajectories $\alpha_P(q^2)$, $\alpha_\rho(q^2)$, $\alpha_\omega(q^2)$, $\alpha_R(q^2)$ are taken as in (8.8) to be linear in q^2,

$$\alpha_i(q^2) = \alpha_i + \beta_i q^2$$

for i = P, ω, ρ, and R, and the residue constants P, ρ, ω, and R are real. In terms of these Regge amplitudes we have

$$f_A(s,q^2) = F_P(s,q^2) - F_\omega(s,q^2) \tag{8.17a}$$

$$f_{\bar{A}}(s,q^2) = F_P(s,q^2) + F_\omega(s,q^2) \tag{8.17b}$$

$$f_B(s,q^2) = F_\rho(s,q^2) - F_R(s,q^2) \tag{8.17c}$$

$$f_{\bar{B}}(s,q^2) = F_\rho(s,q^2) + F_R(s,q^2) \quad . \tag{8.17d}$$

For the scattering of the strange λ quark by the nucleon we assume that asymptopia has been reached and keep only the contribution of the Pomeranchuk pole. The scattering of quark and antiquark is then identical, and we have

$$f_C(s,q^2) = f_{\bar{C}}(s,q^2) = C_P(s,q^2) \equiv - C_P\left(\frac{s}{is_o}\right)^{\alpha_P(q^2)} \quad . \tag{8.18}$$

It is, of course, possible that the other I = 0 pole, the ω, could contribute to f_C and $f_{\bar{C}}$. In the single-scattering amplitudes, however, it is impossible to distinguish whether this is happening, because, as is shown by the antisymmetric sum rule, the equations

for the meson-nucleon amplitudes are linearly related. If we did include such a contribution by writing

$$f_C(s,q^2) = C_P(s,q^2) - C_\omega(s,q^2)$$

$$f_{\bar{C}}(s,q^2) = C_P(s,q^2) + C_\omega(s,q^2)$$

with

$$C_\omega(s,q^2) = -i\, C_\omega \left(\frac{s}{is_o}\right)^{\alpha_\omega(q^2)}$$

then the single-scattering parts of the meson-nucleon amplitudes would contain $C_\omega(s,q^2)$ only in the term $(F_\omega(s,q^2) + C_\omega(s,q^2))$. The determination of C_ω would depend then on the double-scattering terms in $K^{\pm}N$ scattering. The fitting program we have undertaken is probably not sufficiently sensitive to resolve C_ω, so we have omitted it.

It is convenient now to separate the amplitudes into single-scattering and double-scattering parts by writing

$$F_{MN}(s,q^2) = F^1_{MN}(s,q^2) + F^2_{MN}(s,q^2) . \qquad (8.19)$$

Then the contributions of the single-scattering terms to the six meson-nucleon elastic amplitudes are

$$F^1_{\pi^+P}(s,q^2) = 2\, F_P(s,q^2) + 2\, F_\rho(s,q^2) \qquad (8.20a)$$

$$F^{1}_{\pi^- P}(s,q^2) = 2\,F_P(s,q^2) - 2\,F_\rho(s,q^2) \qquad (8.20b)$$

$$F_{K^+P}(s,q^2) = F_P(s,q^2) - F_\omega(s,q^2) + F_\rho(s,q^2) - F_R(s,q^2) + C_P(s,q^2) \qquad (8.20c)$$

$$F_{K^+N}(s,q^2) = F_P(s,q^2) - F_\omega(s,q^2) - F_\rho(s,q^2) + F_R(s,q^2) + C_P(s,q^2) \qquad (8.20d)$$

$$F_{K^-P}(s,q^2) = F_P(s,q^2) + F_\omega(s,q^2) - F_\rho(s,q^2) - F_R(s,q^2) + C_P(s,q^2) \qquad (8.20e)$$

$$F_{K^-N}(s,q^2) = F_P(s,q^2) + F_\omega(s,q^2) + F_\rho(s,q^2) + F_R(s,q^2) + C_P(s,q^2) \; . \qquad (8.20f)$$

The double-scattering integrals can be performed using the result (7.18). We have seen already that the resulting terms depend explicitly upon both the slopes of the Regge trajectories and the normalization energy s_o, but only in that the slope of the diffraction peak must be correctly given. Rather than attempt to vary the slopes of the four trajectories, and also s_o, independently in fitting the data, we have chosen a common value for all the slopes and a value of s_o which give approximately the correct values for the physically observed diffraction peaks. Our choice is simply $\beta_P = \beta_\rho = \beta_\omega = \beta_K = 0.5\ \text{GeV}^{-2}$, $s_o = 0.002\ \text{GeV}^2$, which corresponds to a diffraction peak slope of around $9\ \text{GeV}^{-2}$ for s in the range 15-25 GeV^2. The results were tested and found insensitive to simultaneous variation of the β's and s_o in such a way that this slope remained relatively unchanged. Writing then $\beta_i = \beta$ for all the trajectories, we have for $q^2 = 0$ the

following contributions from double scattering:

$$F^2_{\pi^+P}(s,0) = \frac{i}{4k\beta\ln(\frac{s}{is_o})} \left\{ (-P(\frac{s}{is_o})^{\alpha_P} + i\omega(\frac{s}{is_o})^{\alpha_\omega} + i\rho(\frac{s}{is_o})^{\alpha_\rho} - R(\frac{s}{is_o})^{\alpha_R}) \times \right.$$

$$\left. \times (-P(\frac{s}{is_o})^{\alpha_P} - i\omega(\frac{s}{is_o})^{\alpha_\omega} + i\rho(\frac{s}{is_o})^{\alpha_\rho} + R(\frac{s}{is_o})^{\alpha_R}) \right\} \qquad (8.21a)$$

$$F^2_{\pi^-P}(s,0) = \frac{i}{4k\beta\ln(\frac{s}{is_o})} \left\{ (-P(\frac{s}{is_o})^{\alpha_P} + i\omega(\frac{s}{is_o})^{\alpha_\omega} - i\rho(\frac{s}{is_o})^{\alpha_\rho} + R(\frac{s}{is_o})^{\alpha_R}) \times \right.$$

$$\left. \times (-P(\frac{s}{is_o})^{\alpha_P} - i\omega(\frac{s}{is_o})^{\alpha_\omega} - i\rho(\frac{s}{is_o})^{\alpha_\rho} - R(\frac{s}{is_o})^{\alpha_R}) \right\} \qquad (8.21b)$$

$$F^2_{K^+P}(s,0) = \frac{i}{4k\beta\ln(\frac{s}{is_o})} \left\{ (-P(\frac{s}{is_o})^{\alpha_P} + i\omega(\frac{s}{is_o})^{\alpha_\omega} + i\rho(\frac{s}{is_o})^{\alpha_\rho} - R(\frac{s}{is_o})^{\alpha_R}) \times \right.$$

$$\left. (-C_P(\frac{s}{is_o})^{\alpha_P}) \right\} \qquad (8.21c)$$

$$F^2_{K^+N}(s,0) = \frac{i}{4k\beta\ln(\frac{s}{is_o})} \left\{ (-P(\frac{s}{is_o})^{\alpha_P} + i\omega(\frac{s}{is_o})^{\alpha_\omega} - i\rho(\frac{s}{is_o})^{\alpha_\rho} + R(\frac{s}{is_o})^{\alpha_R}) \times \right.$$

$$\left. (-C_P(\frac{s}{is_o})^{\alpha_P}) \right\} \qquad (8.21d)$$

$$F^2_{K^-P}(s,0) = \frac{i}{4k\beta\ln(\frac{s}{is_o})} \left\{(-P(\frac{s}{is_o})^{\alpha_P} - i\omega(\frac{s}{is_o})^{\alpha_\omega} - i\rho(\frac{s}{is_o})^{\alpha_\rho} - R(\frac{s}{is_o})^{\alpha_R}) \times \right.$$

$$\left. (-C_P(\frac{s}{is_o})^{\alpha_P}) \right\} \qquad (8.21e)$$

$$F^2_{K^-N}(s,0) = \frac{i}{4k\beta\ln(\frac{s}{is_o})} \left\{(-P(\frac{s}{is_o})^{\alpha_P} - i\omega(\frac{s}{is_o})^{\alpha_\omega} + i\rho(\frac{s}{is_o})^{\alpha_\rho} + R(\frac{s}{is_o})^{\alpha_R}) \times \right.$$

$$\left. (-C_P(\frac{s}{is_o})^{\alpha_P}) \right\} . \qquad (8.21f)$$

Taking the parametrizations of the scattering amplitudes given in equations (8.20) and (8.21), we have used the MINROS function minimization program to find the least-χ^2 fit to the data of Galbraith et al.[6] A comparison of the data and the fit obtained is shown in Figure 8-2. The fit is reasonably good, yielding a value of χ^2 = 65.53 for 42 data points and eight parameters.

In this fit α_P, the intercept of the Pomeranchuk trajectory, was held fixed at 1, corresponding to constant asymptotic total cross sections. The asymptote for pion-nucleon scattering is

$$\sigma_\infty(\pi N) = (19.6 \pm 3.8) \text{ mb} \qquad (8.22a)$$

and for kaon-nucleon

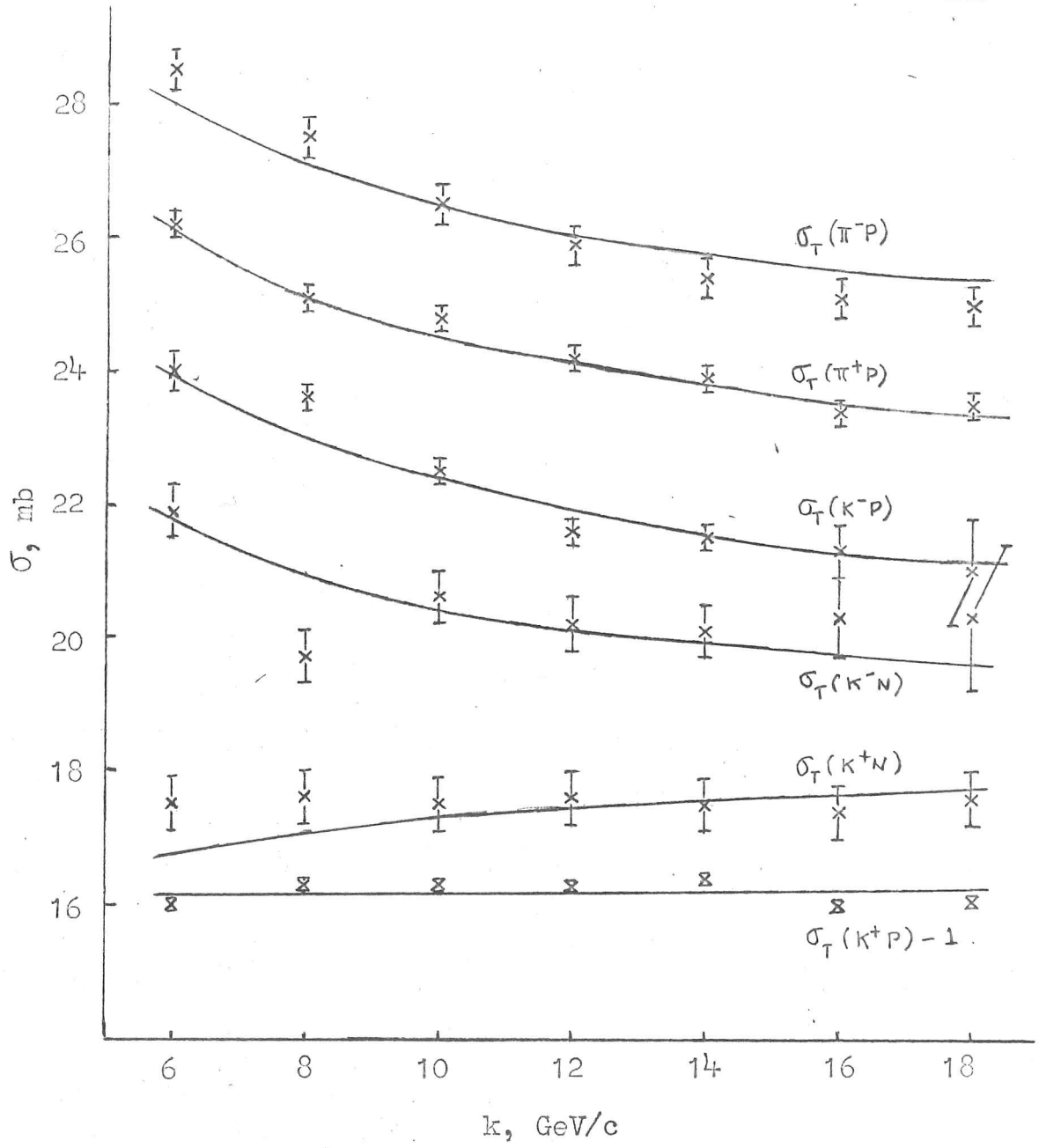

Figure 8-2 Comparison of the experimental data[2] with the fit obtained using P, ω, ρ and R poles to parametrize the quark-nucleon amplitude. The (K^+P) data have been displaced by 1 mb for clarity.

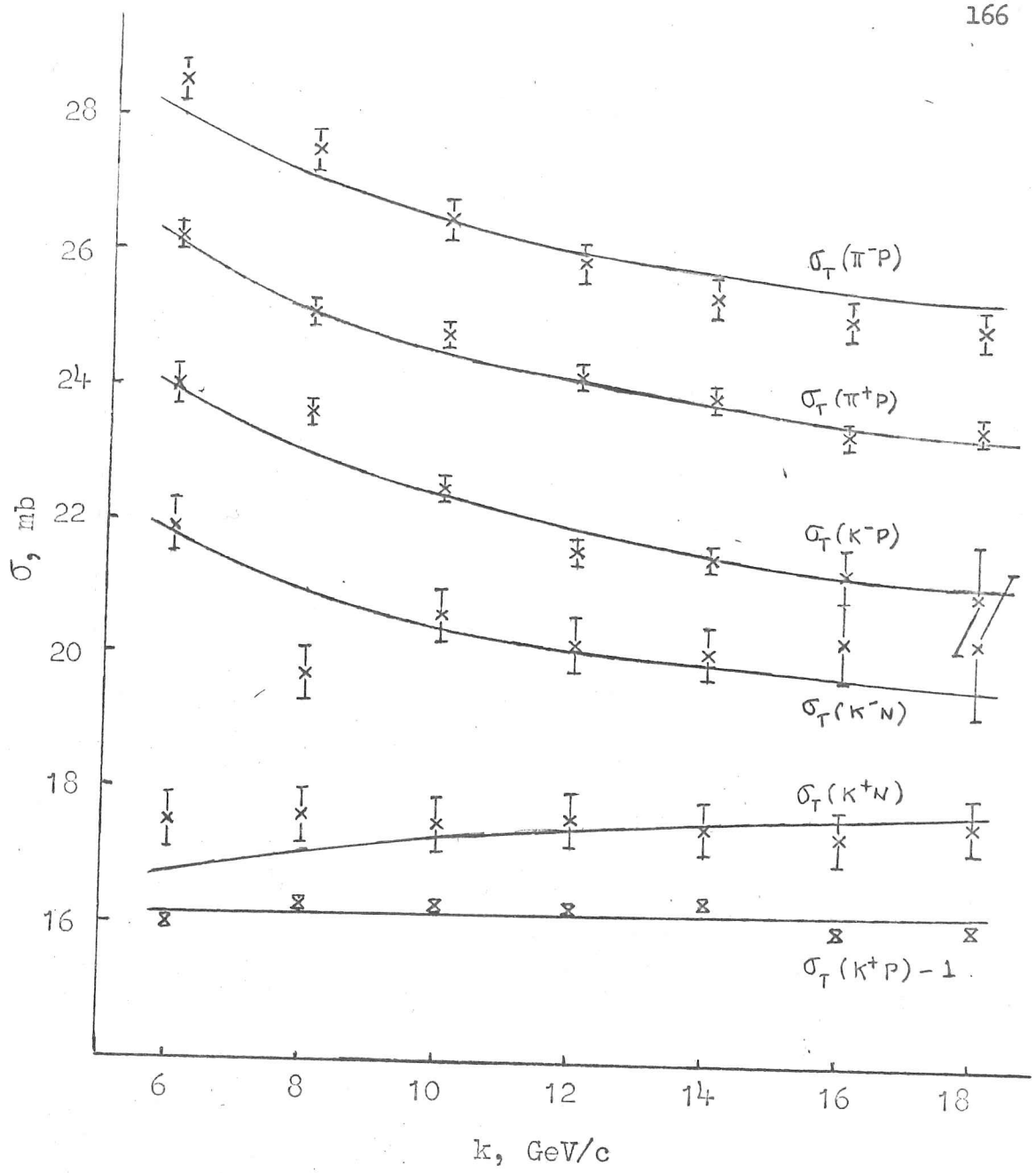

Figure 8-2 Comparison of the experimental data[2] with the fit obtained using P, ω, ρ and R poles to parametrize the quark-nucleon amplitude. The (K^+P) data have been displaced by 1 mb for clarity.

$$\sigma_{\infty}(KN) = (19.3 \pm 3.8) \text{ mb} \quad . \tag{8.22b}$$

The best fit values for the intercepts of the other three poles are

$$\alpha_{\rho} = 0.972 \pm 0.001 \tag{8.23a}$$

$$\alpha_{\omega} = 0.336 \pm 0.011 \tag{8.23b}$$

$$\alpha_{R} = 0.225 \pm 0.012 \quad . \tag{8.23c}$$

We notice in particular the high value of α_{ρ}. The reason for obtaining such a large intercept is twofold. Firstly, part of the shrinkage of the I=1 contribution to the pion-nucleon cross sections is now obtained from the logarithmic decrease of the double scattering term, so that the single scattering does not need to fall off quite as rapidly as in traditional Regge theory. Secondly, the double-scattering contributions of the ρ to the pion-nucleon total cross sections can be positive if α_{ρ} is near 1. These contributions come primarily from the combination of the ρ with the P and with itself in (8.21a) and (8.21b). Specifically, we have

$$\text{Im}\left[iP\left(\frac{s}{is_o}\right)^{\alpha_P} \times i\rho\left(\frac{s}{is_o}\right)^{\alpha_\rho} \right] \propto \cos\frac{\pi}{2}\alpha_{\rho} \tag{8.24a}$$

contributing oppositely to $(\pi^{+}P)$ and $(\pi^{-}P)$, while

$$\text{Im}\left[i(i\rho(\frac{s}{is_o})^{\alpha_\rho})^2\right] = -\rho^2(\frac{s}{s_o})^{2\alpha_\rho}\cos\pi\alpha_\rho \qquad (8.24b)$$

has the same sign in both the amplitudes. If α_ρ is greater than $\frac{1}{2}$, the right-hand side of (8.24b) is positive so that a part of the decreasing behaviour of the total cross sections is accounted for. If α_ρ is near 1, this term is quite important, while the splitting between (π^+P) and (π^-P) produced by (8.24a) is small.

The magnitudes of the different pole terms and their standard deviations are determined by the best fit values of the four residue parameters, which are

$$P = (8.31 \pm 0.16) \times 10^{-4} \qquad (8.25a)$$

$$C_P = (8.11 \pm 0.16) \times 10^{-4} \qquad (8.25b)$$

$$\rho = -(2.45 \pm 0.06) \times 10^{-3} \qquad (8.25c)$$

$$\omega = -(9.98 \pm 0.92) \times 10^{-2} \qquad (8.25d)$$

$$R = (0.129 \pm 0.018) \qquad (8.25e)$$

(In (8.25), and hereafter in this chapter, the dimensions of the residue constants will be mb GeV/c.) We show in Figure 8-3 the contributions of the different pole terms to single scattering, and in Figure 8-4 the double scattering contributions to the various total cross sections. The double scattering effects are fairly sizeable in all cases. In particular it should be noticed that the

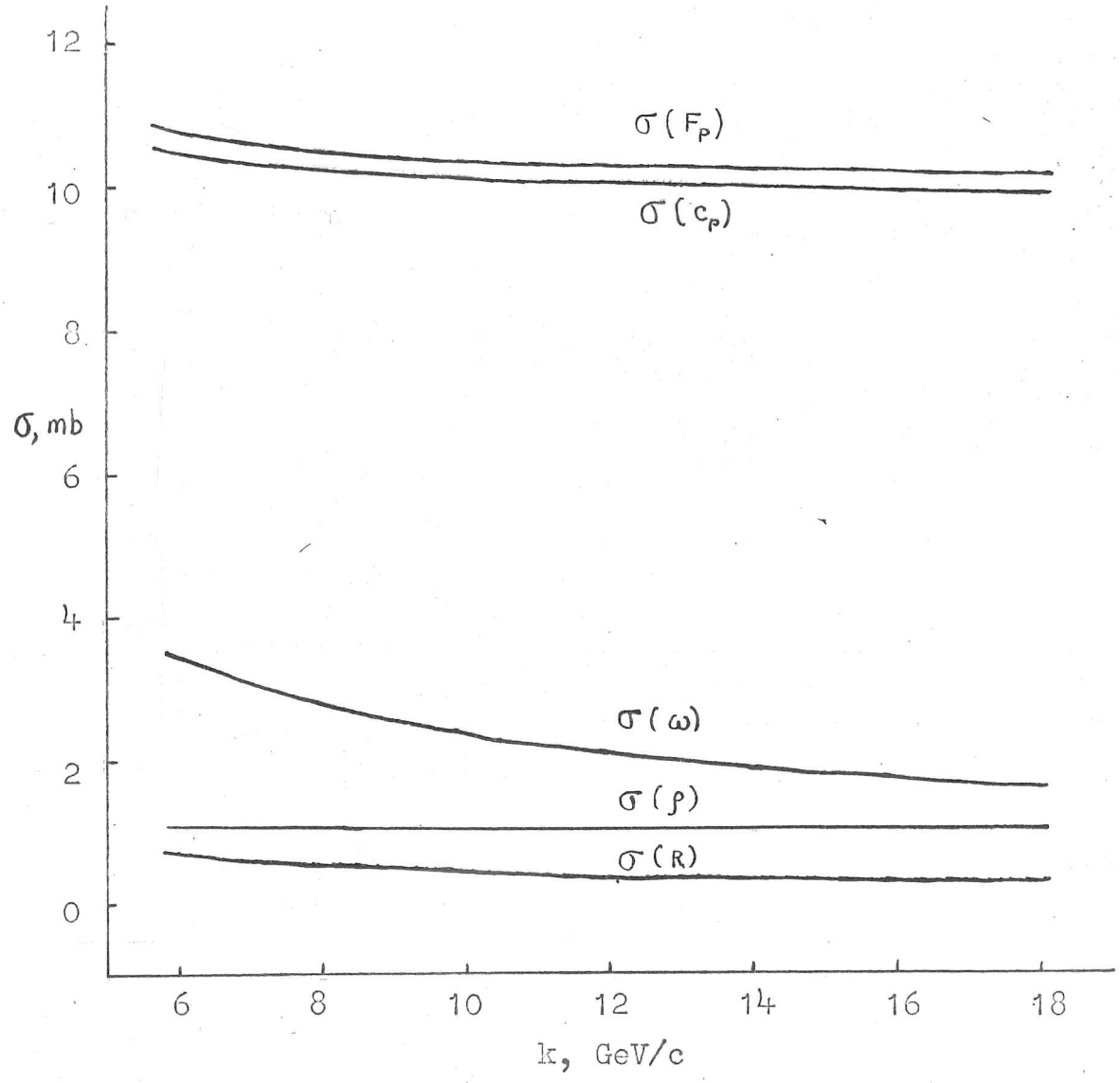

Figure 8-3 Contributions of the P, ω, ρ and R poles to single scattering in the fit shown in Figure 8-2.

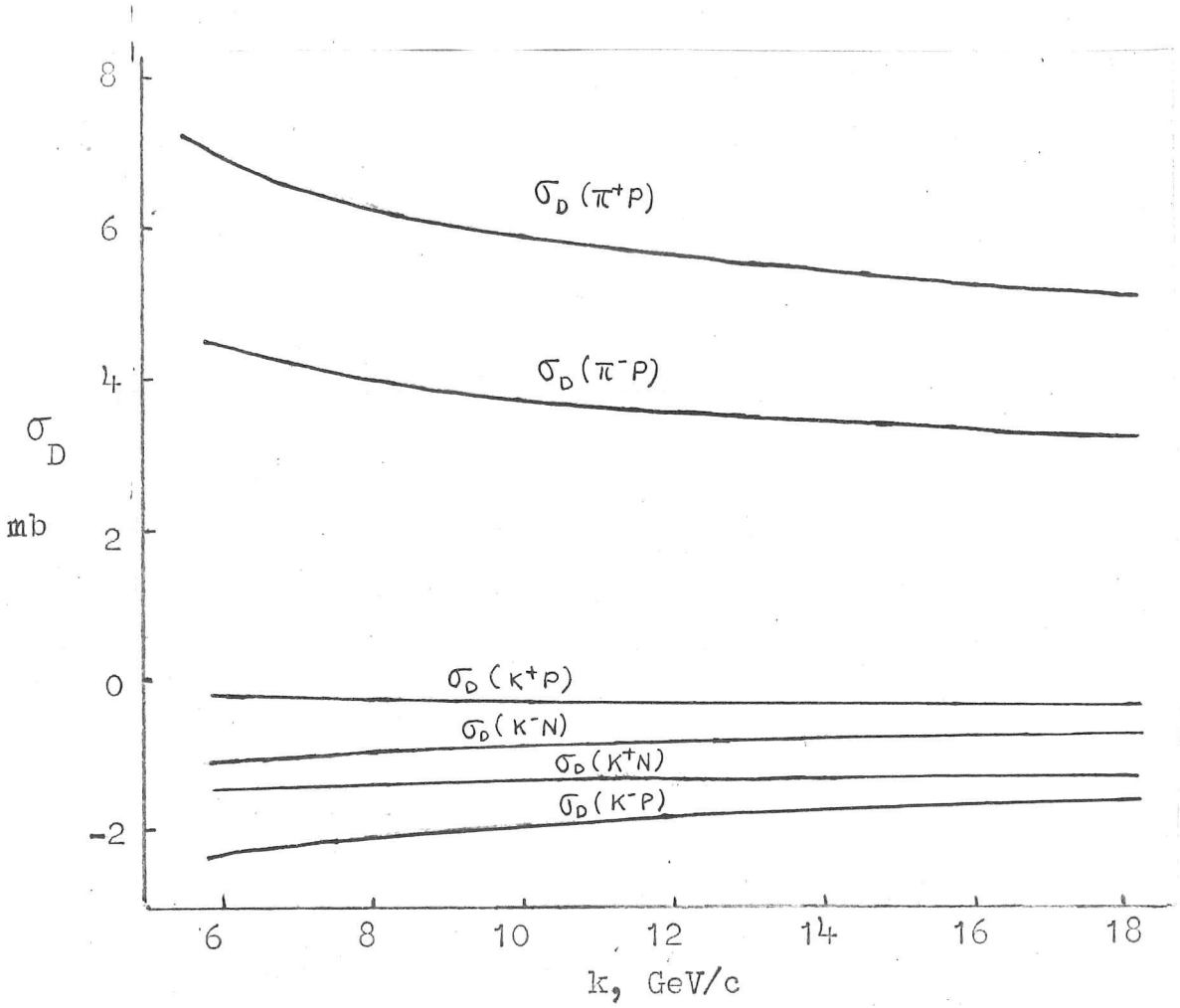

Figure 8-4 Double scattering contributions to the meson-nucleon total cross sections in the fit shown in Figure 8-2.

(K^+N) total cross sections are expected to increase toward $\sigma_\infty(KN)$ at higher energies as these effects disappear.

Although the decreasing behaviour of the pionic total cross sections is well reproduced by this fit, we can attempt to improve agreement still further by adding a second vacuum trajectory. We therefore replace $F_P(s,q^2)$ by

$$F_P(s,q^2) = -P\left(\frac{s}{is_o}\right)^{\alpha_P(q^2)} - P\left(\frac{s}{is_o}\right)^{\alpha_{P'}(q^2)} \qquad (8.16e)$$

and proceed exactly as before. A minimum value of χ^2 occurs with approximately the same parameters as in the fit without the P'. The P' intercept has a best fit value $\alpha_{P'} = 0.58$, and the contribution of the P' is only about 0.4 mb. The value of χ^2 is decreased to 61.94, which, in view of the addition of two new parameters, corresponds to no better fit than the original one.

The variance matrix for this fit has a negative diagonal element, indicating that the minimum found may not in fact be the true absolute minimum, although the MINROS program was unable to find any lower value of χ^2. The recommended procedure in such a case is to alter the χ^2 distribution in some manner which may remove the observed questionable minimum. We therefore changed the normalization energy to $s_o = 0.2$, thereby effectively increasing the importance of double scattering. A new minimum was then found with $\chi^2 = 49.67$ and positive diagonal elements for the variance matrix. Unfortunately, in this fit the contribution of the P trajectory was $\sim (-9 \pm 22)$ mb, and

the intercept of the P′ went to $\alpha_{P'} = 0.95$. This result is clearly not reasonable physically. It appears therefore that the addition of a second vacuum trajectory is not helpful in fitting this model to the data.

The third possibility used in the fitting, which was suggested by the unsuccessful attempt to include the P′ trajectory, is simply to let the intercept of the Pomeranchuk trajectory be a free parameter. This technique has previously been used in the traditional Regge framework by Cabibbo, Kokkedee, Horwitz, and Ne'eman[7], after whom it is called the CKHN model. With α_P free we obtain a best fit having $\chi^2 = 59.64$, a slight improvement over the original fit. The parameters are not appreciably different from those found previously, viz. for the intercepts

$$\alpha_P = 0.987 \pm 0.006 \qquad \alpha_\rho = 0.969 \pm 0.002$$
$$\alpha_\omega = 0.287 \pm 0.027 \qquad \alpha_R = 0.276 \pm 0.029 \tag{8.26}$$

and for the residues

$$P = (9.90 \pm 0.81) \times 10^{-4} \qquad C_P = (8.69 \pm 0.43) \times 10^{-4}$$
$$\omega = -0.146 \pm 0.032 \qquad \rho = -(2.31 \pm 0.14) \times 10^{-3} \tag{8.27}$$
$$R = (6.16 \pm 2.10) \times 10^{-2} \ .$$

We show in Figure 8-5 a comparison of this fit with the data, and in Figures 8-6 and 8-7 respectively the contributions of the different

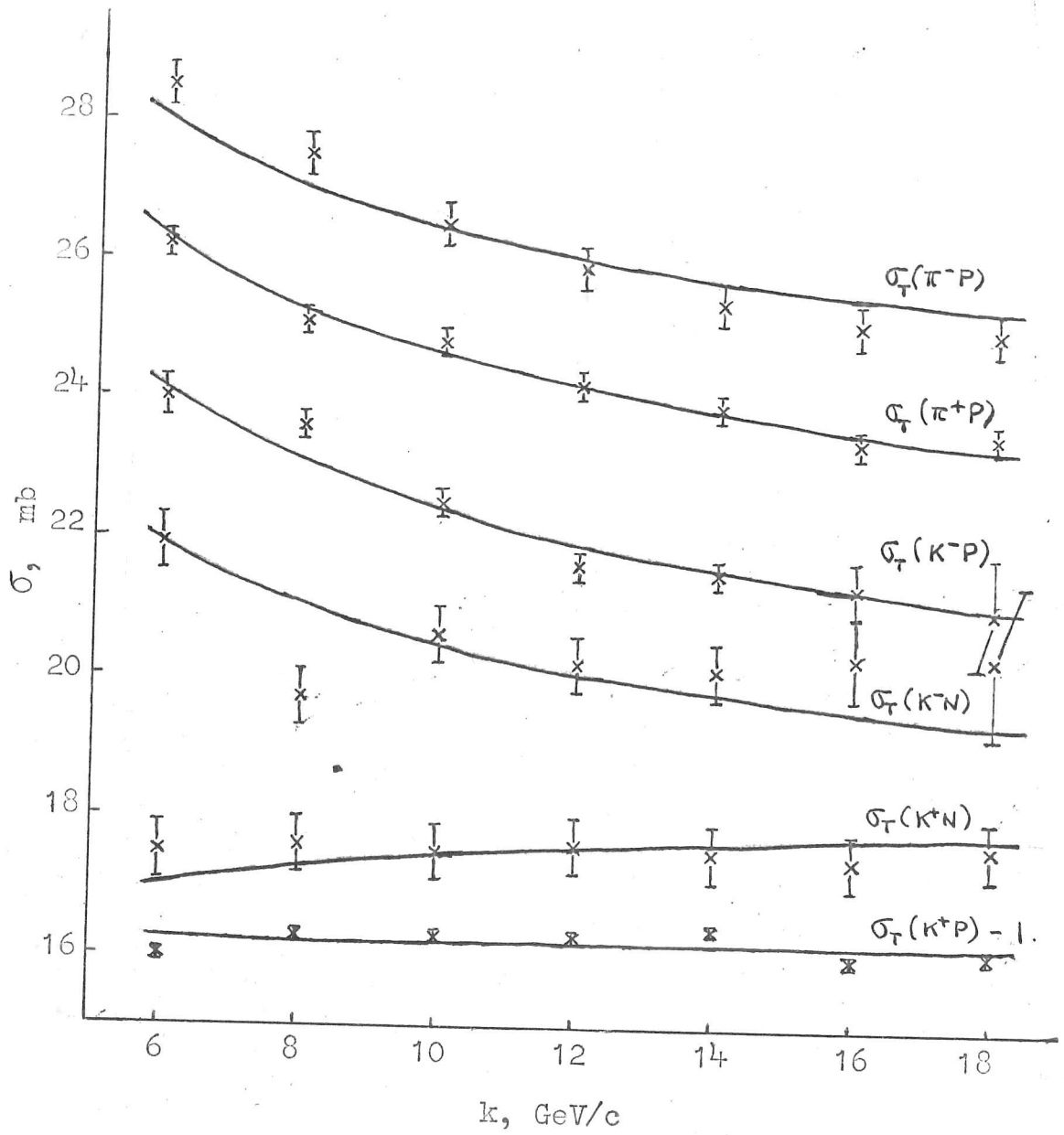

Figure 8-5 Comparison of the experimental data[2] with the fit obtained using a CKHN model to parametrize the quark-nucleon amplitude. The (K^+P) data have been displaced by 1 mb for clarity.

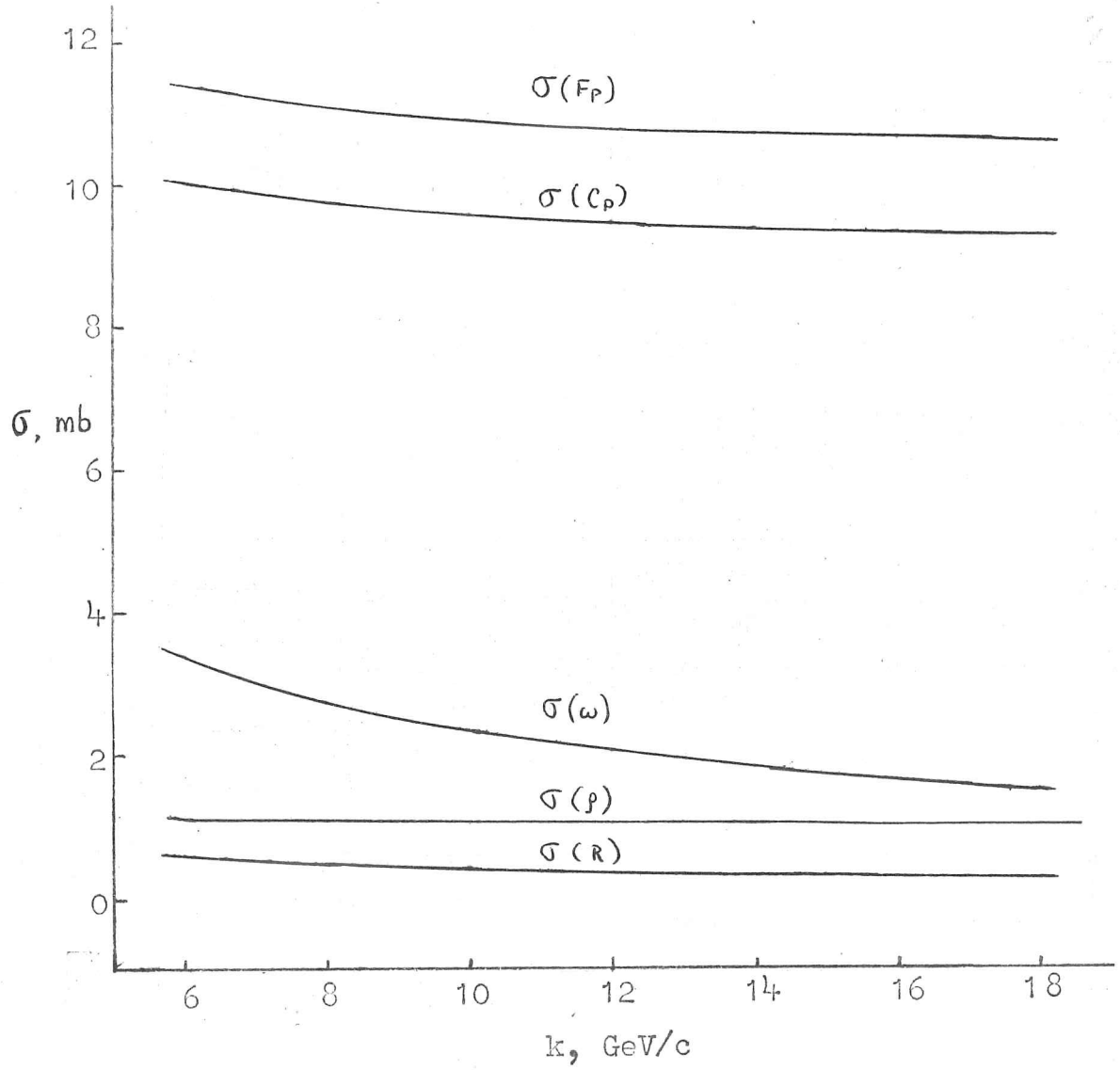

Figure 8-6 Contributions of the P, ω, ρ and R poles to single scattering in the fit shown in Figure 8-5.

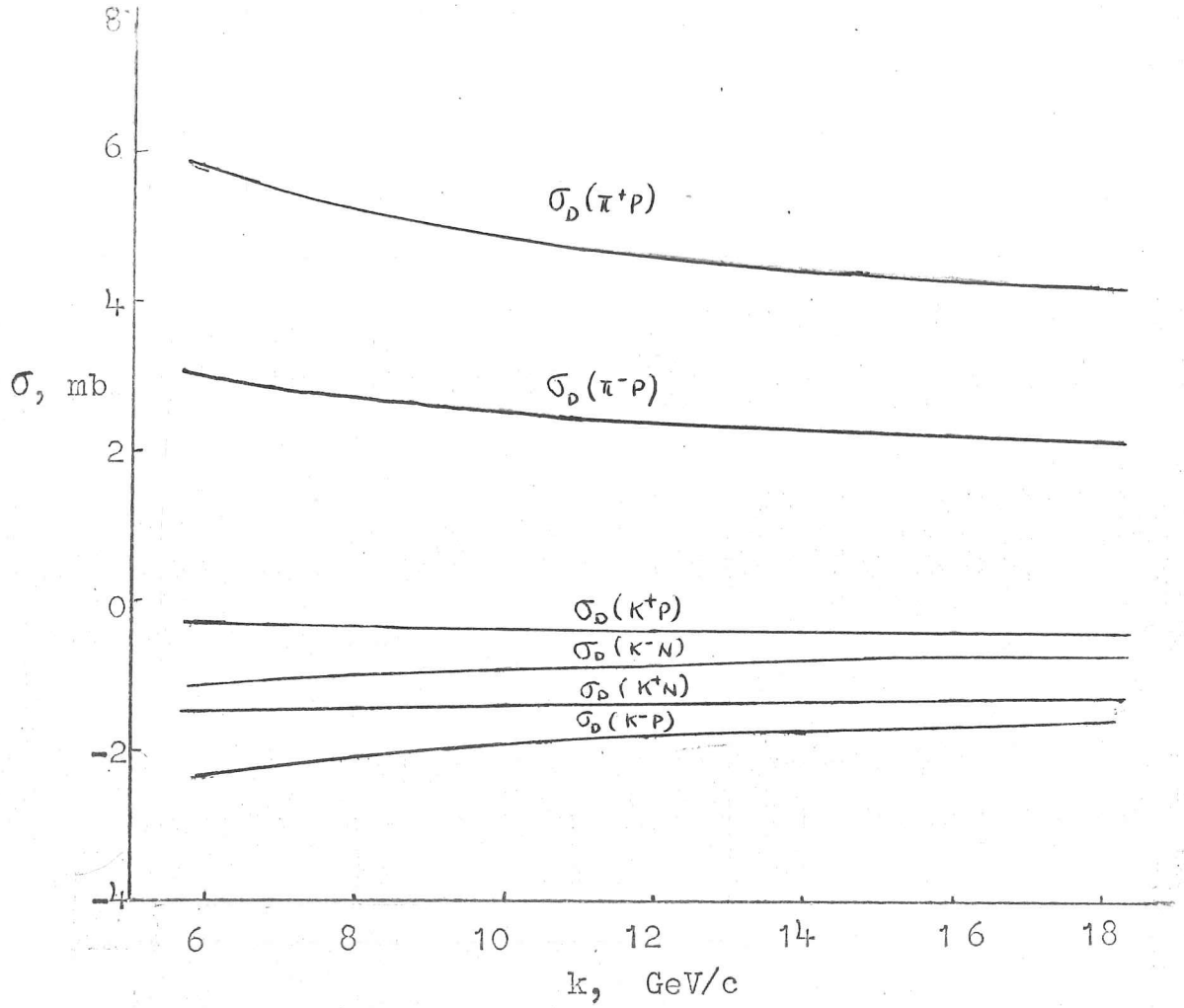

Figure 8-7 Double scattering contributions to the meson-nucleon total cross sections in the fit shown in Figure 8-5.

poles to single scattering and of the double scattering terms. For this fit, of course, the total cross sections go asymptotically to zero.

It is clear that the CKHN model is contained within the preceding parametrization using two vacuum trajectories; it corresponds to the constraint P = 0 in equation (8.16e). That the minimum for this model is less than the value found there confirms the prediction of the negative diagonal variance matrix element. There are, in other words, two regions of low χ^2 in the parameter space, corresponding to the difference in the physical concepts of the two models; between these regions there is a "mountain range" of high χ^2 values.

We next consider the possibility that the quark-quark interaction, rather than the quark-nucleon, should be put equal to the Regge pole term. Since the multiple scattering decomposition now contains up to sextuple-scattering terms, the results are much more complicated; they can, however, be obtained directly from what has already been done by simply finding the structure of the quark-nucleon amplitudes in terms of the Reggeized quark-quark interactions. This calculation is tedious but straightforward, and we shall only give the results. The quark-quark amplitudes are exactly analogous in terms of the Regge poles exchanged to the quark-nucleon amplitudes already written down. The interaction between two non-strange quarks is given by the P, ω, ρ, and R poles exactly as in (8.17), except that f_A and $f_{\bar{A}}$ (f_B and $f_{\bar{B}}$) now refer

to the quark-quark interactions with I = 0 (I = 1) in the crossed channel. Similarly the interaction between strange and non-strange quarks is again assumed to have reached asymptopia and is expressed by using only the Pomeranchuk trajectory, as in (8.18). We break up the meson-nucleon amplitudes into the contributions of the different orders of multiple scattering, writing this time

$$F_{M\mathcal{N}}(s,q^2) = \sum_{i=1}^{6} F^i_{M\mathcal{N}}(s,q^2) \quad . \tag{8.28}$$

Again all trajectory slopes are chosen equal, $\beta_i = \beta = 0.5$, and we put $s_o = 0.002\ \text{GeV}^2$. For $q^2 = 0$, the contributions of the Regge amplitudes to the various terms are then conveniently expressed by writing

$$A = -P\left(\frac{s}{is_o}\right)^{\alpha_P} - i\omega\left(\frac{s}{is_o}\right)^{\alpha_\omega} \tag{8.29a}$$

$$\bar{A} = -P\left(\frac{s}{is_o}\right)^{\alpha_P} + i\omega\left(\frac{s}{is_o}\right)^{\alpha_\omega} \tag{8.29b}$$

$$B = i\rho\left(\frac{s}{is_o}\right)^{\alpha_\rho} - R\left(\frac{s}{is_o}\right)^{\alpha_R} \tag{8.29c}$$

$$\bar{B} = i\rho\left(\frac{s}{is_o}\right)^{\alpha_\rho} + R\left(\frac{s}{is_o}\right)^{\alpha_R} \tag{8.29d}$$

$$C = -C\left(\frac{s}{is_o}\right)^{\alpha_P} \tag{8.29e}$$

in terms of which we obtain the following equations.

Single Scattering:

$$F^{1}_{\pi^+P}(s,0) = 3(A + \bar{A}) + B + \bar{B}$$

$$F^{1}_{\pi^-P}(s,0) = 3(A + \bar{A}) - B - \bar{B}$$

$$F^{1}_{K^+P}(s,0) = 3(A + C) + B$$

$$F^{1}_{K^+N}(s,0) = 3(A + C) - B \qquad (8.30)$$

$$F^{1}_{K^-P}(s,0) = 3(\bar{A} + C) - \bar{B}$$

$$F^{1}_{K^-N}(s,0) = 3(\bar{A} + C) + \bar{B}$$

Double Scattering:

$$F^{2}_{\pi^+P}(s,0) = \frac{1}{4k\beta \ln(\frac{s}{is_o})} \left\{ 3[A^2+\bar{A}^2]+AB+\bar{A}\bar{B}-3[B^2+\bar{B}^2]+(3A+B)(3\bar{A}+\bar{B}) \right\} \qquad (8.31)$$

$$F^{2}_{\pi^-P}(s,0) = \frac{1}{4k\beta \ln(\frac{s}{is_o})} \left\{ 3[A^2+\bar{A}^2]-AB-\bar{A}\bar{B}-3[B^2+\bar{B}^2]+(3A-B)(3\bar{A}-\bar{B}) \right\} \qquad \text{(cont.)}$$

$$F^2_{K^+P}(s,0) = \frac{i}{4k\beta\ln(\frac{s}{is_o})}\left\{3A^2+AB-3B^2+3C^2+3C(3A+B)\right\}$$

$$F^2_{K^+N}(s,0) = \frac{i}{4k\beta\ln(\frac{s}{is_o})}\left\{3A^2-AB-3B^2+3C^2+3C(3A-B)\right\}$$

$$F^2_{K^-P}(s,0) = \frac{i}{4k\beta\ln(\frac{s}{is_o})}\left\{3\bar{A}^2-\bar{A}\bar{B}-3\bar{B}^2+3C^2+3C(3\bar{A}-\bar{B})\right\} \qquad (8.31)$$

$$F^2_{K^-N}(s,0) = \frac{i}{4k\beta\ln(\frac{s}{is_o})}\left\{3\bar{A}^2+\bar{A}\bar{B}-3\bar{B}^2+3C^2+3C(3\bar{A}+\bar{B})\right\}$$

Triple Scattering:

$$F^3_{\pi^+P}(s,0) = \tfrac{1}{3}\left(\frac{i}{2k\beta\ln(\frac{s}{is_o})}\right)^2\left\{A^3+\bar{A}^3+\tfrac{2}{3}\left[A^2B+\bar{A}^2\bar{B}\right]-2\left[AB^2+\bar{A}\bar{B}^2\right]\right.$$

$$\left.-\tfrac{5}{3}\left[B^3+\bar{B}^3\right]+(3A+B)\left[3\bar{A}^2+\bar{A}\bar{B}-3\bar{B}^2\right]+(3\bar{A}+\bar{B})\left[3A^2+AB-3B^2\right]\right\}$$

$$F^3_{\pi^-P}(s,0) = \tfrac{1}{3}\left(\frac{i}{2k\beta\ln(\frac{s}{is_o})}\right)^2\left\{A^3+\bar{A}^3-\tfrac{2}{3}\left[A^2B+\bar{A}^2\bar{B}\right]-2\left[AB^2+\bar{A}\bar{B}^2\right]\right. \qquad (8.32)\ \text{(cont.)}$$

$$\left.+\tfrac{5}{3}\left[B^3+\bar{B}^3\right]+(3A-B)\left[3\bar{A}^2-\bar{A}\bar{B}-3\bar{B}^2\right]+(3\bar{A}-\bar{B})\left[3A^2-AB-3B^2\right]\right\}$$

$$F^3_{K^+P}(s,0) = \tfrac{1}{3}\left(\frac{i}{2k\beta\ln(\frac{s}{is_o})}\right)^2\left\{A^3+\tfrac{2}{3}A^2B-2AB^2-\tfrac{5}{3}B^3+C^3+3C^2(3A+B)\right.$$

$$\left.+\,3C[3A^2+AB-3B^2]\right\}$$

$$F^3_{K^+N}(s,0) = \tfrac{1}{3}\left(\frac{i}{2k\beta\ln(\frac{s}{is_o})}\right)^2\left\{A^3-\tfrac{2}{3}A^2B-2AB^2+\tfrac{5}{3}B^3+C^3+3C^2(3A-B)\right.$$

$$\left.+\,3C[3A^2-AB-3B^2]\right\} \qquad (8.32)$$

$$F^3_{K^-P}(s,0) = \tfrac{1}{3}\left(\frac{i}{2k\beta\ln(\frac{s}{is_o})}\right)^2\left\{\bar{A}^3-\tfrac{2}{3}\bar{A}^2\bar{B}-2\bar{A}\bar{B}^2+\tfrac{5}{3}\bar{B}^3+C^3+3C^2(3\bar{A}-\bar{B})\right.$$

$$\left.+\,3C[3\bar{A}^2-\bar{A}\bar{B}-3\bar{B}^2]\right\}$$

$$F^3_{K^-N}(s,0) = \tfrac{1}{3}\left(\frac{i}{2k\beta\ln(\frac{s}{is_o})}\right)^2\left\{\bar{A}^3+\tfrac{2}{3}\bar{A}^2\bar{B}-2\bar{A}\bar{B}^2+\tfrac{5}{3}\bar{B}^3+C^3+3C^2(3\bar{A}+\bar{B})\right.$$

$$\left.+\,3C[3\bar{A}^2+\bar{A}\bar{B}-3\bar{B}^2]\right\}$$

Quadruple Scattering:

$$F^4_{\pi^+P}(s,0) = \tfrac{1}{4}\left(\frac{i}{2k\beta\ln(\frac{s}{is_o})}\right)^3 \Big\{(3A+B)[\bar{A}^3+\tfrac{2}{3}\bar{A}^2\bar{B}-2\bar{A}\bar{B}^2-\tfrac{5}{3}\bar{B}^3] +$$

$$+ (3\bar{A}+\bar{B})[A^3+\tfrac{2}{3}A^2B-2AB^2-\tfrac{5}{3}B^3]+[3A^2+AB-3B^2][3\bar{A}^2+\bar{A}\bar{B}-3\bar{B}^2]\Big\}$$

$$F^4_{\pi^-P}(s,0) = \tfrac{1}{4}\left(\frac{i}{2k\beta\ln(\frac{s}{is_o})}\right)^3 \Big\{(3A-B)[\bar{A}^3-\tfrac{2}{3}\bar{A}^2\bar{B}-2\bar{A}\bar{B}^2+\tfrac{5}{3}\bar{B}^3] +$$

$$+ (3\bar{A}-\bar{B})[A^3-\tfrac{2}{3}A^2B-2AB^2+\tfrac{5}{3}B^3]+[3A^2-AB-3B^3][3\bar{A}^2+\bar{A}\bar{B}-3\bar{B}^2]\Big\}$$

$$F^4_{K^+P}(s,0) = \tfrac{1}{4}\left(\frac{i}{2k\beta\ln(\frac{s}{is_o})}\right)^3 \Big\{C^3(3A+B)+3C^2[3A^2+AB-3B^2]$$

$$+ 3C[A^3+\tfrac{2}{3}A^2B-2AB^2-\tfrac{5}{3}B^3]\Big\} \qquad (8.33)\ (\text{cont.})$$

$$F^4_{K^+N}(s,0) = \tfrac{1}{4}\left(\frac{i}{2k\beta\ln(\frac{s}{is_o})}\right)^3 \Big\{C^3(3A-B)+3C^2[3A^2-AB-3B^2]$$

$$+ 3C[A^3-\tfrac{2}{3}A^2B-2AB^2+\tfrac{5}{3}B^3]\Big\}$$

$$F^4_{K^-P}(s,0) = \tfrac{1}{4}\left(\frac{i}{2k\beta\ln(\frac{s}{is_o})}\right)^3 \Big\{C^3(3\bar{A}-\bar{B})+3C^2[3\bar{A}^2-\bar{A}\bar{B}-3\bar{B}^2]$$

$$+ 3C[\bar{A}^3-\tfrac{2}{3}\bar{A}^2\bar{B}-2\bar{A}\bar{B}^2+\tfrac{5}{3}\bar{B}^3]\Big\}$$

$$F^{4}_{K^-N}(s,0) = \tfrac{1}{4}\left(\frac{i}{2k\beta\ln(\frac{s}{is_o})}\right)^3 \left\{C^3(3\bar{A}+\bar{B})+3C^2[3\bar{A}^2+\bar{A}\bar{B}-3\bar{B}^2]\right.$$

$$\left. + 3C[\bar{A}^3+\tfrac{2}{3}\bar{A}^2\bar{B}-2\bar{A}\bar{B}^2-\tfrac{5}{3}\bar{B}^3]\right\} \qquad (8.33)$$

Quintuple Scattering:

$$F^{5}_{\pi^+P}(s,0) = \frac{1}{5}\left(\frac{i}{2k\beta\ln(\frac{s}{is_o})}\right)^4 \left\{[3A^2+AB-3B^2][\bar{A}^3+\tfrac{2}{3}\bar{A}^2\bar{B}-2\bar{A}\bar{B}^2-\tfrac{5}{3}\bar{B}^3]\right.$$

$$\left. + [A^3+\tfrac{2}{3}A^2B-2AB^2-\tfrac{5}{3}B^3][3\bar{A}^2+\bar{A}\bar{B}-3\bar{B}^2]\right\}$$

$$F^{5}_{\pi^-P}(s,0) = \frac{1}{5}\left(\frac{i}{2k\beta\ln(\frac{s}{is_o})}\right)^4 \left\{[3A^2-AB-3B^2][\bar{A}^3-\tfrac{2}{3}\bar{A}^2\bar{B}-2\bar{A}\bar{B}^2+\tfrac{5}{3}\bar{B}^3]\right.$$

$$\left. + [A^3-\tfrac{2}{3}A^2B-2AB^2+\tfrac{5}{3}B^3][3\bar{A}^2-\bar{A}\bar{B}-3\bar{B}^2]\right\} \qquad (8.34)\ (\text{cont.})$$

$$F^{5}_{K^+P}(s,0) = \frac{1}{5}\left(\frac{i}{2k\beta\ln(\frac{s}{is_o})}\right)^4 \left\{C^3[3A^2+AB-3B^2)+3C^2[A^3+\tfrac{2}{3}A^2B-2AB^2-\tfrac{5}{3}B^3]\right\}$$

$$F^{5}_{K^+N}(s,0) = \frac{1}{5}\left(\frac{i}{2k\beta\ln(\frac{s}{is_o})}\right)^4 \left\{C^3[3A^2-AB-3B^2]+3C^2[A^3-\tfrac{2}{3}A^2B-2AB^2+\tfrac{5}{3}B^3]\right\}$$

$$F^5_{K^-P}(s,0) = \frac{1}{5}\left(\frac{i}{2k\beta\ln(\frac{s}{is_o})}\right)^4 \left\{C^3[3\bar{A}^2-\bar{A}\bar{B}-3\bar{B}^2]+3C^2[\bar{A}^3-\tfrac{2}{3}\bar{A}^2\bar{B}-2\bar{A}\bar{B}^2+\tfrac{5}{3}\bar{B}^3]\right\}$$

(8.34)

$$F^5_{K^-N}(s,0) = \frac{1}{5}\left(\frac{i}{2k\beta\ln(\frac{s}{is_o})}\right)^4 \left\{C^3[3\bar{A}^2+\bar{A}\bar{B}-3\bar{B}^2]+3C^2[\bar{A}^3+\tfrac{2}{3}\bar{A}^2\bar{B}-2\bar{A}\bar{B}^2-\tfrac{5}{3}\bar{B}^3]\right\}$$

Sextuple Scattering:

$$F^6_{\pi^+P}(s,0) = \frac{1}{6}\left(\frac{i}{2k\beta\ln(\frac{s}{is_o})}\right)^5 \left\{[A^3+\tfrac{2}{3}A^2B-2AB^2-\tfrac{5}{3}B^3][\bar{A}^3+\tfrac{2}{3}\bar{A}^2\bar{B}-2\bar{A}\bar{B}^2-\tfrac{5}{3}\bar{B}^3]\right\}$$

$$F^6_{\pi^-P}(s,0) = \frac{1}{6}\left(\frac{i}{2k\beta\ln(\frac{s}{is_o})}\right)^5 \left\{[A^3-\tfrac{2}{3}A^2B-2AB^2+\tfrac{5}{3}B^3][\bar{A}^3-\tfrac{2}{3}\bar{A}^2\bar{B}-2\bar{A}\bar{B}^2+\tfrac{5}{3}\bar{B}^3]\right\}$$

$$F^6_{K^+P}(s,0) = \frac{1}{6}\left(\frac{i}{2k\beta\ln(\frac{s}{is_o})}\right)^5 \left\{C^3[A^3+\tfrac{2}{3}A^2B-2AB^2-\tfrac{5}{3}B^3]\right\}$$

(8.35)

$$F^6_{K^+N}(s,0) = \frac{1}{6}\left(\frac{i}{2k\beta\ln(\frac{s}{is_o})}\right)^5 \left\{C^3[A^3-\tfrac{2}{3}A^2B-2AB^2+\tfrac{5}{3}B^3]\right\}$$

$$F^6_{K^-P}(s,0) = \frac{1}{6}\left(\frac{i}{2k\beta\ln(\frac{s}{is_o})}\right)^5 \left\{C^3[\bar{A}^3-\tfrac{2}{3}\bar{A}^2\bar{B}-2\bar{A}\bar{B}^2+\tfrac{5}{3}\bar{B}^3]\right\}$$

$$F^6_{K^-N}(s,0) = \frac{1}{6}\left(\frac{i}{2k\beta\ln(\frac{s}{is_o})}\right)^5 \left\{C^3[\bar{A}^3+\tfrac{2}{3}\bar{A}^2\bar{B}-2\bar{A}\bar{B}^2-\tfrac{5}{3}\bar{B}^3]\right\}$$

With this parametrization we follow again the same procedure, using the MINROS function minimization routine to fit the meson-nucleon total cross section data. Taking first only the four poles P, ρ, ω, and R, with the Pomeranchuk intercept α_P fixed at 1, results in the fit pictured in Figure 8-8. The parametrization is not capable of reproducing the decreasing behaviour of the pion-nucleon total cross sections. The best fit passes below the lower energy (πP) data and above the higher, and the resulting value of $\chi^2 = 190.02$ reflects the poorness of the fit to these points. Since $\alpha_P = 1$, the total cross sections become constant as $s \to \infty$ with asymptotes

$$\sigma_\infty(\pi N) = (27.2 \pm 0.8) \text{ mb} \qquad (8.36a)$$

$$\sigma_\infty(KN) = (20.1 \pm 1.3) \text{ mb} \; . \qquad (8.36b)$$

The value of $\sigma_\infty(\pi N)$ is influenced by the poor fit to the (πP) data; therefore it is not surprising that it is considerably above the measured cross sections at the fitted energies. More faith can be put in $\sigma_\infty(KN)$, since it is much less dependent on the fit to the (πP) data.

The results are generally satisfactory in other respects. The best fit values for the intercepts of the three free trajectories are

$$\alpha_\rho = 0.644 \pm 0.061 \qquad (8.37a)$$

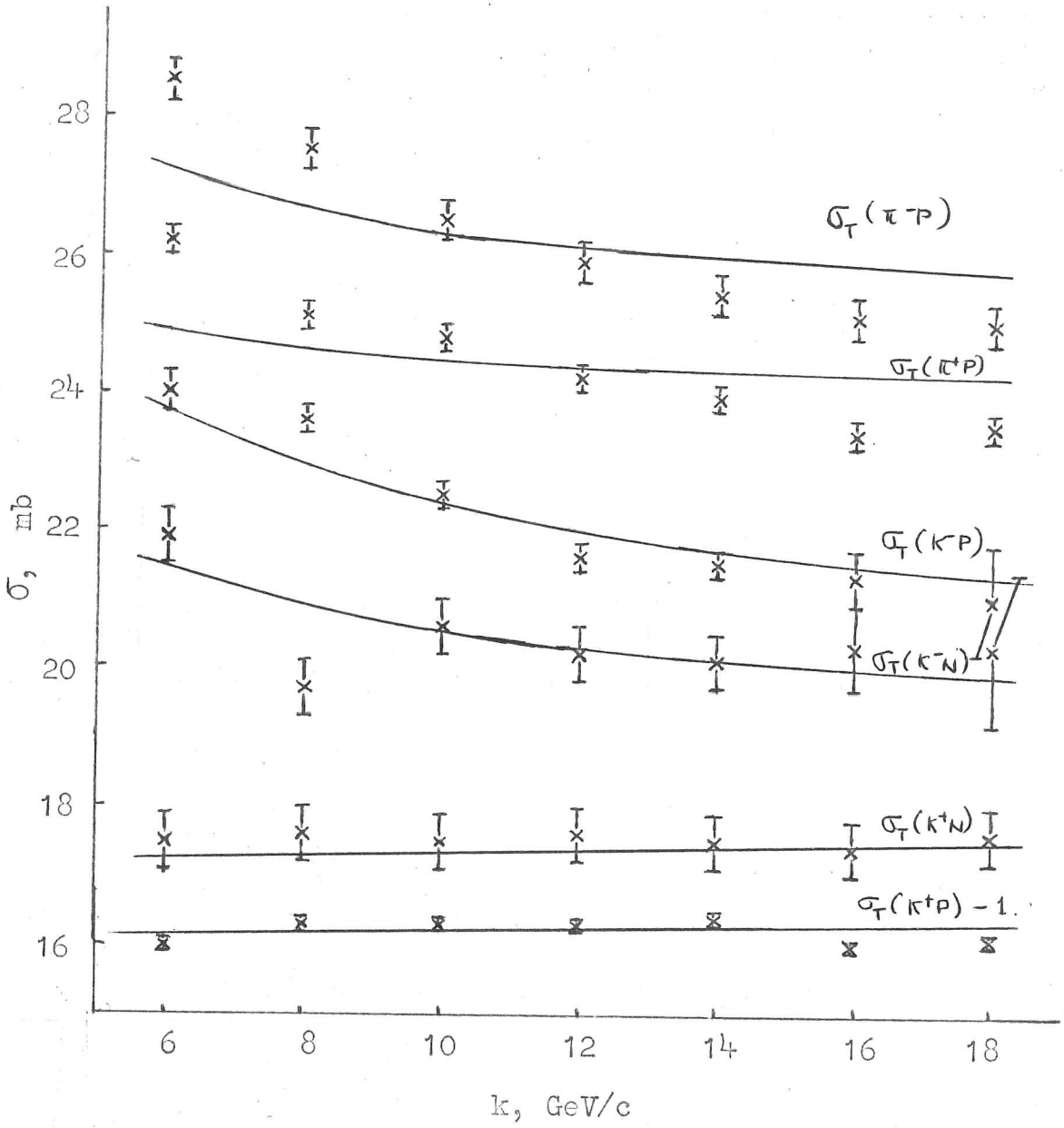

Figure 8-8 Comparison of the experimental data[2] with the fit obtained using P, ω, ρ and R poles to parametrize the quark-quark amplitude. The (K^+P) data have been displaced by 1 mb for clarity.

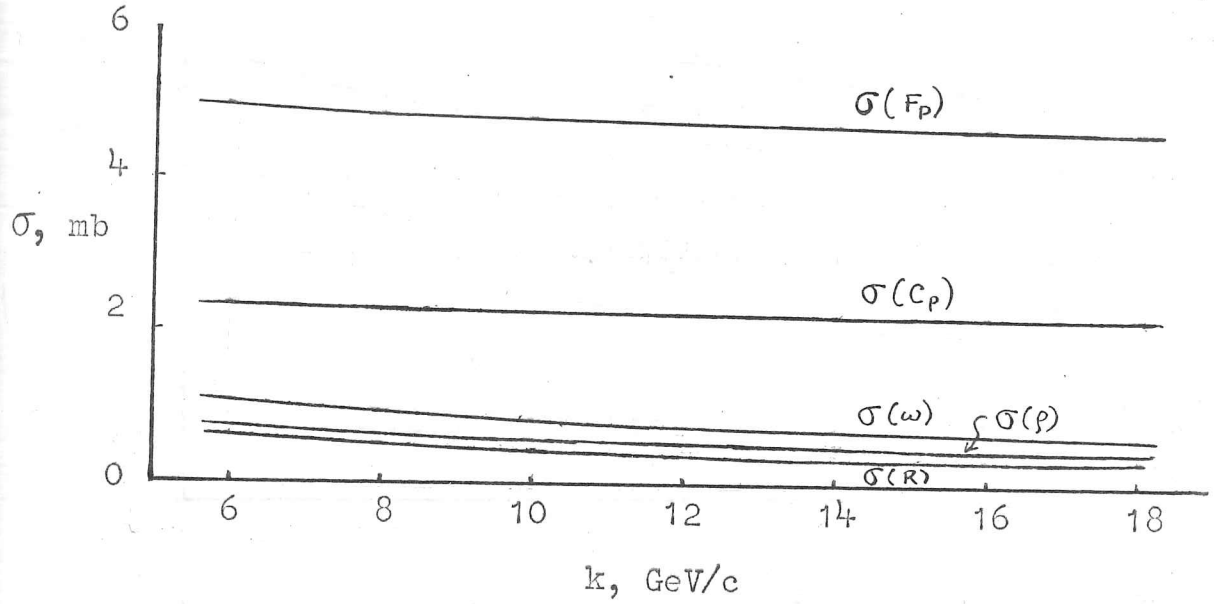

Figure 8-9 Contributions of the P, ω, ρ and R poles to single scattering in the fit shown in Figure 8-8.

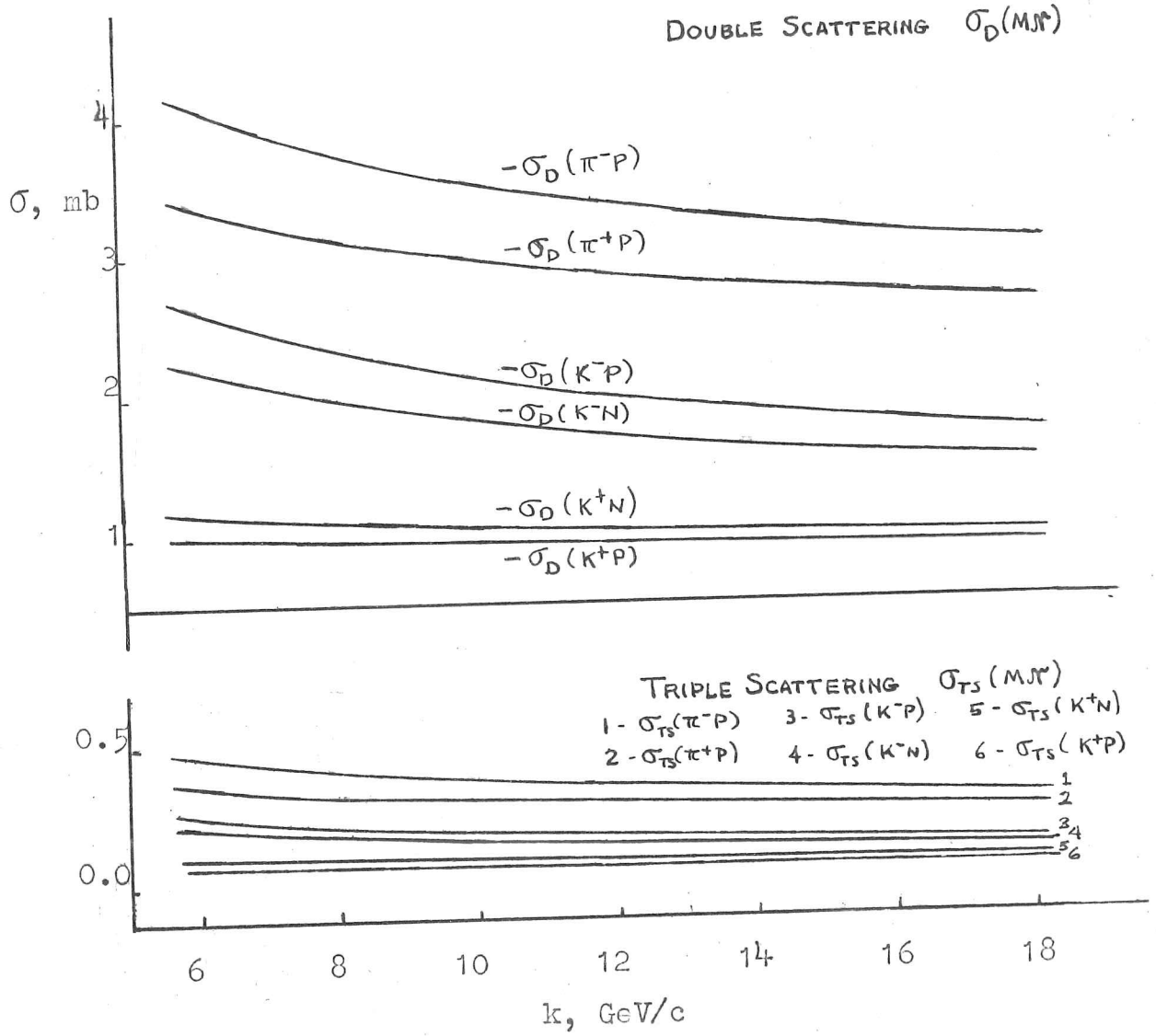

Figure 8-10 Double scattering contributions to the meson-nucleon total cross sections in the fit shown in Figure 8-8.

$$\alpha_\omega = 0.532 \pm 0.035 \qquad (8.37b)$$

$$\alpha_R = 0.529 \pm 0.138 \qquad (8.37c)$$

while the residue constants are

$$P = (3.85 \pm 0.01) \times 10^{-4} \qquad C_P = (1.82 \pm 0.02) \times 10^{-4}$$

$$\omega = -(7.53 \pm 1.94) \times 10^{-4} \qquad \rho = -(2.37 \pm 0.95) \times 10^{-3} \qquad (8.38)$$

$$R = (3.90 \pm 5.62) \times 10^{-3} \ .$$

We show in Figure 8-9 the contributions of the four Regge poles to the single scattering terms, and in Figure 8-10 the contributions of double and triple scattering to the different total cross sections. The double scattering terms are negative and amount to ten to fifteen per cent of the measured σ_T values, whereas the triple-scattering effects are positive but much smaller, typically 0.3 mb. The contributions of higher scattering terms are entirely negligible.

The fit to the (πP) data can be improved either by adopting the CKHN model for the Pomeranchuk amplitude or by adding a second vacuum trajectory. Choosing the second alternative, we obtain a much improved fit to the data, which is shown in Figure 8-11. That the comparison with the (πP) data points is much better is mirrored in the fact that the value of χ^2 is reduced to 90.11. The asymptotic cross sections for this fit are

$$\sigma_{\infty}(\pi N) = (24.40 \pm 0.09) \text{ mb} \tag{8.39a}$$

and

$$\sigma_{\infty}(KN) = (18.67 \pm 0.06) \text{ mb} \ , \tag{8.39b}$$

which are about ten per cent lower than the values given in (8.36) but are still higher than the observed $(\pi^{+}P)$ and $(K^{+}N)$ total cross sections. This model therefore predicts, as have the preceding ones, a slight rise in some of the observed total cross sections at higher energies.

The value of the intercept $\alpha_{P'}$ of the second vacuum trajectory is fully in accordance with our expectations, namely

$$\alpha_{P'} = (0.507 \pm 0.009) \ . \tag{8.40a}$$

The contribution of this pole is about ten to fifteen per cent of that due to the Pomeranchuk. The intercepts we find for the other three adjustable trajectories are

$$\alpha_{\rho} = 0.700 \pm 0.019 \tag{8.40b}$$

$$\alpha_{\omega} = 0.483 \pm 0.004 \tag{8.40c}$$

$$\alpha_{R} = 0.423 \pm 0.008 \ , \tag{8.40d}$$

which are all quite reasonable; the residue constants are

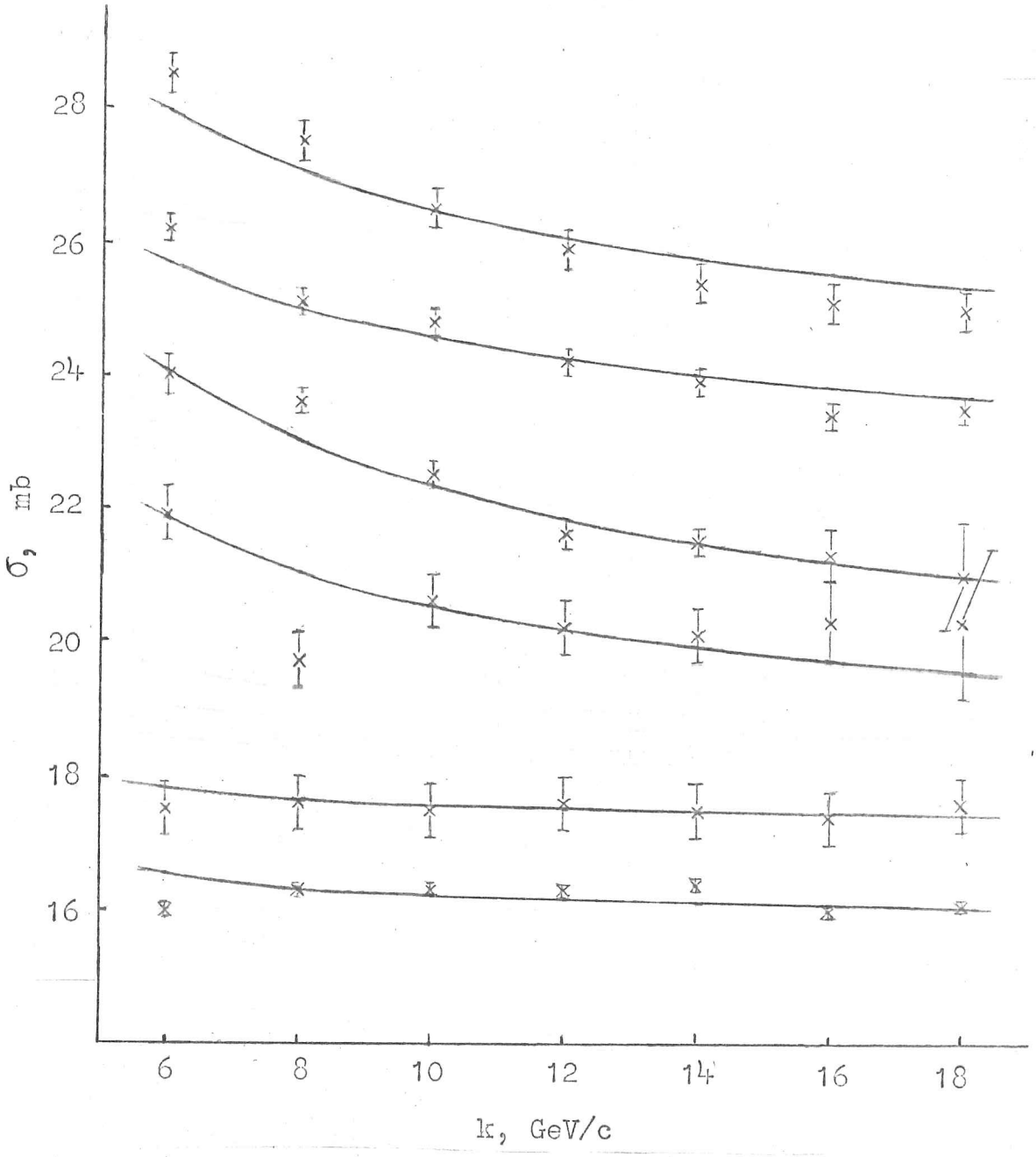

Figure 8-11 Comparison of the experimental data[2] with the fit obtained using P, P′, ω, ρ, and R poles to parametrize the quark-quark amplitude. The (K^+P) data have been displaced by 1 mb for clarity.

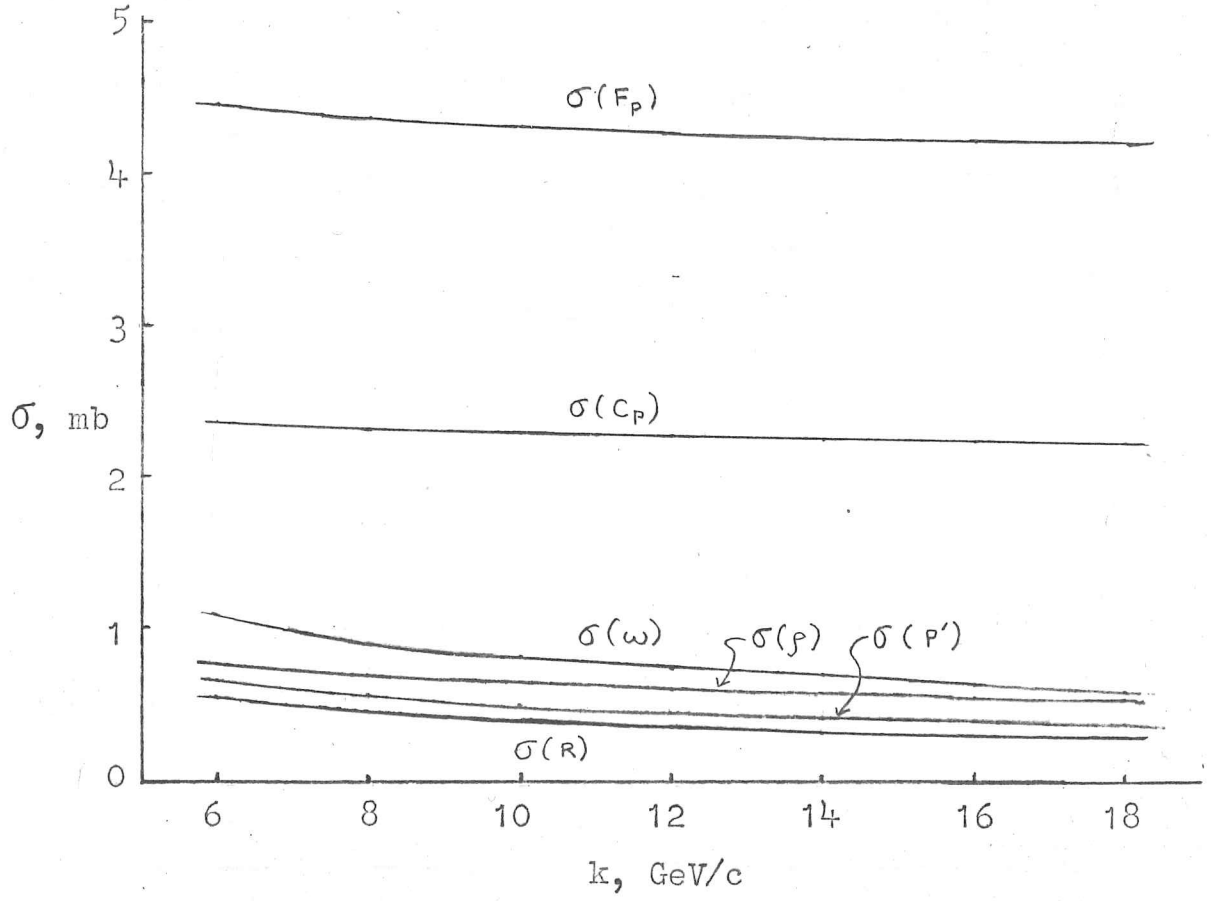

Figure 8-12 Contributions of the P, ω, ρ and R poles to single scattering in the fit shown in Figure 8-11.

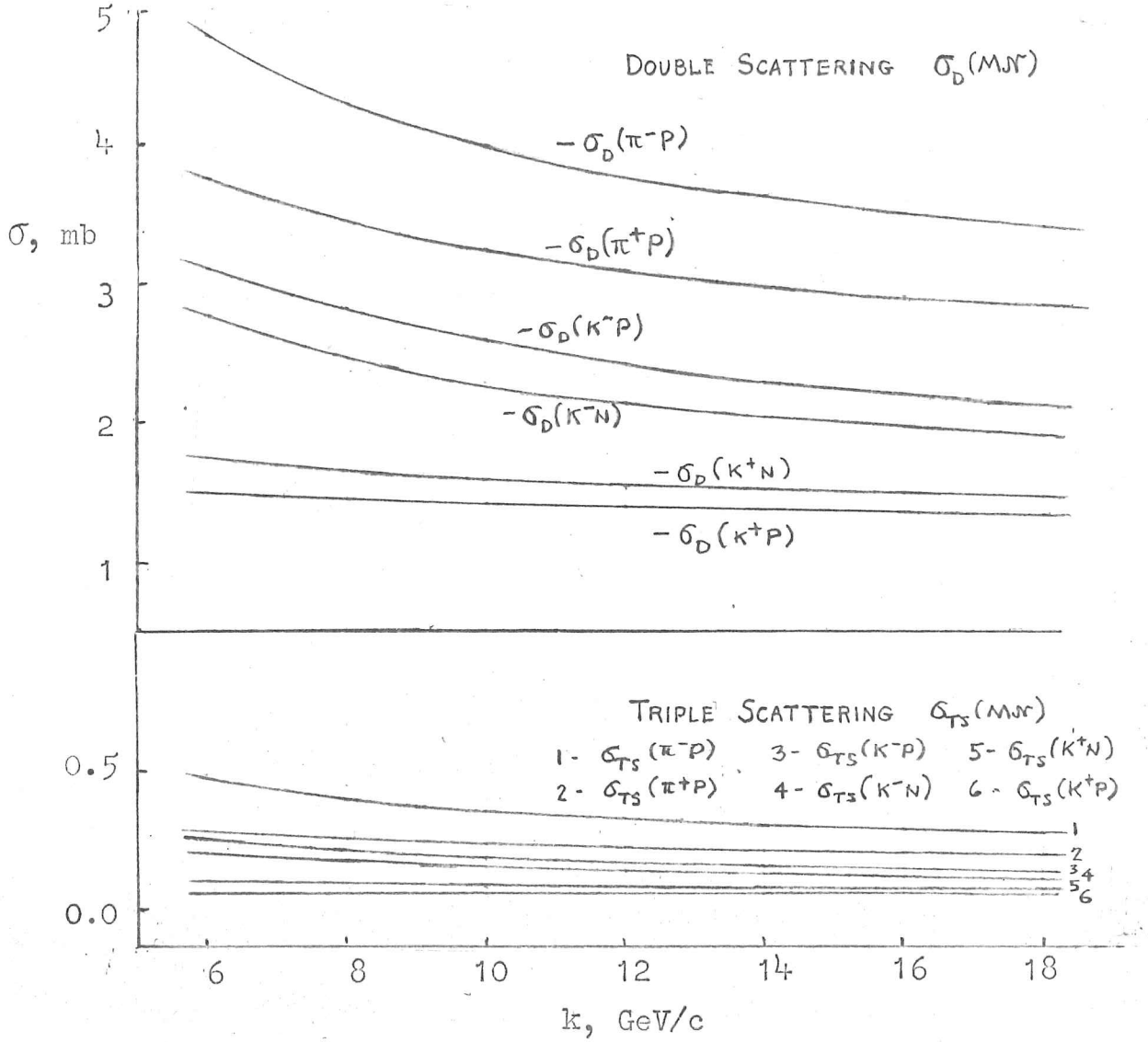

Figure 8-13 Double scattering contributions to the meson-nucleon total cross sections in the fit shown in Figure 8-11.

$$P = (3.46 \pm 0.01) \times 10^{-4} \qquad C_P = (1.833 \pm 0.004) \times 10^{-4}$$

$$P' = (5.22 \pm 0.48) \times 10^{-3} \qquad \omega = -(1.05 \pm 0.03) \times 10^{-2} \tag{8.41}$$

$$\rho = -(1.80 \pm 0.20) \times 10^{-3} \qquad R = (1.04 \pm 0.09) \times 10^{-2} \ .$$

The contributions of double and triple scattering, which are shown in Figure 8-13, are about the same as in the preceding case.

Finally we turn to the CKHN model for the quark-quark amplitudes. Although a satisfactory fit was obtained using the P + P′ model, it is not unlikely that a different, and perhaps better, result can be obtained in this way; we have already seen how this may come about. In fact the best fit using the CKHN model, shown in Figure 8-14, is considerably better than either of the previous ones, producing a χ^2 value of 65.21. The intercept of the Pomeranchuk trajectory has the value

$$\alpha_P = (0.935 \pm 0.001) \tag{8.42a}$$

corresponding to vanishing asymptotic total cross sections. The intercepts of the other trajectories and the residue constants are given by

$$\alpha_\rho = 0.638 \pm 0.027 \tag{8.42b}$$

$$\alpha_\omega = 0.129 \pm 0.010 \tag{8.42c}$$

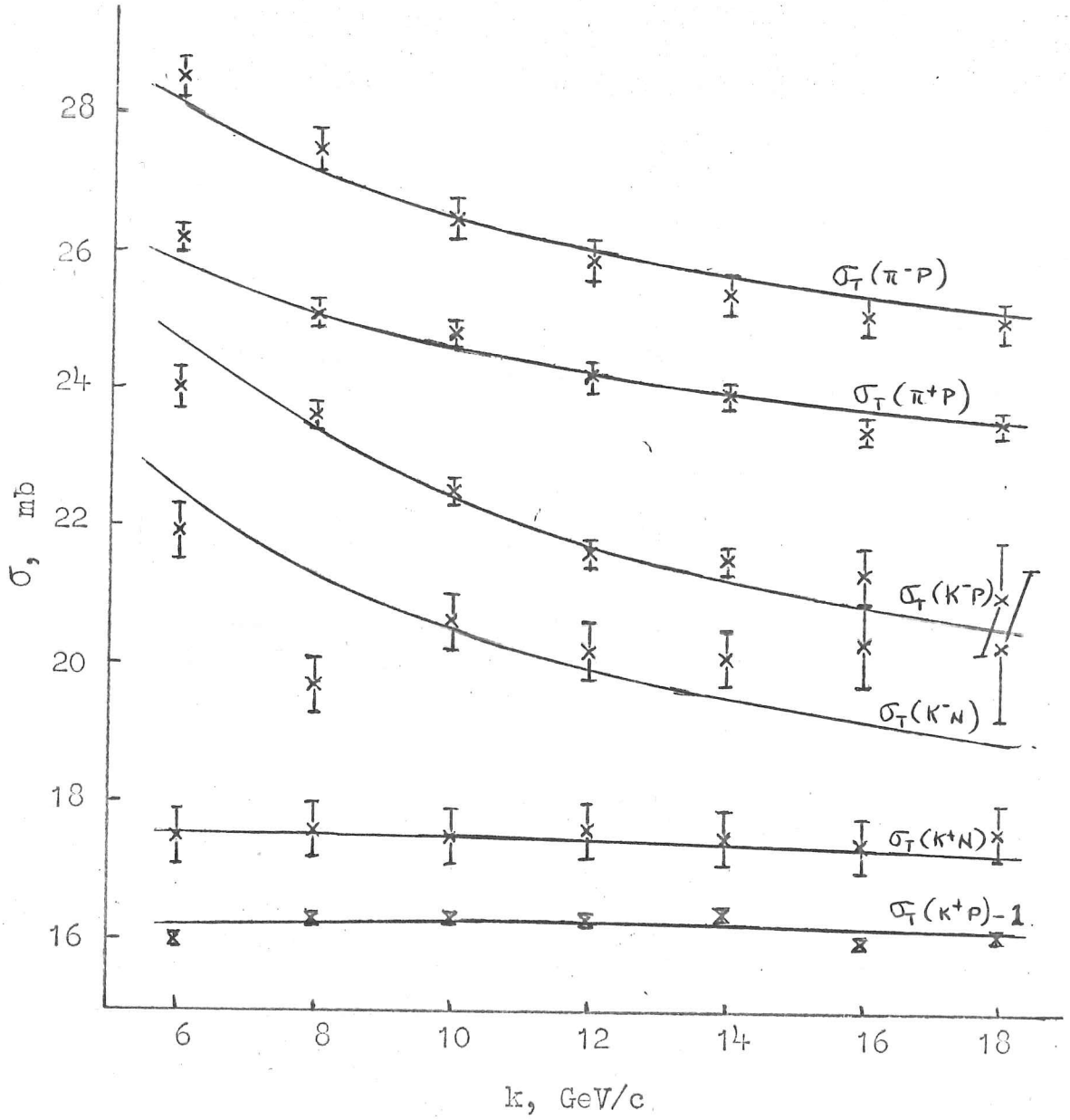

Figure 8-14 Comparison of the experimental data[2] with the fit obtained using a CKHN model to parametrize the quark-quark amplitude. The (K^+P) data have been displaced by 1 mb for clarity.

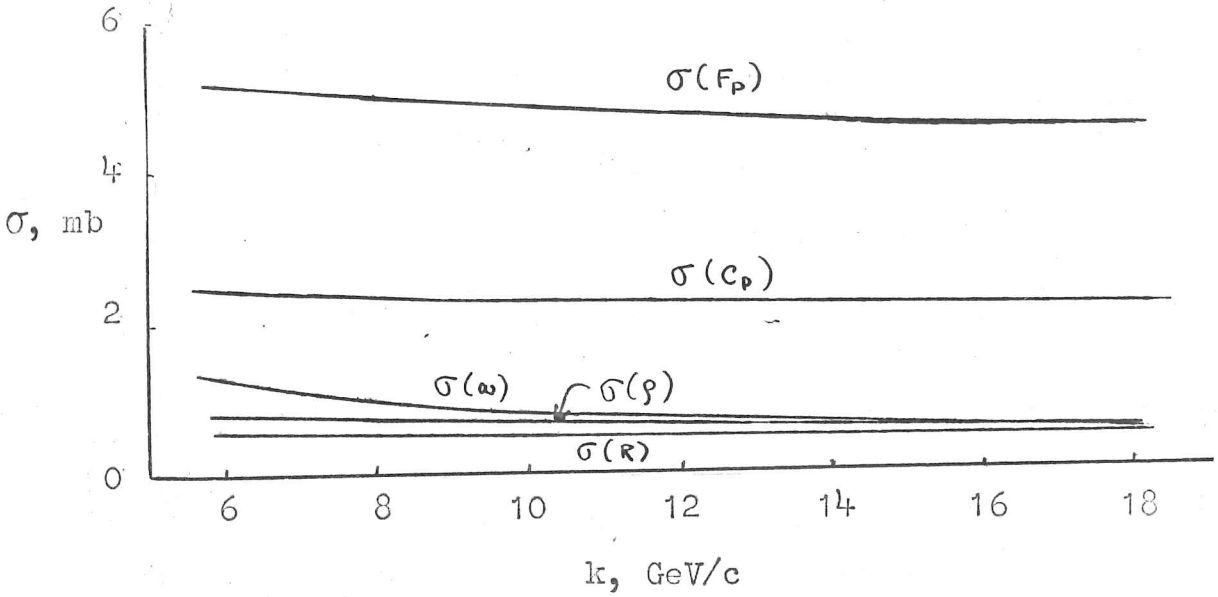

Figure 8-15 Contributions of the P, P′, ω, ρ, and R poles to single scattering in the fit shown in Figure 8-14.

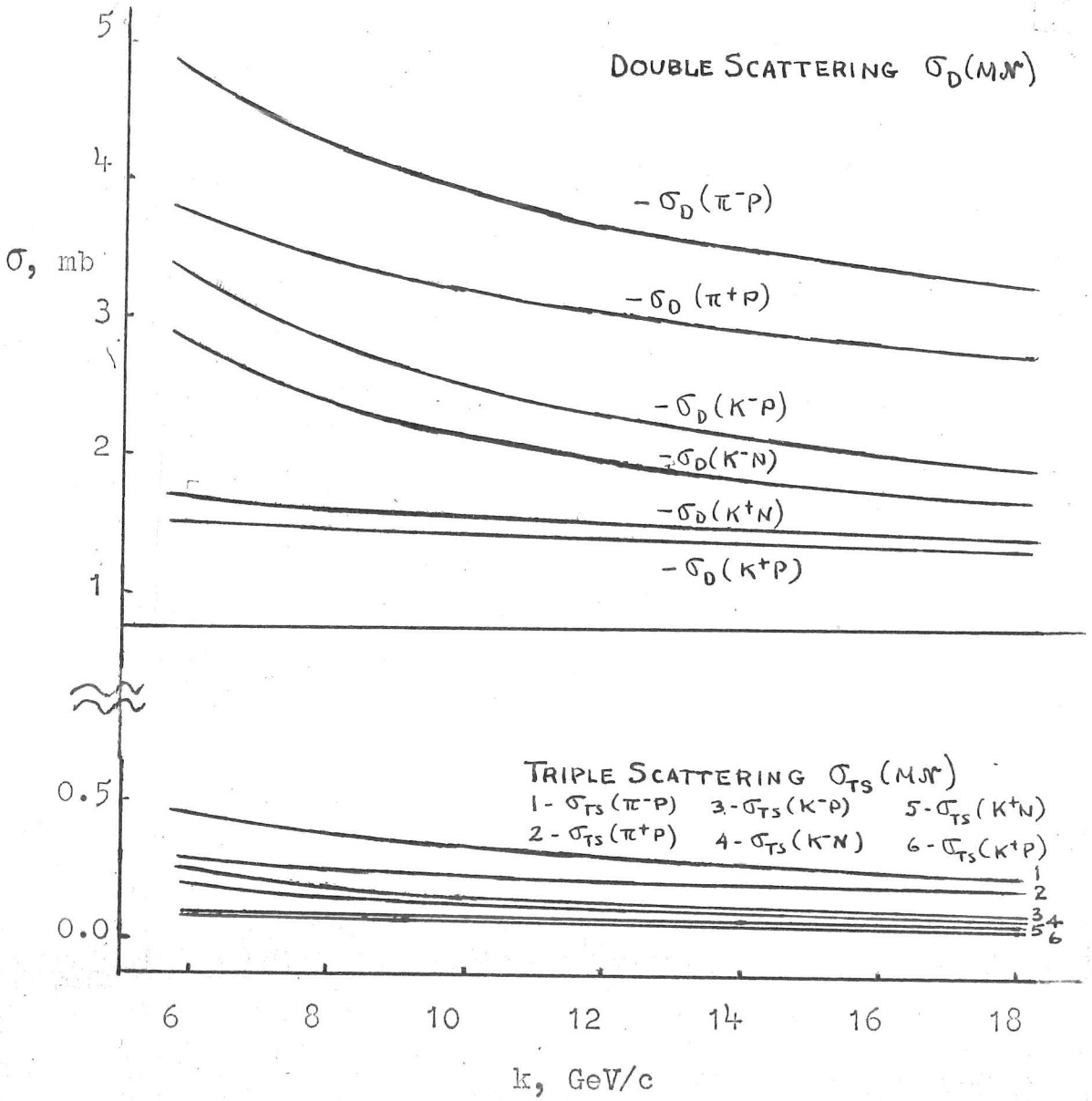

Figure 8-16 Double scattering contributions to the meson-nucleon total cross sections in the fit shown in Figure 8-14.

$$\alpha_R = 0.803 \pm 0.043 \qquad (8.42d)$$

and

$$P = (7.04 \pm 0.07) \times 10^{-4} \qquad C_P = (3.31 \pm 0.04) \times 10^{-4}$$

$$\omega = -(0.199 \pm 0.016) \qquad \rho = -(2.69 \pm 0.47) \times 10^{-3} \qquad (8.43)$$

$$R = (2.44 \pm 1.01) \times 10^{-4} \ .$$

The surprisingly high value of the R intercept is probably caused by the fluctuations in the (K^+P) total cross section, which amount to considerably more than the experimental errors. We note in this connection that the contribution of this pole is quite small; furthermore, it is rather poorly determined, as shown by the large standard deviation of the residue constant R. We show the variation of the different pole terms in Figure 8-15. The magnitudes of the double and triple scattering terms, which are shown in Figure 8-16, are about the same as in the preceding fit.

Let us close this chapter by reiterating the phenomenological nature of the fits we have obtained and of the considerations leading to them. Our intention has been to show the quark model with multiple scattering is capable of describing the energy variation of meson-nucleon total cross sections, and to obtain thereby an estimate of the magnitude of the multiple scattering effects. The approximations that were necessary were not severe. Taking all the

pertinent Regge trajectories to be parallel, for example, eliminates to some extent the possibility of different slopes for the different diffraction peaks; but the magnitude of the double scattering terms should surely depend much more on the average behaviour of these slopes than on the interplay of the different trajectories. Similarly, the intercepts of the trajectories are expected to be only reasonably sensitive to the precise form of the parametrization. They generally turn out to be consistent with what has been found before, and more accurate treatment of the slopes should not alter this result. Even the fact that the CKHN model seems to provide better fits to the data than models predicting a constant asymptotic total cross section may be an effect introduced by the particular forms we have assumed; but that either type of model produced reasonable fits with important multiple scattering effects is clearly a result of a more basic nature.

The significance of these considerations, then, lies in the general behaviour resulting from the concept of multiple scattering, rather than in the numerical details. The comparison with experiment of the quark model with multiple scattering indicates that a sizeable part of the observed total cross sections is due to double scattering effects. This conclusion is reached regardless of whether the total cross section is constant or vanishing asymptotically.

If it is constant, however, the model makes the prediction that, at higher energies, an increase toward an asymptotic value larger than those presently measured should become apparent. The rate at which this asymptote is approached is determined by the shrinkage

of the diffraction peak, and thus depends crucially on the normalization constant s_o. Since we have chosen a small value for s_o, the decrease of the double scattering terms is very slow, and the increasing behaviour is not expected to become evident until quite high energies have been attained. To illustrate this point we show in Figure 8-17 the extension of the fits leading to (8.39) up to k = 10000 GeV/c. More rapid shrinkage of the diffraction peak would, of course, lead to the appearance of the increasing total cross sections at lower energies.

We expect, in any case, that this property is a general one and will still be present in any version of the multiple scattering model. We shall see in the next chapter, for example, that a more comprehensive treatment of the complete pion-nucleon amplitude, with spin included, does not alter it. If this increasing behaviour of the total cross sections should be observed, it would constitute excellent evidence in favour of multiple scattering in the quark model.

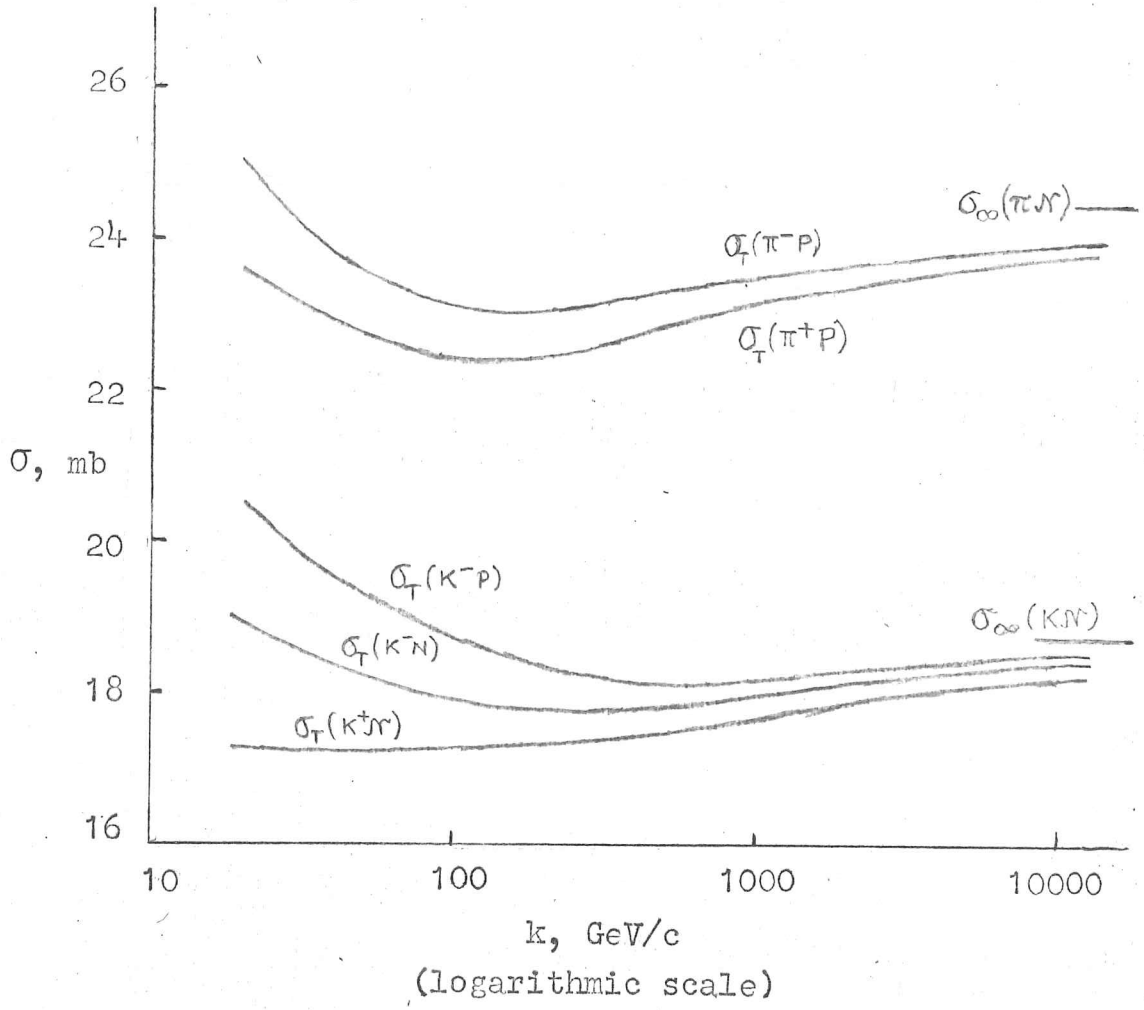

Figure 8-17 Extension of the fit shown in Figure 8-11 to superhigh energies.

References

1. R. J. Phillips and W. Rarita, Phys. Rev. 139B, 1336 (1965).

2. R. J. Eden, Physics Letters 19, 695 (1965).

3. D. Amati, A. Stanghellini, and S. Fubini, Nuovo Cimento 26, 896 (1962).

4. S. Mandelstam, Nuovo Cimento 30, 1127, 1148 (1963).

5. We are very grateful to Dr. Ian Drummond for an interesting discussion of this problem.

6. W. Galbraith et al., Phys. Rev. 138, B913 (1965).

7. N. Cabibbo, J. J. J. Kokkedee, L. Horwitz, and Y. Ne'eman, Nuovo Cimento 45A, 275 (1966).

CHAPTER IX

Application to Pion-Nucleon Interactions with Spin Effects

It is well known by now that although Regge theory is generally successful in describing a great many two-body processes, it is unable to explain simply the non-vanishing polarization observed in the reaction $\pi^- P \to \pi^o N$. The nature of this charge exchange process is such that a single set of quantum numbers, corresponding to the ρ pole, can be exchanged, but the polarization due to the exchange of a single Regge pole vanishes. In the usual Regge framework there have been attempts to explain the observed polarization of about 15% as resulting from the interference of the ρ with direct channel resonances[1], with a second pole ρ' having the same quantum numbers as the ρ [2], or with a Regge cut term[3].

We have noted in the preceding chapter that if the single scattering amplitude is written in Regge form, then the multiple scattering terms possess the s dependence characteristic of a Regge cut. Our model therefore provides a natural mechanism for the explanation of the charge exchange polarization. It is clear, of course, that we cannot meaningfully analyse this effect without considering simultaneously the entire body of pion-nucleon elastic and charge exchange phenomena in a formalism complete with all spin

and isospin complications. To that task we shall devote this chapter.

Before becoming deeply involved with the detailed calculations of the multiple scattering effects which result when spin and isospin are included, however, we wish to show in a simpler model the essential features which arise. We therefore return to the basic deuteron model considered in Chapters VII and VIII. The simplest technique for the inclusion of spin in this model is to keep the composite particle and its components spinless and assign spin one-half to the incident particle. The derivation of the Glauber model given in Chapter VII is valid even in the presence of spin provided any possible ordering ambiguities are resolved, which is accomplished by taking the anticommutator. The expected generalization of (7.16) is then

$$F_D(\bar{q}) = F_N(\bar{q})[S_D(\tfrac{\bar{q}}{2})+S_D(-\tfrac{\bar{q}}{2})] + \frac{i}{4\pi k}\int d^2\bar{q}'S(\bar{q}')\{F_N(\tfrac{\bar{q}}{2}-\bar{q}'),F_N(\tfrac{\bar{q}}{2}+\bar{q}')\}_+ \tag{9.1}$$

Both $F_D(\bar{q})$ and $F_N(\bar{q})$ are now taken to be matrices in the spin space of the system. A convenient form giving $F_N(\bar{q})$ in terms of scalar amplitudes is

$$F_N(\bar{q}) = f(\bar{q}) + 2g(\bar{q})\,\bar{k}\times\bar{q}\cdot\bar{\sigma} \tag{9.2}$$

where $\bar{\sigma}$ is the spin operator for the incident particle. In terms of this definition we find that

$$\left\{F_N(\tfrac{\bar{q}}{2}+\bar{q}'),F_N(\tfrac{\bar{q}}{2}-\bar{q}')\right\}_+ = 2\Big[f(\tfrac{\bar{q}}{2}+\bar{q}')f(\tfrac{\bar{q}}{2}-\bar{q}')+g(\tfrac{\bar{q}}{2}+\bar{q}')g(\tfrac{\bar{q}}{2}-\bar{q}') - k^2(\tfrac{q^2}{4}-q'^2)\Big]$$
$$+\bar{k}\times\bar{q}.\bar{\sigma}\Big[f(\tfrac{\bar{q}}{2}+\bar{q}')g(\tfrac{\bar{q}}{2}-\bar{q}')+f(\tfrac{\bar{q}}{2}-\bar{q}')g(\tfrac{\bar{q}}{2}+\bar{q}')\Big] \qquad (9.3)$$
$$+2\bar{k}\times\bar{q}'.\bar{\sigma}\Big[f(\tfrac{\bar{q}}{2}+\bar{q}')g(\tfrac{\bar{q}}{2}-\bar{q}')-f(\tfrac{\bar{q}}{2}-\bar{q}')g(\tfrac{\bar{q}}{2}+\bar{q}')\Big].$$

We evaluate (9.1) now under the assumptions first made in Chapter VII, namely that the amplitudes are exponentials in q^2 and that the form factor $S(\bar{q})$ is approximately unity throughout the region in which there are important contributions to the amplitudes. Specifically, we write

$$f(\bar{q}) = f_N e^{-\gamma q^2} \qquad (9.4a)$$

$$g(\bar{q}) = g_N e^{-\gamma q^2} . \qquad (9.4b)$$

We have taken the same slope γ for both spin flip and non-flip terms for the sake of simplicity. The results are not crucially dependent upon this equality; for example, the last term in equation (9.3) vanishes upon integration even if different slopes are used. The integrations in the double scattering term can be performed, yielding

$$F_D(\bar{q}) = 2f_N e^{-\gamma q^2} + \frac{i}{2k\gamma}\left(f_N^2 + g_N^2 k^2\left(\frac{q^2}{4} - \frac{1}{2\gamma}\right)\right) e^{-\frac{\gamma}{2} q^2}$$

$$+ \bar{k} \times \bar{q}.\bar{\sigma}\left(2g_N e^{-\gamma q^2} + \frac{i}{2k\gamma} f_N g_N e^{-\frac{\gamma}{2} q^2}\right) . \qquad (9.5)$$

We relate this result to the Regge model used in the preceding chapter in the obvious way. As before we write for the non-flip amplitude

$$f_N e^{-\gamma q^2} = - C\left(\frac{s}{is_o}\right)^{1-\beta q^2} \qquad (9.6)$$

i.e.

$$f_N = - C\left(\frac{s}{is_o}\right) \qquad (9.7a)$$

$$\gamma = \beta \ln\left(\frac{s}{is_o}\right) \qquad (9.7b)$$

For the spin-flip amplitude we define a simplified version of the usual Regge formula

$$G_f(s,t) = \alpha R_f(t) \frac{1 + \tau\, e^{-i\pi\alpha(t)}}{\sin \pi\alpha(t)}\, s^{\alpha(t)-1} \qquad (9.8)$$

by writing

$$kg_N e^{-\gamma q^2} = i\, D\left(\frac{s}{is_o}\right)^{1-\beta q^2} . \qquad (9.9)$$

Then in the high energy limit, using the approximations $s \approx 2Mk$ and $\ln(\frac{s}{is_o}) \approx \ln(\frac{s}{s_o})$, we obtain for the Reggeized amplitude corresponding to $F_D(\bar{q})$

$$F_R(s,q^2) = -2C(\frac{s}{is_o})^{1-\beta q^2} + \frac{Ms_o}{\beta \ln(\frac{s}{s_o})}\left[C^2 - D^2\left(\frac{q^2}{4} - \frac{1}{2\beta\ln(\frac{s}{s_o})}\right)\right](\frac{s}{is_o})^{1-\frac{\beta}{2}q^2}$$

$$+ \bar{k}\times\bar{q}.\bar{\sigma}\,(\frac{2M}{s_o})\left\{2D(\frac{s}{is_o})^{-\beta q^2} - \frac{Ms_o CD}{\beta\ln(\frac{s}{s_o})}(\frac{s}{is_o})^{-\frac{\beta}{2}q^2}\right\} . \qquad (9.10)$$

It should be noted here that the spin-flip term in the single-scattering amplitude can contribute via double scattering to the forward non-flip amplitude, and therefore to the total cross section. The simple physical meaning of this fact is that two consecutive spin-flip processes with opposite momentum transfers will produce forward non-flip scattering. Should this effect be large, it would preclude the possibility of neglecting spin in considering forward scattering, as we did in Chapters VII and VIII. We shall find, reassuringly, that the contributions to the total cross sections of such terms are very small.

The polarization resulting from (9.10) can be calculated using scalar amplitudes, which are conveniently defined by writing

$$F_R(s,q^2) = F(s,q^2) + \bar{k}\times\bar{q}.\bar{\sigma}\,G(s,q^2) . \qquad (9.11)$$

The polarization parameter P is then determined by

$$P\frac{d\sigma}{d\Omega} = 2\mathrm{Re}[F^{*}(s,q^2)G(s,q^2)]\,\lambda(s,q^2) \tag{9.12}$$

with the kinematical factor $\lambda(s,q^2)$ given by

$$\lambda(s,q^2) \equiv kk'\sin\theta = [(k+k')^2-q^2)(q^2-(k-k')^2)]^{\frac{1}{2}} \ , \tag{9.13}$$

k' and θ being the final momentum of the incident particle and the scattering angle. We note that the asymptotic behaviour of $\lambda(s,q^2)$ for non-zero q^2 is given by

$$\lambda(s,q^2) \to 2kq \qquad \text{as} \qquad s \to \infty \tag{9.14}$$

and that

$$\lambda(s,0) = 0 \ . \tag{9.15}$$

From (9.10) we have

$$F(s,q^2) = -2C\left(\frac{s}{is_o}\right)^{1-\beta q^2} + \frac{Ms_o}{\beta\ln\left(\frac{s}{s_o}\right)}\left[C^2-D^2\left(\frac{q^2}{4}-\frac{1}{2\beta\ln\left(\frac{s}{s_o}\right)}\right)\right]\left(\frac{s}{is_o}\right)^{1-\frac{\beta}{2}q^2} \tag{9.16a}$$

$$G(s,q^2) = \left(\frac{2M}{s_o}\right)\left[2D\left(\frac{s}{is_o}\right)^{-\beta q^2} - \frac{Ms_o CD}{\beta\ln\left(\frac{s}{s_o}\right)}\left(\frac{s}{is_o}\right)^{-\frac{\beta}{2}q^2}\right] \ . \tag{9.16b}$$

The single-scattering terms in $F(s,q^2)$ and $G(s,q^2)$ are 90° out of phase, so that they produce, as expected, no polarization. The same is true of the two double-scattering terms. Contributions

to the polarization thus come only from interference between the single-scattering amplitude in $F(s,q^2)$ and the double-scattering in $G(s,q^2)$, and vice versa. Asymptotically then (9.12) yields

$$P\frac{d\sigma}{d\Omega} \approx 8q\frac{DMs_o}{\beta\ln(\frac{s}{s_o})}\left[2C^2-D^2\left(\frac{q^2}{4}-\frac{1}{2\beta\ln(\frac{s}{s_o})}\right)\right](\frac{s}{s_o})^{2-\frac{3}{2}\beta q^2}\sin\frac{\pi\beta}{4}q^2. \quad (9.17)$$

The differential cross section $\frac{d\sigma}{d\Omega}$ is given in this case by

$$\frac{d\sigma}{d\Omega} = |F(s,q^2)|^2 + |\lambda(s,q^2)G(s,q^2)|^2 \quad (9.18)$$

and at high energy the dominant contribution for $q^2 > 0$ comes, as before, from the multiple scattering terms. Asymptotically, then, we have

$$\frac{d\sigma}{d\Omega} \approx \left(\frac{Ms_o}{\beta\ln(\frac{s}{s_o})}\right)^2\left[(C^2-D^2\left(\frac{q^2}{4}-\frac{1}{2\beta\ln(\frac{s}{s_o})}\right))^2+4q^2C^2D^2\right](\frac{s}{s_o})^{2-\beta q^2}. \quad (9.19)$$

It follows from (9.17) and (9.19) that for $q^2 > 0$ the asymptotic behaviour with s of the polarization parameter is given by

$$P \propto (\frac{s}{s_o})^{-\frac{1}{2}\beta q^2}\ln(\frac{s}{s_o}). \quad (9.20)$$

The polarization thus goes to zero, but only extremely slowly. As an example, we take typical values of the parameters to be $\frac{1}{2}\beta q^2 = 0.2$, $s_o = .002$; when s increases from 2 to 2000, the polarization

decreases only by a factor $\frac{1}{2}$.

We see therefore that a non-vanishing polarization will result from multiple scattering effects even if the single scattering process involved permits the exchange of only one Regge pole, and that this polarization will decrease asymptotically toward zero at high energy so slowly as to appear almost constant. These observations are fully consistent with the experimental facts regarding the reaction $\pi^- P \to \pi^o N$. We therefore turn now to a detailed calculation of pion-nucleon interactions in terms of the Reggeized quark model with multiple scattering.

The general pion-nucleon scattering amplitude with full spin and isospin complexity included can be written conveniently in the form

$$F_{\pi N}(s,q^2) = F_{00}(s,q^2) + 2F_{01}(s,q^2)\,\bar{T}_\pi \cdot \bar{T}_N + \bar{k} \times \bar{q}.\bar{\sigma}_N(F_{10}(s,q^2) + 2F_{11}(s,q^2)\,\bar{T}_\pi \cdot \bar{T}_N) \tag{9.21}$$

where $\bar{T}_\pi$, $\bar{T}_N$, and $\bar{\sigma}_N$ denote respectively the isospin operators of the pion and of the nucleon and the spin operator of the nucleon. In the scalar functions $F_{ij}(s,q^2)$ it is clear that i and j correspond to the spin and isospin exchanged. The actual amplitudes for the pertinent physical scattering processes are obtained in the obvious way, by taking the (matrix) form (9.21) between the appropriate spin-isospin states; for spin exchange i,

$$F_i^{\pm}(s,q^2) \equiv F_{i0}(s,q^2) \pm F_{i1}(s,q^2) \tag{9.22a}$$

describes elastic $\pi^{\pm}P$ interactions, while

$$F_i^{x}(s,q^2) \equiv \sqrt{2}\, F_{i1}(s,q^2) \tag{9.22b}$$

describes the charge exchange reaction.

We shall review briefly here the connection between these amplitudes and the quantities measured experimentally. The total cross section for $(\pi^{\pm}P)$ scattering is given through the optical theorem,

$$\sigma^{\pm}(s) = \frac{4\pi}{k} \operatorname{Im} F_0^{\pm}(s,0) \quad . \tag{9.23}$$

The phases of the forward non-flip elastic amplitudes also are known and are usually specified by giving the ratio of the real to the imaginary part, which we shall denote by

$$\eta^{\pm}(s) \equiv \frac{\operatorname{Re} F_0^{\pm}(s,0)}{\operatorname{Im} F_0^{\pm}(s,0)} \quad . \tag{9.24}$$

At non-zero momentum transfer the differential cross sections and the polarizations are measured for all three processes. The former are given in the laboratory frame by

$$\frac{d\sigma}{d\Omega_L}(s,q^2) = |F_0(s,q^2)|^2 + |\lambda(s,q^2)F_1(s,q^2)|^2 \quad , \tag{9.25}$$

where $F_i(s,q^2)$ refers to any of the three amplitudes defined in (9.22), and $\lambda(s,q^2)$ is the kinematical factor defined in (9.13). This quantity is converted to an invariant distribution

$$\frac{d\sigma}{dt}(s,q^2) = C(s,q^2)\,\frac{d\sigma}{d\Omega_L}(s,q^2) \tag{9.26a}$$

with

$$C(s,q^2) = \frac{\pi}{kk'^3}\left\{[(k^2+\mu^2)(k'^2+\mu^2)]^{\frac{1}{2}} - \mu^2\left(1 - \frac{q^2}{2M^2}\right)\right\} \tag{9.26b}$$

in terms of the previously defined quantities, $\mu(M)$ being the pion (nucleon) mass. The polarization, finally, is calculated as in (9.12),

$$P(s,q^2) = \frac{2\,\mathrm{Re}[F_0^*(s,q^2)\,F_1(s,q^2)]\,\lambda(s,q^2)}{\frac{d\sigma}{d\Omega_L}}\,. \tag{9.27}$$

The first step in applying the multiple scattering formalism in the pion-nucleon system is to decompose the nucleon into its quark structure, which we assume to be given by the SU(6) spin-isospin wave functions

$$P_{\pm} = \frac{1}{\sqrt{18}}\Big[\pm 2(p_\pm p_\pm n_\mp + p_\pm n_\mp p_\pm + n_\mp p_\pm p_\pm)$$

$$\mp (p_\pm p_\mp n_\pm + p_\mp p_\pm n_\pm + p_\pm n_\pm p_\mp + p_\mp n_\pm p_\pm + n_\pm p_\pm p_\mp + n_\pm p_\mp p_\pm)\Big] \tag{9.28a}$$

$$N_{\pm} = \frac{1}{\sqrt{18}} \Big[\mp 2(n_{\pm}n_{\pm}p_{\mp} + n_{\pm}p_{\mp}n_{\pm} + p_{\mp}n_{\pm}n_{\pm})$$

$$\pm (n_{\pm}n_{\mp}p_{\pm} + n_{\mp}n_{\pm}p_{\pm} + n_{\pm}p_{\pm}n_{\mp} + n_{\mp}p_{\pm}n_{\pm} + p_{\pm}n_{\pm}n_{\mp} + p_{\pm}n_{\mp}n_{\pm}) \Big] \, . \quad (9.28b)$$

In (9.28) P_+ (P_-) denotes a proton with spin up (down), and $N_{\pm}$, $p_{\pm}$, and $n_{\pm}$ analogously represent the spin states of the neutron and the non-strange quarks. The total pion-nucleon scattering amplitude $F_{\pi N}(s,q^2)$ then consists of three terms,

$$F_{\pi N}(s,q^2) = \sum_{i=1}^{3} F^{i}_{\pi N}(s,q^2) \, , \quad (9.29)$$

corresponding to single, double, and triple scattering of the pion by the three quarks of the nucleon. If we denote the pion-quark scattering amplitude by $F_{\pi Q}(s,q^2)$, which is a matrix in the spin and isospin spaces of the pion-quark system, then in the strong binding approximation the $F^{i}_{\pi N}(s,q^2)$ are given by

$$F^{1}_{\pi N}(s,q^2) = \sum_{i} F_{\pi Q_i}(s,q^2) \quad (9.30a)$$

$$F^{2}_{\pi N}(s,q^2) = \frac{i}{4\pi k} \int d^2q' \sum_{i \neq j} F_{\pi Q_i}\left(s,\left(\frac{\bar{q}}{2} - \bar{q}'\right)^2\right)$$

$$F_{\pi Q_j}\left(s,\left(\frac{\bar{q}}{2} + \bar{q}'\right)^2\right) \quad (9.30b)$$

$$F^{3}_{\pi N}(s,q^2) = \frac{1}{6}\left(\frac{i}{2\pi k}\right)^2 \int d^2\bar{q}' \int d^2\bar{q}'' \sum_{i\neq j\neq k} F_{\pi Q_i}\left(s,(\tfrac{\bar{q}}{2} - \bar{q}')^2\right)$$

$$F_{\pi Q_j}\left(s,(\tfrac{\bar{q}}{2} - \bar{q}'')^2\right) F_{\pi Q_k}\left(s,(\bar{q}' + \bar{q}'')^2\right) \quad . \qquad (9.30c)$$

The summations over Q_i, etc., in (9.30) refer to the three quarks, and have been so taken that symmetry under the interchange of quark labels is guaranteed.

The pion-quark amplitude can be expressed by scalar functions precisely as was the pion-nucleon amplitude itself,

$$F_{\pi Q}(s,q^2) = f_{00}(s,q^2) + 2\, f_{01}(s,q^2)\, \bar{T}_\pi \cdot \bar{T}_Q +$$

$$\bar{k}\times\bar{q} \cdot \bar{\sigma}_Q \left(f_{10}(s,q^2) + 2f_{11}(s,q^2)\, \bar{T}_\pi \cdot \bar{T}_Q\right) . \qquad (9.31)$$

The contributions to the $F_{ij}(s,q^2)$ of single, double, and triple scattering, denoted hereafter by $F^{n}_{ij}(s,q^2)$, n = 1, 2, 3, are then calculated in terms of the $f_{ij}(s,q^2)$ by inserting (9.31) into the expressions (9.30). To evaluate the matrix elements of the spin and isospin operators, using the SU(6) wave functions (9.28), is then a matter of a large amount of tedious but straightforward arithmetic. In fact we shall neglect entirely the triple scattering effects, which we expect to be small, and thus we summarize below the contributions of only those matrix elements necessary for considering single and double scattering. Using the $(\pi^+ P)$ states we find that spin non-flip terms arise only from the matrix elements

$$\langle \pi^+ P_\pm | \sum_i 1_{Q_i} | \pi^+ P_\pm \rangle = 3 \tag{9.32a}$$

$$\langle \pi^+ P_\pm | \sum_i \bar{T}_\pi \cdot \bar{T}_{Q_i} | \pi^+ P_\pm \rangle = \tfrac{1}{2} \tag{9.32b}$$

$$\langle \pi^+ P_\pm | \sum_{i \neq j} (\bar{k} \times (\tfrac{\bar{q}}{2} - \bar{q}') \cdot \bar{\sigma}_{Q_i}) (\bar{k} \times (\tfrac{\bar{q}}{2} + \bar{q}') \cdot \bar{\sigma}_{Q_j}) | \pi^+ P_\pm \rangle =$$

$$- 2 (\tfrac{q^2}{4} - q'^2) \tag{9.32c}$$

$$\langle \pi^+ P_\pm | \sum_{i \neq j} (\bar{T}_\pi \cdot \bar{T}_{Q_i}) (\bar{T}_\pi \cdot \bar{T}_{Q_j}) | \pi^+ P_\pm \rangle = - \tfrac{1}{2} \tag{9.32d}$$

$$\langle \pi^+ P_\pm | \sum_{i \neq j} (\bar{k} \times (\tfrac{\bar{q}}{2} - \bar{q}') \cdot \bar{\sigma}_{Q_i}) (\bar{k} \times (\tfrac{\bar{q}}{2} + \bar{q}') \cdot \bar{\sigma}_{Q_j}) (\bar{T}_\pi \cdot \bar{T}_{Q_i} + \bar{T}_\pi \cdot \bar{T}_{Q_j}) | \pi^+ P_\pm \rangle =$$

$$\tfrac{4}{3} (\tfrac{q^2}{4} - q'^2) \tag{9.32e}$$

$$\langle \pi^+ P_\pm | \sum_{i \neq j} (\bar{k} \times (\tfrac{\bar{q}}{2} - \bar{q}') \cdot \bar{\sigma}_{Q_i}) (\bar{k} \times (\tfrac{\bar{q}}{2} + \bar{q}') \cdot \bar{\sigma}_{Q_j}) (\bar{T}_\pi \cdot \bar{T}_{Q_i}) (\bar{T}_\pi \cdot \bar{T}_{Q_j}) | \pi^+ P_\pm \rangle =$$

$$\tfrac{4}{3} (\tfrac{q^2}{4} - q'^2) \ , \tag{9.32f}$$

while spin flip terms result from

$$\langle \pi^+ P_\pm | \sum_i (\bar{k} \times \bar{q} \cdot \bar{\sigma}_{Q_i}) | \pi^+ P_\mp \rangle = - kq \tag{9.33a}$$

$$\langle \pi^+ P_\pm | \sum_i (\bar{T}_\pi \cdot \bar{T}_{Q_i}) (\mathbf{k} \times q \cdot \sigma_{Q_i}) | \pi^+ P_\mp \rangle = - \tfrac{5}{6} kq \tag{9.33b}$$

$$\langle \pi^+ P_\pm | \sum_{i \neq j} (\bar{T}_\pi \cdot \bar{T}_{Q_i}) (\bar{k} \times \bar{q} \cdot \bar{\sigma}_{Q_j}) | \pi^+ P_\mp \rangle = \tfrac{1}{3} kq \tag{9.33c}$$

$$\langle \pi^+ P_{\pm} | \sum_{i \neq j} (\bar{k} \times \bar{q} . \bar{\sigma}_{Q_i})(\bar{T}_\pi . \bar{T}_{Q_i})(\bar{T}_\pi . \bar{T}_{Q_j}) | \pi^+ P_{\mp} \rangle = -\tfrac{1}{2} kq \qquad (9.33d)$$

(For simplicity in (9.33) we have defined $\bar{q}$ to be in the y direction.)

It is easily verified that isosymmetry is maintained for the double-scattering terms. Consequently it suffices to calculate the $(\pi^+ P)$ amplitudes; those for $(\pi^- P)$ are obtained by changing the sign of $\bar{T}_\pi$, and the amplitudes for the charge exchange are related to the elastic amplitudes by the familiar equation

$$\sqrt{2}\, M(\pi^- P \to \pi^0 N) = M(\pi^+ P \to \pi^+ P) - M(\pi^- P \to \pi^- P)$$

where M denotes any of the above matrix elements. This result is tantamount to f_{i0} (f_{i1}) being even (odd) under charge conjugation.

To carry out the integrations necessary in the double scattering terms now requires a parametrization of the pion-quark amplitude. As we have pointed out in Chapter VIII, the most basic premise would be the use of a simple representation for the quark-quark interactions; the pion-quark amplitude would then be obtained by applying the multiple scattering formalism again, this time decomposing the pion into quark and antiquark. Effectively, however, this procedure leads only to an extremely complicated parametrization of the pion-quark interactions. The quark-quark scattering process has five helicity amplitudes, each of which involves at least four Regge poles. As a result both the complexity of the algebra and the number of parameters are vastly larger than

would result from simply Reggeizing the pion-quark amplitude. Since our parametrization must be amenable to computerized fitting programs, we choose this less complicated technique.

For the pion-quark amplitude, analogously to the usual pion-nucleon Regge theory, only trajectories with positive G-parity, namely the vacuum and the ρ trajectories, are allowed. We do not expect that the Pomeranchuk trajectory alone will be able to reproduce satisfactorily the decreasing total cross sections, so we shall invoke the traditional mechanism of a second vacuum trajectory P′. A substantial reduction of the computer time required can be achieved by taking the two vacuum trajectories to be parallel. We therefore parametrize the I = 0 amplitudes as

$$f_{00}(s,q^2) = -R_0 \left(\frac{s}{is_o}\right)^{1-\beta_P q^2} \tag{9.34a}$$

$$f_{10}(s,q^2) = -R_1 \left(\frac{s}{is_o}\right)^{-\beta_P q^2} \tag{9.34b}$$

with residues R_0 and R_1 containing the energy dependence of both the P and P′ poles, i.e.

$$R_0 = P_0 + P_0' \left(\frac{s}{is_o}\right)^{\alpha_{P'}-1} \tag{9.35a}$$

$$R_1 = P_1 + P_1' \left(\frac{s}{is_o}\right)^{\alpha_{P'}-1} . \tag{9.35b}$$

The I = 1 amplitudes are those corresponding to the ρ pole only,

$$f_{10}(s,q^2) = i\,\rho_0 \left(\frac{s}{is_o}\right)^{\alpha_\rho - \beta_\rho q^2} \tag{9.36a}$$

$$f_{11}(s,q^2) = i\,\rho_1 \left(\frac{s}{is_o}\right)^{\alpha_\rho - 1 - \beta_\rho q^2} . \tag{9.36b}$$

These equations define the real constants P_i, P_i', ρ_i, $\alpha_{P'}$, α_ρ, β_P, β_ρ, and s_o on which our calculation will depend.

The double scattering integrations can be carried out using the parametrizations above, and employing these results along with the matrix elements summarized in (9.32) and (9.33) we find eventually that the various $F^n_{ij}(s,q^2)$ are given by the following equations.

$$F^1_{00}(s,q^2) = -3\,R_0 \left(\frac{s}{is_o}\right)^{1-\beta_P q^2} \tag{9.37a}$$

$$F^1_{01}(s,q^2) = i\,\rho_0 \left(\frac{s}{is_o}\right)^{\alpha_\rho - \beta_\rho q^2} \tag{9.37b}$$

$$F^1_{10}(s,q^2) = -R_1 \left(\frac{s}{is_o}\right)^{-\beta_P q^2} \tag{9.37c}$$

$$F^1_{11}(s,q^2) = \frac{5}{3}\, i\,\rho_1 \left(\frac{s}{is_o}\right)^{\alpha_\rho - 1 - \beta_\rho q^2} \tag{9.37d}$$

$$F_{00}^{2}(s,q^2) = \frac{i}{2k}\left\{\frac{F_0^{PP}(s,q^2)}{2\beta_P \ln(\frac{s}{is_o})}\left(\frac{s}{is_o}\right)^{-\frac{\beta_P}{2}q^2} + \frac{F_0^{\rho\rho}(s,q^2)}{2\beta_\rho \ln(\frac{s}{is_o})}\left(\frac{s}{is_o}\right)^{-\frac{\beta_\rho}{2}q^2}\right\} \quad (9.38a)$$

$$F_0^{PP}(s,q^2) = 3\,(R_0\,\frac{s}{is_o})^2 + (kR_1)^2\left[\frac{1}{2\beta_P \ln(\frac{s}{is_o})} - \frac{q^2}{4}\right]$$

$$F_0^{\rho\rho}(s,q^2) = \left(\rho_0(\frac{s}{is_o})^{\alpha_\rho}\right)^2 - \frac{8}{3}\left(k\rho_1(\frac{s}{is_o})^{\alpha_\rho - 1}\right)^2\left[\frac{1}{2\beta_\rho \ln(\frac{s}{is_o})} - \frac{q^2}{4}\right]$$

$$F_{01}^{2}(s,q^2) = \frac{i}{2k}\,\frac{F_0^{P\rho}(s,q^2)}{(\beta_P+\beta_\rho)\ln(\frac{s}{is_o})}\left(\frac{s}{is_o}\right)^{-\frac{\beta_P\beta_\rho}{\beta_P+\beta_\rho}q^2} \quad (9.38b)$$

$$F_0^{P\rho}(s,q^2) = \frac{5}{3}\,i\rho_0 R_0(\frac{s}{is_o})^{\alpha_\rho+1} - \frac{4}{3}\,i\rho_1 R_1 k^2(\frac{s}{is_o})^{\alpha_\rho-1}\left[\frac{1}{(\beta_P+\beta_\rho)\ln(\frac{s}{is_o})} - \frac{q^2}{4}\right]$$

$$F_{10}^{2}(s,q^2) = \frac{i}{2k}\left\{\frac{F_1^{PP}(s)}{2\beta_P \ln(\frac{s}{is_o})}\left(\frac{s}{is_o}\right)^{-\frac{\beta_P}{2}q^2} + \frac{F_1^{\rho\rho}(s)}{2\beta_\rho \ln(\frac{s}{is_o})}\left(\frac{s}{is_o}\right)^{-\frac{\beta_\rho}{2}q^2}\right\} \quad (9.38c)$$

$$F_1^{PP}(s) = R_0\,R_1\,(\frac{s}{is_o})$$

$$F_1^{\rho\rho}(s) = -\,\rho_0\,\rho_1\,(\frac{s}{is_o})^{2\alpha_\rho - 1}$$

$$F_{11}^{2}(s,q^2) = \frac{i}{2k} \frac{F_1^{P\rho}(s)}{(\beta_P+\beta_\rho)\ln(\frac{s}{is_o})} (\frac{s}{is_o})^{-\frac{\beta_P\beta_\rho}{\beta_P+\beta_\rho} q^2} \qquad (9.38d)$$

$$F_1^{P\rho}(s) = \left[\frac{5}{3} i \rho_1 R_0 - \frac{2}{3} i \rho_0 R_1\right] (\frac{s}{is_o})^{\alpha_\rho} .$$

The amplitudes for the relevant physical processes are obtained by inserting these forms into (9.22). Our Reggeized quark model can then be tested by performing a least chi-square fit to the experimental data using the amplitudes calculated in (9.37) and (9.38) above. For this purpose we choose from the extensive literature a selection of 230 data points describing all the physical quantities listed above at various energies and momentum transfers. The total cross sections and phase measurements are taken from the high precision data recently obtained by Foley et al.[4,5], which cover a range in laboratory momentum from about 7 GeV/c to about 22 GeV/c for (π^+P), and to about 28 GeV/c for (π^-P), with errors of the order of only 0.3% in σ and of 15% in η. The differential cross sections are taken from the measurements by Foley et al.[6] for the elastic scattering and from those by Stirling et al.[7] for the charge exchange process; the polarization data are due to Borghini et al.[8] for elastic scattering and to Bonemy et al.[9] for charge exchange. The range of laboratory momentum in these measurements is from around 6 GeV/c to 18 GeV/c

for $\frac{d\sigma}{dt}$, and to 12 GeV/c for the polarization. The range in momentum transfer has been arbitrarily limited; in order to reduce the importance of the strong binding assumption, we used only points for which the invariant four-momentum transfer was such that $-t \leq 0.36$ GeV^2. As in preceding chapters, we carried out the fitting procedure using the MINROS minimization program and the CERN CDC 6600 computer. All eleven of the parameters defined in equations (9.34) - (9.36) were taken to be free. The best fit obtained to the data produces a chi-square value of 583.8 for 219 degrees of freedom, with the parameters given by:

$$\alpha_{P'} = 0.1632 \pm 0.0002$$

$$\alpha_{\rho} = 0.5254 \pm 0.0001$$

$$\beta_P \ (= \beta_{P'}) = (0.4817 \pm 0.0005) \text{ GeV}^{-2}$$

$$\beta_{\rho} = (0.7889 \pm 0.0008) \text{ GeV}^{-2}$$

$$P_0 = (4.666 \pm 0.026) \times 10^{-3} \text{ mb GeV}$$

$$P_1 = -(0.1041 \pm 0.0018) \text{ mb/GeV}$$

$$P_0' = (0.6339 \pm 0.0013) \text{ mb GeV}$$

$$P_1' = -(21.97 \pm 0.16) \text{ mb/GeV}$$

$$\rho_0 = (2.887 \pm 0.010) \times 10^{-2} \text{ mb GeV}$$

$$\rho_1 = (12.39 \pm 0.04) \text{ mb/GeV}$$

$$s_0 = (0.01285 \pm 0.00007) \text{ GeV}^2$$

Except for the rather low value of the P′ intercept, the parameters of the Regge trajectories are in accord with the results of earlier Regge models. It is also interesting to note that the best fit value of the normalization constant s_0 is roughly the pion mass squared.

The ratio of χ^2 to the number of degrees of freedom is 2.67, which is somewhat high to be considered a good fit. Qualitatively, however, the results are in reasonably good agreement with the experimental situation. A detailed comparison of the model with the fitted data is given in Figures 9-1 through 9-7.

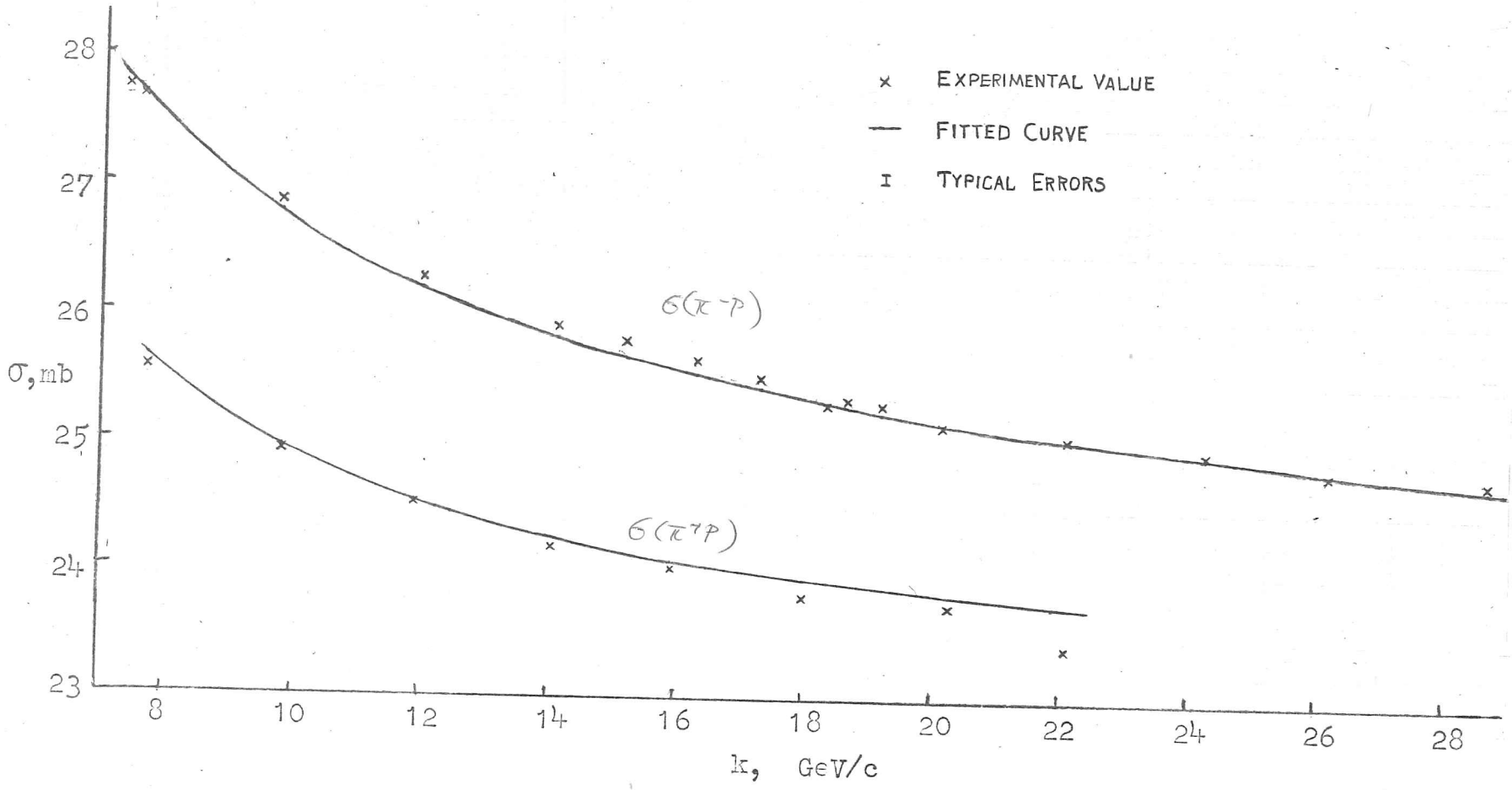

Figure 9-1 Comparison with the experimental data of the fit obtained for the total cross sections.

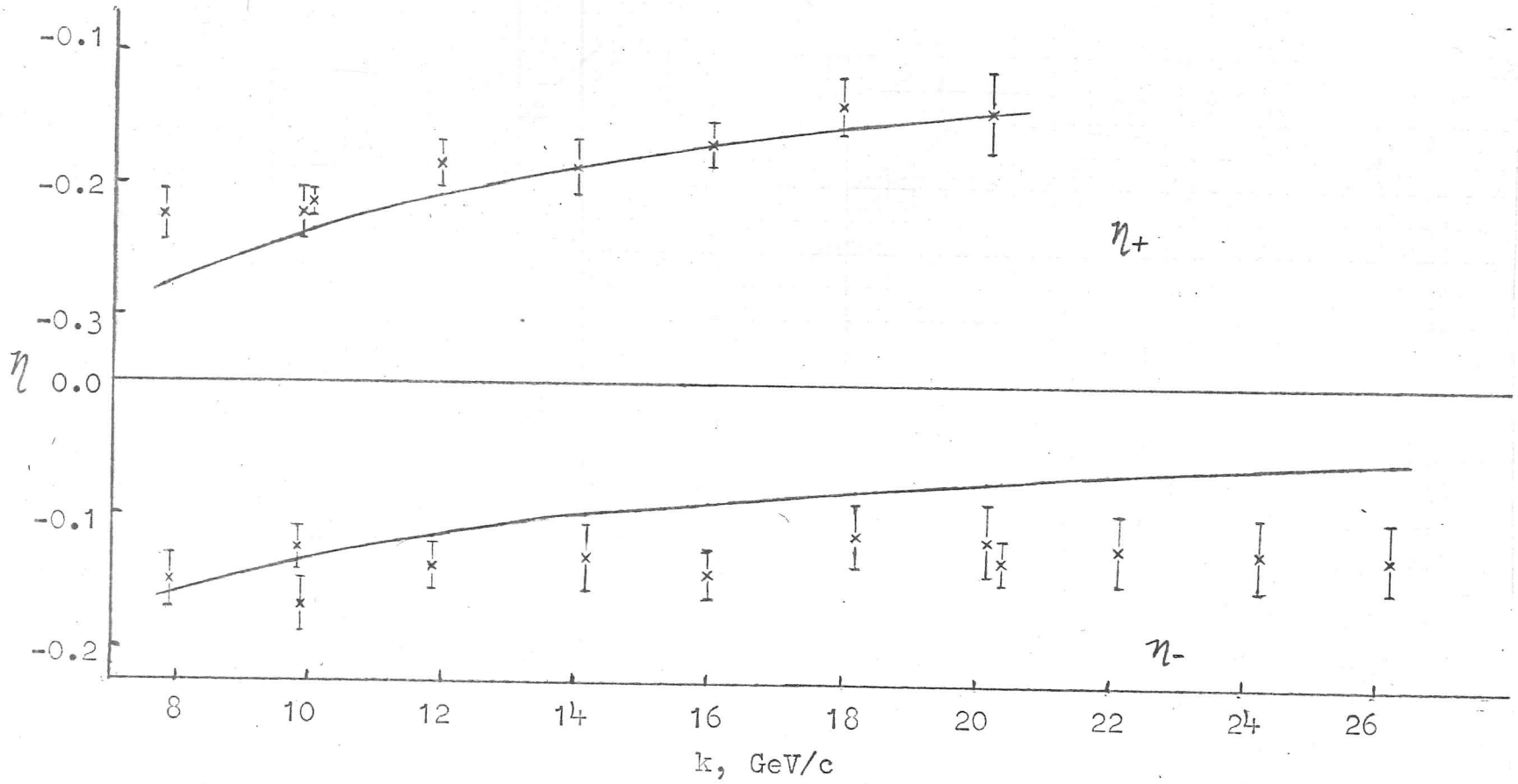

Figure 9-2 Comparison with the experimental data of the fit obtained for the ratio of real and imaginary parts of the amplitude.

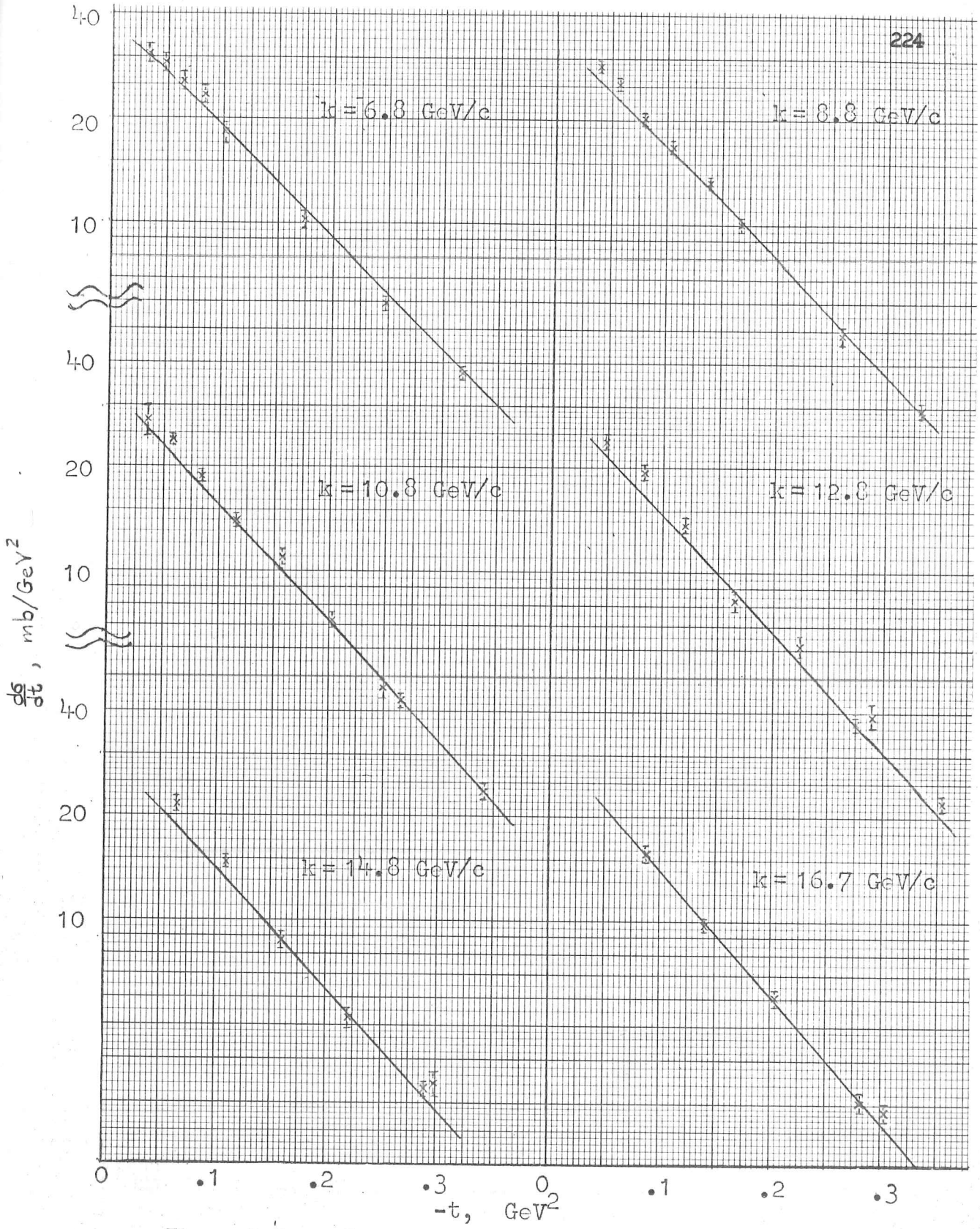

Figure 9-3 Comparison with the experimental data of the fit obtained for the differential cross sections for $(\pi^+ P)$ elastic scattering.

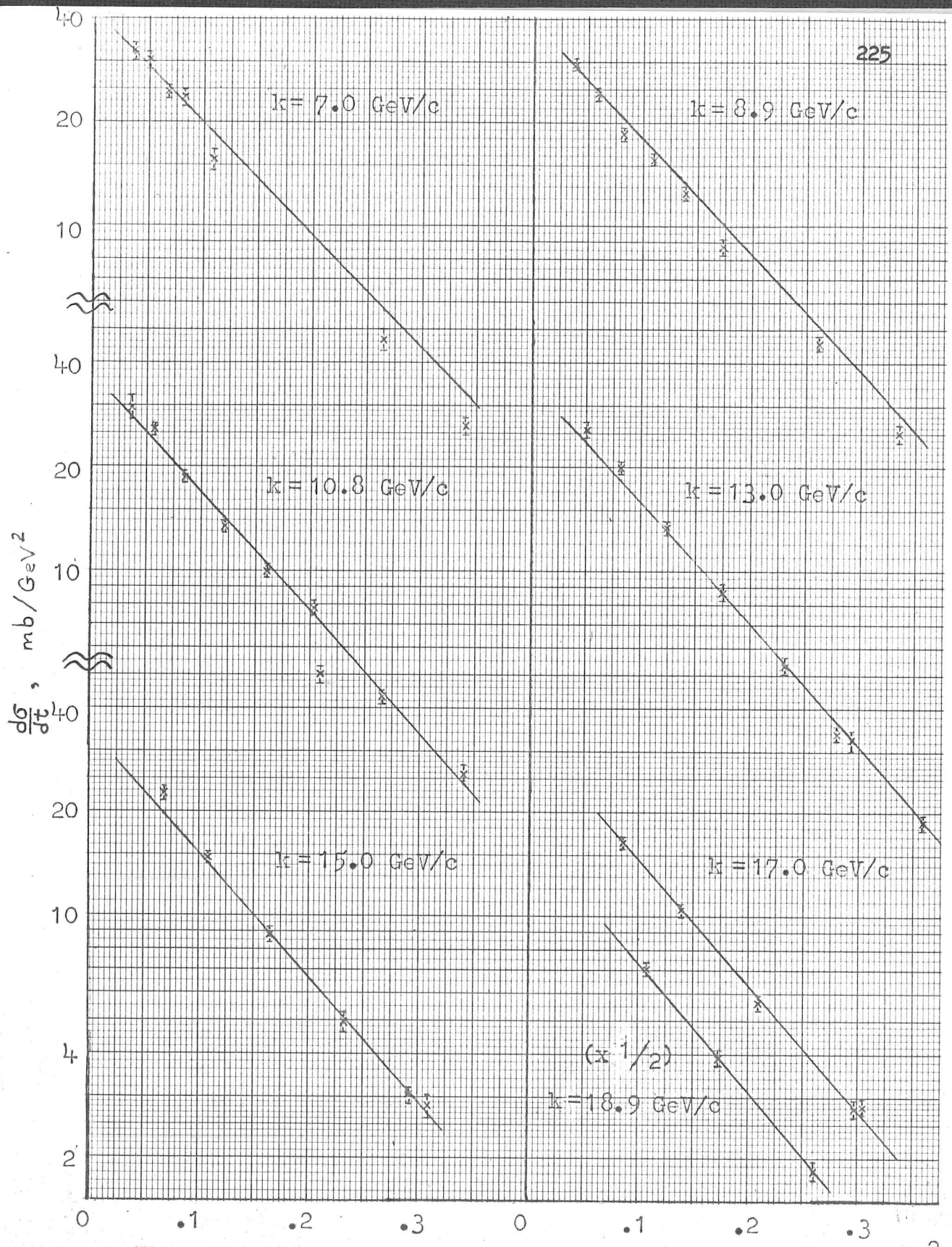

Figure 9-4 Comparison with the experimental data of the fit obtained for the differential cross sections for $(\pi^- P)$ elastic scattering.

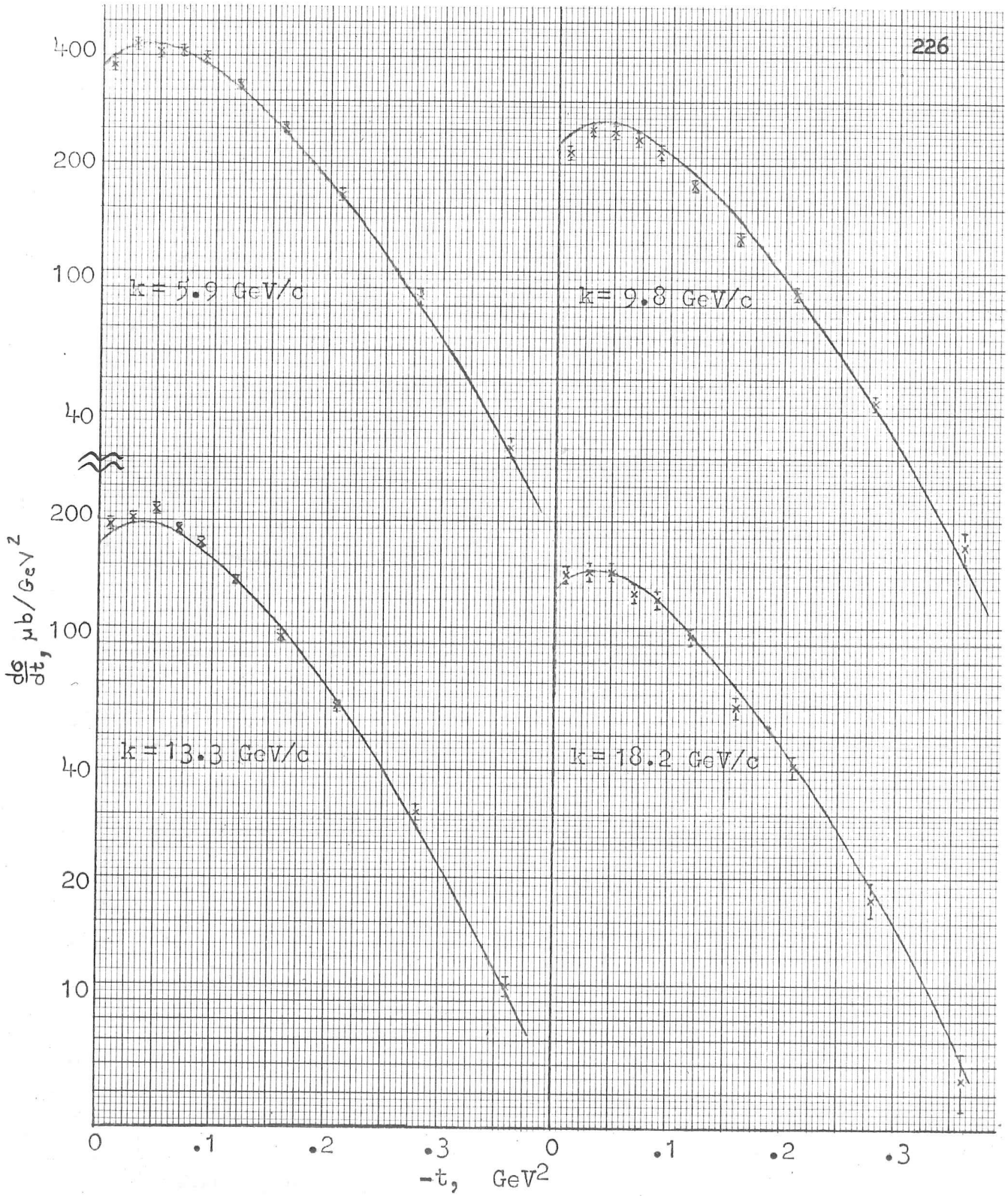

Figure 9-5 Comparison with the experimental data of the fit obtained for the differential cross sections for (πP) charge exchange.

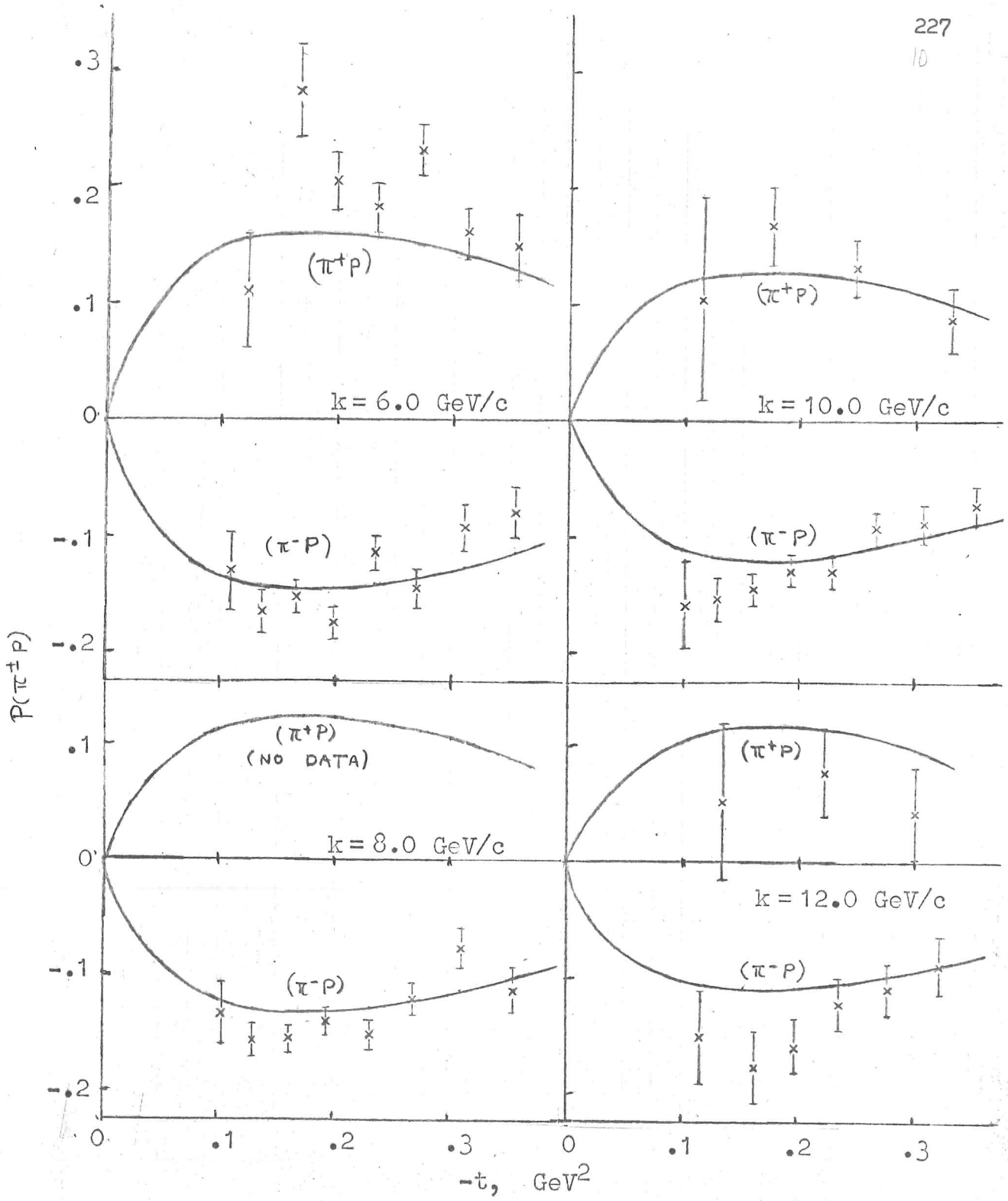

Figure 9-6 Comparison with the experimental data of the fit obtained for the polarization parameter in elastic $(\pi^{\pm}P)$ scattering.

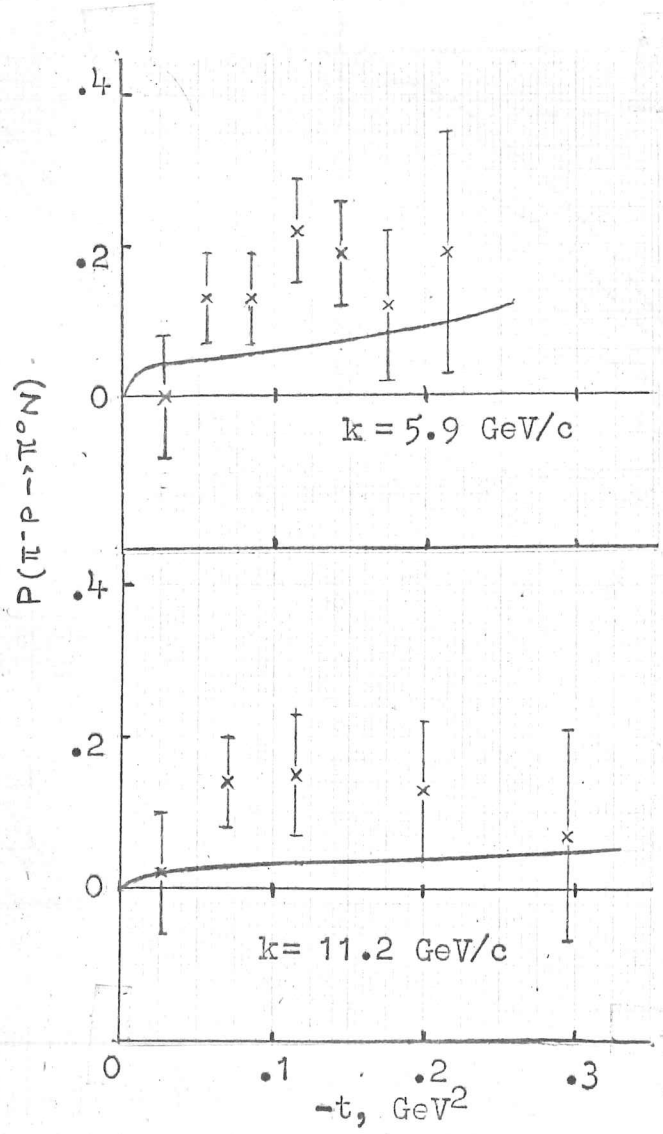

Figure 9-7 Comparison with the experimental data of the fit obtained for the polarization parameter in (πP) charge exchange scattering.

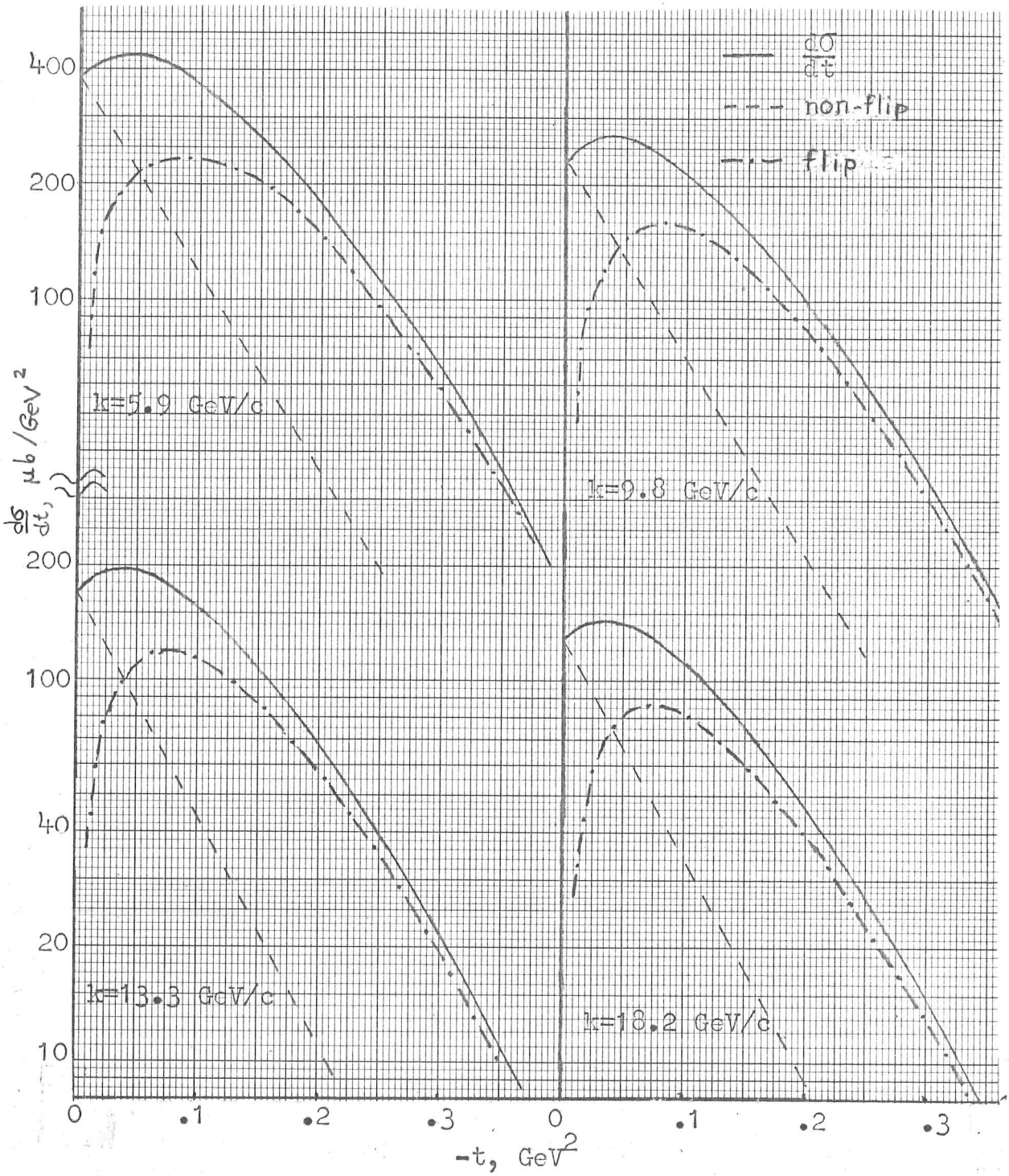

Figure 9-8 Contributions of spin flip and non-flip terms to the charge exchange differential cross sections.

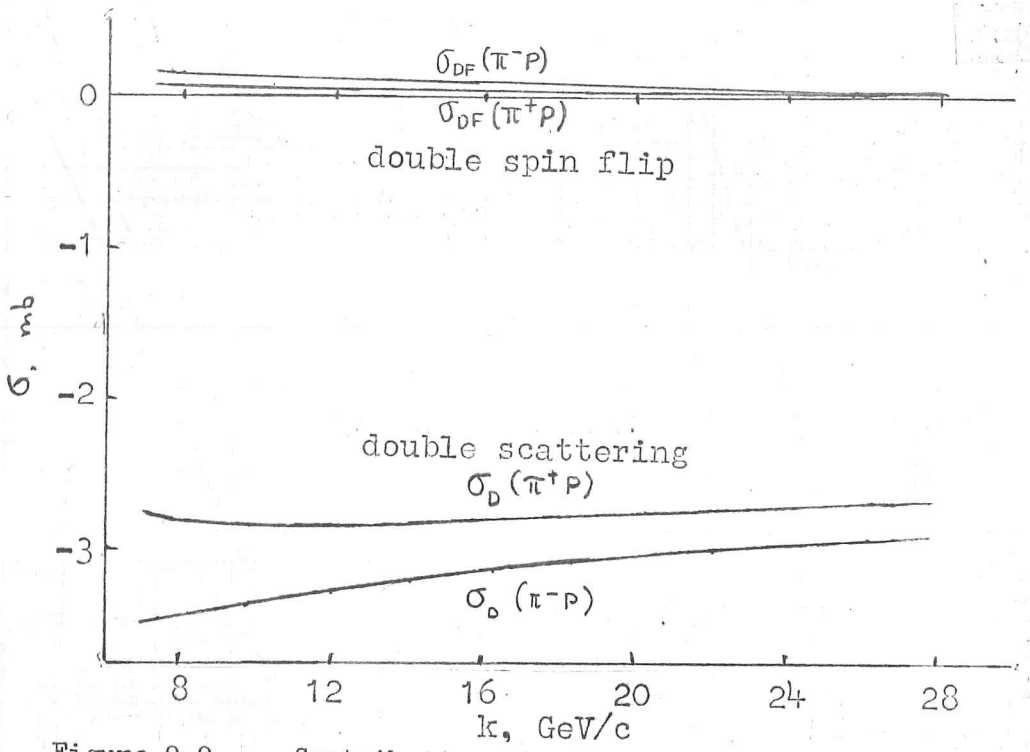

Figure 9-9 Contributions to the total cross section of double scattering and of double spin flip terms.

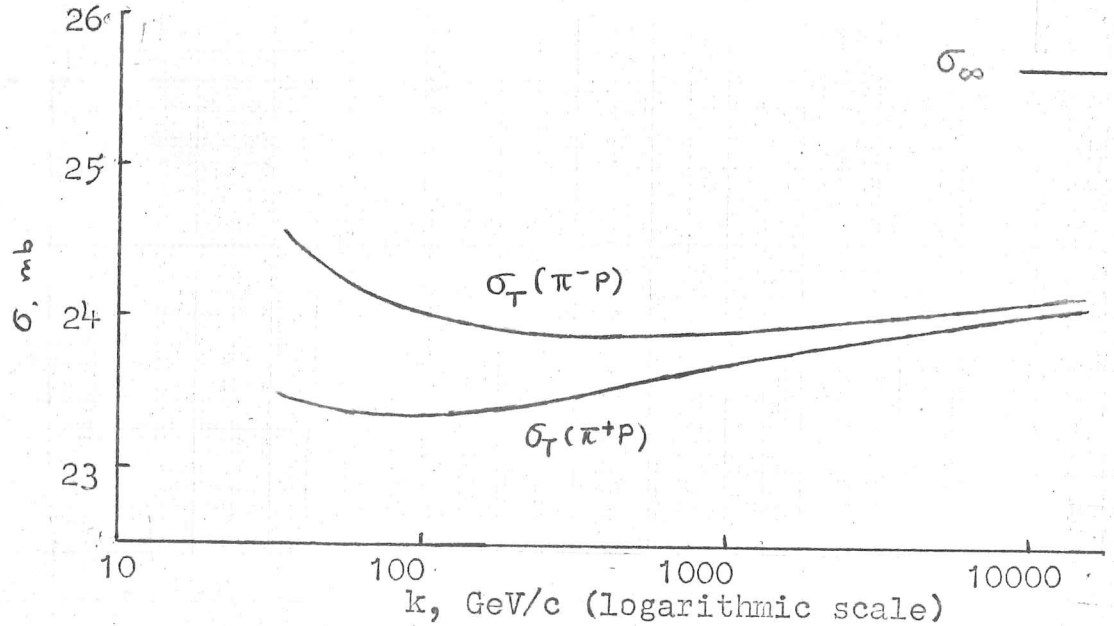

Figure 9-10 Extension of the fit obtained for the total cross sections to the superhigh energy region.

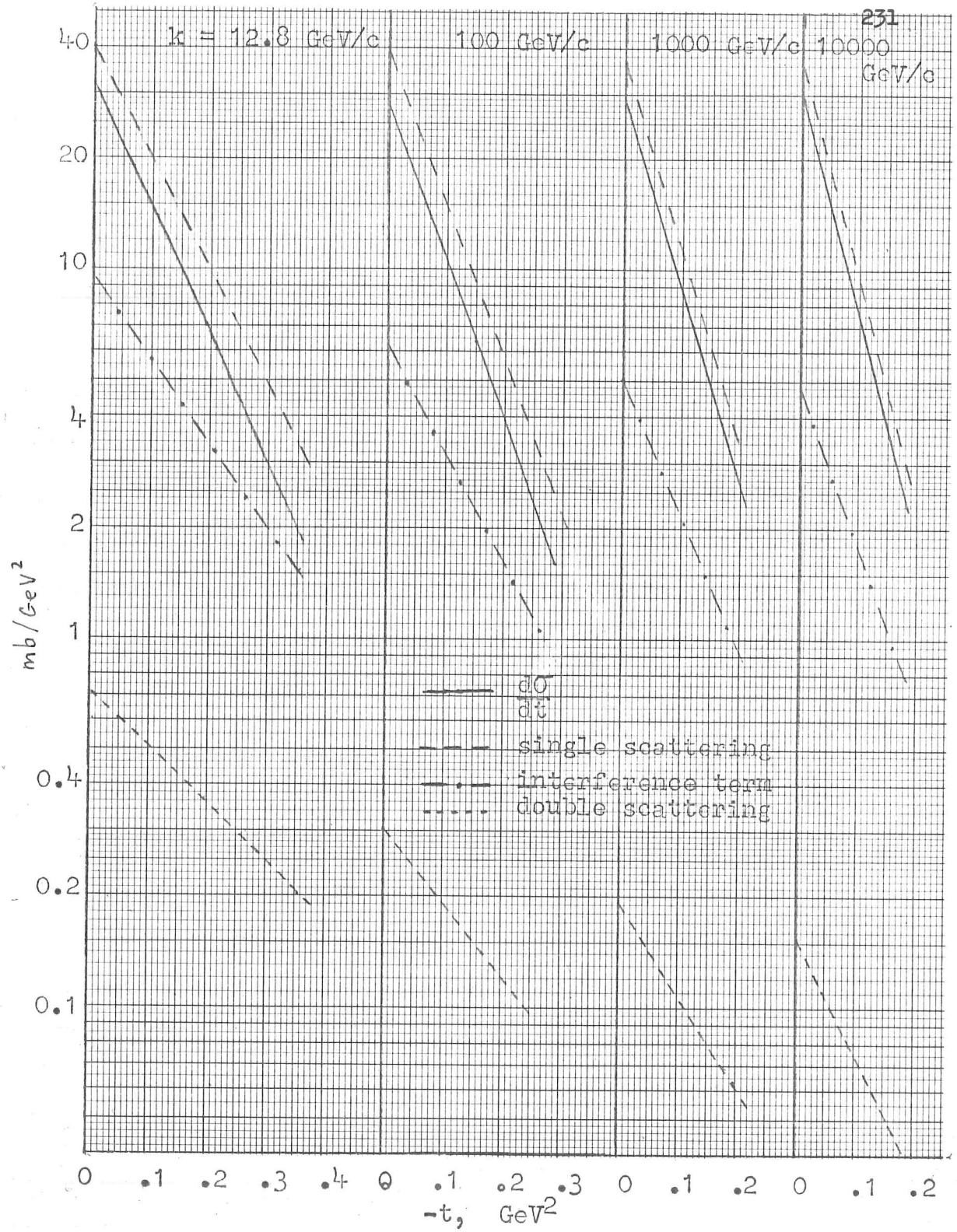

Figure 9-11 Contributions of single scattering, double scattering, and the interference between them, to the differential cross sections at superhigh energies.

It must be pointed out that for the charge exchange polarization, which provided the original motivation for use of the model, the best fit values are generally somewhat smaller than the measured ones. The agreement with the data is quite good for the elastic polarizations, however, and, in fact, for almost all of the other experimental quantities. Only in the case of $\eta^{-}(s)$, where the measured values are generally larger than the model predicts, is there any other consistent disparity between fit and data. The total and differential cross sections are very well fitted, including particularly the structure in the charge exchange process at near-forward angles. To reproduce this dip by means of exponential amplitudes requires that spin-flip terms, negligible in the elastic reaction, must be quite important here (Figure 9-8).

In general the effects of double scattering are fairly significant in these results. Their contribution to the total cross sections are shown in Figure 9-9, along with that resulting particularly from the double spin flip terms. The smallness of the latter is reassuring evidence that the neglect of spin effects in earlier chapters was not unreasonable. As we have noted in Chapter VIII, the disappearance of the double scattering effects at higher energies will cause the total cross sections to increase slightly toward an asymptotically constant value; from the parameters of this model we deduce that this limit is

$$\sigma_{\infty}(\pi N) = (25.65 \pm 0.28) \text{ mb} \quad .$$

The leading multiple scattering contributions decrease only logarithmically, however, so that the increasing behaviour becomes apparent only at superhigh energies. In order to see how rapidly $\sigma_{\infty}(\pi N)$ is approached we give in Figure 9-10 an extension of the model up to k = 10000 GeV/c. It is again evident that the advent of asymptopia is still rather distant.

The importance of double scattering can also be seen in the differential cross sections. Interference between double and single scattering leads to a subtractive term with magnitude about one-third of that resulting purely from the single scattering term. The evolution with energy of the contributions of single and double scattering, and of their interference, to the $(\pi^{+}P)$ curves can be seen in Figure 9-11. The situation for the other reactions is very similar. In all three cases the range of t we are studying is still dominated by the single scattering term.

It appears, then, that the quark model with multiple scattering is capable of reproducing, qualitatively and, to a reasonable extent, quantitatively, the pion-nucleon scattering amplitude. In view of the approximations made, the results must be considered encouraging; in particular we would hope that a proper treatment of the form factor and the use of a completely free P′ trajectory would lead to a more comprehensive fit of the data, including even the dips observed at larger angles. A further extension of the model would be the calculation and comparison with experiment of the amplitudes

for the production of nucleon resonances. Since the form factor in this case involves the overlap of the octet and decuplet spatial wave functions, the strong binding assumption we have used may not be valid. We expect that future research efforts may clarify both of these possibilities.

References

1. R. K. Logan and L. Sertorio, Phys. Rev. Letters 17, 835 (1966).
2. H. Hogaasen and A. Frisk, Phys. Letters 22, 91 (1966);
H. Hogaasen and W. Fischer, Phys. Letters 22, 516 (1966).
3. C. B. Chiu and J. Finkelstein, Nuovo Cimento 48A, 820 (1967).
4. K. J. Foley et al., Phys. Rev. Letters 19, 330 (1967).
5. K. J. Foley et al., Phys. Rev. Letters 19, 193 (1967).
6. K. J. Foley et al., Phys. Rev. Letters 11, 425 (1963).
7. A. V. Stirling et al., Phys. Rev. Letters 14, 763 (1965).
8. M. Borghini et al., Phys. Letters 24B, 77 (1967).
9. P. Bonamy et al., Phys. Letters 23, 501 (1966).

CHAPTER X

Conclusion

The phenomenological approach basic to this thesis has perhaps been more apparent in the second part of it. Our consideration of multiple scattering effects in the quark model has been directed towards parametrization of the experimental facts; our principal conclusion is that this model seems to describe quite satisfactorily a large number of high energy scattering phenomena.

Clearly, there are many further applications of this idea yet to be investigated. On the theoretical side, the entire question of Regge cuts and multiple scattering is an interesting unsolved problem. For high energy phenomenology the model offers numerous possibilities, particularly with reference to the inelastic reactions. As more accurate data become available it will be possible to study the multiple scattering terms as corrections to the predictions of additivity, as well as in the cases where the single scattering yields a null result. In the three examples of the latter which we have considered, namely the antisymmetric sum rule, the double exchange reactions, and the charge exchange polarization, the model seems quite successful.

Many other calculations are possible within this framework; for example, we note in passing that it provides a natural mechanism for the Deck effect.

The principal quantitative conclusion we have reached is that the multiple scattering effects are not negligible. The simple Regge framework employed indicates that they vanish logarithmically, leading to an extremely slow increase of total cross sections toward an asymptote somewhat higher than current values. The implications of this result on dispersion theory should be investigated, since it indicates that integrals over the total cross sections should be slightly larger than present estimates. The details of the model we have fitted to the meson-nucleon scattering are open to considerable refinement, as we have pointed out. We hope that in the near future it will be possible to improve both the accuracy of the phenomenological treatment and the precision of the experimental data. The obvious extension of these techniques to the scattering of nucleons and antinucleons should also be mentioned here, although the choice of energy for comparison of mesonic and baryonic amplitudes will remain a problem.

We feel, therefore, that the concept of multiple scattering in the quark model which we have presented has great potential as a tool for describing and understanding the high energy interactions of fundamental particles.